

A 'Top-Down' Approach For The Synthesis of Diverse Lead-Like Molecular Scaffolds

Chloe Elizabeth Townley

Submitted in accordance with the requirements for the degree of
Doctor of Philosophy

The University of Leeds

School of Chemistry

August, 2020

The candidate confirms that the work submitted is her own and that appropriate credit has been given where reference has been made to the work of others.

This copy has been supplied on the understanding that it is copyright material and that no quotation from the thesis may be published without proper acknowledgement.

The right of Chloe Elizabeth Townley to be identified as Author of this work has been asserted by her in accordance with the Copyright, Designs and Patents Act 1988.

© 2020 The University of Leeds and Chloe Elizabeth Townley

Acknowledgements

Firstly, I am extremely grateful to Adam and Steve for giving me the opportunity to complete a PhD under their supervision. The support and guidance they have both shown me throughout my studies has been exceptional and I cannot thank them enough for this. I would also like to thank my industrial supervisor Lindsay McMurray who has always been very supportive and made my placement at AstraZeneca even more enjoyable.

Next, I would like to say a huge thank you to the other members (past and present) of the Nelson group. You are all wonderful and have made my time in Leeds even more enjoyable. I look forward to seeing what you all achieve in the future as I am sure it will be exceptional. Special mention must go to Sam, Jacob, Adam, Shiao and Joan with whom I have forged great friendships. Thanks to Joan who gave me so much great advice in the lab – you will always be the b.g.e. Adam, I couldn't have hoped for a better person to go through this PhD process with and I will always be grateful for your support, friendship and the countless trips to Opposite. I have never been mocked nor made to laugh by anyone more than by Jacob. Thanks for never letting me take it too seriously and one day I will get you back for the 'beast from the east'. I will always treasure the time spent at pottery classes, on road trips and city breaks with Sam and Shiao. Sam has undoubtedly become one of my closest friends throughout my time at Leeds which looking back, has been a real highlight for me. I really couldn't have wished for a more supportive friend or a better proof-reader.

Finally, I would like to thank my friends and family without whom this would not have been possible. Sophie, I couldn't live so happily if it weren't for your unwavering friendship over the last 20 years, you will always be my family. I cannot thank David enough for his continuing and enduring love and support, you inspire me to be the best I can be. You have never failed to believe in me and for that I will be forever grateful. I am lucky to have so many people in my life I can call parents; Mum, Dad, Andrew, Rukhsana and Ros – you have all done so much for me, especially Mum, and all I can say is thank you, I really could not have done this without you, your support is incredible.

Abstract

Control of molecular properties is essential in the design of new bioactive compounds, due to the inherent link between molecular properties of lead compounds and their successful progression through the stages of clinical development. Through the optimization process compounds tend to gain in molecular weight, lipophilicity and complexity, therefore a set of guidelines have been established to aid the design of lead-like molecules.

In order to realise efficient lead-oriented synthesis a “top-down” approach has been employed whereby complexity is encoded to give a key polycyclic intermediate. It is vital that this intermediate contains functionality that can facilitate annulations, ring contractions and ring cleavage reactions. A small number of candidates was identified from the literature, all of which underwent investigation into their suitability for the approach. The use of this approach was demonstrated using [5+2] cycloaddition chemistry as the complexity generating reaction.

A toolkit of reactions was identified and was applied to the parent compounds, creating a diverse range of lead-like scaffolds. Four approaches were applied which include; ring addition, ring fusion, ring cleavage and ring expansion. The application or combination of these approaches yielded over twenty distinct molecular scaffolds. All but one scaffold was found to contain a novel Murcko framework and originate from nine parent ring systems, so are both diverse and novel in nature.

Out of the 21 synthesised scaffolds 11 scaffolds were selected for decoration with medicinally relevant capping groups. The application of the top-down approach has led to the synthesis of a library of screening compounds with all but one of the compounds possessing the correct properties to target lead-like chemical space (as assessed by LLAMA). Library analysis also highlights the improved exploration of chemical space with increased three-dimensionality and F_{sp^3} . This diverse library of lead-like compounds has the potential to be used to support new drugs and/or chemical probes.

List of Abbreviations

9-BBN	9-Borabicyclo[3.3.1]nonane
Ac	acetyl
ADMET	absorption, distribution, metabolism, excretion and toxicity
AIBN	azobisisobutyronitrile
app.	apparent
B/C/P	build/couple/pair
BBB	blood brain barrier
BLA	biological license application
Bn	benzyl
Boc	tert-butyloxycarbonyl
Bu	butyl
ca	around, about
CAS	Chemical Abstracts Service
Cbz	carboxybenzyl
CNS	central nervous system
cod	cyclooctadiene
d	doublet
d.e	diastereomeric excess
d.r	diastereomeric ratio
Da	Daltons
DCE	dichloroethane
DIAD	diisopropyl azodicarboxylate
DIBAL	diisobutylaluminium hydride
DMAP	4-(Dimethylamino)pyridine
DMF	N,N'-dimethylformamide
DMP	Dess-Martin periodinane
DOS	diversity-oriented synthesis
e.g.	example gratia; for example
Et	ethyl
FBDD	fragment-based drug discovery
FDA	Food and Drug Administration
Fmoc	fluorenylmethyloxycarbonyl
Fsp ³	fraction of sp ³ hybridised carbons
GNB	graph-node-bond
GSK	GlaxoSmithKline
HA	heavy atom
hept	heptet
HFIP	hexafluoroisopropanol
Hsp90	Heat shock protein 90
HTS	High throughput screening
IC50	half-maximal inhibitory concentration
IPA	isopropanol

<i>J</i>	spin-spin coupling constant
LC-MS	liquid chromatography mass spectrometry
LE	ligand efficiency
LLAMA	Lead-Likeness And Molecular Analysis
logP	octanol-water partition coefficient
LOS	lead-oriented synthesis
L-selectride	Lithium tri- <i>sec</i> -butylborohydride
<i>m</i>	multiplet
<i>m</i> -	meta
<i>m</i> -CPBA	3-chloroperoxybenzoic acid
MDAP	mass directed auto purification
Me	methyl
MeCN	acetonitrile
MPO	multiple parameter optimisation
NBS	<i>N</i> -bromosuccinamide
NME	New molecular entity
NMP	<i>N</i> -methyl-2-pyrrolidone
NMR	nuclear magnetic resonance
<i>n</i> Oe	nuclear Overhauser effect
NOESY	nuclear Overhauser effect spectroscopy
<i>p</i> -	para
PCA	principal component analysis
PD	pharmacodynamic
Ph	phenyl
PIFA	[Bis(trifluoroacetoxy)iodo]benzene
PK	pharmacokinetic
PMI	principle moment of inertia
ppm	parts per million
PPTS	pyridinium <i>p</i> -toluenesulfonate
PSA	polar surface area
R&D	research and development
R _f	retention factor
Ro5	rule of five
rt	room temperature
<i>s</i>	singlet
S _N Ar	nucleophilic aromatic substitution
SPR	surface plasma resonance
SuRE	successive ring expansion
<i>t</i>	triplet
TBS	<i>tert</i> -butylsilyl
<i>tert</i>	tertiary
TES	triethylsilane
TFAA	trifluoroacetic anhydride
TFT	trifluorotoluene
THF	tetrahydrofuran

THP	tetrahydropyran
TLC	Thin layer chromatography
TMEDA	<i>N,N,N',N'</i> -Tetramethylethylenediamine
TOSMIC	tosylmethyl isocyanate
troc	2,2,2-trichloroethoxycarbonyl chloride
Ts	toluenesulfonyl
TST	temporary silicon tether
δ	chemical shift

Table of Contents

Acknowledgements	iii
Abstract	iv
List of Abbreviations	v
Table of Contents	viii
Chapter 1 Introduction	1
1.1 An overview of the drug discovery process	1
1.1.1 The role of chemistry in the drug development process	3
1.1.2 Decline in productivity within the pharmaceutical industry	3
1.2 Molecular properties pertinent to drug discovery.....	6
1.2.1 Characteristics of Drug-like molecules	6
1.2.2 Characteristics of lead-like molecules	7
1.2.3 Characteristics of fragment-like molecules	10
1.3 The exploration of chemical space.....	13
1.3.1 Scaffold diversity and the poor exploration of chemical space	13
14	
1.4 Approaches to small-molecule library synthesis.....	17
1.4.1 Diversity-oriented synthesis (DOS)	17
1.4.2 Lead-Oriented synthesis (LOS).....	20
1.4.3 The 'top-down' approach to lead-oriented synthesis	26
1.5 Summary.....	29
1.6 Thesis overview and aims.....	30
1.6.1 Objective 1: To select an appropriate complexity generating reaction towards the synthesis of lead-like compounds.....	31
1.6.2 Objective 2: Establish and harness a toolkit of reactions for the preparation of sp ³ rich, lead-like scaffolds.....	32
1.6.3 Objective 3: To design, prepare and evaluate the library of decorated lead-like scaffolds.....	34
Chapter 2 Synthesis and selection of complex synthetic intermediates	36
2.1 The use of a Rh-catalysed C-H insertion as a complexity generating reaction	36
2.1.1 Synthesis of the precursors and framework <i>via</i> a C-H insertion reaction.....	37

2.1.2 Analysis and assignment of the framework formed using a C-H insertion reaction	38
2.1.3 Attempted optimisation of the C-H insertion reaction	38
2.2 The use of dearomatisation chemistry as a complexity generating reaction	42
2.2.1 Synthesis of the cyclisation precursors and carbocyclic analogue	43
2.2.2 Synthesis of the heteroatom analogues of the dearomatisation framework.....	45
2.3 Tropone cycloaddition chemistry as a complexity generating reaction	49
2.3.1 Synthesis of tropone complex intermediate.....	50
2.3.2 Formation of enone functionality via deprotection.....	51
2.3.3 Formation of enone functionality via reduction and protection	52
2.4 [5+2] Oxido-pyridinium alkene cyclisation as a complexity generating reaction	57
2.4.1 Synthesis of the cyclisation precursor and construction of the complex intermediate	57
2.5 Intramolecular [5+2] Oxido-pyrillium alkene cyclisation as a complexity generating reaction.....	60
2.5.1 Synthesis of the acetoxypyranone-alkene cyclisation precursor and its cyclisation.....	61
2.6 Analysis and selection of the complex intermediates for use in the synthesis of a library of lead-like compounds.....	62
Chapter 3 Synthesis of diverse molecular scaffolds	66
3.1 The application of ring addition chemistry	66
3.1.1 Rh catalysed 1,4-addition of aryl boronic acids	66
3.2 Application of ring fusion reactions.....	70
3.2.1 Pyrrolidine formation <i>via</i> a [3+2] dipolar cycloaddition	71
3.2.2. Pyrrole formation <i>via</i> a [3+2] cycloaddition.....	74
3.2.3 Gold catalysed pyridine formation	75
3.3 Application of ring expansion chemistry	78
3.3.1 Testing of the Beckmann ring expansion	78
3.3.2 Application of the Baeyer-Villiger ring expansion	79
3.4 Application of ring cleavage chemistry to the complex intermediates.....	81
3.4.1 Cleavage of the enone C-C double bond	81
3.4.2 Cleavage of a C-N bond.....	83

3.4.3 Attempted cleavage of the lactone	87
3.5 Synthesis of scaffolds using two approaches	87
3.5.1 Ring addition followed by ring fusion	88
3.5.2 Ring expansion followed by ring fusion	89
3.6 Summary and analysis of the synthesised scaffolds	89
3.6.1 Summary of scaffolds synthesised	89
3.6.2 Novelty assessment of synthesised scaffolds	90
3.6.3 Diversity assessment of the scaffolds	91
3.6.4 Conclusions	92
Chapter 4 Design and preparation of a library of decorated lead-like scaffolds.	94
4.1 Selection of scaffolds for decoration	94
4.2 Strategy used in the design of lead-like compounds	95
4.2.1 Decoration strategy	96
4.2.2 Desirable properties for cell permeability	97
4.3. Decoration on oxygen	97
4.3.1 Reduction of the ketone	98
4.3.2 O-arylation <i>via</i> S _N Ar	102
4.4 Reductive aminations applied as a decoration technique	104
4.5 Decorations on the nitrogen functionality	108
4.5.1 Deprotection of benzylamines	109
4.5.2 Reductive amination as a method for decoration	109
4.5.3 Sulfonamide formation as a decoration	111
4.5.4 Amide formation	112
4.6 Computational assessment of the prepared screening compounds	114
4.6.1 Analysis of the decoration reactions	114
4.6.2 Lead-like assessment of the library of compounds	115
4.6.3 Assessment of the shape diversity of the library of lead-like compounds	116
4.6.4 F _{sp} ³ assessment of the library compounds	118
4.6.5 Summary of the computational assessment	120
Chapter 5 Summary, conclusions and future work	121
5.1 Selection of an appropriate complexity generating reaction towards the synthesis of lead-like compounds	121
5.2 Establishment and implementation of a toolkit of reactions for the preparation of sp ³ rich, lead-like scaffolds	123

5.3 Design, preparation and evaluation of the library of decorated lead-like scaffolds.....	124
5.4 Future perspectives.....	125
Chapter 6 Experimental	129
6.1 General Information and Instrumentation.....	129
6.2 General experimental.....	130
6.3 Compound Series	134
List of References	196
Appendix A: NMR data for complex intermediates and scaffolds included in the final library.....	208
Appendix B NOESY NMR Spectrum's used in the assignment of stereochemistry.	228

Chapter 1

Introduction

Small-molecule drugs are a powerful tool in combating disease, with 28 of the 48 FDAs new approved drugs being small molecules in 2019.¹ However, the discovery of bioactive small molecules has been a constant challenge to medicinal chemists. The rate of drug discovery has remained constant for nearly 60 years despite a sharp increase in investment within the sector.²⁻⁴ The cost of bringing a new molecular entity (NME) to market is estimated to be ca. \$2.6 billion,⁵ which accounts for the costs incurred on failed campaigns and post-approval costs. There are several reasons why a molecule can fail to progress through the stages of clinical trials however, one major reason is that candidates have poor ADMET (absorption, distribution, metabolism, excretion and toxicity) properties.⁶ Consequently, consideration of these molecular properties at an earlier stage in the drug development process could allow for an improvement in the success rates of small molecules.⁷

1.1 An overview of the drug discovery process

The drug discovery process is initiated when an unmet medical need is identified, an existing treatment is deemed sub-optimal^{8,9} or by a fundamental scientific discovery. The drug discovery process is complex and can be divided into five key stages (Figure 1). Initially, the biological target must be selected, which is a key decision point in a drug discovery programme, as this shapes the property requirements for the subsequent compounds.⁸



Figure 1: An overview of the drug discovery process. Adapted from references ^{8,10}

There are several methods used in the generation of new leads for drug discovery programmes. Analysis of 66 published clinical candidates identified the most common methods for successful lead generation (Figure 2). The most frequently successful strategy employed is utilising a known compound as starting point (43%), followed by a random high throughput screen (HTS, 29%). Structure based drug design (14%), focussed screening (8%), fragment screening (5%) and DNA-encoded libraries (DEL, 1%) make up the remaining methods utilised to produce a successful drug candidate.¹¹

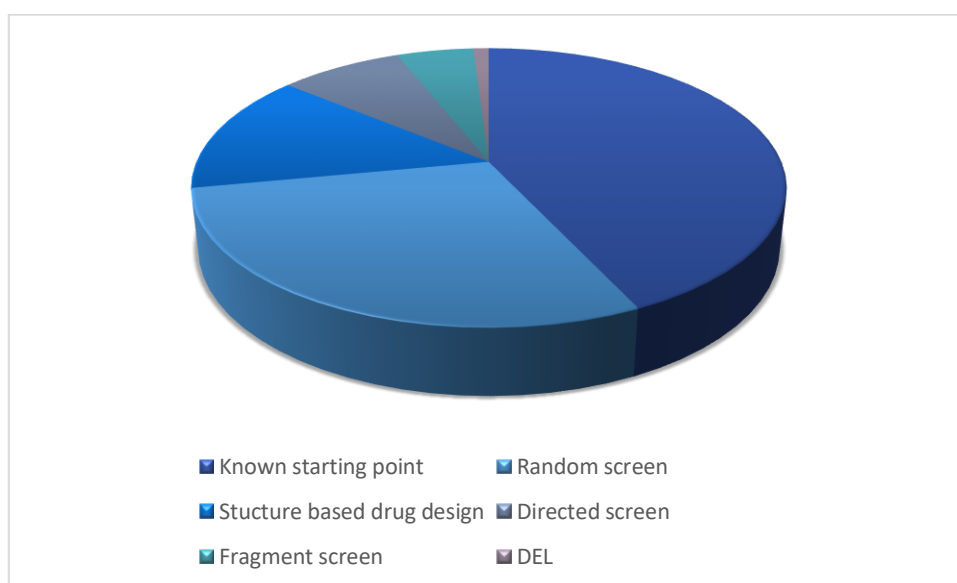


Figure 2 lead generation approaches towards clinical candidates. Adapted from¹¹

HTS is a common method used to identify starting points for drug discovery programmes^{8,12-14} where a large library ($>10^5$)¹⁵ of small molecules are screened against the biological target to identify compounds which interact with the desired target or affect the function of a target. A compound that can bind to the target resulting in inhibition or activation is called a 'hit'.⁸ These initial hits can then undergo rounds of optimisation to generate 'lead' compounds, which should have the correct properties to target lead-like chemical space and demonstrates efficacy in an in vivo model of the disease of interest. Lead compounds can then be further optimised through analogue synthesis and the fine tuning of molecular properties to improve affinity and safety.^{8,16,17} The final compound is termed a 'drug candidate' which is then entered in to pre-clinical and clinical trials and must successfully complete all stages to become an approved drug.⁸

1.1.1 The role of chemistry in the drug development process

The drug development process is complex and requires multi-disciplinary teams for successful drug discovery campaigns.¹⁸ Chemistry is one of the main drivers in the early stage drug discovery as it enables chemical matter to be prepared for biologically testing.⁸ Synthetic chemistry is used for the preparation of screening libraries whether that is through the synthesis of HTS libraries¹⁹ or preparation of more focussed libraries (<100 compounds) using different approaches, for example DOS (diversity-oriented synthesis),^{20–22} FBDD (fragment-based drug discovery)^{23,24} and LOS (lead-oriented synthesis)^{25,26} all of which will be discussed below (Section 1.4.1, Section 1.2.3 and Section 1.4.2 respectively).

The lead-optimisation process is also heavily reliant on chemistry to evolve and improve the initial lead into a clinical candidate. Numerous chemistries have been established to aid the optimisation of leads, including C-H activation, fluorinations and numerous other late-stage functionalisations.^{27–29} The use of new reactions is likely to increase the diversity of the compounds synthesised.³⁰

1.1.2 Decline in productivity within the pharmaceutical industry

Research and Development (R&D) investment within the pharmaceutical industry has been increasing year on year, totalling \$1.36 trillion from 2007–2016 and forecasts predict that annual investment will be \$181 billion by 2020.³¹ The number of approvals of both NMEs and BLAs has fluctuated over the past 25 years (Figure 3). The five-year average of approvals highlights the slump in productivity observed in the mid 2000's. Since then the number of approvals has recovered with 2018 seeing the highest number of approvals since 1996.¹

Biologics have had a sharp increase in the number of approvals over recent years. It is estimated that by the end of 2020 biologics will make up over a quarter of the therapies available on the pharmaceutical market. The drive towards biological treatments is due to their ability to reach targets which are thought to be 'undruggable' targets for small molecules.^{32,33}

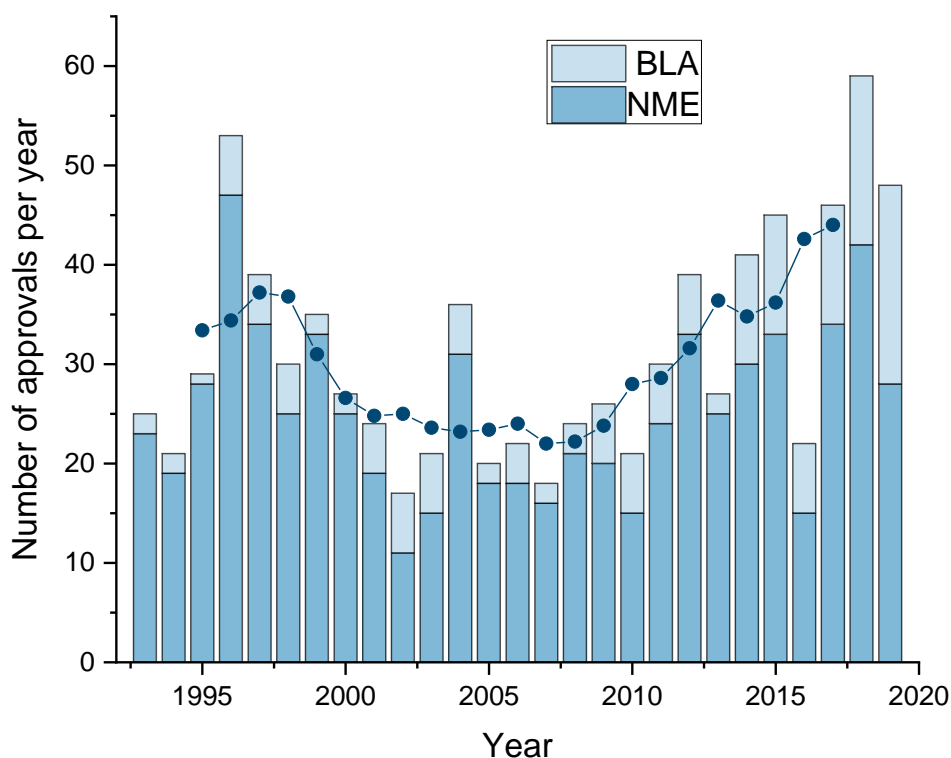


Figure 3: The number of BLA's and NME's 1993-2019. Bar chart indicating the yearly approvals with left hand axis, with overlain scatter and line plot with right hand axis showing the five-year moving average of the approvals. NME – New molecular entity (dark blue), BLA – biological licence application (light blue). Adapted from ³⁴

This decline in productivity can be attributed in part to rising costs and stricter safety regulations;⁵ however drug candidate attrition rates remain the most significant challenge. There are several reasons why a candidate may fail to progress through clinical trials. Previously, poor bioavailability and pharmacokinetics were thought to be the primary cause of failure though it is now understood to result from a lack of efficacy and safety issues, meaning more costlier late-stage failures.³⁵⁻³⁷

This can be seen by the attrition rates in phase II clinical trials with only 25% of small-molecule candidates successfully validating their efficiency at treating the target disease (Figure 4).³⁸ Unexpected safety issues can sometimes be linked to pharmacokinetics and subsequently its molecular properties, which are defined through lead-optimisation, therefore preparing leads with more desirable molecular properties could reduce attrition rates and subsequently costs.^{7,39}

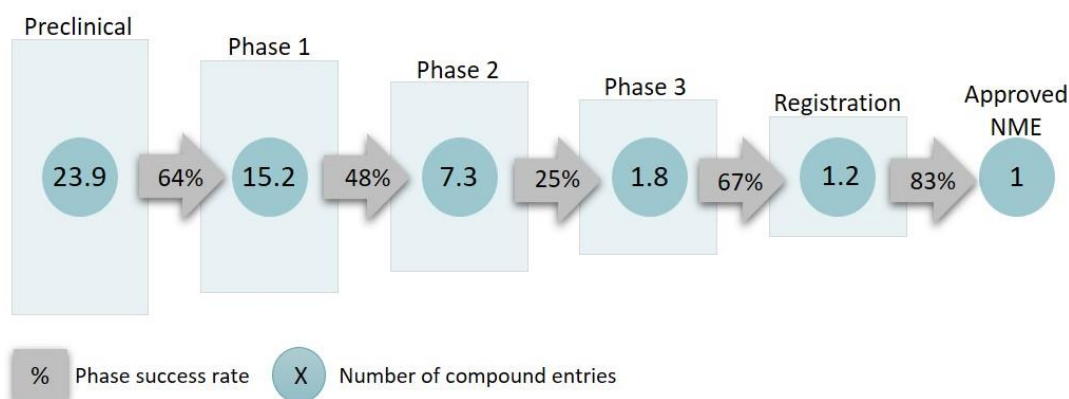


Figure 4: NME approval success rates by phase averaged from 9 pharmaceutical companies. Adapted from reference.³⁸

The decline in R&D productivity is described as the industry's grand challenge, although this issue is compounded by the so-called 'patent cliff'. The drug discovery process is a very costly and time consuming enterprise, with the average drug taking 13 years³⁸ to reach the market and costs totalling ca. \$2.6 billion.⁵ Ensuring long term profitability after the launch of a drug is vital to all companies within the pharmaceutical industry. Loss of patent protection is known to result in a severe cut in sales and profit as generic manufacturers step in and make the product at a much lower price, typically 40% lower than the original. This is beneficial for public health spending but detrimental to the industry. The increasing cost of a drug combined with the patent cliff mean it is more difficult for a company to create a new blockbuster drug.^{40,41} Reducing attrition rates throughout the drug discovery process is one key way to help improve productivity, to achieve this the reasons for attrition must be addressed.

Many pharmaceutical companies have actively tried to address these issues, one example of this is AstraZeneca. Improvements to success rates were achieved by implementation of a new strategy working on a focused range of disease types. Considerable investment has been made in target selection and validation, lead generation, pharmacokinetic/pharmacodynamic (PK/PD) modelling which has allowed for selection of the most appropriate candidate. This approach is having a positive impact with success rates from candidate drug selection to competition of clinical trials increasing from 4% in 2005–2010 to 19% in 2012–2016.⁴²

1.2 Molecular properties pertinent to drug discovery

As previously mentioned, a compound's success through the development process and clinical trials is linked to its molecular properties.^{7,39} There are a number of key molecular properties that have turned out to be pertinent to the process of identifying new, bioactive compounds. These are molecular weight, lipophilicity, and 3-dimensionality. Each of these key properties are discussed below within the context of drug, lead and fragment-likeness.

1.2.1 Characteristics of drug-like molecules

The phrase 'drug-like' describes the ideal molecular properties for small molecules which are consistent with most known drugs.⁴³ Lipinski developed the rule of 5 (Ro5) guidelines after analysis of approved drugs and their typical molecular properties, which medicinal chemists now use as guidelines for controlling molecular properties in the design of orally bioavailable drug candidates (Table 1).⁴⁴⁻⁴⁶

Undesirable molecular properties are understood to be a significant reason for the failure of clinical candidates.⁴⁷ Lipophilicity* (describing a molecule's affinity for a lipophilic environment) is thought to be one of the most important properties to control. Molecules with higher lipophilicity (clogP > 3) generally have higher activity but this also results in reduced selectivity and thus increased off-target interactions.^{48,49} Therefore in the design of drug-like molecules lipophilicity (clogP) should be kept below five.

* LogP is measured lipophilicity by the n-octanol/water partition system, and is reported on a logarithmic scale,⁹⁷ whereas cLogP is the calculated lipophilicity of a molecule.

Physiochemical property	Drug-like compounds ⁴⁶	Lead-like compounds ³⁹	Fragment-like compounds ⁵⁰
Molecular weight	≤500	≤350	140 – 230
Heavy atom count	≤38	14 – 26	10 – 16
clogP	≤5	≥ -1 – ≤3	≥0 – ≤2
H-bond donors	≤5	≤5 ^a	≤3
H-bond acceptors	≤10	≤10 ^a	≤3
Shape	-	Higher Fsp ³ 1 – 3 Aromatic rings	Number of rotatable bonds 0 – 3 Chiral centres ≤1
Substructure	-	Avoid chemically reactive, electrophilic and redox active groups	Remove highly reactive functional groups.

Table 1: the physiochemical property parameters for drug, lead and fragment like molecules ^anot covered in the first GSK guidelines so taken from ⁵¹

1.2.2 Characteristics of lead-like molecules

To consistently synthesise drug-candidates that fall within drug-like chemical space (defined by Lipinski's Ro5 or similar) chemists must be able to prepare high quality lead compounds. Lead-like molecules have different molecular properties to that of drug-like properties (Figure 5).³⁹ Comparison of 62 leads and 75 drugs highlights the key differences between the compound classes. On average lead molecules are lower in molecular weight (by ca. 70 Da) and lipophilicity (by ca. 0.43).⁵² Lead structures also exhibit less molecular complexity, fewer rotatable bonds, and a lower number of hydrogen-bond donors and acceptors. Therefore, chemists must prepare leads which have suitable molecular properties to allow for the tendency for increases in these properties throughout the discovery process.^{25,39,51,53–55}

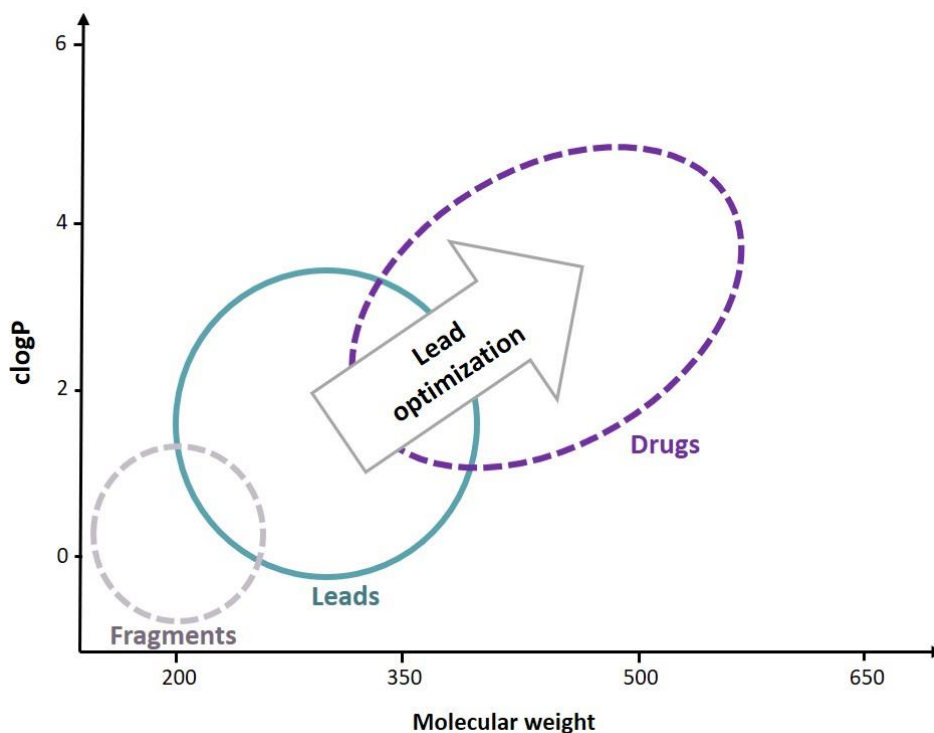


Figure 5: A graph highlighting the relationship between fragment, lead and drug like chemical space. Adapted from ³⁹

The search for smaller, less complex molecules as starting points for leads has additional benefits, as these molecules sample chemical space more effectively. The number of possible compounds decreases significantly with the number of heavy atoms.^{56,57} These smaller compounds lead to a higher number of hits with a larger number of targets (with potentially lower potency).^{24,39,58} Therefore, screening libraries containing compounds with a lower molecular weight can sample a greater proportion of chemical space. HTS libraries used in the identification of lead compounds should reflect this and be of low average molecular weight and complexity. Ideally a HTS library compound will also contain a synthetic handle which is useful for optimisation and analogue synthesis, making them a practical starting point for lead compounds.⁵¹

A stricter set of physicochemical property guidelines were developed for the purpose of lead-oriented synthesis by GSK to define their interpretation of lead-like chemical space. These stricter guidelines should allow greater flexibility for optimisation in the drug discovery process. In addition to the tighter clogP and molecular weight constraints (Table 1), the lead-like

guidelines also include restrictions on the number of aromatic rings and suggest filters to remove undesirable functionality from the molecules that could result in unwanted promiscuity (for example chemically reactive, electrophilic or redox active groups).³⁹ Although there are specific applications where for example electrophilic compounds are required, in general, they are undesirable in lead compounds.

Molecular shape is now understood to be an important feature of a molecule, and this is a key difference between lead-like and drug-like parameters (Table 1). Molecular shape is captured in terms of the fraction of sp^3 carbons (F_{sp^3}) where $F_{sp^3} = (\text{number of } sp^3 \text{ hybridized carbons} / \text{total carbon count})$.^{59,60} A higher F_{sp^3} and an increased number of chiral centres (and thus the number of possible isomers of the compound) could improve the interactions with the target potentially enhancing potency, and thus have a higher rate of success throughout the drug discovery process.^{61–63} An increased F_{sp^3} has been found to have a higher rate of success throughout the drug discovery process, due to improved properties such as solubility.^{61,62}

This is in good agreement with the observation that compounds which are found in patent applications, which move on to be drug candidates and subsequently launched drugs have an increase in the mean F_{sp^3} (0.34, 0.37 and 0.42 respectively).⁶⁴ The mean number of aromatic rings is also seen to decrease (2.9, 2.6 and 2.1 respectively).⁶⁴ Candidates with a higher number of aromatic rings correlates with poorer developability and consequently has an increased level of attrition.⁶⁵ The hybridisation (F_{sp^3}) of the molecules also influences the compounds physiochemical properties. Fully saturated molecules have a higher aqueous solubility and lower lipophilicity both of which are desirable properties in drug candidates, and could improve their success throughout clinical trials.^{59,60,63,66}

1.2.2.1 HTS in lead generation

High-throughput screening (HTS) is the second most common method for hit identification in the pharmaceutical industry¹¹ and has been widely reported in its use for the past two decades.^{8,13,67} It is challenging to develop a large screening library which possess desirable molecular properties with a

high level of diversity.²⁵ There have been a few noteworthy initiatives aimed at creating such libraries, for example the release of the AstraZeneca and Bayer screening collections⁶⁸ as well as the European Lead Factory, which generated new diverse screening compounds in an academic and industrial collaboration.^{69,70} Many primary assays are now available meaning compounds can be efficiently screened against a wide number of targets.^{11,71,72}

One example of the successful application of a HTS campaign is the identification of an initial lead which led to approval of Maraviroc **3** (Figure 6).⁷³ Maraviroc is an antiviral drug which displays selective and potent antagonism against anti-human immunodeficiency virus type 1 (HIV-1). The initial hit identified in the HTS screen (*ca.* 500,000 compounds) was an imidazopyridine compound **1** which was a weakly binding CCR5 ligand but had limited cellular antiviral activity. An extensive SAR programme was undertaken with over 4000 compounds synthesised to overcome affinity for hERG ion channels which is involved in the electrical activity of the heart. The key SAR evolution was the introduction of polar substituents into regions of the molecule which were believed to be involved with hydrophobic interactions with the hERG ion channel.^{74–76} This extensive effort achieved a potent chemokine receptor antagonist, which prevents the HIV virus entering the host cell.^{71,73}

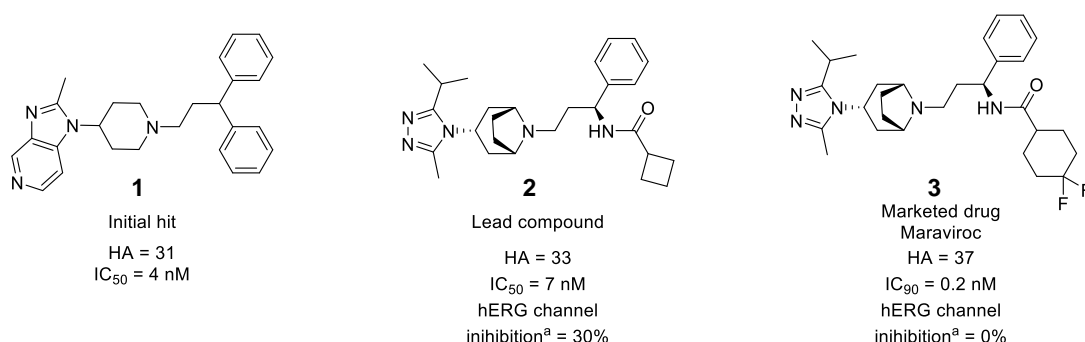


Figure 6: The marketed drug Maraviroc **3** and its initial hit and developed lead compound. ^a measured at 300nM

1.2.3 Characteristics of fragment-like molecules

Recently fragment-based discovery in which small fragments are developed into leads and subsequently drugs has become popular. Guidelines have been developed to aid in the design of these fragment-like

molecules. The guidelines for fragment-like chemical space were developed by Murray and Rees of Astex Pharmaceuticals (Table 1).⁵⁰ A fragment is characterised by having a molecular weight (<250 Da), and is typically aromatic, less complex, soluble and chemically stable. The lower molecular weight allows for a more effective sampling of chemical space.^{58,77} Again, control of lipophilicity is key, as there is a clear trend towards greater promiscuity, as the lipophilicity of a fragment increases, which will increase the chance of unhelpful off target effects.⁵⁸

Molecular shape is also a consideration in fragments as solubility is a key physiochemical property to allow screening at high concentrations, with solubility increasing with increased F_{sp} .⁵⁹ The suggested number of chiral centres by Murray and Rees is one (Table 1), which can impart some molecular shape whilst limiting molecular complexity. A variety of 3-dimensional shapes should be captured in each scaffold and pharmacophore allowing shape diversity across the library of fragments.⁵⁰

It is widely accepted that screening smaller molecules allows for a more efficient sampling of chemical space. This is because the number of possible fragment-like molecules with 17 heavy atoms or less is around 10^{11} ,^{57,78} however increasing the number of heavy atoms to 30, which can be considered lead-like, increases the number of possible molecules to 10^{63} .^{57,79} Consequently, fragment libraries are typically much smaller (*ca.* 10^3) than high throughput screening (HTS) libraries (*ca.* 10^6),^{80,81} and this efficient sampling of fragment-like chemical space often results in higher hit rates.⁸²

FBDD allows for the identification of compounds which bind efficiently to a biological target. The smaller size of the compounds often results in lower potency, despite this, the interactions formed are often higher quality.⁸³ The quality of such interactions are judged by the binding energy per atom, known as ligand efficiency, which is a useful metric when comparing molecules of different sizes.^{84,85} As such a principal requirement of FBDD is that the process requires very sensitive biophysical detection techniques. These techniques include X-ray crystallography, surface plasma resonance (SPR) and NMR screening techniques.^{86,87} Surface plasma resonance is one of the

primary methods employed due to its low protein consumption and label free methodology.⁸⁸

Fragment based drug discovery (FBDD) is a widely used approach to lead generation. A number of approaches have been implemented to develop these fragment hits. The identified fragment binders can then be grown,^{89,90} linked⁹¹ or merged^{92,93} through an iterative process of design, synthesis and testing cycles to obtain potent lead compounds.

1.2.3.1 The use of fragment-based drug discovery in the discovery of bioactive molecules

Two separate inhibitors from a library of *ca.* 1600 fragments were discovered using NMR (water-LOGSY) to identify the hits against Hsp90.⁹⁴ Hsp90 is a commonly investigated target as it is a chaperone protein that enables other proteins to fold, stabilises them against heat stress and aids in protein degradation. It is also known to stabilize several proteins involved in tumour growth.⁹⁵

A total of 125 fragments was taken forward into crystallography studies, resulting in 26 co-crystal structures. In the first series, compound **4** was identified as a weak hit (Figure 7), virtual screening led to the identification of compound **5** whereby the additional chlorine atom led to a *ca* 100-fold improvement in affinity. A bi-aryl twist (i.e. the bond connecting the two aromatic rings) was observed in the crystal structure of **6**, substituting the pyridine for a phenyl resulted in another *ca.* 20-fold increase in affinity, further optimisation, including addition of a solubilising group gave compound **7**, which has low nanomolar (nM) binding affinity.⁹⁴

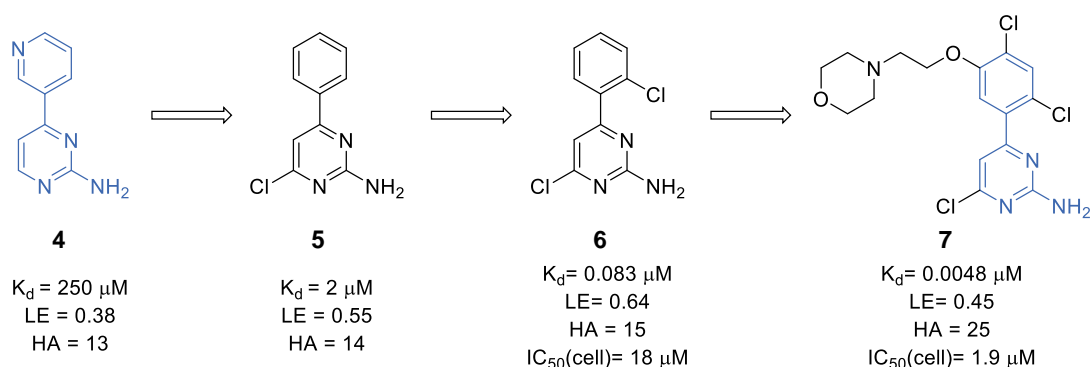


Figure 7: the development of fragment 7 which targets Hsp90.⁹⁴

1.3 The exploration of chemical space

As previously mentioned the pharmaceutical industry is facing a war of attrition, whereby more funds are being invested without a large increase in productivity.^{2,38,96,97} So far exploration of chemical space has been asymmetrical and disordered.^{98,99} Chemical space is vast and although estimates of the number of possible molecules vary widely⁹⁹⁻¹⁰³ it is believed that there are as many as 10^{33} possible drug-like molecules based on exploration of GDB17 (which is a general database comprising of all possible enumerated compounds with up to 17 heavy atoms). Chemical space is shown to increase rapidly with molecular size; there are 26 million possible compounds which contain up to 11 heavy atoms (C, N, O, F), 977 million compounds with up to 13 heavy atoms (C, N, O, S, Cl) and 166 billion compounds containing up to 17 heavy atoms (C, N, O, S, Hal).¹⁰⁴

1.3.1 Scaffold diversity and the poor exploration of chemical space

In 2008 Lipkus highlighted the poor scaffold diversity in the chemical abstracts service (CAS) registry and observed a 'top-heavy' distribution of frameworks, meaning a small number of frameworks are present in a large number of compounds.¹⁰⁵ A framework is defined as the ring system that remains when all functionality has been removed from the molecule, except the ring heteroatoms and the atoms that connect the rings (Panel A, Figure 8).^{105,106} In the last decade attempts have been made towards a more systematic exploration of chemical space, which has been reflected in the

frameworks synthesised. The CAS registry now contains more than 30 million cyclic compounds which can be classified by 4.2 million frameworks. Before 2009 31.7% of registry compounds were based on just 250 frameworks, whereas over the past decade (2009-2018) that number has fallen to 23.8%. This improvement highlights the efforts made by chemists to explore uncharted areas of chemical space. This updated analysis shows the synthesis of new, structurally novel frameworks by chemists, but the reuse of frameworks which have a high level of structural similarity is still common. It is important for chemists to keep targeting this uneven distribution of frameworks to increase diversity within the compounds synthesised.¹⁰⁶

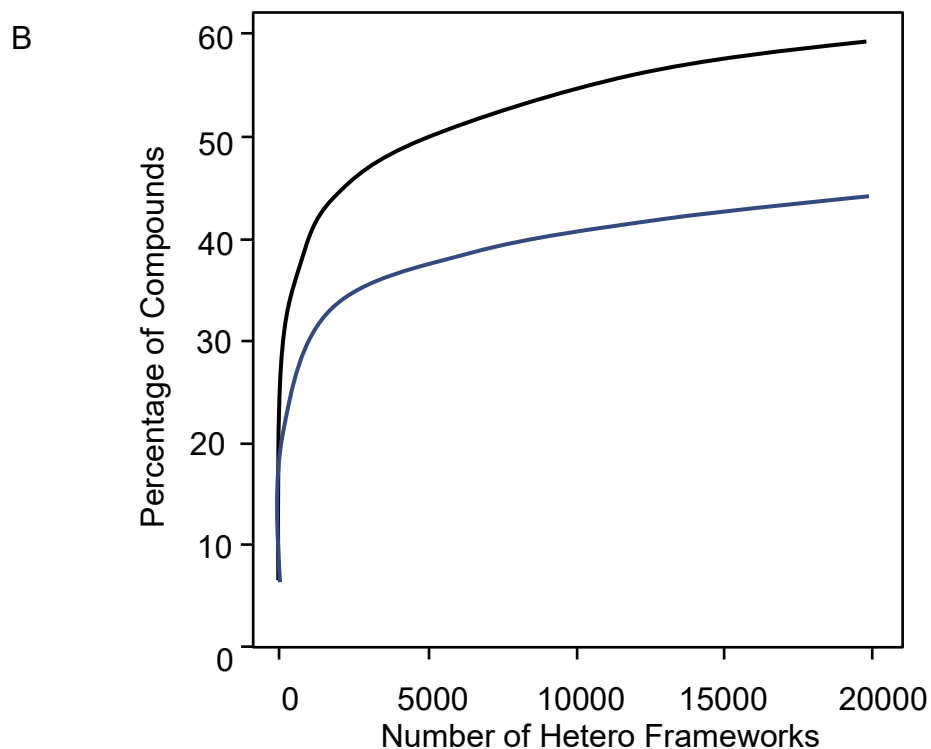
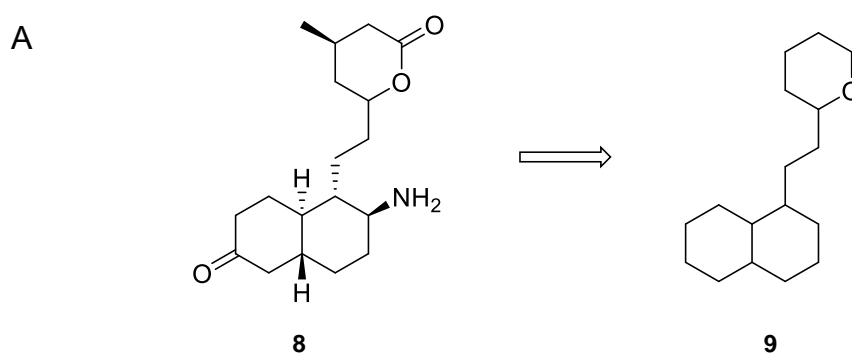


Figure 8: Poor scaffold diversity in the CAS database. Panel A, illustration of the relationship between compound **8** and the graph-node framework that remains when all functionality is removed **9**. Panel B: the number of scaffolds in the 30 million cyclic compounds in the CAS registry in 2008 (black line) and in 2009-2018 (blue line). Adapted from¹⁰⁶

This same overreliance on well represented frameworks can also be seen in medicinally relevant chemical space. The scaffold diversity of seven representative commercial and proprietary compound collections were assessed using framework and scaffold tree analysis, which groups compounds based on their related structural frameworks. These compound collections contain a small number of highly populated frameworks with a high number of singleton scaffolds. This high concentration of certain frameworks may reduce efficiency in screening as collections of structurally similar compounds are repeatedly screened. These results further highlight the need for enrichment of medicinally relevant compound libraries.¹⁰⁷

1.3.2 The medicinal chemists' toolkit of reactions

The limited scaffold diversity observed in the CAS database is largely attributed to an overreliance on a remarkably narrow toolkit of robust chemical reactions used by medicinal chemists.¹⁰⁸⁻¹¹⁰ An analysis of 7315 reactions from 430 papers published by major pharmaceutical companies was undertaken.¹¹¹ Nine common classes of reaction were identified which accounted for *ca.* 63% of all reactions undertaken (Table 2). Upon closer inspection three classes of reaction are deprotections and the other six generate flat, sp^2 rich compounds, such as amide formations, Suzuki-Miyaura and S_NAr reactions.

Reaction type	Number of reported reactions	Percentage of reported reactions (%)
Amide formation	1165	16.0
<i>N</i> -alkylation	776	10.6
<i>N</i> heterocycle formation	537	7.4
<i>N</i> -arylation	458	6.3
Carboxylic acid deprotection	395	5.4
<i>N</i> -Boc deprotection	357	4.9
Suzuki reaction	338	4.6
<i>O</i> -substitution	319	4.4
NH deprotections	212	2.9
Total	4557	62.4

Table 2: nine commonly used reaction classes used by medicinal chemists.¹¹¹

Walters of Vertex pharmaceuticals¹¹² analysed more than 400,000 molecules which were reported in the *Journal of Medicinal Chemistry* over the past 50 years and it highlights how dramatically molecular properties have changed. Generally they are flatter, more aromatic and therefore have a lower fraction of sp^3 carbons.¹¹² The over-reliance of chemistries that leads to flat, sp^2 rich compounds feeds back into the poor exploration of drug-like chemical space and decreases diversity among compounds synthesised, but it also limits the exploration of three-dimensional chemical space. There also appears to be a slow uptake of new and emerging chemistries into drug development programmes which also results in low diversity.^{113,114} This is exemplified when a random 1% of the ZINC database (90911 compounds) is assessed based on their three-dimensionality (Figure 9).¹¹⁵ A PMI (principal moment of inertia) plot is a commonly used method to depict three-dimensionality, with the three extremes of molecular geometry represented on each axis. The compounds are represented as green dots and can clearly be seen to lie heavily along the rod-disk like axis with very few compounds moving away from this trend. Clearly there has also been a very poor exploration of three-dimensional chemical space and attempts should be made to improve this.

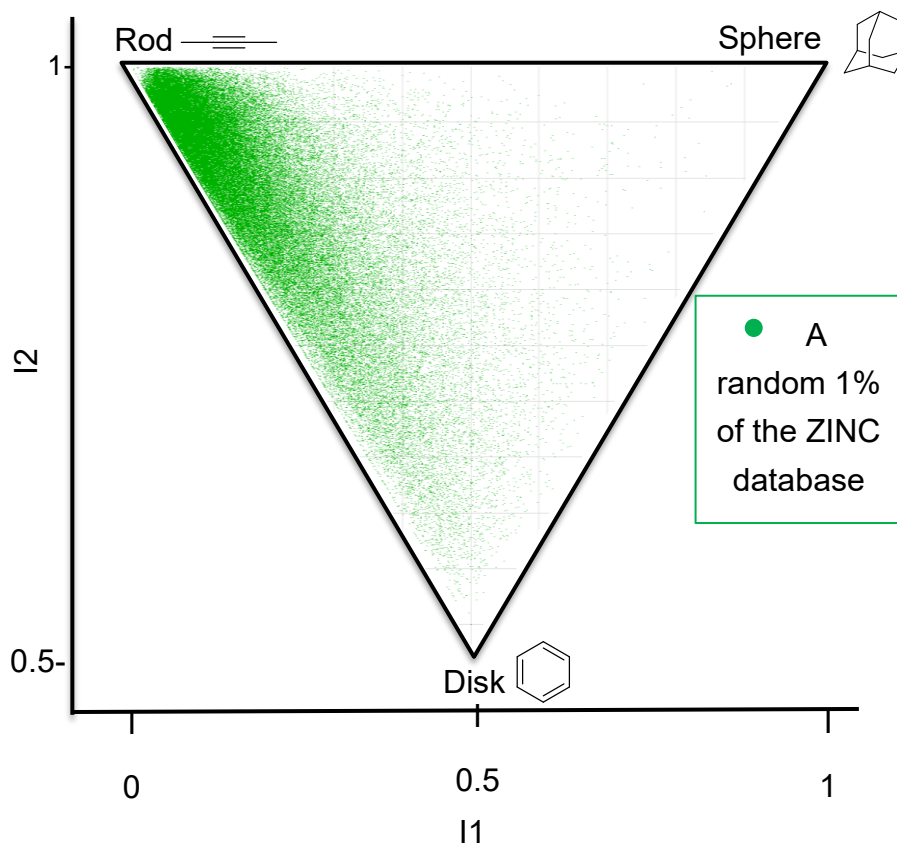


Figure 9: a PMI plot of 90911 virtual compounds from a random 1% of the ZINC database.¹¹⁵

1.4 Approaches to small-molecule library synthesis

To address the challenge of chemical space exploration, two approaches - termed diversity-oriented synthesis (DOS) and lead-oriented synthesis (LOS) - were developed to enable access to new chemical matter.^{39,116} More structurally diverse compounds are believed to increase the odds of addressing a broad range of biological targets.

1.4.1 Diversity-oriented synthesis (DOS)

For two decades, DOS has provided a practical approach towards the synthesis of diverse small molecule libraries^{20,22,117-122} and has been described as 'the deliberate, simultaneous and efficient synthesis of more than one target compound in a diversity-driven approach'.¹²³ This approach focuses on generating a high level of skeletal diversity within the library to achieve a higher degree of chemical space sampling.¹²⁴ This differs from

traditional target-oriented approach, where linear sequences lead to a single specific molecule which occupies a specific area of chemical space.¹²⁵ It differs from LOS as the DOS approach gives no consideration to the molecular properties of the products, whereas LOS, the molecules are specifically designed with molecular properties in mind.

To sample chemical space effectively a high degree of diversity is required and the literature identifies three types of diversity that should be incorporated into a successful DOS strategy.¹²⁶ These include skeletal diversity (differing molecular frameworks resulting from variation of ring size or structure), substitutional/appendage diversity (variation in the core building block and substituents/functionality around the scaffold) and stereochemical diversity (variation in the spatial arrangement of different functionality around the framework).¹²⁶

1.4.1.1 Diversity-oriented synthesis: A case study

There have been many reported applications of the DOS strategy^{118,119,121,127–129} broadly these fall in to two approaches; the folding pathway¹³⁰ in which multiple substrates are converted into multiple products under common conditions and branching pathway^{131–133} where a single starting material is converted into multiple products using a range of reaction conditions. The branching pathway is commonly achieved using the build, couple, pair (B/C/P) approach^{120,127}, where building blocks are synthesised, coupled together, then cyclised in a number of ways to generate a range of scaffolds.^{118,127}

In 2018 Spring published a reagent-based DOS approach using a branching pathway to generate a library of 40 diverse small molecules.¹³⁴ The single starting material used in this approach was an α,α -disubstituted amino ester building block. This flexible starting material contained many distinct functionalities which could be reacted intra- or intermolecularly in several different combinations. This allows generation of a range of ring sizes and frameworks with a select few examples are shown below (Figure 10). The starting material contained an *N*-substituted quaternary carbon which incorporated quaternary centres in the screening library, as well as instilling

three-dimensionality. Moreover, the library also contained modifiable functional groups which would allow for elaboration and fragment growth.¹³⁴

The 40 compounds generated via this approach include desirable functionality including *N*-containing stereocentres, polar functionalities, and *N*-based heterocycles. The molecular properties of the library fall within the rule of three guidelines highlighting the ability of DOS to form ‘fragment-like’ compounds which could then be used in biological screening. Analysis of the library highlights a wide molecular shape distribution, stemming from the sp^3 rich nature of the library.¹³⁴

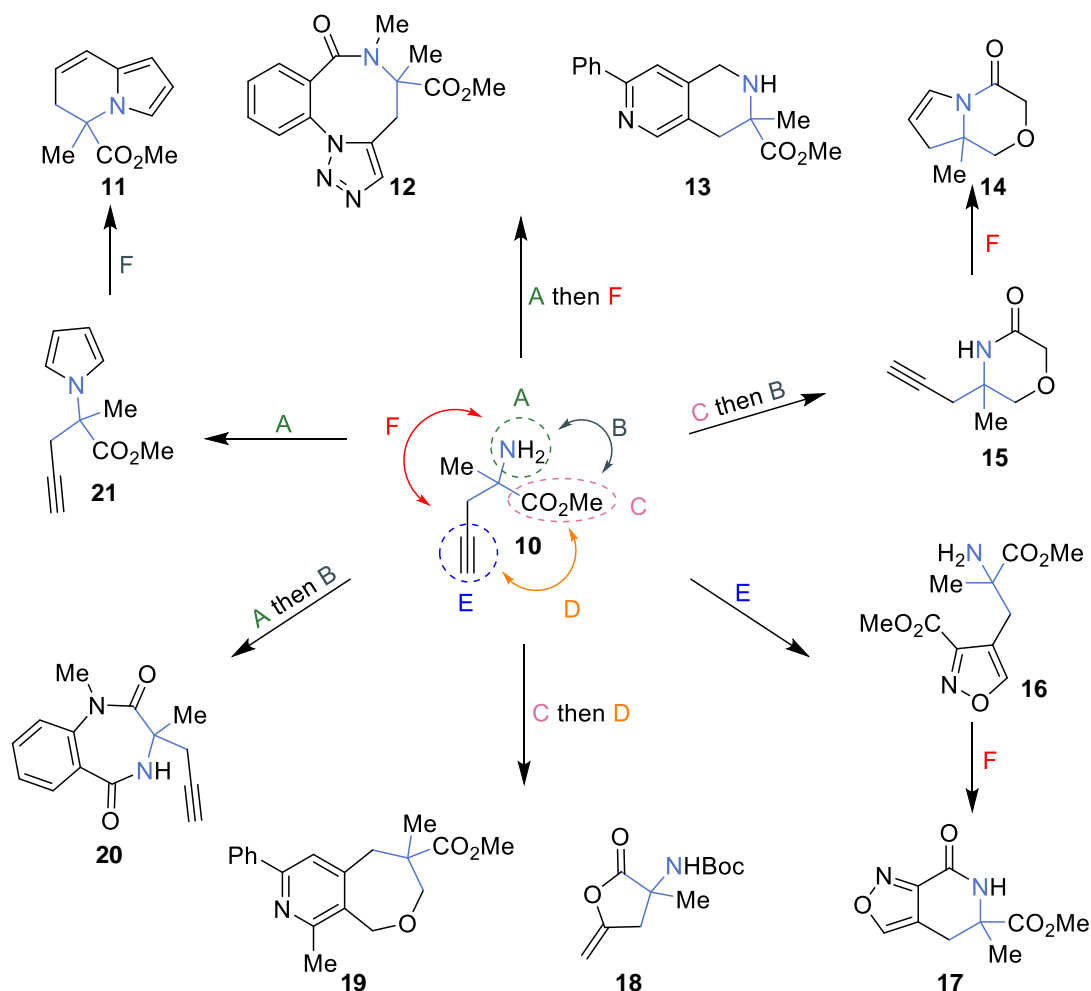


Figure 10: Synthesis of structurally diverse *N*-substituted quaternary carbon from an α, α -disubstituted amino ester. The pairing methods A- amine derivatisation; B pairing of the amine and ester; C ester derivatisations; D reaction of the alkyne and ester moieties; E alkyne functionalisation; F coupling of the amine and alkyne. The bonds in blue highlight the quaternary centre found in the starting material.

1.4.2 Lead-Oriented synthesis (LOS)

Lead-oriented synthesis (LOS) is the strategy employed to prepare compounds with lead-like molecular properties (outlined in Section 1.2.2).³⁹ LOS is a fundamentally similar approach to DOS, whereby diversity and three-dimensionality are encoded into the library; however LOS also places focus on the control of molecular properties.³⁹ This is an attempt to manage the associated problems with the development of lead compounds into drugs, such as increase in logP and molecular weight.^{6,39,135} For the creation of successful hits, the compounds must be able to interact with biological targets.³⁹ The synthesis of lead like compounds should be efficient and tolerant of different functionality.¹³⁵ Two approaches to the LOS strategy have been employed known as the 'bottom-up' and 'top-down' approaches which are described below.

1.4.2.1 The 'bottom up approach' to lead-oriented synthesis case studies

The first example of the 'bottom-up' approach to lead-oriented synthesis has been successfully applied to the synthesis of a library of CNS lead-like compounds. The bottom up approach relies on the facile synthesis of a pair of building blocks which can be coupled to create a cyclisation precursor. Which in turn should contain multiple functionalities which can be paired in multiple combinations to create a range of diverse frameworks (Figure 11). The guidelines used in the LOS approach can be tuned to target different areas of chemical space relevant to different disease types (Figure 12). Drugs which act on the central nervous system must cross the blood brain barrier (BBB). To achieve this the compounds must have finely tuned molecular properties.¹³⁶

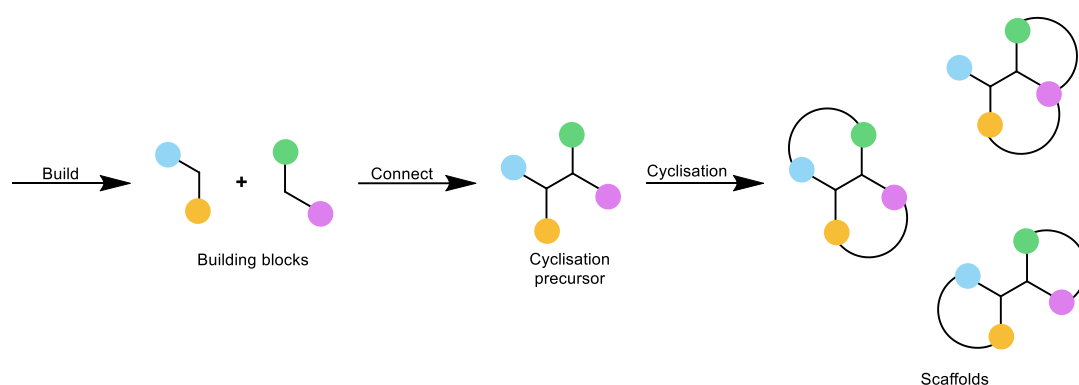


Figure 11: The overview of 'bottom up' approach to lead-oriented synthesis.

CNS lead compounds tend to have lower molecular weight and higher lipophilicity when compared to lead compounds which focus on oral bioavailability (Figure 12).¹³⁶ To assess the suitability of compounds as CNS leads, a multi parameter optimisation (MPO) scoring system was adapted and employed to guide the synthesis of CNS lead-like compounds. This computational tool assesses and scores the compounds on factors such as molecular weight, clogP, clogD_{7.5}, pKa and polar surface area (PSA), using parameters adapted from GSK.^{136,137}

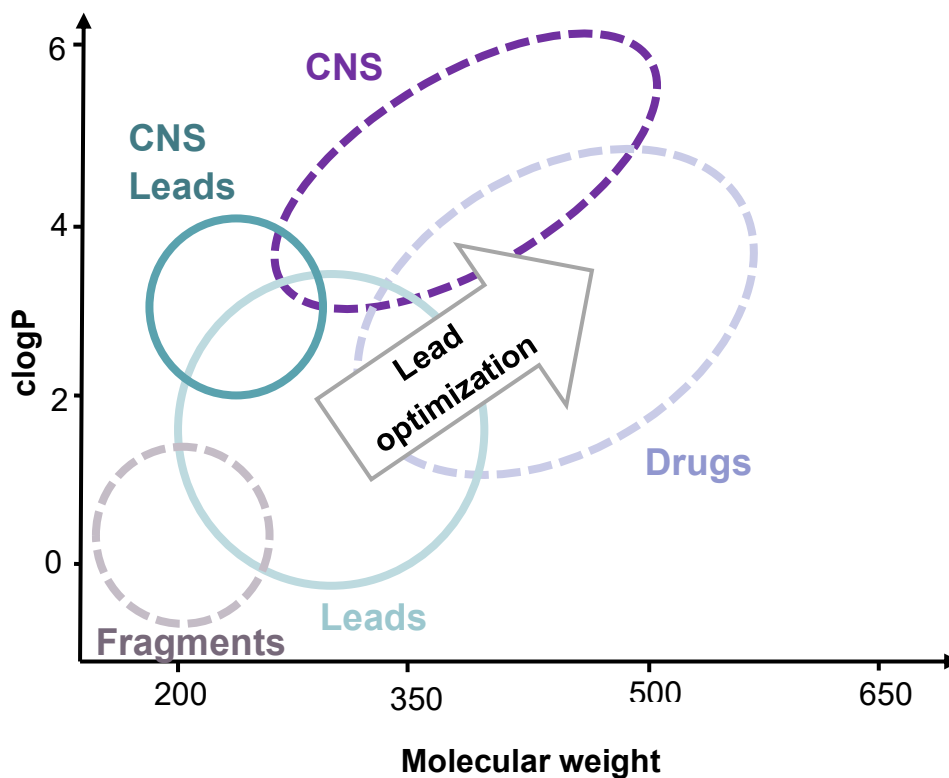


Figure 12: Relationship between typical leads and CNS leads

The starting material selected in this case is a cyclic β -keto ester, which was a flexible starting material allowing variation in the ring size and the heteroatom within the ring. This β -keto ester then underwent an alkylation and Tsuji-Trost reaction to form the cyclisation precursor, which contains four different functionalities. Several different cyclisations were tested which yielded 12 scaffolds. Out of the 12, five were prioritised based on yields and *d.r.s.* These five cyclisations were then applied to five different starting materials with varied ring sizes and heteroatoms (Figure 13).¹³⁶

The resultant scaffolds were assessed for their potential to serve as high quality CNS leads. Potential scaffolds were decorated once or twice with capping groups often found in medicinal chemistry. Desirability scores (ranging from 0.05-1) were determined based on six properties *clogP*; *clogD* at pH 7.4; number of H bond donors; molecular weight; *pKa* and topological polar surface area. The score for each of the properties were combined to give a CNS lead MPO score (0.3-6). Ideally CNS lead-like compounds will have an MPO score of four or above. Most of the scaffolds synthesised achieved this, clearly validating the approach with all the compounds synthesised being suitable for a CNS lead discovery programme.¹³⁶

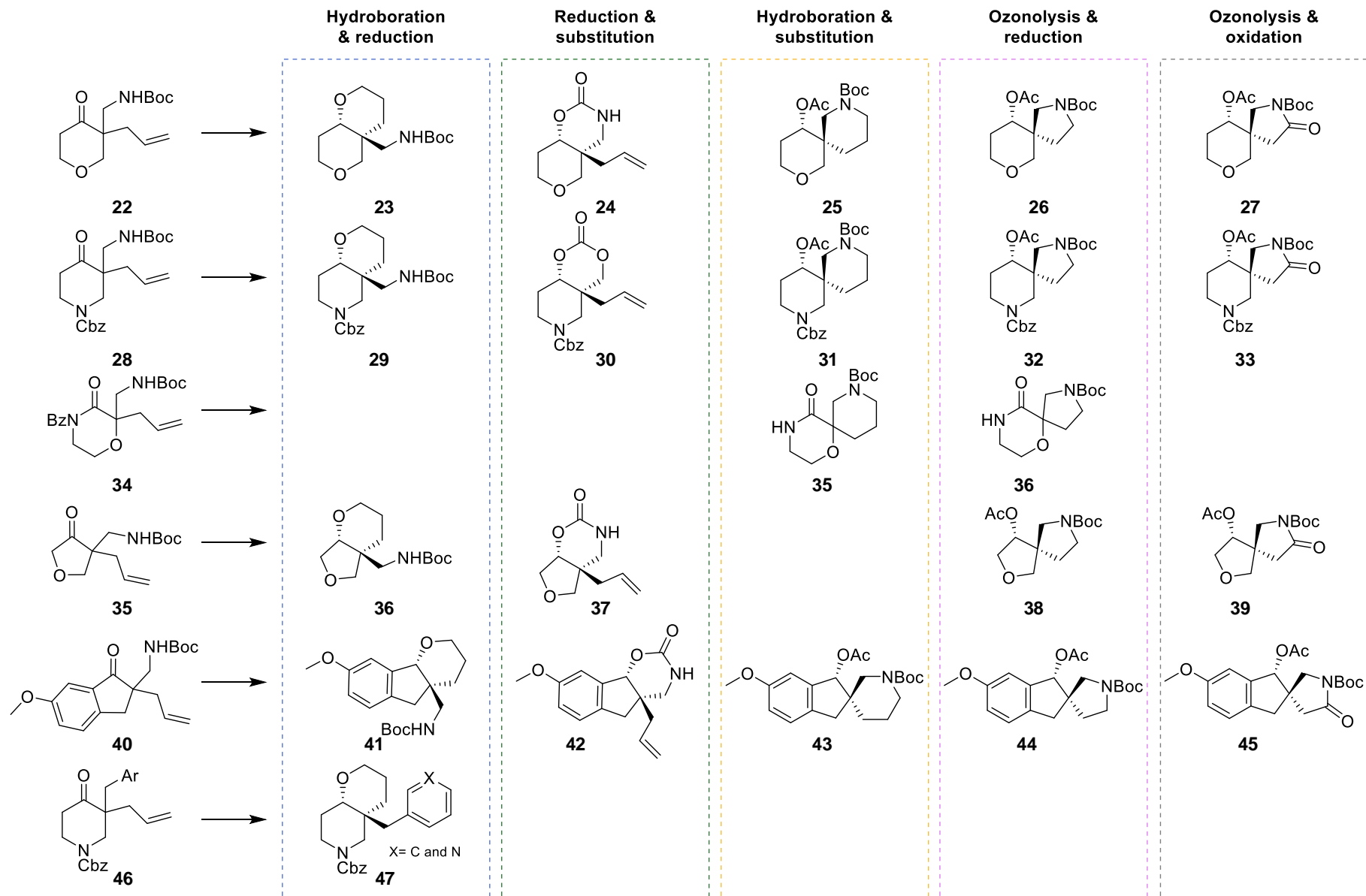


Figure 13: the library of scaffolds synthesised using the five shortlisted cyclisation reactions. Adapted from ¹³⁶

The second example is a similar approach was used in the synthesis of a library of 30 lead-like medium ring frameworks.¹³⁸ Five- and six-membered rings are commonplace in drug and lead-like compounds, however in recent years interest has risen in developing libraries of larger ring compounds. Medium sized rings (8-11) are frequently found in diverse bioactive natural products, although they are present in some marketed drugs (Figure 14) they are vastly underrepresented. This could be due to the challenges associated with their synthesis due to unfavourable transannular interactions.^{138,139}

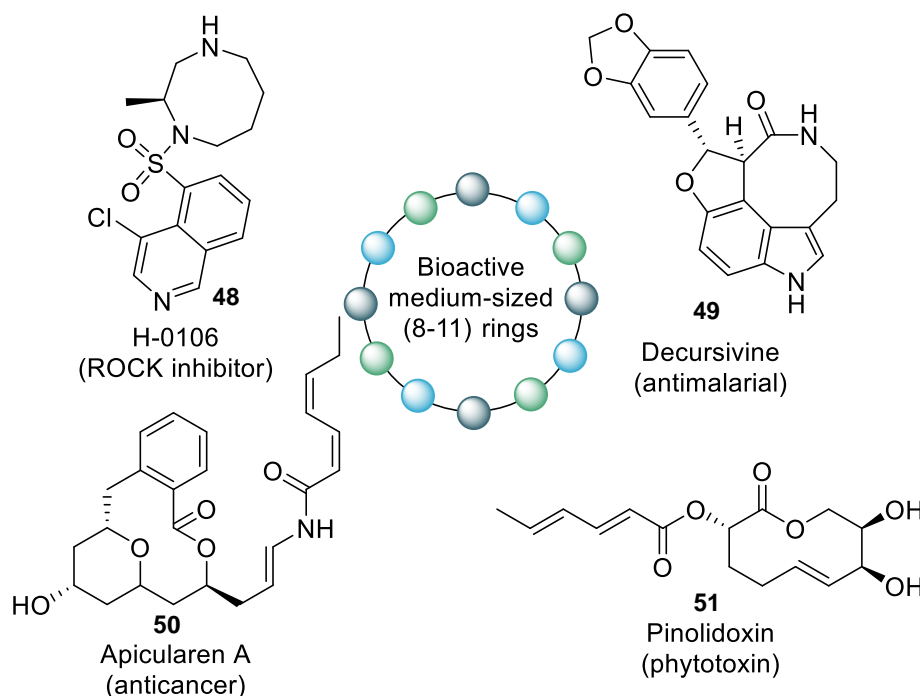


Figure 14: medium sized rings present in marketed drugs. Adapted from ¹³⁹

Forming medium rings *via* ring expansion is an attractive approach as the kinetic challenges associated with direct cyclisation can be avoided.¹³⁹ This approach utilised a successive ring expansion (SuRE) protocol which allows for the insertion of an amino acid three or four atom fragment into the cyclic β -keto ester via an acylation and ring expansion to form medium ring lactones. This process also retains the β -keto ester functionality in the product which is not only a useful functional handle for derivatisation but also makes this approach an iterative one, thereby allowing access to a wide array of ring sizes from medium to macrocycles.^{138,140}

This approach facilitated the synthesis of a library of 30 medium ring products. A range of ring sizes were achieved (8-12) by varying the cyclic β -keto ester. A range of examples are highlighted below (Figure 15), including examples with fused or appended aromatic rings and rings containing heteroatoms.

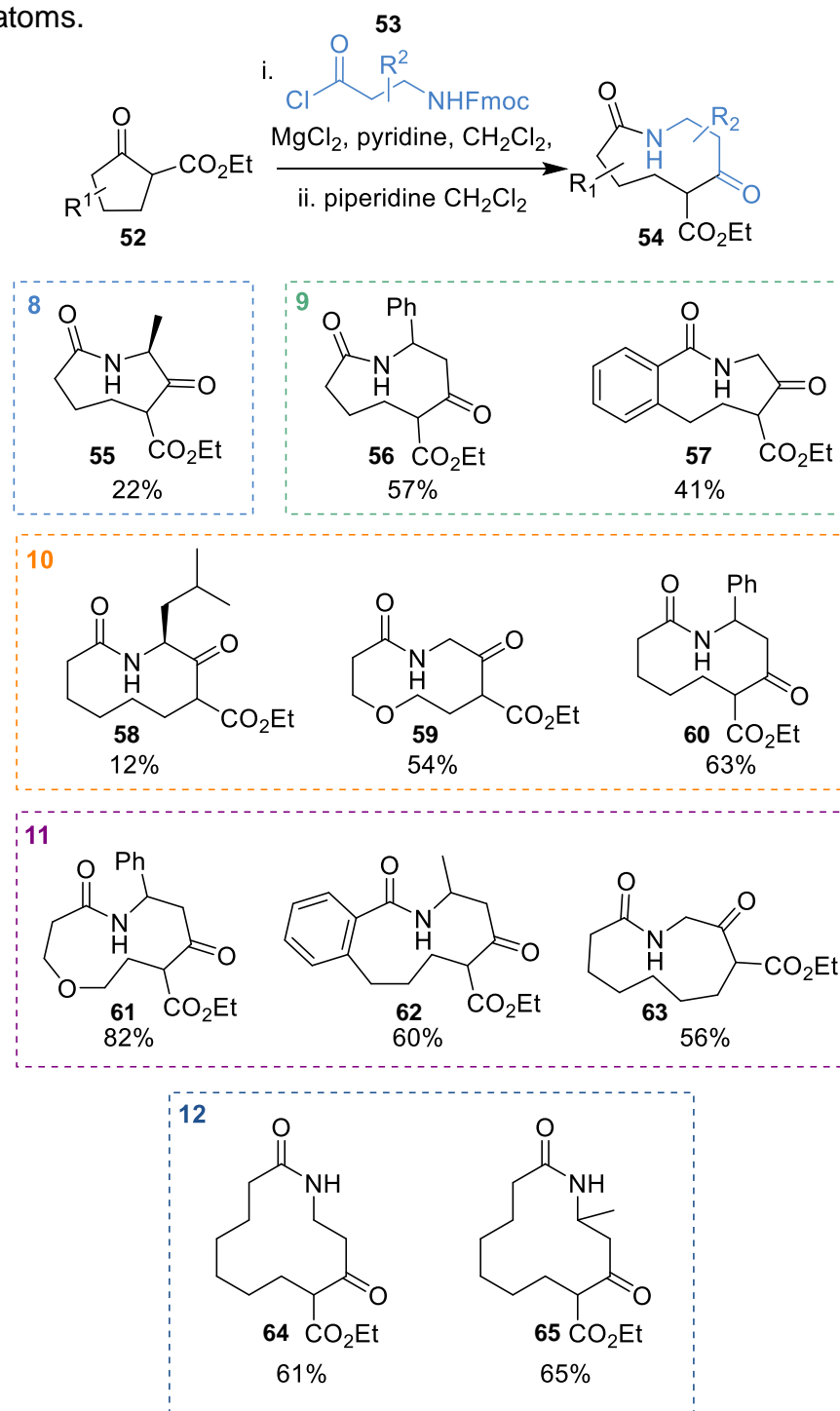


Figure 15: the ring expansion protocol yielding a range of 8-12 membered rings. The compounds are sorted according to their ring size. Adapted from ¹³⁸

The library of 30 medium-sized ring compounds were assessed for their lead-like properties using LLAMA (lead-likeness and molecular analysis) which is a computational tool which assess the lead-likeness of compounds based on specific scaffolds.¹⁴¹ The enumerated virtual library of ca 400 compounds was based on the hydrolysis product of the ethyl ester, with focus on 5 reaction classes for the decorations (reductive aminations, sulfonamide formation, secondary amine alkylation or arylation and amide formation). A high proportion (70%) of the enumerated library had the correct molecular properties to target lead-like chemical space. Furthermore, analysis of the libraries 3-dimensionality using a PMI plot suggest that the virtual library occupies a wide range of chemical space, highlighting the shape diversity found within medium sized ring. This research highlights the value of the ring expansion approach along with its potential to synthesis a library of shape diverse lead-like medium ring scaffolds.

1.4.3 The ‘top-down’ approach to lead-oriented synthesis

The ‘top-down’ synthetic approach to LOS uses the formation of complex cycloadducts, which can then be converted into alternative small molecule scaffolds, through the exploitation of the complexity and functionality within the cycloadducts. This is achieved using three distinct approaches; ring expansion, ring addition and ring cleavage (Figure 16). These small molecule scaffolds should, again, target lead-like chemical space, so attention should be paid to molecular properties such as heavy atom count when forming the cycloadducts.¹⁴²

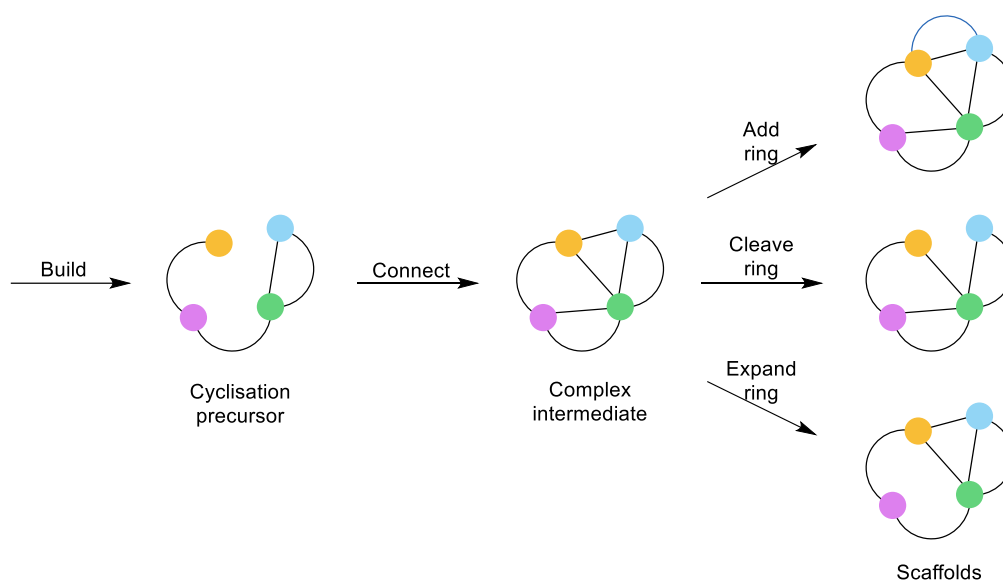


Figure 16: overview of the top down approach to LOS.

Natural products are produced via function driven pathways and occupy biology relevant chemical space.¹⁴² Diversity oriented approaches have been developed utilising natural products as starting materials. Exploiting the complexity found in nature has proved to be an efficient way of generating chemical libraries rich in diversity.^{143–145} Natural products are often highly three-dimensional, as a result, compounds inspired by them often have a high Fsp³. As previously mentioned, this is an attractive feature and can be linked to a candidate's clinical success.^{59,60,63,142}

With this in mind, [5+2] cycloaddition chemistry was selected as this allowed the efficient generation of complexity and therefore three-dimensionality. The [5+2] cycloaddition reaction allowed access to four different frameworks (Panel A, Figure 17), which were exploited in this project. A toolkit of synthetic methodologies was applied to the complex intermediates. The approach of ring addition allowed both the fusion and appendage of a ring. The ring expansion and cleavage reactions appeared to be the most effective in this project. As they resulted in a change to the core frameworks of the molecule, increasing the diversity of the compound collection. Using this approach resulted in 28 unique frameworks (Panel B, Figure 17).¹⁴²

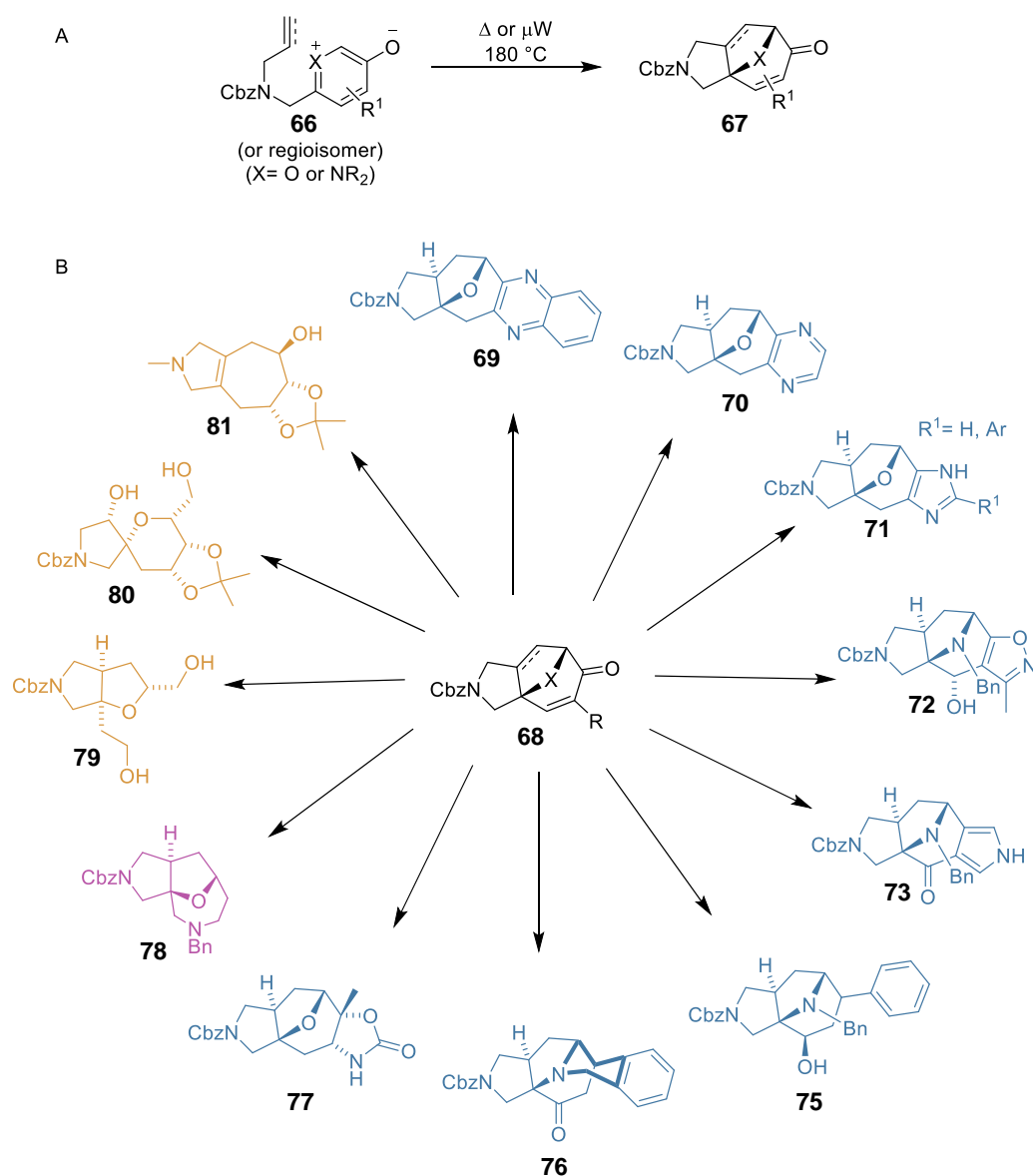


Figure 17: The top-down approach to lead-oriented synthesis. Panel A, the [5+2] cycloaddition utilised in this project. Panel B, a selection of scaffolds synthesised in this project. The colour of the compound indicates how it was synthesised, blue (ring addition), pink (ring expansion) and red (ring cleavage).

From the 23 of the 28 scaffolds, a library of 52 fragments (with less than 19 heavy atoms in size and $-1.5 < \text{clogP} > 3$) was prepared to demonstrate the biological relevance of the compounds. The set were designed to probe fragment-like chemical space to facilitate a more efficient sampling of chemical space. This approach resulted in a compound set which was more three-dimensional and natural product like than a commercial fragment set.¹⁴²

The fragment library was screened against three epigenetics targets from two different mechanistic target classes using high-throughput protein crystallography. The specific target proteins were; ATAD2A and BRD1A bromodomains, and JMJD2DA, a histone demethylase, resulting in 17 novel binders.¹⁴² Furthermore, this included seven hits against ATAD2, a novel oncology target previously deemed to have low 'druggability'.¹⁴⁶ Screening against JMJD2DA also identified two novel binders. This target has several reported binders all of which interact with the enzyme active site. In contrast the two fragments identified from this library were seen to target a peripheral binding site, which have not previously been identified using traditional fragment sets. All the bioactive compounds identified in this screen would serve as distinctive starting points for ligand discovery as their natural product scores are similar to the natural product screening collection which is dramatically different to the score calculated from the commercial screening library. This case demonstrates the biological relevance of creating such libraries.¹⁴²

1.5 Summary

Historically, the exploration of chemical space has been asymmetrical which can be attributed to a limited toolkit of reactions used by medicinal chemistry, which has resulted in overpopulated areas of chemical space, with limited diversity and undesirable molecular properties. Many approaches have been developed to target this uneven exploration and generate new chemical matter. Diversity oriented synthesis has many published examples and generates high levels of diversity within the compound libraries, however there is no consideration to molecular products. Therefore, the lead-oriented synthesis approach was developed to generate diverse chemical libraries whilst controlling molecular properties to make them ideal starting points for a drug discovery program.

1.6 Thesis overview and aims

As previously discussed, there are many different approaches used in the synthesis of bioactive compounds. Diversity oriented synthesis is an efficient tactic in the generation of complexity and diversity and with increased complexity comes an increase in Fsp³. Increased Fsp³ is known to improve physiochemical properties such as solubility and lipophilicity. All approaches to lead generation have their merits, but to synthesise libraries with the best chance of success, control of molecular properties is key. Lead-oriented synthesis (LOS) is a well reported approach in the synthesis of diverse compound libraries whilst maintaining control over molecular properties.

Expansion of the toolkit of reactions used by medicinal chemists will result in newer, under-explored frameworks which will aid in the exploration of chemical space. It was proposed that the identification of a reliable complexity generating reaction that could facilitate the construction of a three-dimensional intermediate would be a good starting point for a LOS project. The complexity of this intermediate could be exploited to generate a range of molecular scaffolds all of which will be intrinsically three-dimensional in nature, due to their parent compound (Figure 18). Utilising a toolkit of reactions not typically used in medicinal chemistry will allow for a modular approach to lead-oriented synthesis. This toolkit or reactions should ideally be applicable to more than one parent framework as an efficient way to achieve scaffold synthesis.

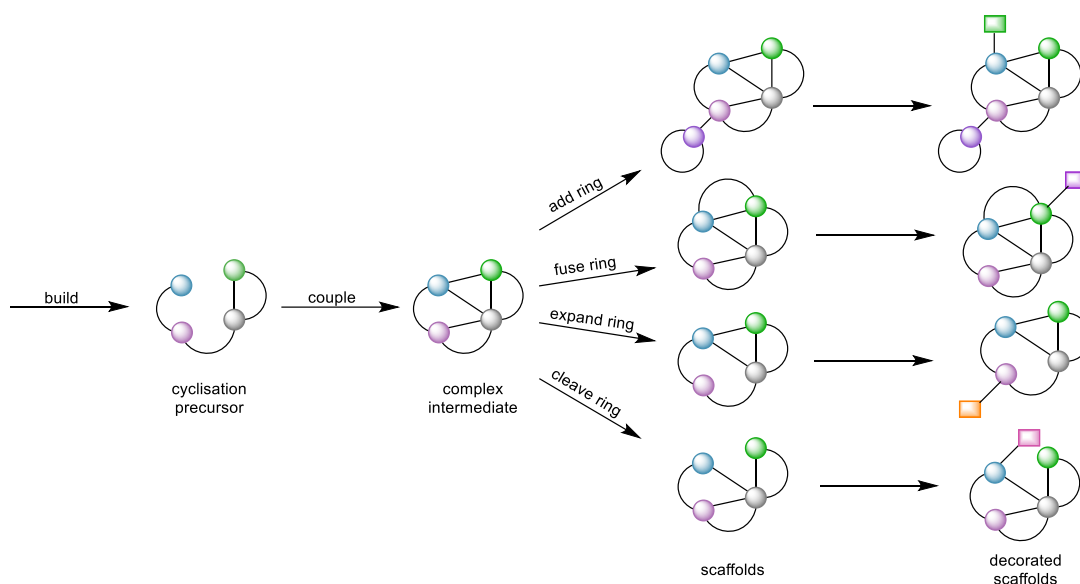


Figure 18: An overview of the 'top-down' approach to LOS.

It was anticipated that decoration of the remaining functionality in the scaffolds with medically-relevant capping groups could form the library of compounds. These groups should aim to sample chemical space as effectively as possible, so should be varied in size and electronics as possible. A series of project objectives was outlined to evaluate the development of a highly three-dimensional library of compounds which should possess the correct molecular properties to target lead-like chemical space.

Objective 1: To select an appropriate complexity generating reaction towards the synthesis of lead-like compounds (Chapter 2).

Objective 2: Establish and harness a toolkit of reactions for the preparation of sp^3 rich, lead-like scaffolds (Chapter 3).

Objective 3: To design, prepare and evaluate the library of decorated lead-like scaffolds (Chapter 4).

1.6.1 Objective 1: To select an appropriate complexity generating reaction towards the synthesis of lead-like compounds.

It was proposed that this project would follow the 'top-down' synthesis approach for the synthesis of a diverse 3-D scaffold library, therefore, generation of complexity was crucial. An appropriate complexity generating reaction must be selected and will form the basis of this project. Therefore, to

ensure the correct choice was made it was proposed that generation of a set of guidelines would inform the selection. It is important for the reaction to construct a highly 3-dimensional parent cycloadduct. Ideally, this will be either a bridged or fused bi- or tricyclic ring system, which forms the first requirement.

Another key criterion for the reaction is practically. This reaction will be used to generate a large amount of the intermediate, so must produce the complex intermediate in a yield higher than 40% (for the cyclisation step). The catalyst loading should be as low as possible and a short synthetic route would also be desirable, ideally fewer than five synthetic steps, so time can be prioritised on scaffold synthesis. Lastly, the reaction must contain suitable functionality to facilitate further reactions. Without this the rest of the project cannot proceed. Ideally this functionality will allow the exploration of multiple vectors. This could allow the compounds to create different or multiple interactions with a biological target.

A shortlist of complexity generating reactions will be compiled following an extensive literature searching (Figure 19). Subsequently, these reactions should be investigated in the lab to ensure reproducibility from the literature. Upon completion of this task the complex intermediates will be analysed to ensure all the criteria are met, any such intermediates will be taken forward into scaffold synthesis.

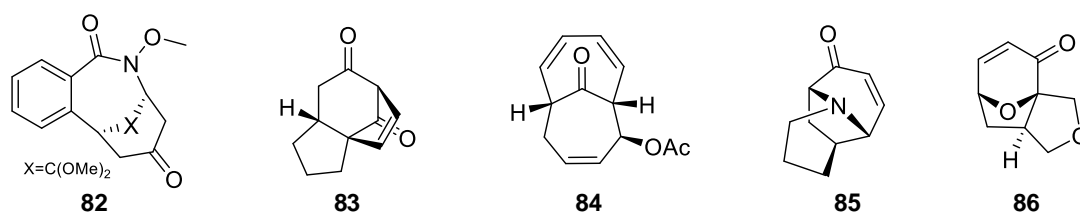


Figure 19: Potential complex intermediates identified from the literature.

1.6.2 Objective 2: Establish and harness a toolkit of reactions for the preparation of sp³ rich, lead-like scaffolds.

With the appropriate complexity generating reaction/s selected the scaffolds can be synthesised. As discussed previously in this chapter, there is still a need to expand the medicinal chemist's toolbox of reactions. It was proposed that utilising different chemistry to that relied on by medicinal

chemists to synthesise scaffolds could explore a wider area of chemical space.

Following the principles of the 'top-down' approach chemistries should be selected to facilitate ring addition, ring fusion, ring cleavage and ring expansion (Figure 20). These chemistries should be modular and applicable to any of the selected scaffolds to facilitate the generation of a toolkit of reactions. It is important to be able to introduce a wide array of ring systems and/or functionality into the scaffolds as this will give different functional handles for decorations.

It is imperative that the molecular properties of all the scaffolds are considered, and to stay within the heavy atom (HA) and lipophilicity guidelines whilst still allowing room for decoration. Ensuring the scaffolds retain their 3-dimensionality will be achieved by following the lead-like guidelines for the number of aromatic rings. Ideally this approach will lead to the synthesis of between 15 – 20 scaffolds formed utilising all the approaches. There should be a high level of diversity and the scaffolds should also have functionality which can be decorated in different ways to achieve object 3.

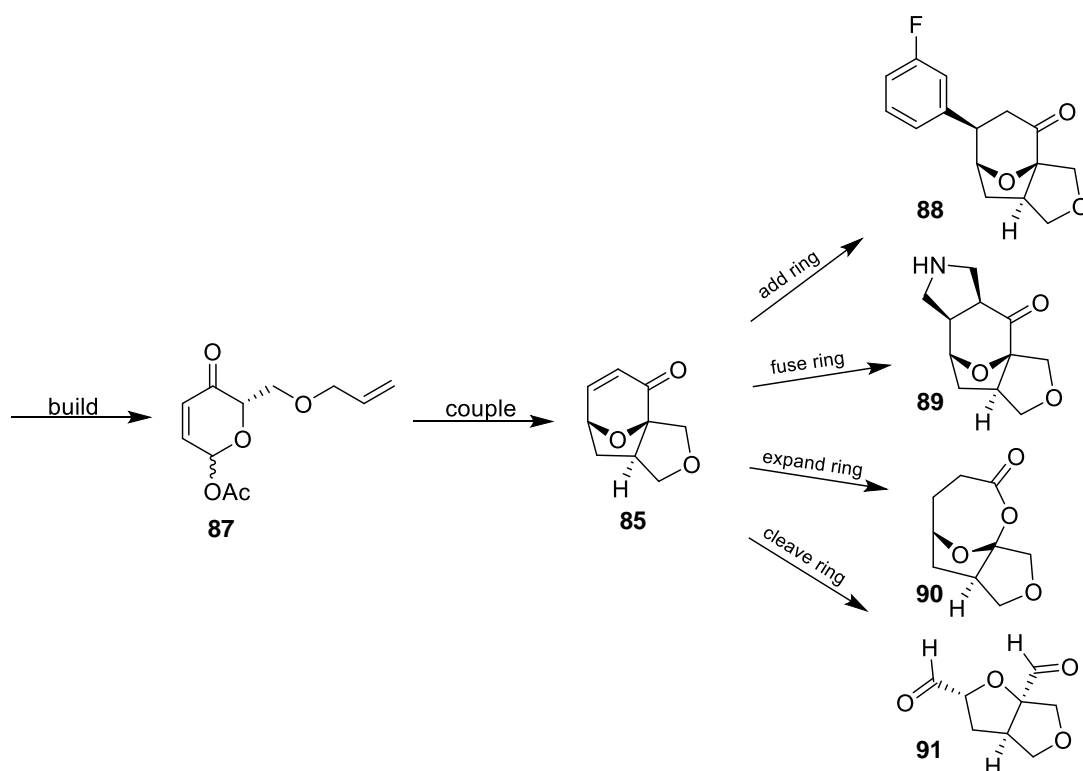


Figure 20: the potential frameworks which could be accessible from complex intermediate **85** via ring addition, fusion, cleavage and expansion chemistry.

1.6.3 Objective 3: To design, prepare and evaluate the library of decorated lead-like scaffolds.

It was anticipated that a single decoration of the synthesised scaffolds with medically relevant capping groups would allow the generation of a library of lead-like scaffolds suitable for screening against biological targets. Each scaffold will be decorated in each of the different functionalities with a range of capping groups, to create a library of *ca.* 50 lead-like compounds (Figure 21). This will allow for exploration of different vectors of the molecule with different functionalities which will hopefully allow the compounds to pick up different interactions against a biological target.

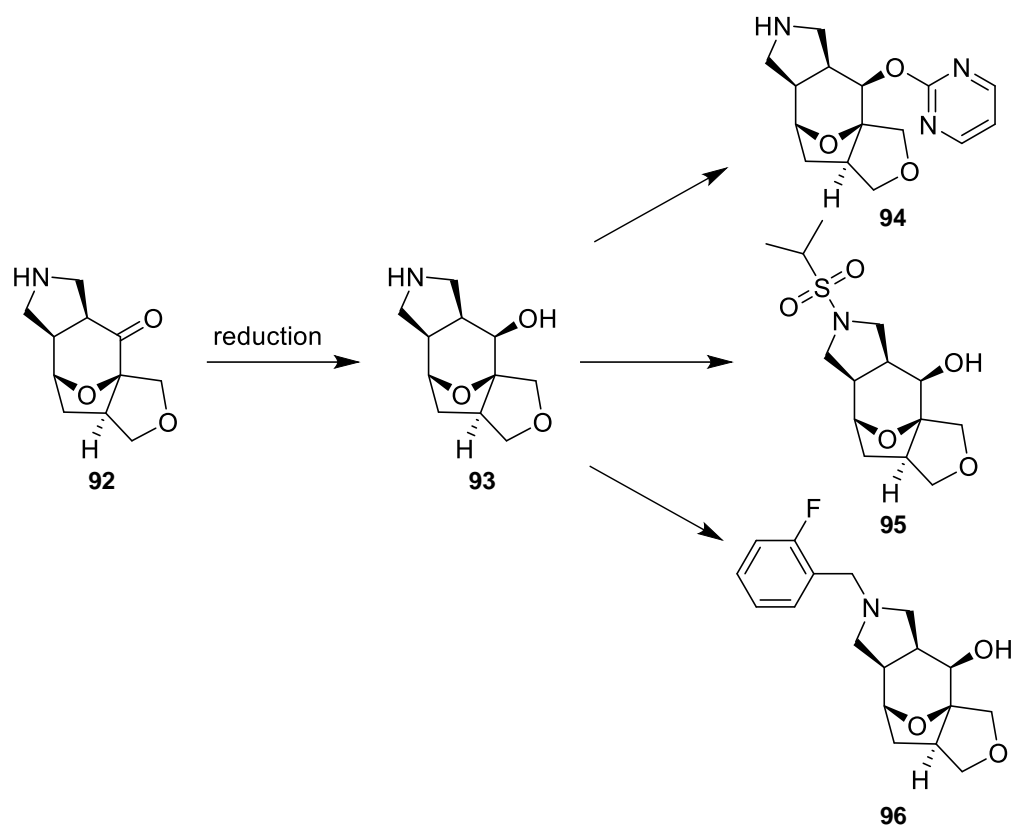


Figure 21: the potential decorations on an exemplar scaffold, generating library compounds.

It was envisioned that the resultant library of decorated compounds will each have their molecular properties analysed using LLAMA. This will allow validation of the approach, analysing what proportion of the final library have the correct properties to target lead-like chemical space. LLAMA will also be used to analyse the 3-dimensionality of the library through the generation of a PMI plot. Finally, diversity of the library should be assessed using scaffold hunter which analyses the parent frameworks found in the library of compounds.

Chapter 2 Synthesis and selection of complex synthetic intermediates

The selection of the appropriate complexity generating reactions is of paramount importance to this project as it forms the basis for all compounds in the final library. As discussed, (Section 1.6.1), there were several key requirements that the complexity generating reaction must meet. These criteria were put in place to ensure the reaction chosen would enable a library of lead-like compounds to be successfully synthesised.

With these requirements in mind, a literature search was undertaken to identify candidates for investigation. The shortlisted reactions detailed in this Chapter met the initial project requirements and gave rise to complex, 3-dimensional polycyclic intermediates in fewer than five synthetic steps and all had reported yields over 40%.

This chapter discusses the synthesis of all cyclisation precursors and complex intermediates in turn, followed by any optimisation undertaken on the reaction. Finally, the complex intermediates were assessed on a number of parameters such as yield, step count and molecular properties to ensure the appropriate choice/s was identified.

2.1 The use of a Rh-catalysed C-H insertion as a complexity generating reaction

The first complex intermediate selected for investigation was based on C-H insertion chemistry.¹⁴⁷ C-H activation has become a powerful tool for synthetic chemists as it allows for disconnections that were not previously possible and its use has been demonstrated in a range of heterocycle syntheses and medium ring systems.^{147,148} This approach, using a masked quinone allowed access to a nine membered fused/bridged ring system (Figure 22), which contain this azepinone structural motif, which is common in many natural products.^{147,149,150} Not only does this compound comprise a complex framework it also contains several/many useful functionalities for scaffold formation and decoration. One notable feature is the acetal, a masked

ketone, on the one carbon bridge as this would remove any selectivity issues and allow for exploration of two separate vectors.

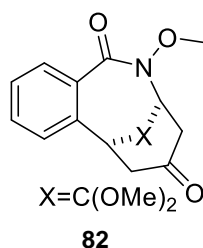
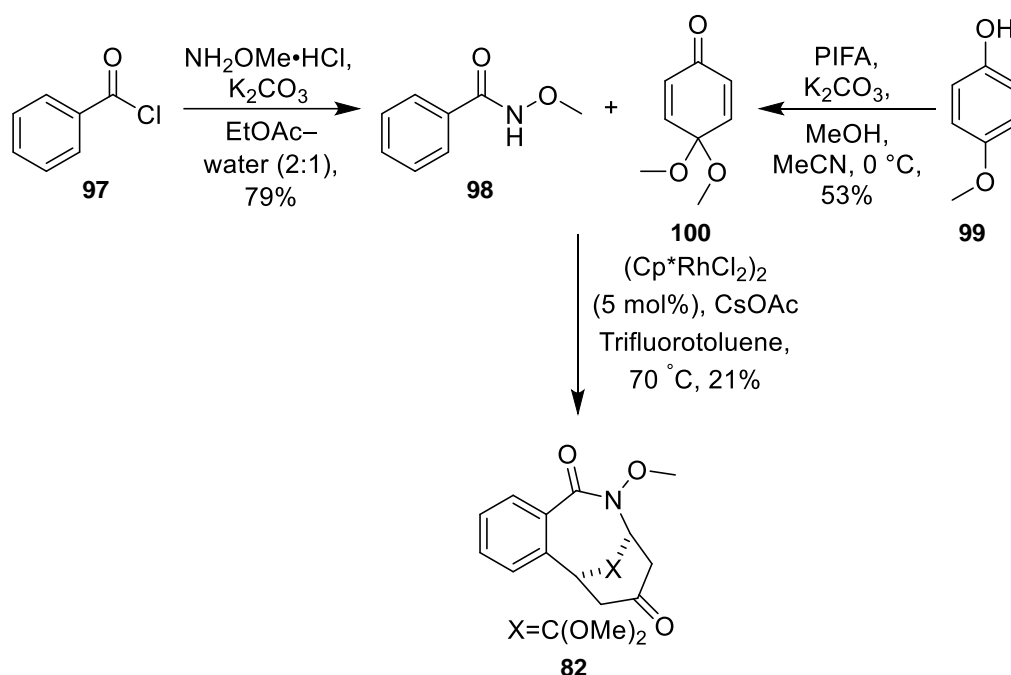


Figure 22: Complex intermediate **82**, synthesised using C-H insertion chemistry.

2.1.1 Synthesis of the precursors and framework *via* a C-H insertion reaction

The first of the two starting materials required for the C-H insertion reaction was the amide **98**, which was synthesised in a single step, whereby benzoyl chloride was reacted with methoxy amine hydrochloride using literature conditions¹⁵¹ with an isolated yield of 79% (Scheme 1). The second starting material was the masked quinone **100**. Again, this compound was synthesised in a single step utilising a literature¹⁵² (Bis(trifluoroacetoxy)iodo)benzene (PIFA) mediated dearomatisation reaction producing the masked quinone **100** in an isolated yield of 53% (Scheme 1).

Reagents **98** and **100** underwent a C-H insertion/Michael addition (Scheme 1),¹⁴⁷ to yield the complex intermediate **82** in a 21% yield. This reaction proceeded open to air and moisture as per the literature conditions, which was an ideal characteristic should the reaction be scaled up for scaffold synthesis. The isolated yield of 21% is well below the reported yield of 91% and did not meet the minimum practical requirements of a 40% yield. This reaction also requires 5 mol% of the Rh catalyst, which is high loading of an expensive catalyst, which also reduces the practicality of this reaction.



Scheme 1: Outline for the synthesis of both cyclisation precursors and the complex intermediate using C-H insertion.

2.1.2 Analysis and assignment of the framework formed using a C-H insertion reaction

The relative configuration of the complex intermediate was determined by Xu et al¹⁴⁷ through the use of X-ray crystallography. Utilising the same reaction conditions, the spectroscopic data of the synthesised product matched that reported in the literature. Interestingly, the 'W' coupling of the bridgehead protons can be observed in the ¹H NMR spectrum (500 MHz) with a coupling constant of 2.60 Hz, confirming their cis relationship (Figure 23).

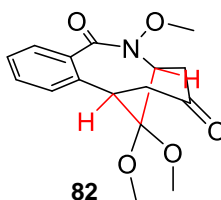


Figure 23: The bridged fused ring system produced through the C-H insertion/Michael addition reaction. The bonds shown in red highlight the 'W' coupling relationship between the two bridgehead protons.

2.1.3 Attempted optimisation of the C-H insertion reaction

The initial yield achieved using the literature conditions was too low to be considered practical for this project; therefore, a range of conditions was

screened to assess if the yield could be increased. In each case, the yield of the reaction was determined using 500 MHz ^1H NMR spectroscopy and one equivalent of an internal standard, limiting the amount of purifications required to ascertain a yield. In this case mandelic acid was selected as an internal standard (Figure 24, Panel A), with the peaks used for comparison highlighted in red.

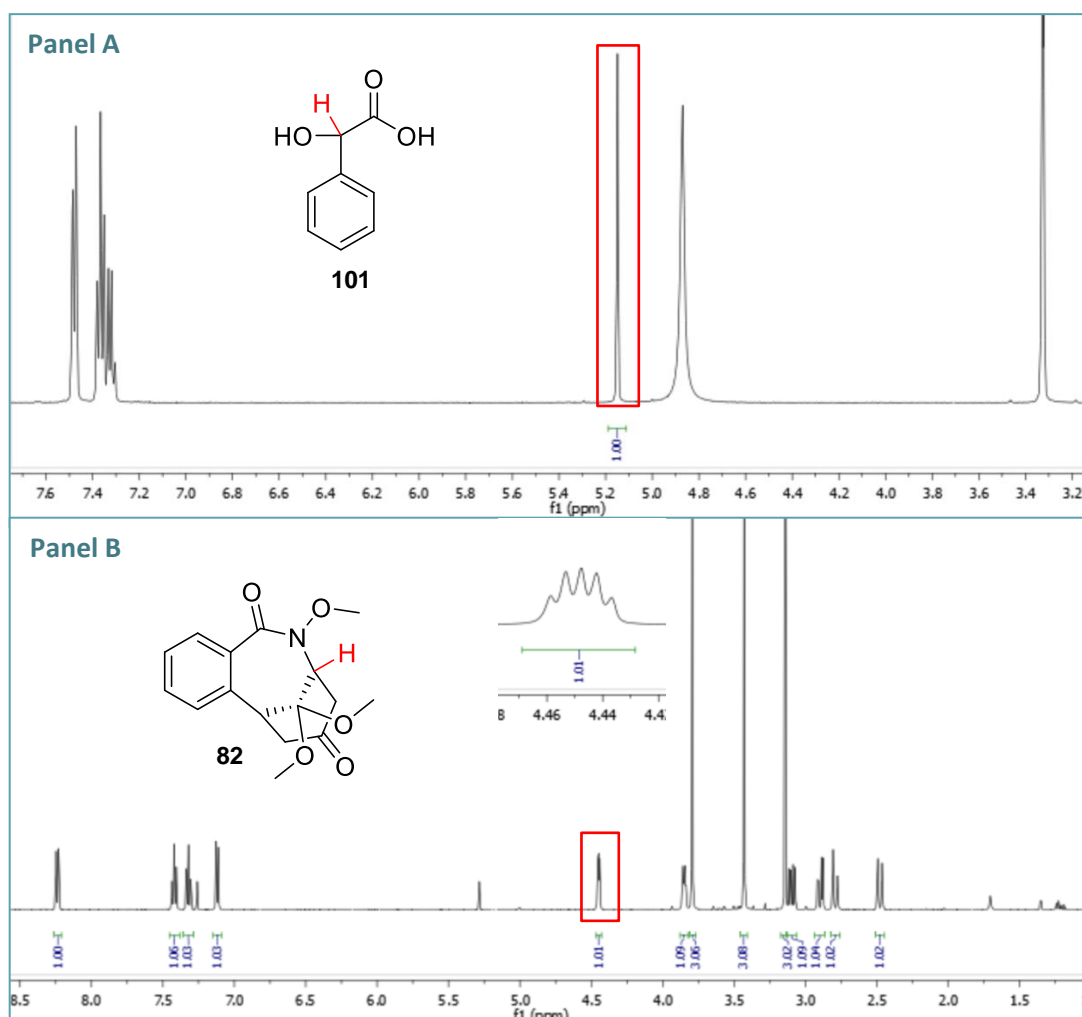
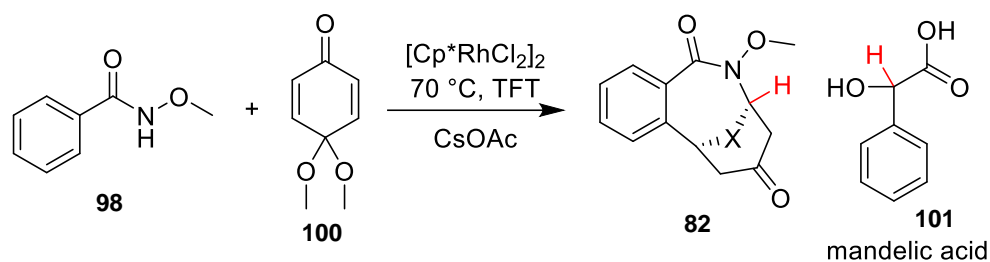


Figure 24: NMR data used to measure yields of the reactions. Panel A: 500 MHz ^1H NMR spectrum of mandelic acid **101**, which was used as the internal standard, the proton in red is the one used for comparison, and the corresponding peak is highlighted in the NMR spectrum. Panel B: shows the ^1H NMR of the product, the proton in red in the compound **82** is the one used for comparison, and the corresponding peak is highlighted in the NMR spectrum.

A range of conditions was screened, firstly the reaction run under literature conditions (Entry 1, Table 3) as a benchmark, and an NMR yield[†] of 21% was observed. Decreasing the catalyst loading to 1 mol% and 2.5 mol% (Table 3, Entries 2 and 3) decreased the yield to 0% (no reaction) and a 6% NMR yield respectively. Increasing the number of equivalents of benzoquinone was investigated; again, this had a detrimental effect and the NMR yield and dropped to 7% (Table 3, Entry 4).

Next, the air sensitivity of the reaction was investigated as the reaction was reported to be tolerant of air and water. Therefore, the reaction was carried out under anhydrous conditions and under an atmosphere of nitrogen (Table 3, Entries 5 and 6); the results of these experiments highlight the dependency of the reaction on oxygen or water as the yields dropped significantly. Similar reactions such as the Rh-catalysed heterocycle synthesis published by Guimond¹⁵³ require an internal oxidant whereas the conditions detailed by Xu¹⁴⁷ may require molecular oxygen to act as an oxidant. Therefore, the reaction was conducted with air bubbled through the reaction mixture (Table 3, Entry 7), and under an atmosphere of oxygen (Table 3, Entry 8) both of which gave a yield of 21% which only matched that of the literature conditions. Finally, the reaction concentration was increased (Table 3, Entry 9), which again resulted in no observed reaction.

[†] NMR yield refers to the amount of product in crude material relative to the internal standard.



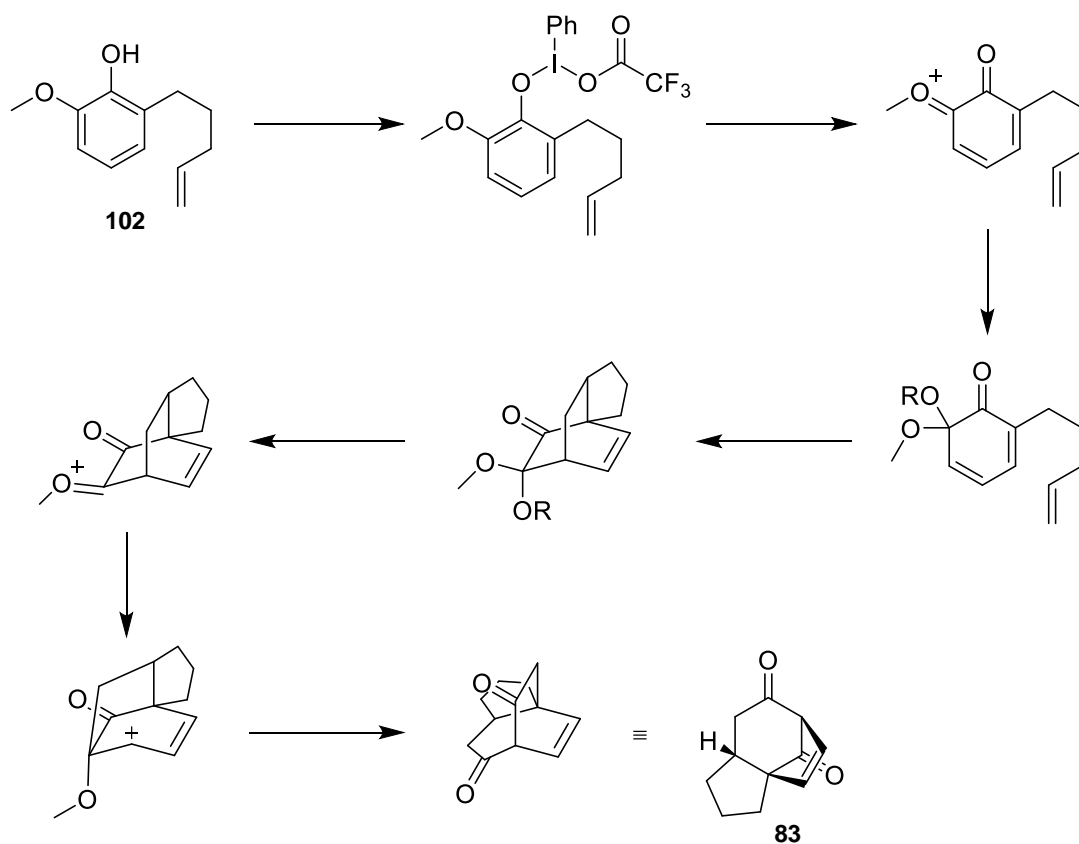
Entry	Deviation from the literature conditions ^a	NMR Yield %
1	Literature conditions ^a	21
V2	1.0 mol% of catalyst	<2
3	2.5 mol% of catalyst	6
4	3.0 eq. of benzoquinone	7
5	Anhydrous reaction	3
6	Reaction run under an atmosphere of nitrogen	9
7	Air bubbled through the reaction mixture	21
8	Reaction run under an atmosphere of oxygen	21
9	1 M reaction concentration	<2

Table 3: Conditions tested to improve the yield of the C-H insertion reaction. The NMR yield was measured using one equivalent of mandelic acid **101** as the internal standard. ^a $[\text{Cp}^*\text{RhCl}_2]_2$ (5 mol%), CsOAc (1.0 eq.), amide (1.0 eq.) quinone (1.5 eq.) TFT (0.1 M) $70\text{ }^\circ\text{C}$, 16 h. $\text{X} = \text{C}(\text{OMe})_2$.

Unfortunately, stepwise changes to the literature reaction conditions did not lead to an increase in yield. The highest yield achieved was 21%, which was well below the minimum requirement of 40%. It was therefore decided this scaffold could not be taken forward for the preparation of a lead-like compound library.

2.2 The use of dearomatisation chemistry as a complexity generating reaction

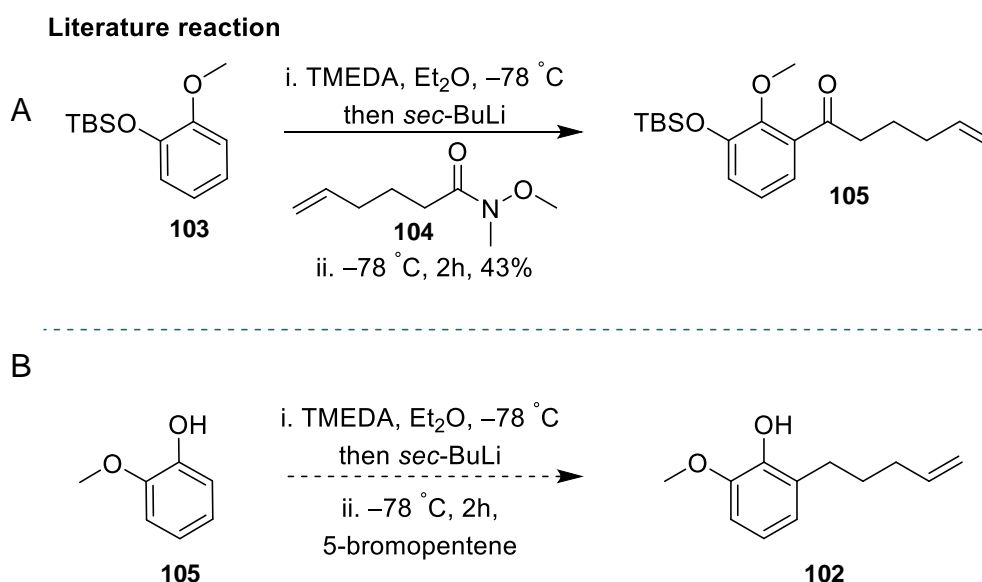
The second shortlisted reaction was the formation of cedrene-type skeleton **83** (Scheme 2).¹⁵⁴ The reaction proceeds via an oxidative dearomatisation, diastereoselective [5+2] cycloaddition and an acyl migration to generate the tricyclic framework. This reaction generates complexity in a very efficient manner, progressing from a flat, aromatic ring to a complex, tricyclic ring system and as such could be effective in this project (Scheme 2). This complex intermediate contains several different functional handles, including two potentially distinguishable ketones which had the potential to be utilised for manipulations such as ring expansion and fusion. The alkene on the two-carbon bridge could also prove to be very useful for ring cleavage chemistries.



Scheme 2: The complex intermediate **83** formed via an oxidative dearomatisation, cyclisation and bond migration.¹⁵⁴

2.2.1 Synthesis of the cyclisation precursors and carbocyclic analogue

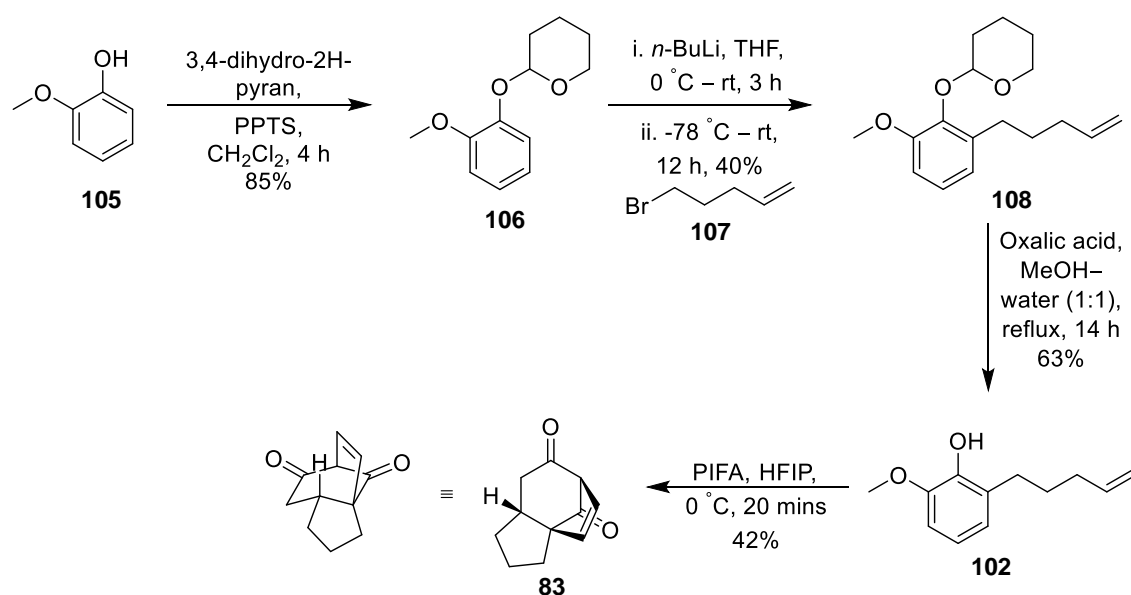
The carbocyclic analogue was initially selected for synthesis as it had a high yielding reported yield of 78%. The synthesis of the cyclisation precursor published by Ding¹⁵⁴ was initially reported by Chen¹⁵⁵ and describes the use of *sec*-BuLi and tetramethylethylenediamine (TMEDA) to lithiate the aromatic ring and trap the metallated intermediate with the Weinreb amide **104** (Scheme 3, Panel A). Utilising these conditions with 5-bromopentene in place of the Weinreb amide, the synthesis of the cyclisation precursor **102** was unsuccessful, with no observed product formed *via* 500 MHz ¹H NMR spectroscopy (Scheme 3, Panel B).



Scheme 3: Approach used in the synthesis of the cyclisation precursor **102**. Panel A details the literature conditions using the Weinreb amide **104** to trap the lithiated aromatic ring. Panel B depicts the same conditions but instead using 5-bromopentene.

The literature procedure was modified by protecting the phenol **105** with a tetrahydropyran (THP) group. The THP can act as a directing group for metalation of the aromatic ring through co-ordination with the oxygen atom in the THP group. This protection was achieved using 3,4-dihydro-2H-pyran and pyridinium *p*-toluene sulfonic acid and the product was isolated in an 85% yield (Scheme 4). With this substrate, lithiation with BuLi and treatment with 5-bromopentene gave **108** in an isolated yield of 40% (Scheme 4). The

successfully alkylated product **108** was then deprotected by refluxing in methanol and water with oxalic acid. This deprotection reaction proceeded in a 63% yield to give the cyclisation precursor **102** (Scheme 4). With this compound in hand the complexity generating reaction could be applied, which utilised [Bis(trifluoroacetoxy)iodo]benzene (PIFA) with hexafluoroisopropanol (HFIP) as solvent.¹⁵⁴ The reaction proceeded quickly (20 minutes) to give the carbocyclic complex intermediate **83** in a 42% yield, which is far lower than the literature yield (78%). However, it did meet the requirement for a yield over 40% and thus could be deemed practical. The relative configuration of the cycloadduct had been unambiguously determined by Ding¹⁵⁴ using X-ray crystallographic data of a bromine containing analogue, and all spectroscopic data collected matched that of the reported analytical data.



Scheme 4: The synthesis of carbocyclic analogue **83** using the modified procedure.

The successful synthesis of the carbocyclic analogue was a promising sign that this complex intermediate could be selected for use in this project, despite the recorded yield being lower than that reported. However, one potential challenge was that the carbocyclic analogue contained no functionality for scaffold formation or decoration in the bottom five membered ring. This could also result in limited diversity and undesirable molecular properties such as high lipophilicity. Therefore, efforts were focussed on synthesising the nitrogen containing analogue which had been reported

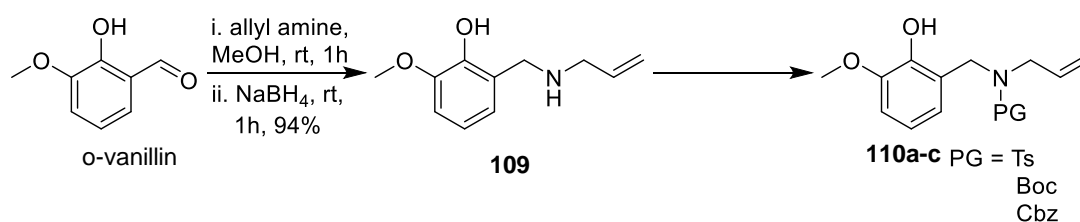
previously in the literature, as this would install functionality into the bottom portion of the molecule and could also serve to modulate molecular properties.

2.2.2 Synthesis of the heteroatom analogues of the dearomatisation framework.

2.2.2.1 Aza-analogue synthesis and optimisation

Ding¹⁵⁴ reported the synthesis of the tosyl protected aza-analogue **111a**, however a tosyl protecting group is not particularly practical as it requires forcing conditions for its removal.¹⁵⁶ Therefore, two other protecting groups were selected for testing alongside the tosyl group, both of which are also electron withdrawing, rendering the nitrogen non-basic, mimicking the electronics of the reported example.

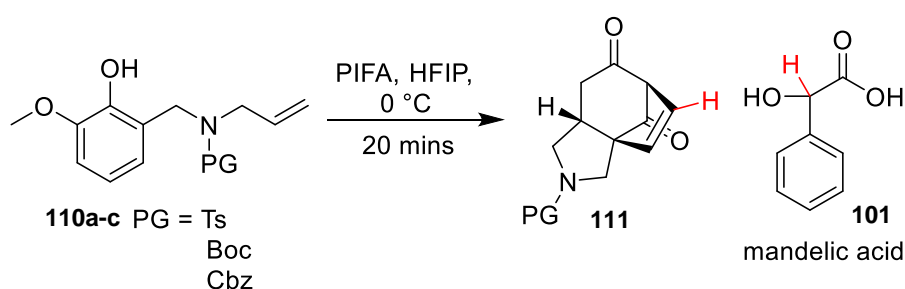
The cyclisation precursors **110a-c** were prepared in two steps. Firstly, reductive amination of *o*-vanillin with allyl amine and sodium borohydride, gave the unprotected amine **109** in a 94% yield. The amine **109** was then split into three portions and protected as the corresponding tosyl, Boc and Cbz derivatives. All three reactions proceeded smoothly and produced the protected amines in good to excellent yields with the specific conditions used are shown below (Table 4).



Entry	PG	Conditions	Yield %
1	110a - Ts	TsCl, K ₂ CO ₃ , CH ₂ Cl ₂ , rt, 2 h.	53
2	110b - Boc	Boc ₂ O, NEt ₃ , CH ₂ Cl ₂ , rt, 16 h.	97
3	110c - Cbz	CbzCl, K ₂ CO ₃ , THF–water (2:1), rt, 16 h.	93

Table 4: The conditions used for protection of the allyl amine with three different protecting groups.

With all three cyclisation precursors in hand, the dearomatisation/cyclisation reaction could be undertaken using PIFA and HFIP. The *N*-Tosyl (Table 5, Entry 1) precursor produced the desired product **111** in a 9% yield as assessed by 500 MHz ¹H NMR spectroscopy with one equivalent of an internal standard (mandelic acid **101**). Again, this fell short of the reported isolated literature yield which was 73%.¹⁵⁴ The formation of what appeared to be an over oxidised product which was identified as the quinone product **112** (Table 5, Entry 1), by the new diagnostic alkene peaks of the quinone, which have a different shift (ppm) and coupling constant (2.0 Hz) to the alkenes observed in the starting material and the product. Both the *N*-Boc and *N*-Cbz were both shown to be unreactive under the literature conditions with only starting material present assessed by 500 MHz ¹H NMR spectroscopy at the end of the reaction (Table 5, Entries 2 and 3).



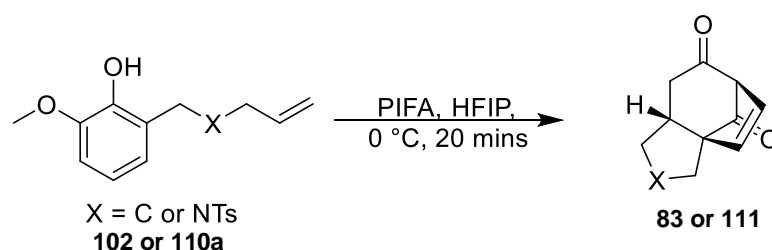
Entry	PG =	NMR Yield ^a %	Unwanted side products
1	Ts	9	 112 40% ^a
2	Boc	<2	Only starting material
3	Cbz	<2	Only starting material

Table 5: The range of protecting groups tested on the nitrogen analogue. ^a measured using ¹H NMR spectroscopy (500MHz) and mandelic acid as an internal standard.

Ding¹⁵⁴ ran the reaction under an atmosphere of nitrogen to eliminate as much air and water from the reaction as possible. However, the only potential source of water or oxygen is the solvent. Ding reported the importance of HFIP to the reaction however it is not possible to purchase

anhydrous HFIP, so instead a range of solvent mixtures were screened where either one or both solvents were anhydrous to see the effect on the yield. All solvent mixtures were screened against both the aza **111a** and carbocycle **102**, with intent to increase the yield further and to observe whether the trends in the yield were consistent between the two analogues, or if selectivity was afforded.

The yield was again assessed using 500 MHz ¹H NMR spectroscopy and an internal NMR standard, using the same internal standard and protons for comparison as before (see above). Despite screening a range of solvents in different ratios it appeared this only served to decrease the yield. It was observed (Table 6) that higher the percentages of HFIP increased the observed NMR yield (Table 6, Entries 1-4) which agrees with the literature, whilst methanol interrupted product formation completely (Table 6, Entry 5).



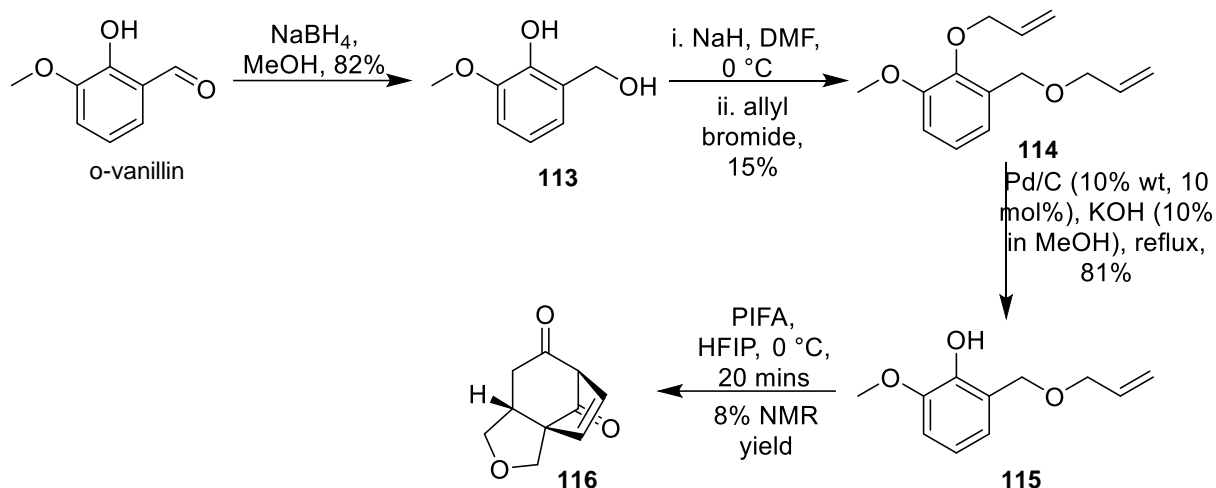
Entry	Solvent mix (ratio)	NMR yield % ^a X=C	NMR yield % X=NTs
1	HFIP (100)	41	9
2	HFIP–MeCN (50:50)	19	<2
3	HFIP–MeCN (75:25)	31	3
4	HFIP–MeCN (90:10)	34	4
5	MeCN–MeOH (50:50)	<2	<2
6	HFIP–CH ₂ Cl ₂ (50:50)	29	6

Table 6: Effect of solvent on the yield of the carbo- and aza- analogues. ^a determined using ¹H NMR spectroscopy and one equivalent mandelic acid as an internal standard.

2.2.2.1 Oxa- analogue synthesis, precursor synthesis and attempted cyclisation

Integration of a nitrogen atom into the parent scaffold could not be practically achieved. However, without the heteroatom present the five-membered ring offered little potential for decoration and the resulting scaffolds would suffer with poor molecular properties and a lack of diversity. Therefore, it was decided it would potentially prove beneficial to prepare the oxygen containing analogue which is previously unreported in the literature. It would have limited reactivity in the five-membered ring for decoration but could contribute in improving the molecular properties compared to the carbocyclic analogue.

The oxo- analogue cyclisation precursor **116** (Scheme 5) was made from the same commercially available starting material, *o*-vanillin, which was subjected to a reduction using NaBH₄ to give the alcohol **113** in an 82% yield. This product was protected using two equivalents of allyl bromide and sodium hydride producing the bis-protected species **114** in a 15% yield. Hara¹⁵⁷ *et al* demonstrated the selective deprotection of allyl phenols over allyl alcohols, which was successfully applied to the bis-protected compound **114**, yielding the cyclisation precursor **115** in an 81% isolated yield (Scheme 5). The cyclisation was attempted using PIFA and HFIP, the yield of this reaction was 8%, but no product was successfully isolated. Again, the reaction was monitored by 500 MHz ¹H NMR spectroscopy using one equivalent mandelic acid.



Scheme 5: The synthetic route devised to the oxo-analogue **116**.

As judged by the low yield of both the aza- and oxo- analogues, the incorporation of heteroatoms into this framework was not possible. The carbocycle **83** could be synthesised in a reasonable yield of 42% however further control of molecular properties would be challenging.

2.3 Tropone cycloaddition chemistry as a complexity generating reaction

Tropone has been used commonly in cycloaddition reactions including [6+4] and [6+3] cycloadditions.^{158–161} Higher-order cycloadditions are synthetically useful, rapidly increase molecular complexity and offer access to functionally rich bicyclic structures.¹⁶² This framework contains attractive features which would enable a diverse lead-like compound library to be prepared (Figure 24). It contains a bridged, bicyclic ring systems, versatile diene functionality, bridged ketone and masked enone functionality, all of which could act as functional handles for the addition, cleavage and expansions of this framework.

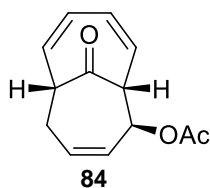


Figure 24: The tropone based scaffold, **84**, formed via a [6+4] cycloaddition reaction.

2.3.1 Synthesis of tropone complex intermediate

The [6+4] tropone cycloadduct **84**, originally published by Ito¹⁵⁸ in 1982 and later by Rigby¹⁶³ was readily prepared in a single step using commercially available starting materials. In this case,¹⁵⁸ tropone, **117**, and 1-acetoxybuta-1,3-diene **118**, were refluxed together for five days (Figure 25, Panel A). The product **84** was isolated in a 57% yield as a single *exo* diastereomer (>95:<5 by 500 MHz ¹H NMR spectroscopy).

The *exo* isomer is the major product formed in this cycloaddition with the exclusion of the *endo* species in virtually every published example.¹⁶² The Newman projection highlights the proximity between the OAc and bridgehead proton as they have a *cis* relationship (Figure 25, Panel B). The *exo* adduct is kinetically favoured as there is repulsion between the filled orbitals in the *endo* transition state (Figure 25, Panel C).¹⁶⁴ Despite the long reaction time, the readily available starting material, acceptable yield and scalability were assessed to be more prominent factors. Therefore, this promising scaffold was chosen for further investigation.

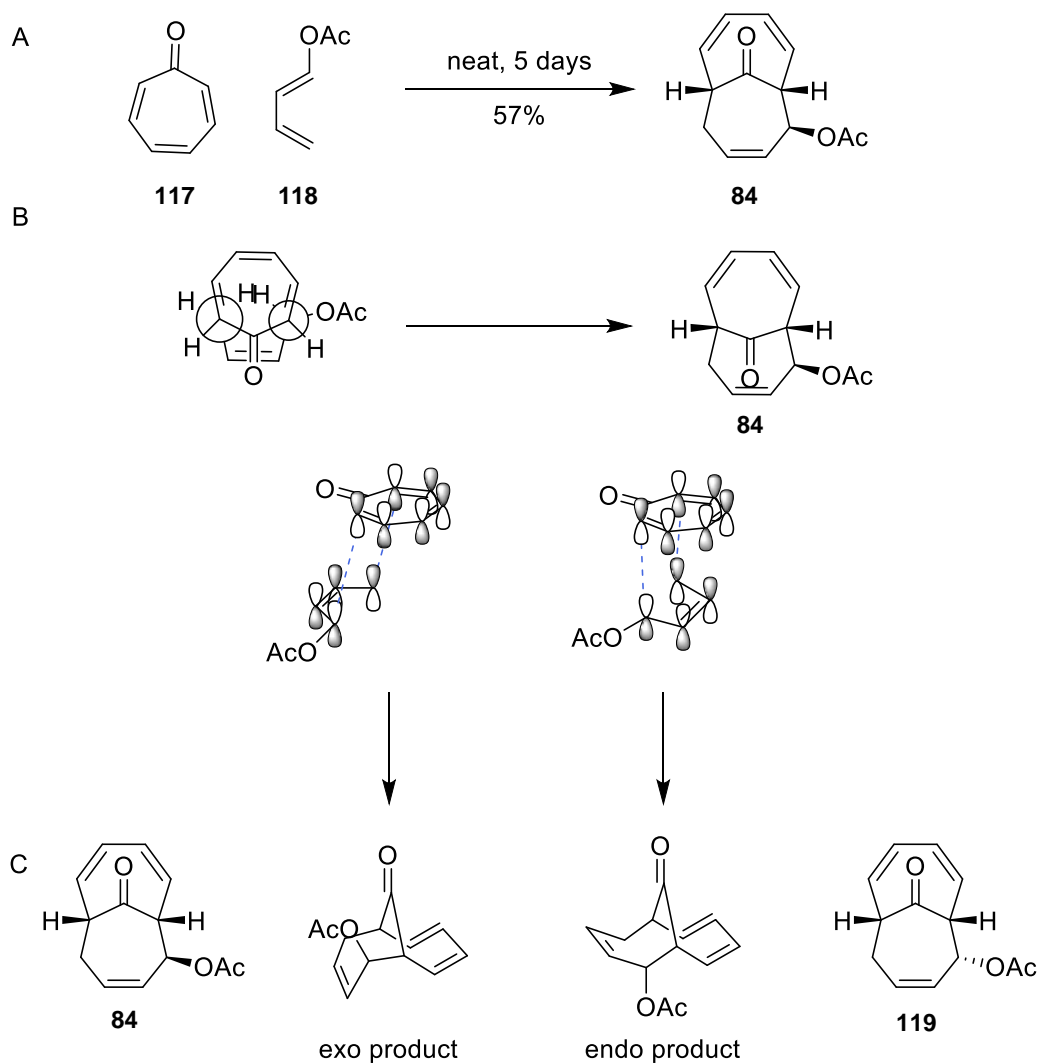
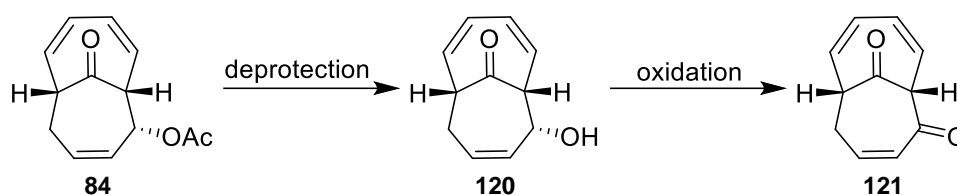


Figure 25: The tropone cycloaddition. Panel A the synthetic route to complex intermediate **84**. Panel B The newman projection for the cycloaddition, indicating the bridged proton and OAc will be on the same face. Panel C The transition states for the exo- and endo- pathways and the products from those pathways.

2.3.2 Formation of enone functionality via deprotection

Conversion of the allylic acetate to the enone was an important transformation to achieve, as this a very useful functional handle for ring addition reactions and some ring cleavage reactions. Formation of the enone would require removal of the acetate group to form the alcohol **120** which can then be oxidised up to the enone **121** (Scheme 6).



Scheme 6: The devised synthetic route to the enone **121**.

Unfortunately, no reaction was observed with (K_2CO_3 in MeOH, Na_2CO_3 or LiOH). Instead, the reaction mixture suffered severe discolouration (turned bright purple) and the formation of multiple spots by TLC analysis was observed. Ito has previously reported that treatment of **84** with KOH results in formation of the highly coloured tetraene **122** (Figure 26).¹⁵⁸ This is an unusual structure as the compound contains an anti-Bredt alkene, however this can be tolerated in bicyclic ring systems with rings larger nine carbon atoms, as they can accommodate the double bond without excessive strain.¹⁶⁵ It is evident that the ketone form of this scaffold was not the ideal substrate for the deprotection of the allylic alcohol.



Figure 26: The tetraene formed when **122** is treated with base.¹⁵⁸

2.3.3 Formation of enone functionality via reduction and protection

As the acetate could not be deprotected directly an alternative route was devised, the first step is the reduction of the bridged ketone followed by protection of the bridged alcohol using an appropriate silyl protecting group. It was believed that this would be a suitable substrate, as these groups can tolerate the conditions for acetate cleavage, followed but oxidation to the enone.

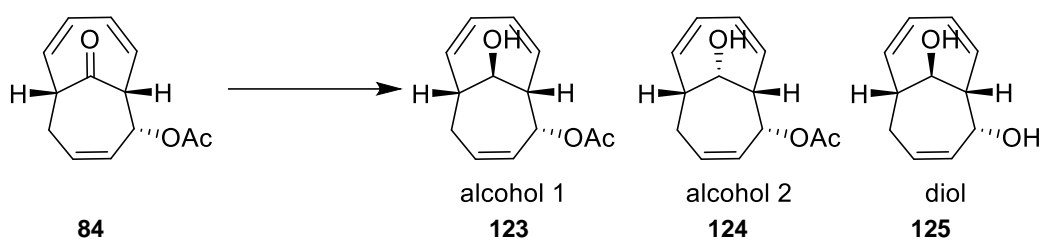
2.3.3.1 Screening of reduction conditions for the bridged ketone

The reduction of the bridgehead ketone was investigated, ideally this would be a selective reduction affording the alcohol as a single diastereoisomer, however the molecule is quite symmetrical, so this was a challenging task. Several reducing agents were screened on a small scale

(ca. 20 mg) (Table 7, Entries 1-6). Analysis of the crude product by 500 MHz ^1H NMR spectroscopy assessed whether a successful reduction had taken place, then the promising reactions were scaled up to evaluate isolated yields.

Reduction of the bridged ketone with sodium borohydride afforded a 50:50 mixture of diastereomers (Table 7, Entries 1 and 2). LiAlH_4 (Table 7, Entry 3) gave a ca. 50:50 mixture of diastereomers. L-selectride and DIBAL (Table 7, Entries 4 and 5) resulted in a complex mixture observed in the crude 500 MHz ^1H NMR spectrum. Brown ¹⁶⁶ demonstrated the use of 9-BBN to successfully reduce a variety of carbonyl compounds including ketones, reduction of **84** with 9-Borabicyclo[3.3.1]nonane (9-BBNH) (Table 7, Entry 6) appeared to produce a single product on a small scale by crude 500 MHz ^1H NMR spectroscopy.

When scaled up (0.5 g) with ethanol as the solvent, NaBH_4 appeared to give three products (Table 7, Entry 7). Upon isolation, it appears that the acetate group had trans esterified with the solvent, which has resulted in a product with two unprotected alcohols. To prevent this isopropanol was used (Table 7, Entry 8), and both diastereomers were produced in a ratio of 38:62. The 9-BBN reduction was scaled up (0.3 g) (Table 7, Entry 9) to assess the isolated diastereomeric ratio of the reaction. On a larger scale the reduction produced a diastereomeric ratio of 56:43. Sodium borohydride appeared to be the most selective and is a widely used reagent and was therefore selected for larger scale synthesis, and to simplify the latter steps only the major diastereomer was taken forward in the synthesis of the enone.



Entry	Conditions	Ratio of diastereomers (A1:A2)	Total yield (%) (A1+A2)	Yield of diol (%)
1	NaBH ₄ , MeOH, rt ^a	50:50	-	/
2	NaBH ₄ , CeCl ₃ ·7H ₂ O, MeOH, rt ^a	50:50	-	/
3	LiAlH ₄ , THF, 0 °C ^a	50:50	-	/
4	L-Selectride, THF, -78 °C ^a	Complex mixture	-	/
5	Bu ₂ AlH, CH ₂ Cl ₂ , -78 °C ^a	Complex mixture	-	/
6	9-BBNH, THF, 0 °C ^a	100	-	/
7	NaBH ₄ , EtOH, rt ^b	reduced product and deprotected diol product 125	23 (A2)	49
8	NaBH ₄ , iPrOH, 0 °C ^b	38:62	63	/
9	9-BBNH, THF, 40 °C ^c	57:43	48	/

Table 7: Reduction conditions for the bridgehead ketone. ^a 20.0 mg scale ^b 0.5 g scale ^c 0.3 g scale, – meaning was not assessed in this case, / not observed.

2.3.3.2 Assignment of the configuration of the bridgehead alcohols

The configuration of the diastereomeric alcohols **123** and **124** were assigned using interactions observed by NOESY NMR spectroscopy (500 MHz, Figure 27). In alcohol **123** there were no diagnostic interactions

observed in the NOESY NMR spectrum (Figure 27). Alcohol 2 **124** displayed one diagnostic interaction, which was between the alpha hydroxy proton, one of the diastereotopic CH₂ protons (position 5 according to the name in Chapter 6, Figure 27), indicating that they are on the same face of the molecule. Therefore, alcohol **123** has the opposite configuration and from the conformational diagram (Figure 27) it can be seen that alpha hydroxy proton is directionally isolated and no NOESY interactions would be expected, which is in agreement with the observations.

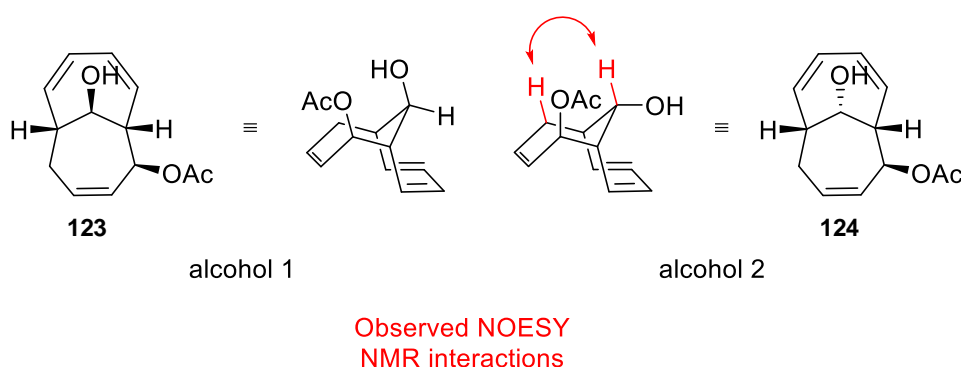
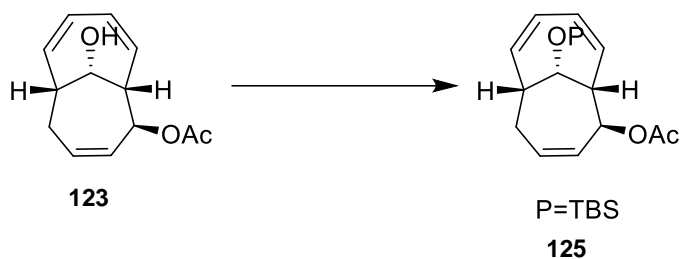


Figure 27: The protons shown in red highlighting the interactions observed in the NOESY NMR spectroscopy (500 MHz) of alcohols **123** and **124**.

2.3.3.3 Conversion of the allylic alcohol into the enone

The next required step in the formation of the enone, was the protection of the alcohol with a suitable protecting group. This protecting group is required to be stable to both basic and oxidising conditions so a *tert*-butyl dimethylsilyl (TBS) group was chosen. Initial attempts using mild conditions were unsuccessful with no product formation observed (Table 8, Entry 1). Slightly more forcing conditions were investigated (Table 8, Entries 2 and 3), raising the temperature resulted in only trace product formation. Instead the reaction was run as concentrated as possible in DMF and left stirring for 3 days and the product was successfully isolated in a 68% yield (Table 8, Entry 3).

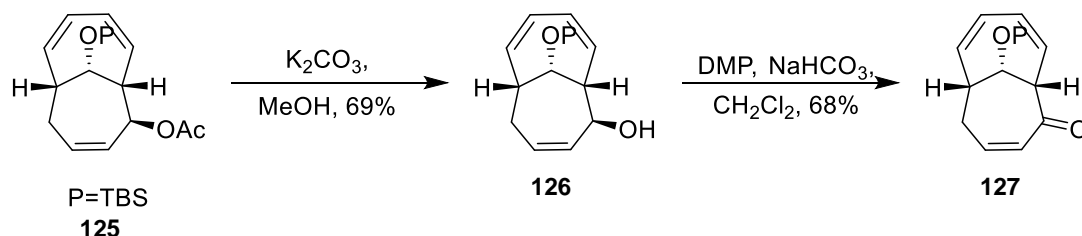


Entry	Reagents and solvent	Temperature (°C)	Reaction time (days)	Outcome
1	TBSCl, NEt ₃ , CH ₂ Cl ₂	rt	1	Starting material ^a
2	TBSCl, NEt ₃ , DMAP (10 mol%), CH ₂ Cl ₂	reflux	2	Trace amount of product ^a
3	TBSCl, imidazole, DMF	rt	3	68% isolated yield

Table 8: the conditions screened for the TBS protection of the alcohol. ^a observed by 500 MHz ¹HNMR spectroscopy and LC-MS

2.3.3.4 Cleavage of the acetate and oxidation to the enone

With the TBS protected alcohol **125** in hand, the acetate was easily cleaved under standard, mild conditions (K₂CO₃, MeOH) to give the allylic alcohol **126** in a reasonable yield (69%, Scheme 7). The final step required for the formation of the enone was oxidation of the allylic alcohol to the enone. Dess-Martin periodinane (DMP) was used for this oxidation as it is mild and therefore tolerated by the TBS protecting group. The oxidation proceeded as expected and produced the enone in a 68% yield (Scheme 7).



Scheme 7: The synthetic route for the removal of the acetate protecting group to give the allylic alcohol **126** followed by an oxidation to the enone **127** with DMP.

The practicality of the route from the unprotected alcohol **123** to the enone **127** can be somewhat improved by telescoping some of the reactions to limit the number of purifications. The overall yield of these telescoped steps is still low at just 32%. This low yield limits the practicality of this framework as

the enone functionality is a valuable functional handle for many diversification reactions and cannot be sufficiently produced.

2.4 [5+2] Oxido-pyridinium alkene cyclisation as a complexity generating reaction

The penultimate shortlisted complex intermediate for investigation was an intramolecular [5+2] oxido-pyridinium cycloaddition, which provides access to seven membered rings, which is a structural motif common among many natural products.^{167,168} The original publication details the formation of a complex, highly 3-dimensional complex intermediate **85** shown below (Figure 28).¹⁶⁹ The high 3-dimensionality of this compound is particularly appealing as it would be a good way to impart this characteristic on the final library of compounds. This complex intermediate also contains both a basic nitrogen, which could help modulate lipophilicity and an enone functional handle, which as previously discussed is very useful for ring fusion chemistry.

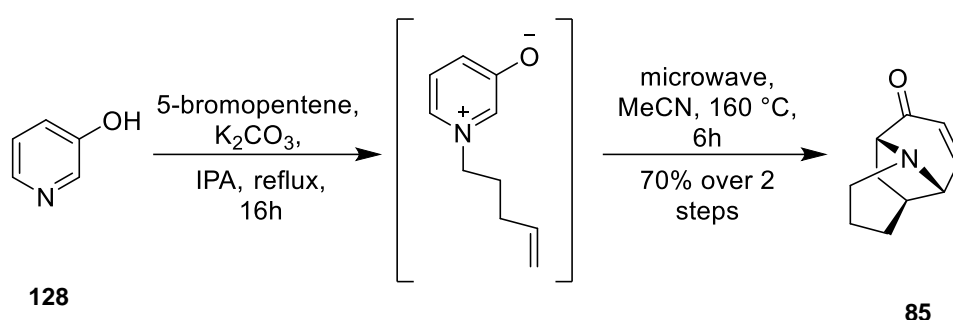


Figure 28: The complex intermediate **85** selected for investigation.¹⁶⁹

2.4.1 Synthesis of the cyclisation precursor and construction of the complex intermediate

One requirement for the complexity generating reaction is that the cyclisation precursor must be synthesised in fewer than five synthetic steps, and in this case the complex intermediate is synthesised in just two steps from 3-hydroxy pyridine, which is very cheap (£37/100 g) making this complexity generating reaction very appealing. The first step in the two-part synthesis is an alkylation of 3-hydroxypyridine, originally achieved using Amberlite IRA-410 ion exchange resin (OH⁻ form) as a base for the alkylation.¹⁶⁹ This resin had limited commercial availability, so instead potassium carbonate was selected. 3-hydroxypyridine, potassium carbonate and 5-bromopentene were refluxed in isopropanol (IPA) overnight to create a dark orange slurry (Scheme

8). The intermediate betaine **129** was not isolated, instead the solvent was removed and rediluted in acetonitrile. The cyclisation requires forcing conditions and this was originally achieved in an autoclave, however a microwave was employed in this case. The cyclisation was achieved at 160 °C under microwave irradiation in acetonitrile for 6 hours, the yield over two steps was good and the complex intermediate **85** was synthesised in a 70% yield (Scheme 8) with excellent selectivity of >20:<1 by ¹HNMR spectroscopy (400 MHz).



Scheme 8: Synthesis of the complex intermediate **85**, the first step is an alkylation of 3-hydroxypyridine, and the second step is the cyclisation achieved in the microwave at 160 °C.

This reaction is very selective and creates a single diastereomer, the configuration of which was assigned using ¹HNMR NMR spectroscopy. The bridged amine complex intermediate **85** displays diagnostic ¹HNMR signals. The observed coupling pattern of proton 8 (shown in green, Figure 29) is a doublet. This is due to the dihedral angles between proton 8 and the adjacent proton 3 (shown in blue) being close to 90°. This configuration is also confirmed by observed NOESY interactions, between a proton alpha to the nitrogen and a bridgehead proton (shown in red, Figure 29).

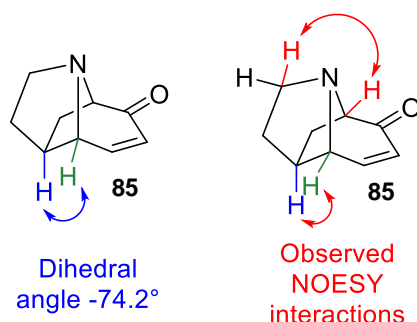


Figure 29: The predicted dihedral angle between proton 8 (green) and proton 3 (blue) is -74.2° which give a predicted coupling constant of 0.8 Hz, the observed splitting was a singlet for proton 8. The red arrows highlight the observed NOESY couplings in the NMR.

This reaction appeared robust with the recorded yield matching that of the literature yield. Sammes¹⁶⁹ only investigated a very limited scope of starting materials and alkyl chains. Therefore, the two variations to this reaction were investigated. Firstly, could the chain length be increased from C5 to C6 and secondly, if the starting hydroxypyridine be varied in any way.

2.4.2 Synthesis of alternate complex intermediates utilising the oxido-pyridinium cyclisation

Increasing the chain length from a five-carbon chain to a six-carbon chain (Table 9, Entry 1) did not affect the alkylation step, with successful formation of the betaine, yet the cyclisation reaction did not proceed under the microwave conditions, with only the alkylated 3-hydroxy pyridine present in the crude ^1H NMR spectrum. Next, different 3-hydroxypyridine substrates were tested, the 4-bromo analogue (Table 9, Entry 2) and the 4-phenyl derivative (Table 9, Entry 3) were both successfully alkylated, but the cyclisation was unsuccessful. Lastly, 4-hydroxyisoquinoline **134** was tested (Table 9, Entry 4), in this case both the alkylation and the cyclisation were successful under the microwave conditions and the desired compound **135** was successfully isolated in a 45% yield.

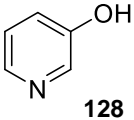
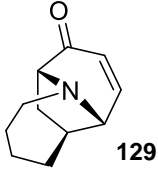
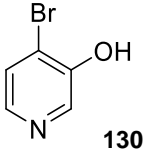
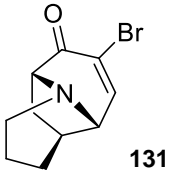
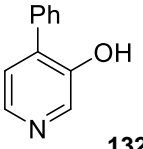
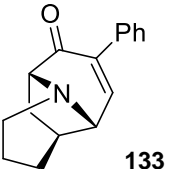
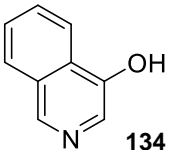
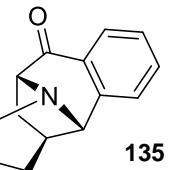
Entry	Hydroxy pyridine reagent	Alkyl reagent	Product	Alkylation ^a	Cyclisation	Yield ^b (%)
1	 128	6-bromo hexene	 129	Y	N	70
2	 130	5-bromo pentene	 131	Y	N	-
3	 132	5-bromo pentene	 133	Y	N	-
4	 134	5-bromo pentene	 135	Y	Y	45

Table 9: The range of starting hydroxypyridines and alkyl chains tested in this cyclisation reaction. The conditions for the alkylation and cyclisation are the same as the original substrates. Y – yes, N – no. ^a determined *via* 500 MHz ¹HNMR analysis of the crude reaction mixture ^b isolated yield.

This oxido-pyridinium cyclisation has generated two complex intermediates **85** and **135** that could be utilised in this project. The first framework synthesised offers many more options for scaffold synthesis due to the enone functionality. Whereas the fused phenyl framework offers fewer options with only the ketone as a functional handle, but it was proposed it could be decorated in several ways to create some final library compounds.

2.5 Intramolecular [5+2] Oxido-pyryllium alkene cyclisation as a complexity generating reaction

The final reaction selected for investigation was another [5+2] cycloaddition but in this case, an oxido-pyryllium intramolecular cycloaddition. This specific class of cycloaddition had previously been reported to construct bridged polycyclic ethers.¹⁷⁰ This example was published by Mitchell¹⁷¹ in

2018, and details the construction of a number of acetoxypyranone-alkene derivatives with a range of functionality in the alkyl chain, to construct a tricyclic, bridged and fused ring system **86** (Figure 30). The ether analogue was shortlisted for this project as it is small, only 12 heavy atoms, which allows for scaffold synthesis and decorations along with two ethers which will moderate the molecular properties of the library compounds. The tricyclic bridged framework again contains an enone functional group so is complimentary to the previous framework **85** and again would facilitate scaffold synthesis.

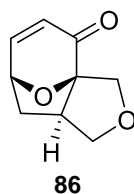
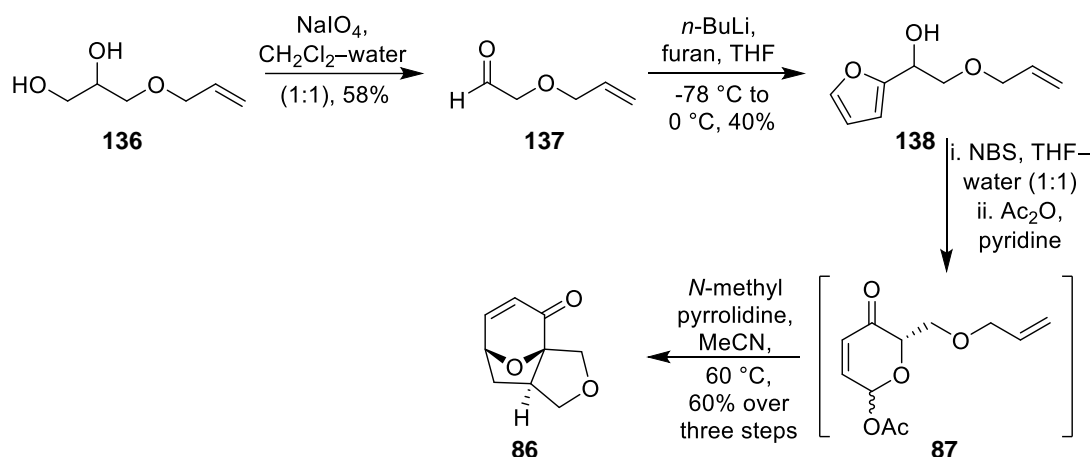


Figure 30: the complex intermediate formed via an intramolecular oxido-pyrylium alkene cycloaddition.

2.5.1 Synthesis of the acetoxypyranone-alkene cyclisation precursor and its cyclisation

Construction of the acetoxypyranone-alkene cyclisation precursor **87** follows the literature procedure (Scheme 9).¹⁷¹ Initially, the diol **136** was treated with sodium periodate to give the aldehyde **137** in a 58% yield (Scheme 9). Next, furan was lithiated with *n*-BuLi at -78 °C and added to the aldehyde **137**, to give the furfuryl alcohol **138** in a 40% yield (Scheme 9). This furfuryl alcohol **138** was treated with NBS to form the crude pyranone, which was taken through into the acetate protection step without purification. At this point in the literature the acetoxypyranone was purified however in practice this was also carried through crude into the final cyclisation step in a one-pot fashion. The cyclisation was achieved with *N*-methylpyrrolidine (NMP) in acetonitrile to yield the complex intermediate **86** as a single diastereomer in a 60% yield over the three steps (Scheme 9). The configuration of the complex intermediate **86** was unambiguously determined by Mitchell¹⁷¹ using X-Ray crystallographic data. All measured spectroscopic data was in agreement with the literature therefore the configuration of the compound was assumed to be the same.



Scheme 9: The synthetic route in the synthesis of complex intermediate **86**. The route involves a periodate cleavage, a lithiation, Achmatowicz ring expansion, acetate protection and [5+2] cyclisation reaction.

This complex intermediate is synthesised in five synthetic steps which meets the requirements laid out for the complexity generating reaction with only two purifications required. Mitchell¹⁷¹ demonstrated the use of a cross metathesis on the terminal alkene of the acetoxy pyranone **87** as a method to install other functional handles. This was attempted following the literature procedure using crotonaldehyde as the metathesis partner, however there was no evidence of product formation. The alkyne analogue was tested in parallel; the same synthetic route was employed with the alkyne equivalents in place of the alkene. The synthesis of the complex intermediate from the alkyne analogue was unsuccessful as the Achmatowicz ring expansion resulted in no isolatable product and therefore deprioritised after the successful synthesis of the alkene derived compound **86**.

2.6 Analysis and selection of the complex intermediates for use in the synthesis of a library of lead-like compounds

So far in this chapter the synthesis of six different complex intermediates have been discussed, the results of which are summarised below (Table 10). Selection of the complexity generating reaction is a crucial decision for this project, as it will determine the downstream success. There are two complex intermediates which were clearly not suitable for this project. Firstly, the Rh catalysed C-H insertion (Table 10, Entry 1), the yield of the

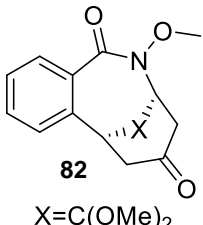
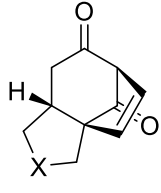
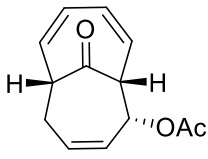
reaction was only 21% and despite attempts to optimise the reaction, it could not be improved. Secondly, the dearomatisation based complex intermediate **83** (Table 10, Entry 2), the carbocyclic analogue was successfully synthesised in a 42% yield, which is much better than the previous reaction. Although this compound would create a library of compounds with limited diversity and poor molecular properties, and neither the oxa nor aza analogues were synthesised in any suitable amounts. Therefore, both reactions were disregarded for this project.

The third complex intermediate **84** (Table 10, Entry 3) was synthesised in a single step using tropone cycloaddition chemistry and the yield over 40% made this scaffold appear very practical. The challenges arose for this framework when attempts were made to convert the allylic acetate into the enone, this added another four steps to the synthesis of the useful complex intermediate **127**, in a low yield of 32%. Initially, it was unclear how to proceed with this framework due to the multi-step route to the enone, but it was decided to take this complex intermediate through to scaffold synthesis and if those reactions were unsuccessful or low yielding a final decision could be made.

The fourth complexity generating reaction was based on an intramolecular [5+2] oxido-pyridinium alkene cycloaddition (Table 10, Entries 4 and 5) and this reaction yielded two amine bridged complex intermediates **85** and **135**. The two-step synthetic route allowed quick access, in yields over the required 40% to both amine bridged frameworks, with the complex intermediate **85** demonstrating the highest isolated yield of all the investigated reactions, at 70% isolated yield. The original complex intermediate **85** (Table 10, Entry 3) is small at only 12 HA, which allows room for growth *via* scaffold synthesis and decoration with groups of varying size, however complex intermediate **135** (Table 10, Entry 4) is larger with 16 HA, so will have more limited options. Both **85** and **135** contain an unfunctionalised carbon chain, however these molecules also contain a basic nitrogen which can modulate the molecular properties. Consequently, complex intermediate **85** would be taken forward for scaffold synthesis and the fused aromatic complex

intermediate **135** will be used as a scaffold itself and will be decorated to yield final library compounds.

The final complex intermediate **86** was successfully synthesised in a 60% yield. The synthetic route consists of five steps, which is the upper limit for this requirement however only two purifications are required, improving its practicality. This complex intermediate appears to meet all the requirements set and is a clear choice to take forward for scaffold synthesis. But all three complex intermediates chosen for scaffold synthesis contain enone functional handle, which could lend itself to a toolkit of reactions being applied to all three complex intermediates, to create a more uniform approach.

Entry	Complex intermediate	Number of synthetic steps	Yield of the cyclisation (%)	Points for comparison	Selected for scaffold synthesis
1	 <p>82 X=C(OMe)₂</p>	3	21 ^a	Yield could not be improved to reach target of 40%.	N
2	 <p>X= C or NTs 83 or 111</p>	4	C = 42 ^a NTs= 9 ^b	Carbocyclic analogue has limited options for scaffold synthesis and NTs the yield is not over the 40% threshold.	N
3	 <p>84</p>	1 (to complex intermediate) 5 (to enone)	54 ^a 32a	Easy synthesis of the complex intermediate, however 4 low yielding steps to reach the useful enone functionality.	Y

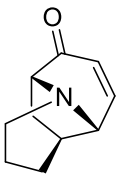
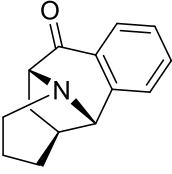
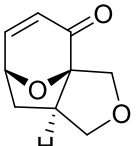
4	 <p>85</p>	2	70 ^a	Concise two step synthesis to the complex intermediate, useful enone functionality.	Y
5	 <p>135</p>	2	45 ^a	Concise two step synthesis to the complex intermediate, limited options for scaffold synthesis but decorations could yield final compounds	Y
6	 <p>86</p>	5	60 ^a	5 step synthesis but only two purifications required, contains useful enone functionality	Y

Table 10: Summary of all six complex intermediates discussed in this chapter, four of which have been chosen for further investigation. ^a indicates an isolated yield, ^b indicated an NMR yield, N denotes no and Y denotes yes.

Chapter 3 Synthesis of diverse molecular scaffolds

To realise our 'top-down' approach, a range of reaction classes were developed to modify the complex intermediates, for example by ring addition, ring fusion, ring cleavage and ring expansion. It was envisaged that the employment of these reactions should result in a diverse collection of frameworks. As three complex intermediates were selected in the previous chapter, it was proposed that the scaffold forming reactions will be applied to all the selected cycloadducts to aid the development of a widely applicable toolbox of reactions and to enable a diverse set of scaffolds to be generated. The successfully formed scaffolds would subsequently be harnessed in the preparation of a diverse set of screening compounds.

3.1 The application of ring addition chemistry

Within the context of our 'top down' approach ring addition is the appendage of a ring to the parent cycloadduct. The appendage of a ring is the connection of a cyclic building block to the cycloadduct. Ring fusion results in addition of a new ring system to the cycloadduct and can introduce aromaticity into the series.

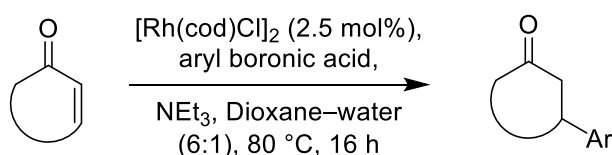
3.1.1 Rh catalysed 1,4-addition of aryl boronic acids

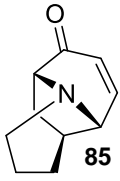
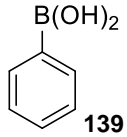
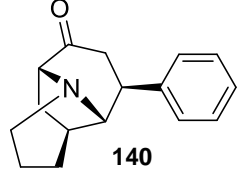
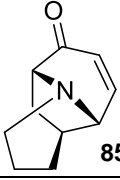
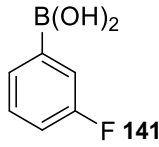
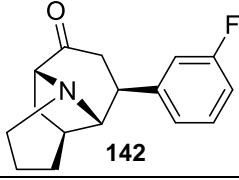
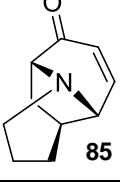
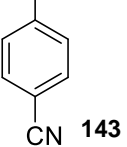
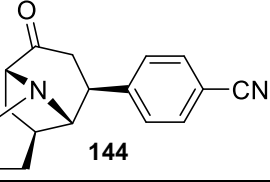
The three selected complex intermediates contained an enone which is a very useful functional handle for ring addition reactions. To achieve the attachment of a new ring, a rhodium catalysed 1,4-addition was selected, as this is an ideal way to incorporate an aromatic ring whilst maintaining three-dimensionality.¹⁷²⁻¹⁷⁵ A 1,4-addition reaction also leaves the ketone free for derivatisations to form a collection of screening compounds.

The enones **85**, **86** and **127** were treated with the cyclooctadiene rhodium chloride dimer (2.5 mol%) and the appropriate aryl boronic acid (5.0 equiv.) and the reaction was heated overnight¹⁷³, producing the desired 1,4-addition product in all but one case. Four different aryl boronic acids were investigated in this reaction. The phenyl, *m*-fluoro and *p*-cyano phenyl

derivatives (Table 11, entries 1-7) all reacted smoothly albeit in varying yields (14-49%).

There are many examples of Rh-catalysed 1,4-additions with a variety of aryl boronic acids.^{172,173,176,177} However, there are substantially fewer examples using heteroaryl boronic acids.¹⁷⁴ Pyridyl boronic acids and esters have been demonstrated for use in a Rh-catalysed 1,4-additions, with all the substitution patterns tested (nitrogen atom in *ortho*- *meta*- and *para*- position). However the 4-pyridyl derivative appears to be a poor substrate (literature yield of 31%) without an electron donating group on the ring.¹⁷⁴ The 4-pyridylboronate ester was unavailable for purchase, instead the corresponding boronic acid was investigated. However, the pyridyl boronic acid was not tolerated, with no product isolated, suggesting incompatible with these specific reaction conditions (Table 11, entry 8). The reaction was highly stereoselective in every case (>95:<5), with only a single diastereomer observed by *via* 400 MHz NMR spectroscopic analysis of the crude product, which was then isolated.



Entry	Cycloadduct	Arylboronic acid	Product	Yield (%)
1	 85	 139	 140	20 ^{a,b}
2	 85	 141	 142	24 ^{a,b}
3	 85	 143	 144	40 ^{a,b}

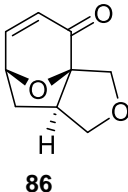
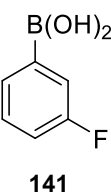
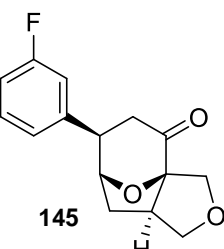
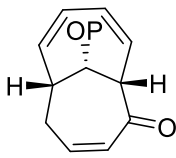
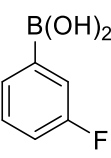
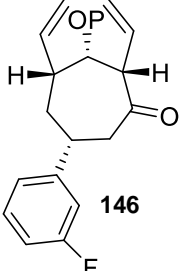
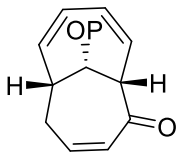
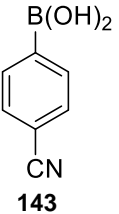
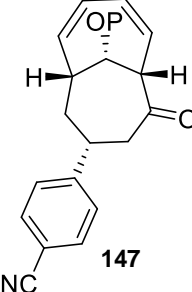
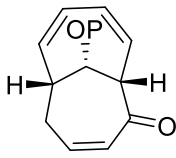
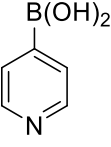
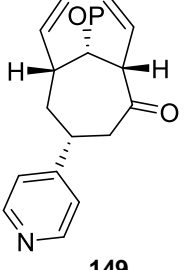
4	 86	 141	 145	49^{a,b}
6	 127	 141	 146	21^{a,b}
7	 127	 143	 147	14^{a,b}
8	 127	 148	 149	<2^c

Table 11: the 1,4-addition series. ^a isolated product, ^b single product isolated, ^c no product isolated
P=TBS

Two different methods were used to ascertain the configuration of the 1,4-addition products. Compounds **140** and **147** were assigned using interactions observed by NOESY NMR spectroscopy (500 MHz), and an X-ray crystal structure was obtained for **145**. For compound **140**, there was a diagnostic interaction observed in the NOESY NMR spectrum (500 MHz), which is highlighted in red (Figure 31, Panel A), as well as a diagnostic splitting pattern on proton 8 shown in blue. This proton appears as a singlet due to the dihedral angles of the two adjacent protons, indicating again that they are on the same face. The if the other diastereomer were present then this dihedral

angle is not possible and thus a different splitting pattern and J values would be observed.

The configuration of compound **145** was unambiguously determined using X-ray crystallography (Figure 31, Panel C). The configuration of the troponone based product **147** was also assigned using a diagnostic interaction observed in the NOESY NMR spectrum (500 MHz), with the two protons involved highlighted in red (Figure 31, Panel B). This key interaction could only be observed in this configuration and therefore they must be on the same face of the molecule.

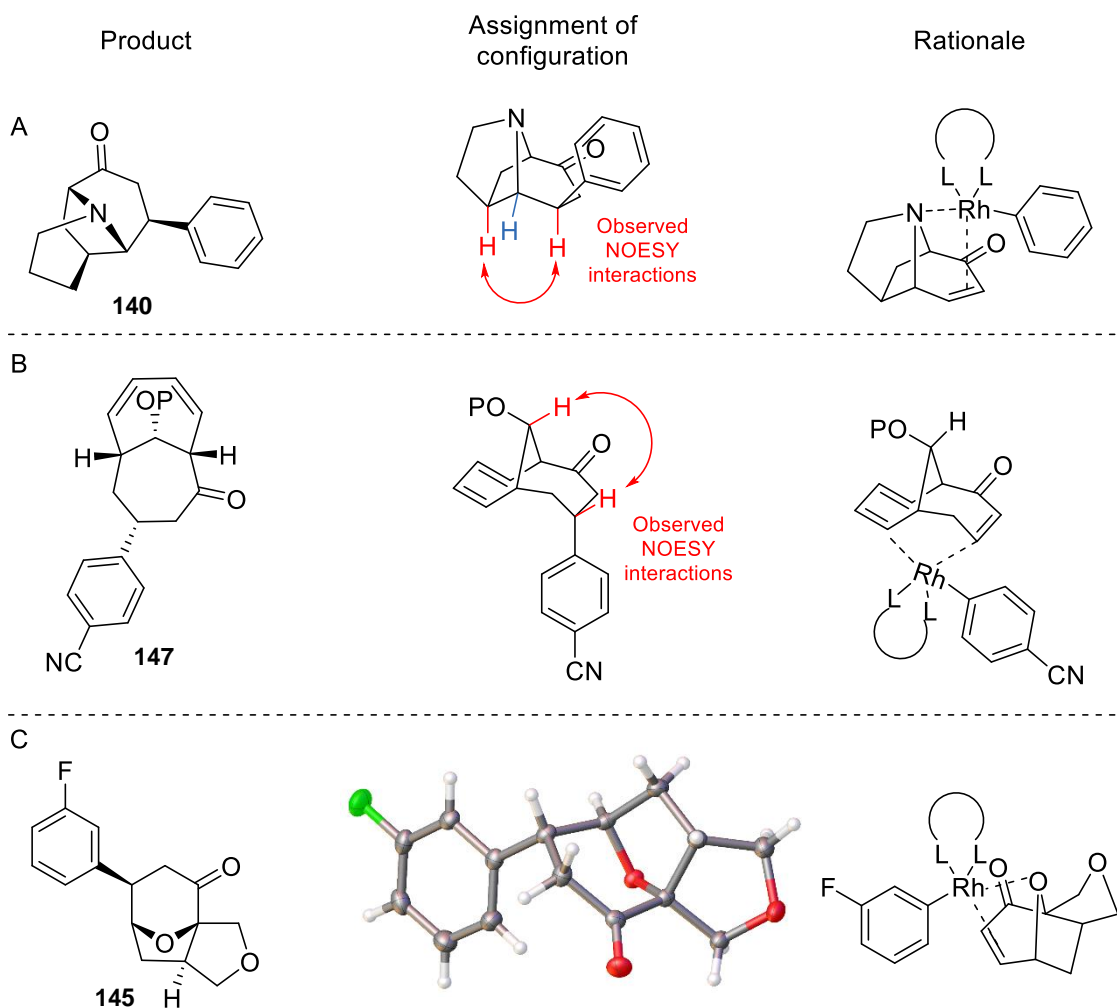
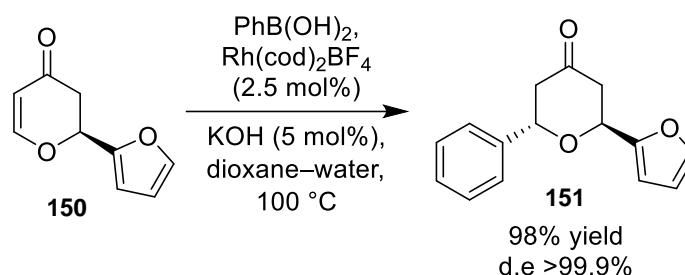


Figure 31: Assignment and rationale for the stereochemistry observed in all three series. Panel A, the product of the 1,4-addition, the NOESY interactions (shown in red) and the rationale for the observed configuration. Panel B, the product from the troponone based scaffold, the observed NOESY interactions (shown in red) and the theorised rationale for this. Panel C, the 1,4-addition product of complex

intermediate **86** and the crystal structure for this compound and the rationale for the observed stereochemistry

Most diastereoselective Rh-catalysed 1,4-additions appear to rely on steric control.^{178–181} For example, in the total synthesis of total synthesis of (–)-diospongins B (Scheme 10).¹⁷⁸ The addition of the ArRh(cod)₂ proceeded from the less hindered R-face of the enone double bond and led to high diastereoselectivity (d.e >99.9%).



Scheme 10: The 1,4-addition used in the synthesis of (–)-diospongins B.¹⁷⁸

Very few examples bridged ring systems with a heteroatom could be found in the literature,¹⁷⁵ most substrate scopes are narrow with only simple cyclic enone ring systems.^{174,180,182,183} The selectivity of this reaction could be explained using the same argument as above, where attack comes from the less hindered face of the enone, past the one atom bridge. One alternative argument could be co-ordination of the Rh complex to the bridgehead heteroatom. This could then direct addition from the top face of the enone (Figure 31). This rationale for selectivity can be applied to both compound **140** and **145**. In the case of the tropone based compound **147** the stereochemical outcome is opposite to the previous cases. As there is no bridging heteroatom for the Rh catalyst to coordinate to, instead it could be postulated that the diene can direct the addition to the bottom face of the enone (Figure 31, Panel C). Which ever argument is most appropriate the outcome of the reaction would be the same.

3.2 Application of ring fusion reactions

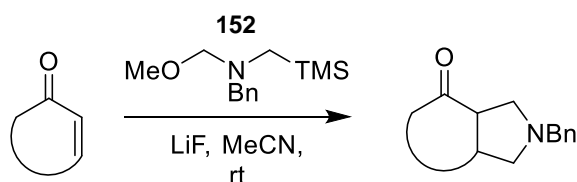
The second approach used in the synthesis of diverse molecular scaffolds was ring fusion, whereby a ring is integrated into the core framework.

This method allows incorporation of biologically relevant rings which have new functional handles. Nitrogen heterocycles are widespread amongst FDA-approved small-molecule drugs, 84% of all small-molecule drugs contain at least one nitrogen atom, and 59% contain at least one nitrogen heterocycle.¹⁸⁴ Several ring fusion reactions were tested utilising both the enone and the ketone and are detailed below.

3.2.1 Pyrrolidine formation *via* a [3+2] dipolar cycloaddition

Out of the FDA approved drugs containing five membered, nonaromatic nitrogen heterocycles, pyrrolidine is the most frequently found.¹⁸⁴ 59% of small-molecule drugs contain a nitrogen heterocycle and therefore are a significant structural feature amongst pharmaceuticals. There are many reported methods for the synthesis of pyrrolidine ring systems,^{185,186} in this case a [3+2] dipolar cycloaddition was selected.¹⁸⁷

The first ring fusion reaction investigated was a [3+2] dipolar cycloaddition between an enone and an azomethine ylide which is generated *in situ*, to achieve the fusion of an *N*-benzyl pyrrolidine ring.¹⁸⁷ This was realised on all three cycloadducts **85**, **86** and **127** by treating the enone and the ylide precursor **152** with LiF in MeCN.¹⁸⁷ The reactions progressed in a range of yields (17-70%, Table 12). The reaction processed a high level of inherent stereoselectivity, with only a single diastereomer (>95:<5) observed *via* 400 MHz NMR spectroscopic analysis of the crude product, which was then successfully isolated.



Entry	Starting material	Product	Yield (%)
1	 85	 153	21 ^a

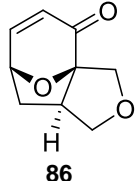
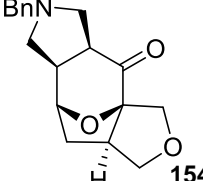
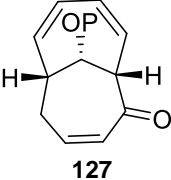
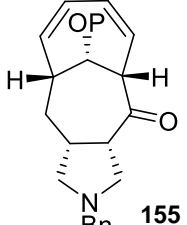
2	 86	 154	70 ^a
3	 127	 155	17 ^a

Table 12: Pyrrolidine synthesis using [3+2] dipolar cycloaddition on all three complex intermediates. P= TBS ^a isolated yields

The configuration of all the products was assigned using interactions observed by NOESY NMR spectroscopy (500 MHz) and analysis of observed coupling constants. For compound **153**, a diagnostic interaction was observed in the NOESY NMR spectrum (500 MHz), which is depicted in red (Figure 32, Panel A), where the two protons interact across the bottom face of the ring, indicating they are on the same face of the molecule. Proton 8 (depicted in blue) appears as a singlet due to the dihedral angles of the two adjacent protons, again, indicating again that they are on the same face. For compound **154**, again, a diagnostic interaction was observed in the NOESY NMR spectrum (500 MHz), the two protons (highlighted in red) have a nOe interaction across the bottom face on the molecule giving the configuration shown below (Figure 32, Panel B). Finally, analysis of the observed coupling constants was used to identify the configuration of the tropone based compound **155** (Figure 32, Panel C). A small coupling constant of 2.2 Hz was measured in the splitting of the two protons depicted in blue consistent with a 'W' arrangement coupling, meaning they must have a *syn* relationship and were assigned as such.

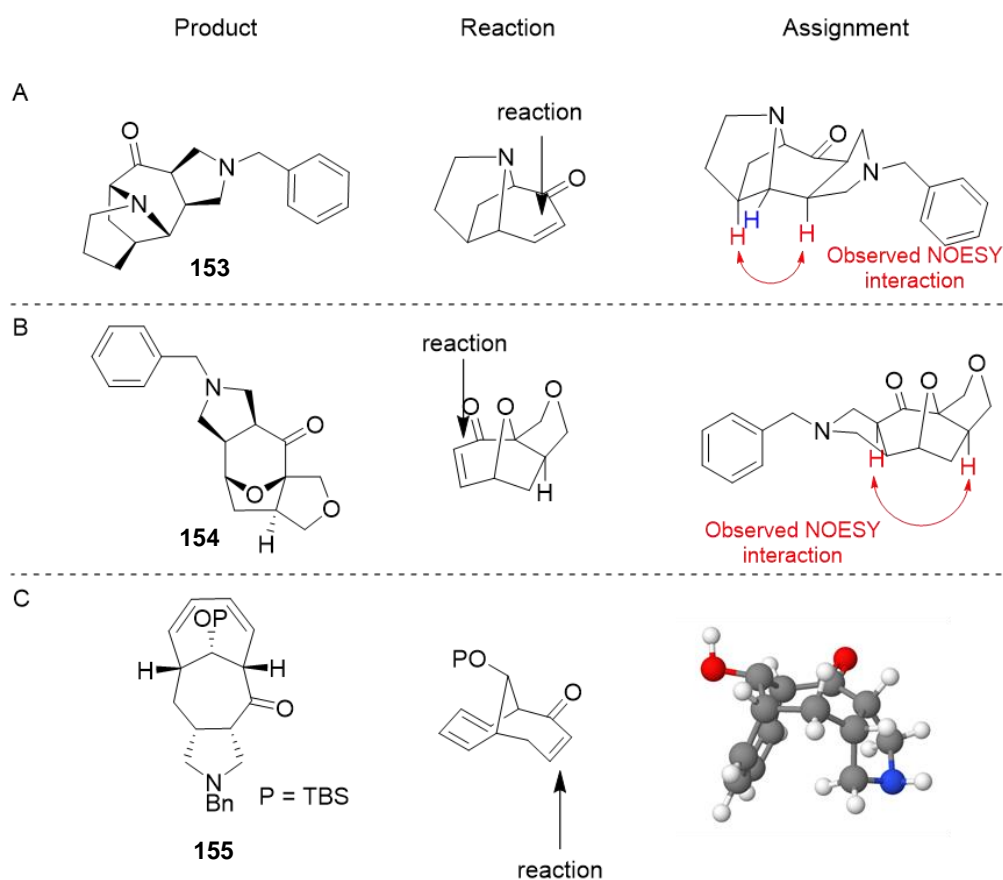


Figure 32: Configuration for the three pyrrolidine scaffolds **153-155**. Panel A the product **153** and assignment of its configuration. Panel B Assignment of the configuration of compound **154**. Panel C The assignment of the configuration of tropane compound **155**. The lowest energy conformation of the pyrrolidine scaffold **155** generated using molview.

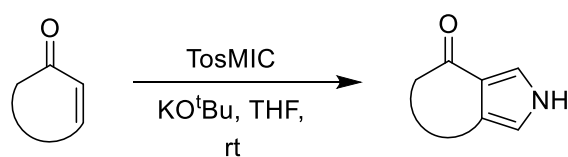
There appears to be a good level of diastereoselectivity in this reaction, with all three complex intermediates forming a single product. From the literature it appears that steric interactions are the influencing factor in diastereoselectivity in these reactions.^{186,188,189} In the case of the three complex intermediates **85**, **86** and **127** the same argument may be applied as rationale for the observed selectivity. It was proposed that the benzyl group imparted stereoselectivity and in the case of compounds **153** and **154** this resulted in attack from the top face of the enone. This was to avoid clashing between the benzyl ring and the protons on the bottom face of the rings. Again, the opposite configuration was observed in the tropane framework **155**, this could be due to the presence of the bulky TBS protecting group have an unfavourable interaction with the benzyl protecting group, favouring attack

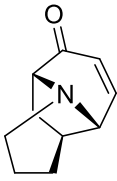
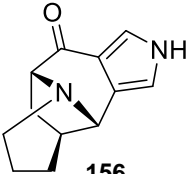
from the bottom face. The same level of stereoselectivity may not be observed if the *N*-benzyl group was replaced with an *N*-methyl group.

3.2.2. Pyrrole formation via a [3+2] cycloaddition

Pyrrole is a framework known to be biologically active, and can be found as a core skeleton in pharmaceuticals and natural products.^{190,191} Therefore, pyrrole containing analogues are considered to be a potential source of biologically active compounds.¹⁹¹ One well reported method of pyrrole fusion is the [3+2] cycloaddition reaction between tosylmethyl isocyanide (TosMIC) with electron-deficient alkenes, known as the van Leusen pyrrole synthesis.¹⁹²

To achieve this Van Leusen cycloaddition the enones **85**, **86** and **127** were treated with potassium *tert*-butoxide and tosylmethylisocyanide (TosMIC) to give the fused pyrroles **156-158**.¹⁹² Though the reaction was successfully applied to all three of the scaffolds (Table 13) the yields of these reactions are low for all the complex intermediates (11-33%). Although the yields of **156-158** are relatively low (24% and 33% respectively) enough material could be generated for decoration as the related starting complex intermediates could be synthesised on scale. In contrast the complex intermediate **127** has a low overall yield coupled with the low yield of the pyrrole (11%, Table 13, Entry 3), suggesting that the tropone framework may not be practical for deprotection and decoration.



Entry	Starting material	Product	Yield %
1	 85	 156	24 ^a

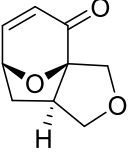
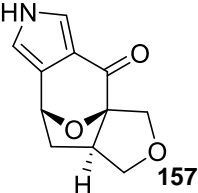
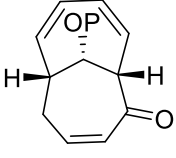
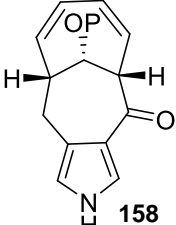
2	 <p style="text-align: center;">86</p>	 <p style="text-align: center;">157</p>	33 ^a
3	 <p style="text-align: center;">127</p>	 <p style="text-align: center;">158</p>	11 ^a

Table 13: Pyrrole synthesis utilising Van Leusen chemistry on all three complex intermediates. ^a isolated yields

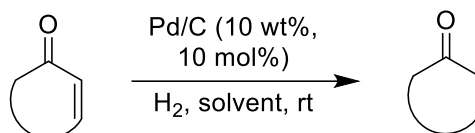
This reaction facilitates the formation of scaffolds which contain two functionalities (ketone and pyrrole N) which can be classed as decoration points. Pyrroles tend to have lower stability towards acids and heat unless they are conjugated with an electron withdrawing group either on the nitrogen or the carbon. Therefore, before decoration on the ketone can take place, an appropriate group must be placed on the nitrogen.

3.2.3 Gold catalysed pyridine formation

As well as diversity, control over the number of aromatic rings in molecular frameworks is important. Pyridine rings are present in many natural products including vitamins such as vitamin B6. One role pyridine plays in medicinal chemistry is to help improve solubility.¹⁹³ There are many reported methods for pyridine formations, most methods are rarely utilised due to the lack of generality and/or selectivity.^{194,195} The conditions selected for formation of the pyridine utilises a ketone and propargyl amine, therefore, the C-C double bond of the enones **85** and **86** must be reduced.

The enones **85** and **86** were treated with palladium on carbon (10 wt%) and hydrogen to achieve the reduction to the ketones (Table 14). Methanol was used as the solvent for the hydrogenation of enone **85** giving the ketone in an 87% yield (Table 14, Entry 1), and was initially chosen for the reduction of enone **86**. However, in this case the use of methanol resulted in formation of both the ketone and the acetal in a ca 60:40 ratio (Table 14, Entry 2). To

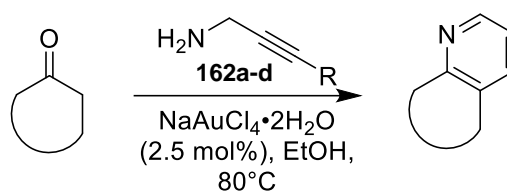
avoid this problem, ethyl acetate was used as the solvent, giving the ketone **161** in an 83% yield (Table 14, Entry 3).



Entry	Starting material	Solvent	Product	Yield %
1	 85	MeOH	 159	87 ^a
2	 86	MeOH	 160 1.0 : 0.7 161	81 ^b
3	 86	EtOAc	 161	83 ^a

Table 14: Hydrogenation conditions for the reduction of the enone. ^a isolated yields ^b isolated mixture of compounds

With the ketones **159** and **161** in hand, the pyridine formation reaction could be applied. The ketones **159** and **161** were treated with sodium tetrachloroaurate (2.5 mol%) and the relevant propargyl amine at 80 °C.¹⁹⁵ When treated with propargyl amine (Table 15, Entry 1) ketone **85** gave the pyridine **163** in a 42% yield. However, when the alkyne was terminally substituted (Table 15, Entries 2 and 3) the reaction was unsuccessful with no product observed *via* LC-MS or 500 MHz NMR spectroscopic analysis of the crude product. Ketone **161** gave pyridine **166** in a 13% yield when reacted with propargyl amine.

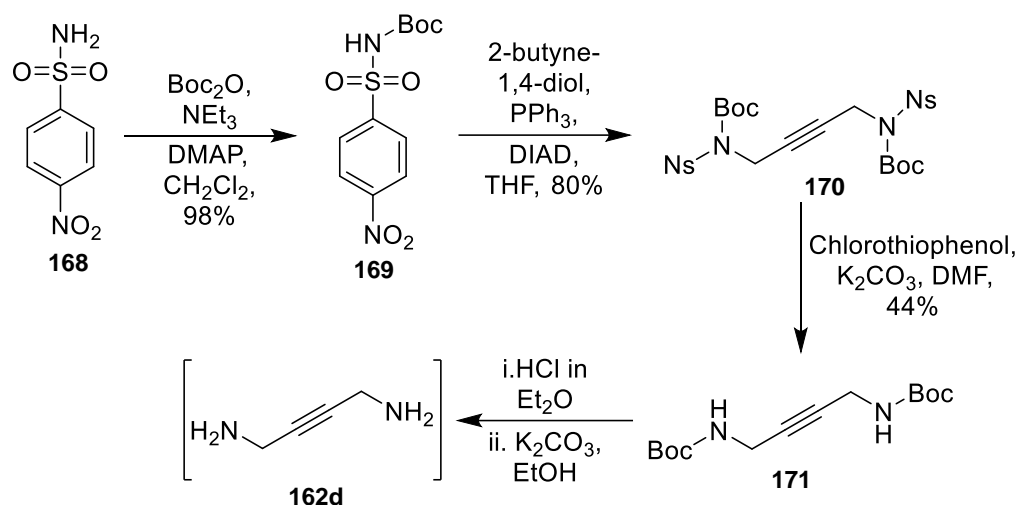


Entry	Starting material	R =	Product	Yield %
1		162a- H		42 ^a
2		162b- Me		<2 ^b
		162c- Ph		<2 ^b
3		162a- H		13 ^a
		162d- CH ₂ NH ₂ ^c		<2 ^b

Table 15: the ketones used in the gold catalysed pyridine formation. ^a isolated yields ^b no product isolated ^c preparation of reagent found in Scheme 11.

The symmetrical propargyl amine **162d** was synthesised in an attempt to create a functionalised pyridine. 4-nitrobenzenesulfonamide **168** was treated with di-*tert*-butyl dicarbonate with triethylamine to give the *bis* protected amine **169** in a 98% yield (Scheme 11). With the amine **169** in hand a Mitsunobu reaction was then accomplished by treating amine **169** with diisopropyl azodicarboxylate (DIAD) and triphenyl phosphine to give the diamine **170** in an 80% yield.¹⁹⁶ Removal of the *p*-nitrobenzenesulfonyl group was achieved by treating the diamine **170** with two equivalents of 4-chlorothiophenol to yield the mono protected diamine **171** in a 44% yield. Finally, the Boc group was removed using HCl in diethyl ether to yield the HCl salt which was then desalted to reveal the diamine **171** in situ and used crude in the pyridine forming reaction. Treatment of the ketone **161** with the

symmetrical diamine **172** resulted in no evidence of product formation via LC-MS or 500 MHz NMR spectroscopic analysis of the crude product.



Scheme 11: the synthetic route undertaken to achieve the synthesis of the symmetrical diamine **172**.

In summary the ring fusion approach has been successfully applied with three different ring fusion reactions applied to the selected complex intermediates and as a result 8 new scaffolds were successfully synthesised. The ring fusion chemistry appears to be a robust way to create new frameworks and install new functional handles for subsequent decorations.

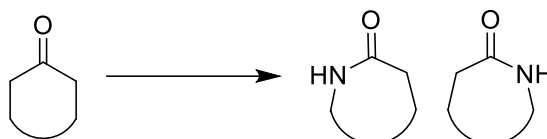
3.3 Application of ring expansion chemistry

The penultimate tactic utilised in the 'top-down' approach was ring expansion chemistry. Ring expansions are a valuable tool in synthetic chemistry as they allow access to larger ring systems. For example, in the pyridyl complex intermediate **85** it would allow access to an eight membered ring. Ring expansion through addition of a heteroatom also has value, as other methods for incorporation may require a de-novo synthesis.

3.3.1 Testing of the Beckmann ring expansion

Firstly, the Beckmann ring expansion was investigated this will allow an increase of ring size of the core framework. The bond migration step involved in this ring expansion can be achieved under both acid and basic conditions. Both ketones **159** and **161** were exposed to the acidic and basic conditions (Table 16). Under all the conditions listed the formation of the

tosylated oxime intermediate was observed via LC-MS. However, there was no evidence of product formation by LC-MS or 500 MHz NMR spectroscopic analysis of the crude product. This could be due to the desired bond migration not taking place under the conditions investigated, or further fragmentation resulting a complex mixture of products.

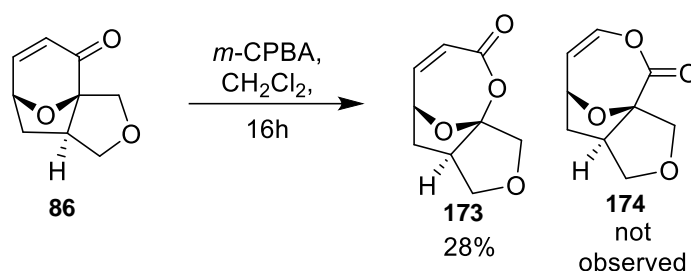


Entry	Starting material	Conditions	Yield %
1	159	i. $\text{NH}_2\text{OH}\cdot 2\text{H}_2\text{O}$, K_2CO_3 , H_2O - EtOH (1:1), reflux ii. TsCl , NEt_3 , DMAP, CH_2Cl_2 iii. H_2SO_4 , EtOH	<2 ^a
2	159	i. $\text{NH}_2\text{OH}\cdot 2\text{H}_2\text{O}$, NaOH , H_2O , EtOH , rt then reflux ii. DME, H_2O , TsCl , K_2CO_3 , 82 °C	<2 ^a
3	161	i. $\text{NH}_2\text{OH}\cdot 2\text{H}_2\text{O}$, K_2CO_3 , H_2O - EtOH (1:1), reflux ii. TsCl , NEt_3 , DMAP, CH_2Cl_2 iii. H_2SO_4 , EtOH	<2 ^a
4	161	i. $\text{NH}_2\text{OH}\cdot 2\text{H}_2\text{O}$, NaOH , H_2O , EtOH , rt then reflux ii. DME, H_2O , TsCl , K_2CO_3 , 82 °C	<2 ^a

Table 16: the conditions investigated for the Beckmann ring expansion ^a no product isolated

3.3.2 Application of the Baeyer-Villiger ring expansion

The reaction of this substrate of this substrate with *m*-CPBA was studied. Although it had been hoped to secure the corresponding epoxide in fact the Baeyer-Villiger ring expansion took place instead, resulting in the formation of the lactone **173** (Scheme 12). Only one of the two possible regioisomers was isolated in a 28% yield.



Scheme 12: The Baeyer-Villiger ring expansion of the cyclic enone **86**.

In the case of compound **86**, it can be assumed that the differentiating feature in this compound is the bridged oxygen atom. The inductive effect of the bridge oxygen must be outweighed by a favourable resonance effect, which can effectively stabilise the build-up of a partial positive charge at the migrating bridgehead atom, thus making it the preferred migratory group.²⁰⁰

In this case ^{13}C NMR spectroscopy was used to identify which regio-isomer was formed. The observed chemical shift of the carbonyl has changed from 194 ppm in the starting material to 165 ppm in the isolated product, which is diagnostic for an ester, confirming the ring expansion has indeed proceeded (Figure 33). The observed chemical shift for the quaternary carbon centre of the hemiacetal is 118 ppm. If the other regio-isomer had formed the shift of this carbon would be significantly lower, which is predicted to be 79 ppm.

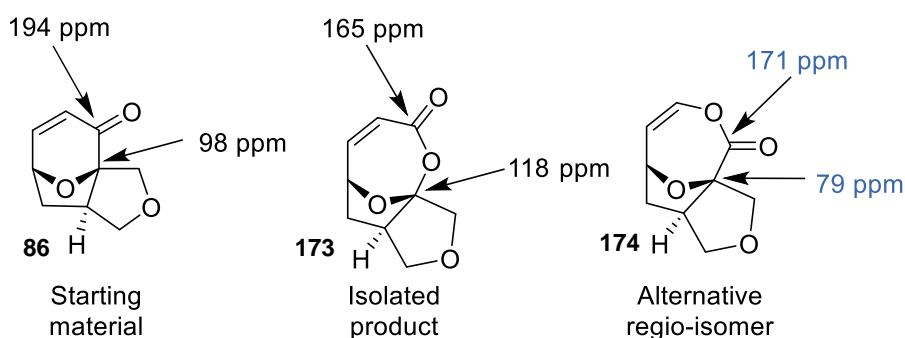
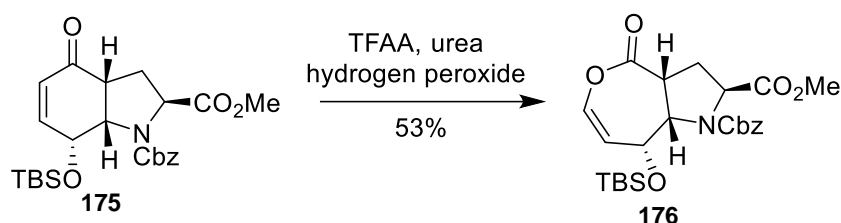


Figure 33: the ^{13}C NMR chemical shifts for the ring expansion. The shifts reported in black are observed chemical shifts and those in blue are predicted chemical shifts using nmrdb.org.

There are limited examples of the successful application of the Baeyer-Villiger to enone substrates,^{197–199} and none could be found with the same substitution on either side of the enone. The closest literature reaction found is shown below, whereby compound **175** undergoes the Baeyer-Villiger ring

expansion (Scheme 13).¹⁹⁷ In this case the alkene migrates preferentially over the tertiary carbon centre. The alkene is also seen to migrate when a methylene group is alpha to a ketone, though this is unsurprising as a methylene group is known to have a lowest migratory aptitude.^{198,199}



Scheme 13: The Baeyer-Villiger ring expansion of compound **175**.¹⁹⁷

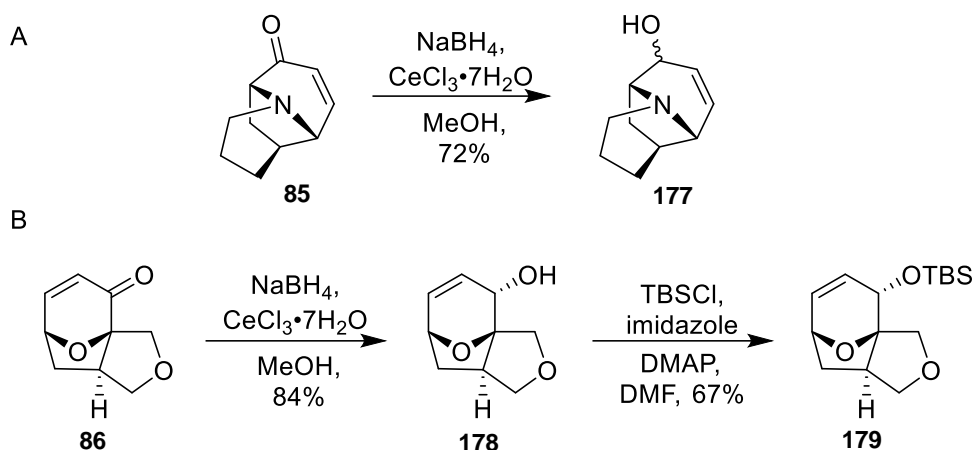
3.4 Application of ring cleavage chemistry to the complex intermediates

The final tactic investigated was ring cleavage reactions, which is a fundamentally more challenging approach, as carbon-carbon bonds are not easily broken.²⁰¹ Ideally, different bonds would be cleaved at different positions in the complex intermediates within the fused ring systems to allow access to new distinct frameworks.

3.4.1 Cleavage of the enone C-C double bond

The first ring cleavage approach investigated was cleavage of the carbon-carbon double bond of the enone. It was envisaged that this would be a more challenging approach than the previous two tested, so the reactions were initially tested on the complex intermediates **85** and **86** to preserve material on the low yielding tropone intermediate **127**. Different methods were identified from the literature and investigated (Table 17).

The first method selected was a dihydroxylation and periodate mediated cleavage. The enones **85** and **86** were treated with sodium borohydride and cerium (III) chloride heptahydrate to yield the corresponding allylic alcohols **177** and **178** in 72% and 84% yield respectively (Scheme 14). Allylic alcohol **178** was then treated with *tert*-butyldimethylsilyl chloride, DMAP and imidazole to give the TBS protected alcohol **179** in a 67% yield (Panel B, Scheme 14).



Scheme 14: formation of the allylic alcohols. Panel A reduction of complex intermediate **85** and **86** with NaBH_4 and $\text{CeCl}_3 \cdot 7\text{H}_2\text{O}$. Panel B formation and TBS protection of allylic alcohol **179**.

The enones (**85** and **86**) and the corresponding allylic alcohols (**177** and **178**) were treated with osmium tetroxide and sodium periodate (Table 17, Entries, 1,2,4 and 5). In the case of enone **85** and allylic alcohol **177**, the reaction resulted in a complex mixture of products; however, the potential diketone products could be unstable. In an attempt to isolate products, benzyl amine was added to the reaction after the periodate cleavage. However, there is a second advantage to this approach which was to achieve a ring expansion (Table 17, Entry 4) or insertion of a heteroatom into the ring (Table 17, Entry 5). Unfortunately, no product was observed *via* LC-MS or 500 MHz NMR spectroscopic analysis of the crude product.

An alternative method for cleavage of the double bond was ozonolysis. To achieve this the TBS protected allylic alcohol **179** was treated with ozone, which was generated *in situ*, followed by treatment with sodium borohydride. There was a complex mixture of products and the desired product could not be detected *via* LC-MS or 500 MHz NMR spectroscopic analysis of the crude product.

Entry	Starting material	Conditions	Yield %
1	85	OsO ₄ (2.5% in tBuOH), 2,6-lutidine, NaIO ₄ , dioxane-water (3:1) ²⁰²	<2 ^a
2	177	OsO ₄ (2.5% in tBuOH), 2,6-lutidine, NaIO ₄ , dioxane-water (3:1) ²⁰²	<2 ^a
3	177	Ru/C (1mol%), NaIO ₄ , MeCN-EtOAc-water (1:1:1) ²⁰³	<2 ^a
4	86	i. OsO ₄ (4% in water), NaIO ₄ , 2,6-lutidine, dioxane-water (3:1) ²⁰² ii. benzylamine, MeOH iii. NaBH ₄ , MeOH	<2 ^a
5	178	i. OsO ₄ (4% in water), NaIO ₄ , 2,6-lutidine, dioxane-water (3:1) ²⁰² ii. benzylamine, MeOH iii. NaBH ₄ , MeOH	<2 ^a
6	179	i. Ozone, CH ₂ Cl ₂ , -78 °C ²⁰⁴ ii. NaBH ₄ , MeOH	<2 ^a

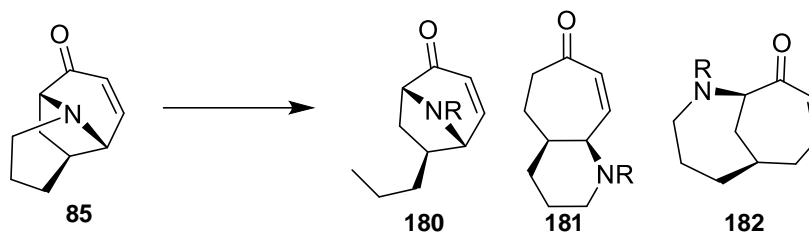
Table 17: conditions investigated for the cleavage of the enone C-C double bond. ^a no product isolated

As this approach to cleaving the C-C double bond of the enone was unsuccessful, instead a different approach was selected. The Eschenmoser fragmentation was considered for cleave of the scaffold **86**. Previously, it has been shown that *m*-CPBA achieved the Baeyer-Villager ring expansion, therefore nucleophilic epoxidation conditions were investigated using dihydrogen peroxide and sodium hydroxide in methanol. Unfortunately, there was no evidence of product formation and the required epoxy ketone substrates could not be synthesised.

3.4.2 Cleavage of a C-N bond

A range of methods have been reported for the activation of tertiary amines and subsequent fragmentation.^{205–207} Complex intermediate **85** contains three C-N bonds and with no examples found on such complex frameworks it was unknown which C-N bond would break preferentially under

the investigated conditions. Tertiary amine **85** has three possible products from bond cleavage which can be seen below (Scheme 15).



Scheme 15: The three possible products of the C-N bond cleavages.

The enone **85** was treated with a range of different conditions (Table 18) to facilitate the cleavage of a C-N bond. All but one of the conditions tested resulted in no observable reaction *via* LC-MS and 500 MHz NMR spectroscopic analysis of the crude product.

Entry	Conditions used for cleavage of 85	Yield %
1	Boc ₂ O, FeCl ₂ (10 mol%), ^t BuOOH, MeCN 85 °C, 1 h ²⁰⁵	<2 ^a
2	Boc ₂ O, FeCl ₂ (10 mol%), ^t BuOOH, MeCN 85 °C, 6 h ²⁰⁵	<2 ^a
3	Cyclopropane carboxaldehyde, FeCl ₂ (10 mol%), ^t BuOOH, MeCN, 85 °C, 6 h ²⁰⁵	<2 ^a
4	CbzCl, DCE, reflux, 16 h ²⁰⁶	<2 ^a
5	i. Benzyl bromide, MeCN, reflux, 16 h ²⁰⁷ ii. TES, THF reflux	<2 ^a
6	i. MeI, acetone, rt 2 h ²⁰⁷ ii. TES, THF reflux	<2 ^a
7	Allyl chloroformate, K ₂ CO ₃ , toluene, 16 h ²⁰⁶	<2 ^a
8	2,2,2-trichloroethyl chloroformate, K ₂ CO ₃ , reflux, toluene, 16 h ²⁰⁶	183 , 8 ^b

Table 18: the conditions screened for the cleavage of a C-N bond. ^a no product isolated ^b isolated yield

Treatment of the enone **85** with 2,2,2-trichloroethyl chloroformate and K_2CO_3 gave the protected alkyl chloride compound **183** in an 8% yield. A single product was isolated, the C-N bond broken resulted in a chloropropyl chain (Figure 34). The C-N bond cleaved in this case does not change the ring structure as the ring is still bridged. However, this bond cleavage has revealed two other points of decoration within the molecule, including the bridged nitrogen.

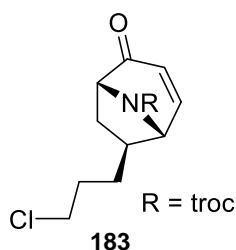
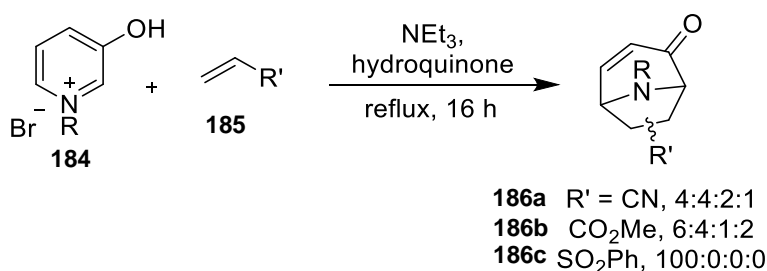


Figure 34: the product isolated from the ring cleavage reaction.

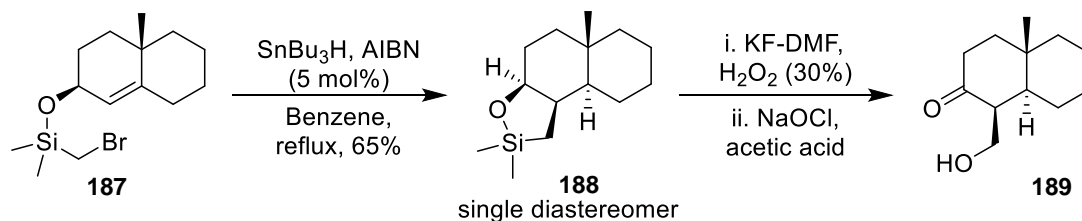
This bond cleavage allows an alternative route to access to a framework which can be made via a [5+2] cycloaddition reaction with dipolarophiles **185** and a pyridinium salt **184** (Scheme 16). However, the regio- and stereo- selectivity of the reaction is very poor unless the dipolarophile has a sterically demanding group attached for example the phenyl vinyl sulfone, therefore this new route allows access to the same framework with stereo and regio control.



Scheme 16: the [5+2] cycloaddition route allowing access to the same framework.

This is a complementary method to that developed by Stork, whereby a temporary silicon tether (TST) aids in the formation of a regiospecific and stereoselective carbon-carbon bond.²⁰⁸ This approach works by using a removable silicon atom to bring two reactive partners into proximity. This approach was initially developed for controlling the stereochemistry of radical reactions (Scheme 17), for example to form a trans decalin ring system **188**.²⁰⁸

This method has also been proved effective in a number of ionic, photochemical and cycloaddition reactions.^{208–210}



Scheme 17: The use of Stork's TST to control the stereochemistry of a radical addition to form a trans decalin ring.²⁰⁸

Another framework where cleavage of a C-N bond is possible is the benzo-fused complex intermediate **135**. This compound contains a benzylic C-N bond which has the potential to be cleaved under hydrogenation conditions. Compound **135** was treated with palladium hydroxide on carbon and hydrogen and produced a single compound in a 93% yield (Figure 35, Panel A). Unfortunately, this was not the product of a bond cleavage, instead the ketone was reduced to the alcohol. The stereochemistry of the alcohol was assigned using NOESY NMR spectroscopy (500 MHz), the diagnostic interaction is highlighted in red (Figure 35, Panel B).

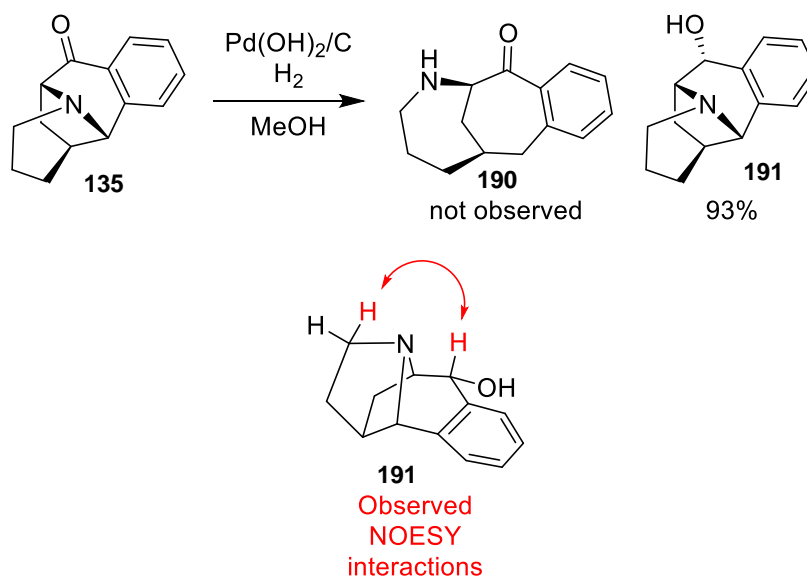
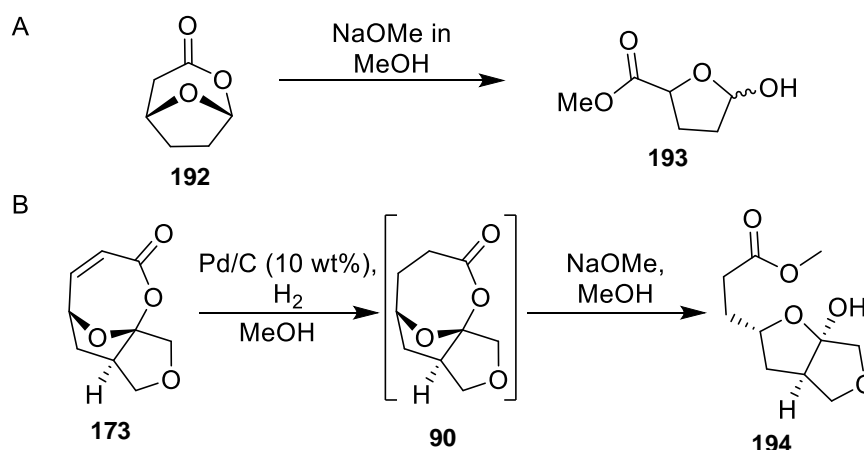


Figure 35: the hydrogenation of compound **135**. Panel A, the conditions used in the attempted C-N bond cleavage which resulted in reduction of the ketone. Panel B the diagnostic NOESY NMR (500 MHz) interactions highlighted in red.

3.4.3 Attempted cleavage of the lactone

The final ring cleavage attempted was cleavage of the lactone produced via ring expansion (Section 3.3.2). Cyclic acetals are present in natural products, for example, Pinnatoxin. However this functionality provides a good opportunity to break open a ring as most acetals can be easily cleaved. Initially, hemiacetal **173** was treated with palladium on carbon and hydrogen to reduce the double bond producing lactone **90**. This compound was not isolated and instead carried forward into the next reaction. Using the conditions detailed by Wege²⁰⁰ (Scheme 18, Panel A), compound **194** was treated with sodium methoxide in methanol (Scheme 18, Panel B). However, no product was identified *via* 500 MHz NMR spectroscopic analysis of the crude product.



Scheme 18: cleavage of lactones using sodium methoxide. Panel A the literature conditions detailed by Wege.²⁰⁰ Panel B attempted cleavage of the lactone **173**.

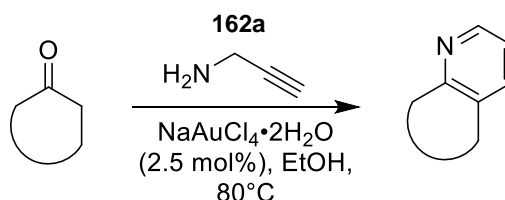
Unfortunately, the ring cleavage tactic utilised in the ‘top-down’ approach has been very challenging and not as productive as desired. From this approach only one scaffold was produced, despite multiple attempts.

3.5 Synthesis of scaffolds using two approaches

Some of the scaffolds already prepared were themselves useful intermediates for the synthesis of further scaffolds. The combination of approaches offers access to a unique assembly of ring systems.

3.5.1 Ring addition followed by ring fusion

The previously described 1,4-addition reaction proved an efficient method of installing an aromatic ring within the molecules (Section 3.1.1). However, the scaffolds formed using the 1,4-addition reaction are themselves interesting substrates for the gold catalysed pyridine formation as the ketone functional handle remains. Using the conditions described previously, the ketones were treated with sodium tetrachloroaurate (2.5 mol%) and propargyl amine at 80 °C (Table 19).¹⁹⁵ Four pyridine compounds were successfully isolated in a range of yields (21–73%). This combination of approaches allows two aromatic rings to be incorporated into the framework in distinct ways.

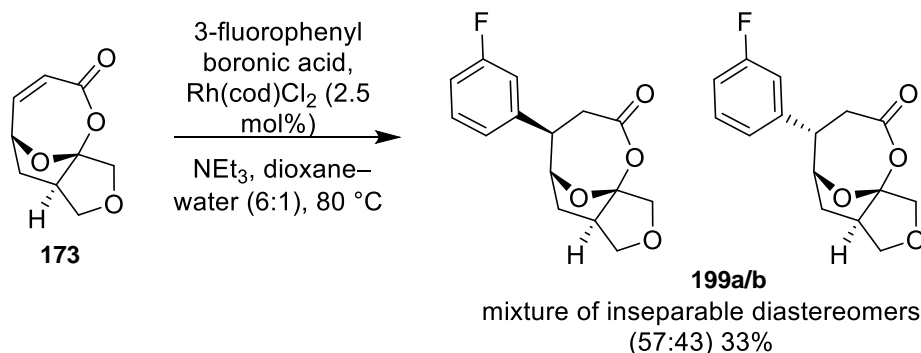


Entry	Starting material	Product	Yield %
1			40
2			25
3			73
4			21

Table 19: Pyridine formation as a decoration reaction.

3.5.2 Ring expansion followed by ring fusion

For compound **173** to be considered as a screening compound it was important to remove the reactive Michael acceptor as per the lead-like guidelines.³⁹ Therefore, the Rh-catalysed 1,4-addition was selected as this method has proved effective on a number of different frameworks (Section 3.1.1) and effectively removes the Michael acceptor functionality. The enone **173** was treated with the cyclooctadiene rhodium chloride dimer (2.5 mol%) and the appropriate aryl boronic acid (5.0 eq.) and the reaction was heated overnight¹⁷³ giving the desired product as an inseparable mixture of diastereomers (*d.r* 57:43, Scheme 19). This scaffold does not exhibit the same selectivity observed in the previous scaffolds (Section 3.1.1) suggesting a reduced directing effect from the bridged heteroatom.



Scheme 19: 1,4-addition addition of the ring expanded product **173**.

3.6 Summary and analysis of the synthesised scaffolds

3.6.1 Summary of scaffolds synthesised

Despite the limited success with the final two approaches a total of 21 scaffolds was synthesised (Figure 36). Some of the synthesised scaffolds have more synthetic utility than others. For example, the pyridine scaffolds **195** – **198** have no remaining functional handles for decoration but can serve as final library compounds. Each complex intermediate gave rise to four or more scaffolds in a single step creating a diverse range of frameworks.

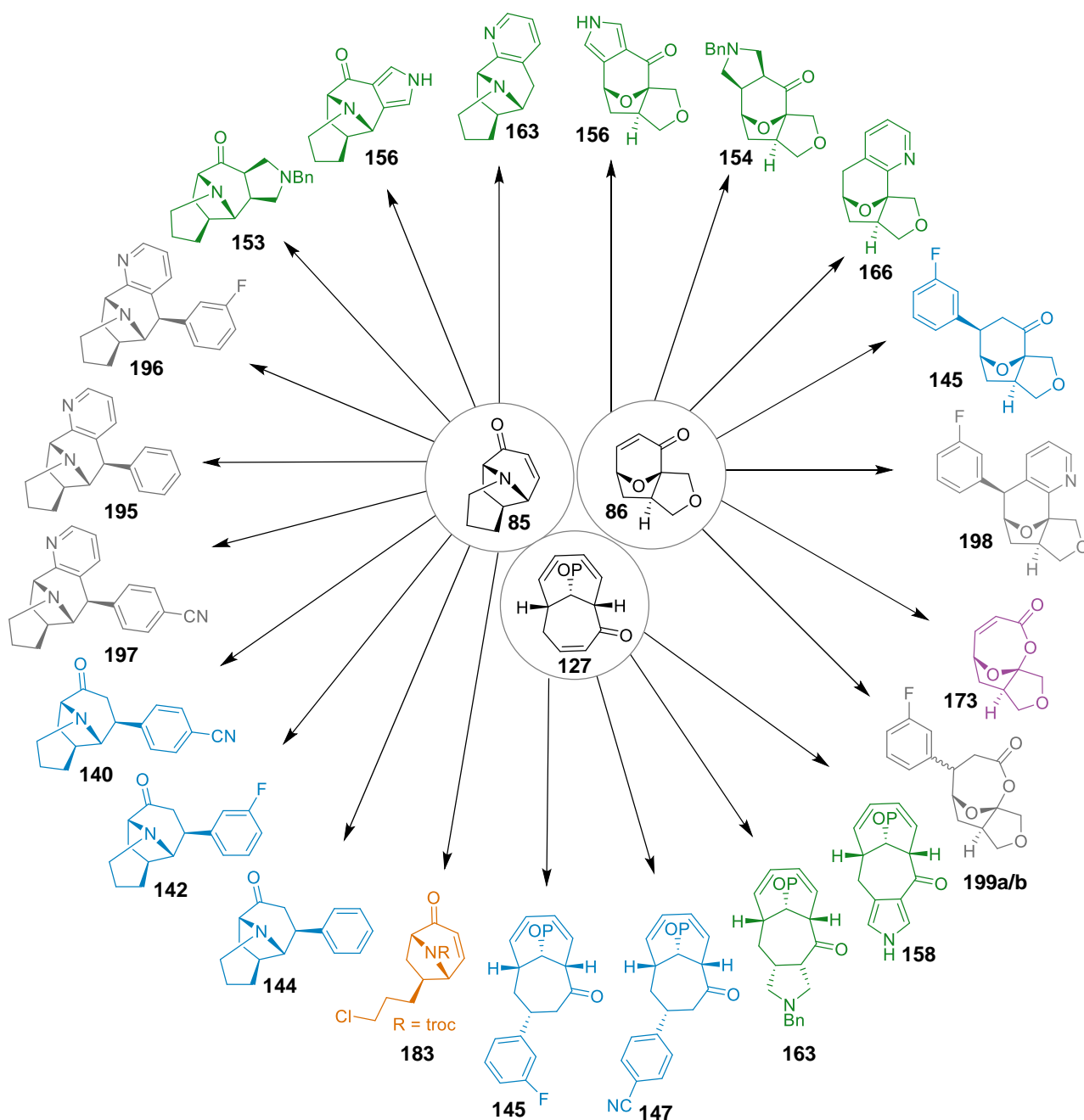


Figure 36: the 21 scaffolds synthesised using all three complex intermediates. The colour indicates the method used in their synthesis; blue – ring addition, green – ring fusion, purple – ring expansion, orange – ring cleavage and grey – combined approach. P=TBS

3.6.2 Novelty assessment of synthesised scaffolds

Computational assessment, namely LLAMA²¹¹, was used evaluate the novelty of the scaffolds synthesised. The Murcko frameworks (and alpha attachments) were generated by LLAMA and searched against a random 2% of the Murcko assemblies of the ZINC database. Although 2% is a small proportion of the library an appreciation for novelty could still be understood

and comparison to a larger subset of compounds from the database would be more computationally demanding. To generate the Murcko framework, all the side chains are removed from a molecule, leaving the ring systems and any linking atoms between them (Figure 37).²¹² A Murcko framework which still contain alpha-attachments details the locations of substitutions from the rings. All but one of the scaffolds synthesised in this chapter are novel with no compounds containing the same framework. The only Murcko assembly derived from compound **183** was found as a substructure match (7 hits).

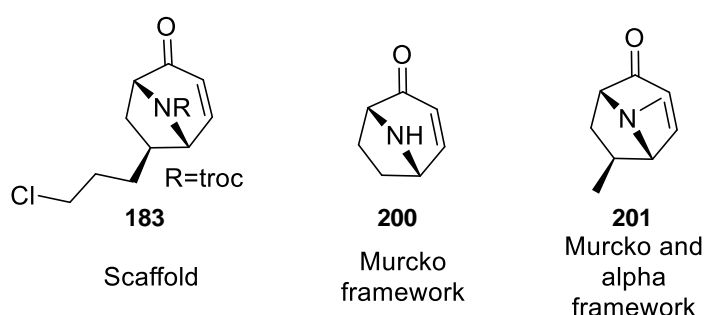


Figure 37: The only compound and its resulting Murcko frameworks that returned a hit from a random 2% of the ZINC database.

3.6.3 Diversity assessment of the scaffolds

The skeletal diversity and relationship between the different scaffolds were assessed using a 'scaffold tree'. This hierarchical method of analysis was developed by Waldmann and applies a set of prioritisation rules to the graph-node-bond (GNB) frameworks which deconstructs the scaffolds via iterative removal of rings until the final parent ring system is reached. These rules were applied to all 21 scaffolds.²¹³ It was found that the 21 compounds analysed were ultimately related to nine parent frameworks (Figure 38). The number of parent rings is significant as all the compounds synthesised are derived from just three complex intermediates. The tropane based scaffolds appeared to be the least diverse with just a single parent ring system, which is due to the diene remaining unmodified in all the compounds.

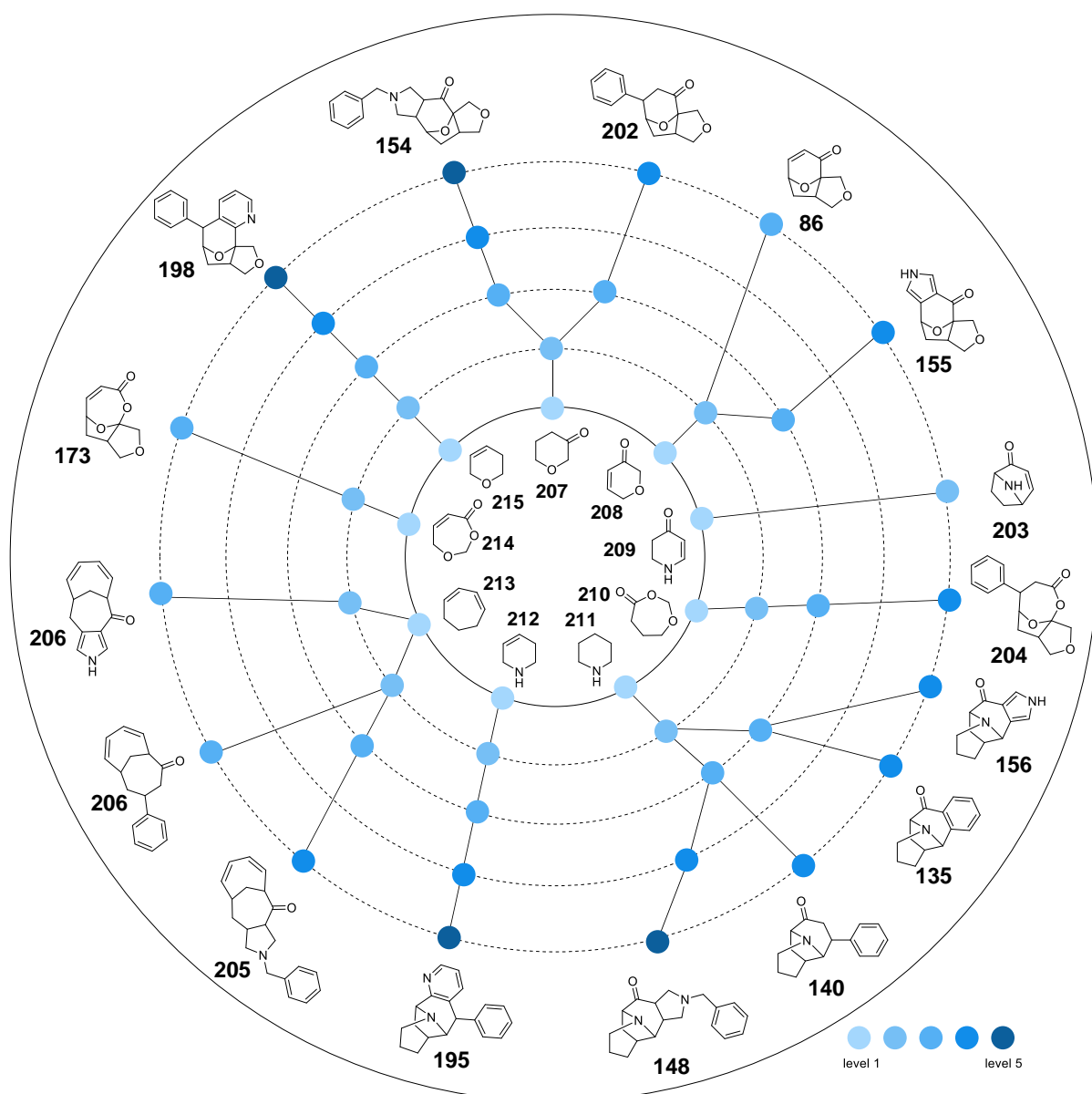


Figure 38: The 'scaffold tree' developed using Waldmann's hierarchical method of analysis showing the nine parent ring systems. The colour of the circles depicts how many iterations was required to reach the parent ring system.

3.6.4 Conclusions

Four different tactics in the application of the 'top-down' approach to the synthesis of diverse scaffolds have been applied successfully to three different complex intermediates. The first approach, ring addition, was successfully applied to all three complex intermediates yielding a total of six new scaffolds in a selective reaction in varying yields. Ring fusion was also a successful approach creating fused pyrroles, pyrrolidines and pyridine ring

systems, again these reactions were applied to the three complex intermediates. These reactions created a total of eight novel scaffolds.

The last two tactics employed in the top-down approach were more synthetically challenging and as a result much less successful. The Baeyer-Villiger ring expansion was the only successful reaction applied to complex intermediate **86**, yielding the only ring expanded product. Despite screening numerous ring cleavage conditions only one successful reaction was identified, which could only be applied to complex intermediate **85**.

Finally, a few of the scaffold forming approaches were successfully combined, as some of the scaffolds formed provided unique starting points for further reactions. The scaffolds formed from the 1,4-addition were ideal for the pyridine ring fusion reaction. This successfully provided access to a further four scaffolds. The only scaffold formed from the ring expansion approach was also a good substrate for the ring addition reaction. Again, this combination of approaches provided access to another novel framework.

A total of 21 scaffolds have been synthesised, all but one was found to contain novel Murcko frameworks. The only compound with a known Murcko framework had a very low number of hits. The scaffold set was assessed as diverse and are derived from nine parent frameworks despite originating from just three complex intermediates. The 'top-down' approach appears to be an efficient method for generating a diverse set of molecular scaffolds.

Chapter 4 Design and preparation of a library of decorated lead-like scaffolds.

Assessment of biological relevance of the diverse scaffolds would require conversion into a suitable series of screening compounds. This will be achieved via decoration of the scaffolds with a medically relevant capping group. Each functional handle will be decorated separately to ensure synthetic expedience and to ensure that the molecules fall within lead-like chemical space. The use of diverse set of different capping groups will allow for the exploration of different vectors of the scaffold molecules. Finally, the molecular properties and shape diversity of the prepared screening compounds were also assessed to determine the success of the 'top-down' approach.

4.1 Selection of scaffolds for decoration

When considering which scaffolds should be decorated it was decided to focus on scaffolds prepared from **85** and **86** because the synthesis was more practical. Therefore, a finalised list of eight synthesised scaffolds (Figure 39) was compiled and these were taken forward for scaffold decoration. Some scaffolds, for example compound **153**, contains more than one functional handle and thus could be decorated more than once. It was decided that these functional handles should both be decorated separately. The benzo-fused complex intermediate **135** was also selected for decoration to generate screening compounds.

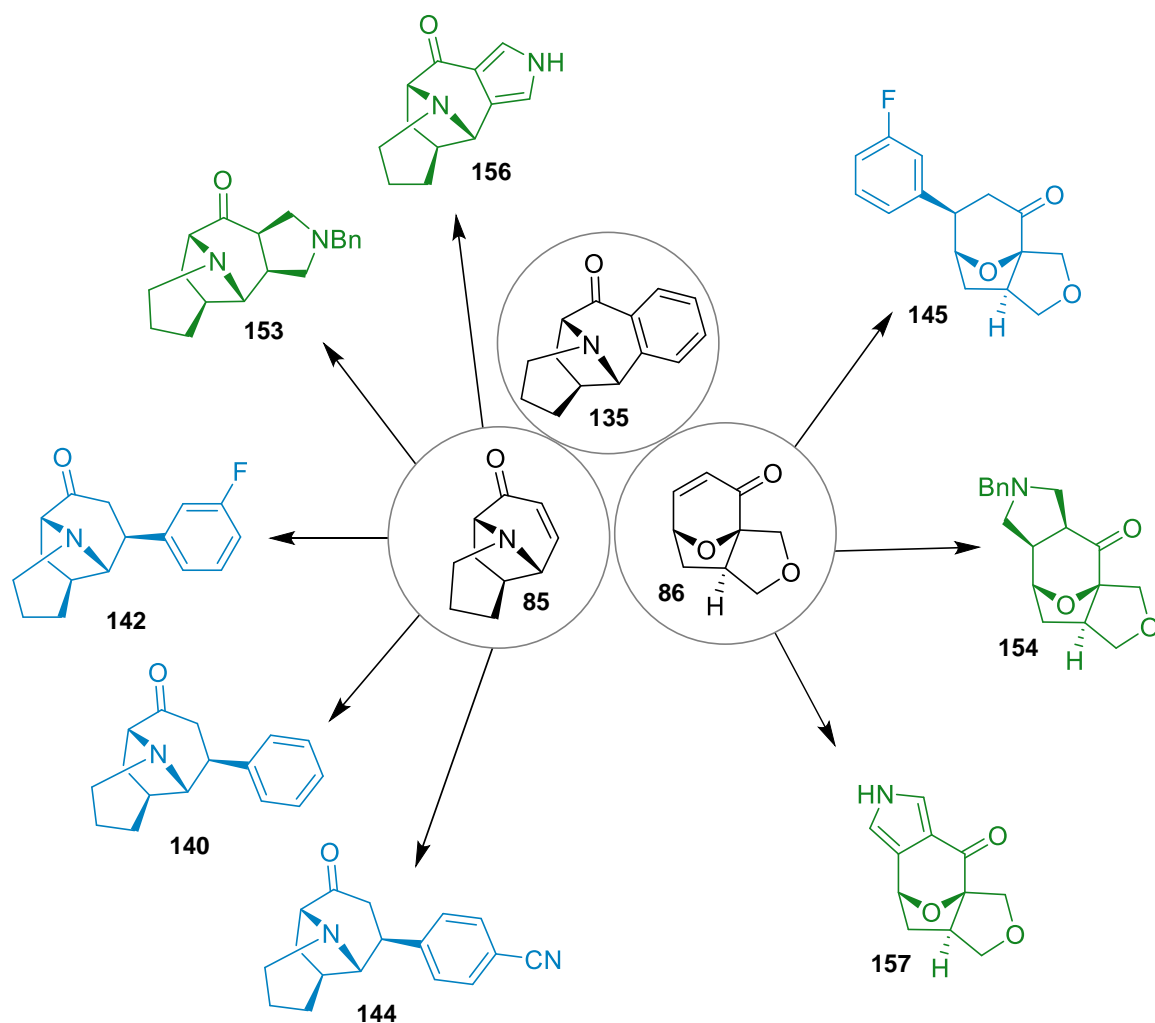


Figure 39: The eight scaffolds and complex intermediate selected for decoration. The colour indicates the method used in their synthesis; blue – ring addition and green – ring fusion.

4.2 Strategy used in the design of lead-like compounds

The aim of lead-oriented synthesis is to generate diverse screening compounds which have molecular properties (in particular molecular weight and lipophilicity) that lie within lead-like chemical space to provide a good starting point for ligand discovery.^{25,39,135} The guidelines applied in the project are not as strict as those originally described by GSK.³⁹ After discussion with Dr Lindsay McMurray of AstraZeneca who was the industrial supervisor to this project, it was decided that compounds with a molecular weight below 400 Da and $\text{clogP} < 4$ would be preferable.

The 10 selected scaffolds and complex intermediate **135** are relatively small, with an average molecular weight of 219 Da, and AlogP of 1.4. This low average molecular weight and lipophilicity allows for flexibility in the capping group strategy, meaning a wide range of capping groups can be explored. To prepare suitable screening compounds from the selected scaffolds it is important to select high quality medicinally relevant capping groups.

4.2.1 Decoration strategy

The importance of capping groups in medicinal chemistry has been noted by design of a new collection of novel capping groups.²¹⁴ The new capping groups were designed so that they would not increase molecular weight by more than 200 Da and lipophilicity (logP) by more than two units. Limits on hydrogen donors (≤ 2) and acceptors (≤ 4)²¹⁴ were also put in place to ensure a capping group is not detrimental to a compound's molecular properties. Therefore, we decided to adopt these guidelines for the selection of capping groups to ensure that the resultant library of compounds will have the correct properties to target lead-like molecular space.

A list of exemplar capping groups was compiled under the guidance of Dr Lindsay McMurray (Figure 40), with groups selected for the decoration of both oxygen and nitrogen atoms. To sample chemical space as effectively as possible, the capping groups were chosen to vary in size but also characteristics. For example, in the decoration of an amine, the electron withdrawing strength of the capping groups should vary, rendering the amine basic (*via* reductive amination) or non-basic (*via* amide coupling). Unfavourable characteristics should also be avoided. For example, in the decoration of the fused pyrrolidine scaffold **153**, efforts should be made to render this additional nitrogen non-basic in all but a few examples, limiting the number of di-basic compounds and thus the polarity of the library compounds.

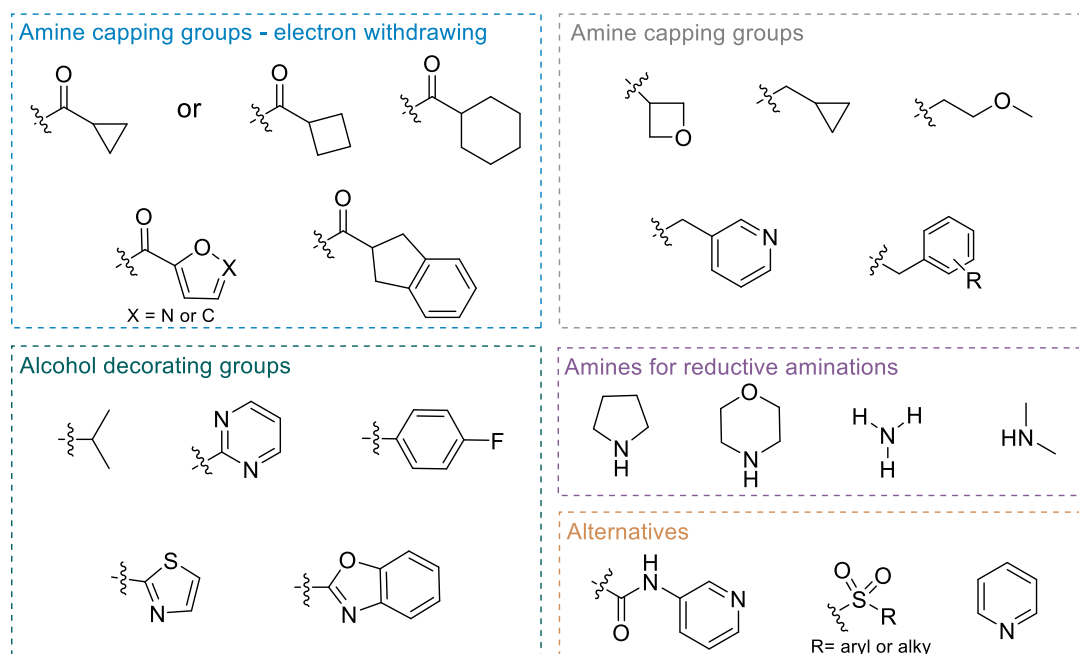


Figure 40: The list of exemplar capping groups collated for the decoration of oxygen and nitrogen functionalities.

4.2.2 Desirable properties for cell permeability

Desolvation, diffusion and resolvation are necessary for the passive permeability of a compound across a cell membrane.²¹⁵ This is reliant on a small number of key molecular properties including a compound's size, polarity and lipophilicity. Generally, the requirements for a compound to have cell permeability are in good agreement with the rule of five guidelines developed by Lipinski,⁴⁴⁻⁴⁶ which includes limiting the size of the molecule and its polarity. This can be achieved by minimising the number of polar groups and charges found within a molecule. As smaller molecules that are more nonpolar in nature can cross a membrane more easily.²¹⁵⁻²¹⁷ Lead-like compounds by their very nature fall within Lipinski's rule of five chemical space and thus the compounds contained in this library should have properties which allow for cell permeability. This should increase the likelihood of eliciting a biological response when the library of compounds is screened.

4.3. Decoration on oxygen

There are several possibilities for the decoration of the ketones contained in each of the scaffolds. The ketone can be reduced to the

subsequent alcohol and decorated via alkylation or S_NAr reaction. These methods were applied to the scaffolds and are detailed below.

4.3.1 Ketone reduction

The first method employed in the functionalisation of the carbonyl was reduction. This is a useful approach as it removes the electrophilic and potentially reactive ketone functionality. Two reducing agents were assessed, with the initial stereoselectivity assessed by ¹H NMR spectroscopy (Table 20, Entry 1). Treatment with sodium borohydride resulted a *ca* 50:50 mixture of diastereomers, therefore purification was not attempted. Next, L-selectride was chosen for testing, 400MHz ¹H NMR analysis of the crude reaction mixture showed a complex mixture and no crude *d.r* could be determined, therefore, only a single diastereomer was isolated after purification, in a yield of 22%.

The remaining β-(het)aryl ketones were treated with L-selectride (Table 20, Entries 2–4). In the case of the *m*-fluorophenyl analogue **142**, both diastereomers were successfully isolated in a yield of 20% and 4% respectively. This provided an insight into the inherent selectivity for the reaction on the pyridinium framework with an isolated *d.r* of 83:17 (Table 20, Entry 2). In the case of the *p*-nitrile analogue 400 MHz ¹H NMR analysis of the crude reaction mixture suggested a complex mixture of products resulting from the reduction of the ketone and the nitrile (Table 20, Entry 3). The final 1,4-addition product **145** also gave rise to a mix of diastereomers, although in this case the selectivity of the reduction is much lower, with an isolated yield of 38% and 15% respectively giving a *d.r* of 72:28 (Table 20, Entry 4).

Reduction of the pyrrolidine scaffolds **153** and **154** was also achieved using L-selectride and appeared to proceed with much high selectivity. 500 MHz ¹H NMR spectroscopic analysis of the crude reaction mixture showed a single product in both cases (Table 20, Entries 5 and 6). The yield of the reduction was also improved, with an isolated yield of 77% and 86% respectively.

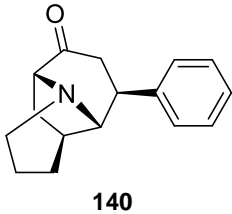
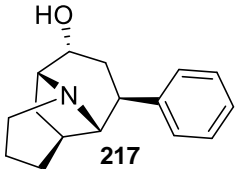
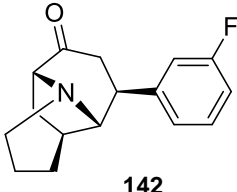
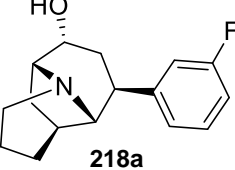
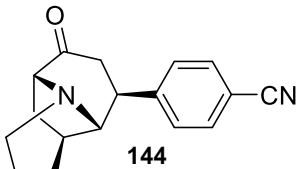
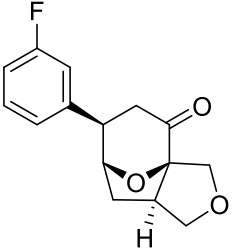
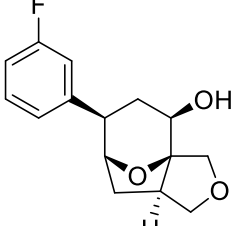
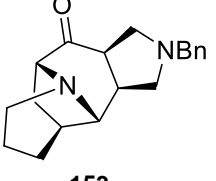
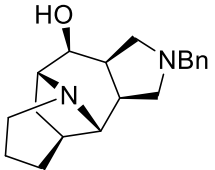
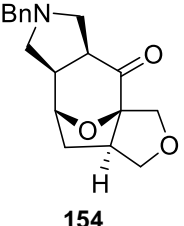
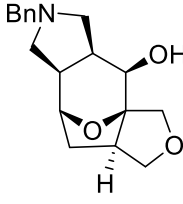
Entry	Scaffold	Reduction conditions	Product	Yield (%)
1	 140	NaBH ₄ , MeOH	1:1 mixture of isomers	<2 ^a
		L-selectride ^b	 217	22 ^c
2	 142	L-selectride ^b	 218a Major isomer	Major- 20 Minor- 4
3	 144	L-selectride ^b	Complex mixture	<2 ^a
4	 145	L-selectride ^b	 219a Major isomer	Major - 38 Minor - 15
5	 153	L-selectride ^b	 220	77 ^d
6	 154	L-selectride ^b	 221	86 ^d

Table 20: Reduction of the carbonyl compounds - ^a not isolated ^b Ketone (1.0 eq.), L-selectride (1.5 eq.), THF, -78 °C. ^c only major diastereomer isolated ^d only a single product observed (>20:<1 by ¹HNMR).

Two different methods were used to determine the relative configuration of the products. Compounds **218a**, **219** and **220** were assigned by analysis of interactions observed by NOESY NMR spectroscopy (500 MHz), and an X-ray crystal structure was obtained for compound **221**. For compound **218a**, there was a diagnostic interaction observed in the NOESY NMR spectrum (500 MHz), where a proton from the aromatic ring interacts with the α -hydroxy proton which is highlighted in red (Figure 41, Panel A). This interaction was not observed in the minor diastereomer. This interaction was observed in all the 1,4-addition products from this series and therefore configuration of the major product was assumed to be the same. The coupling constants correlated across the series. The major isomers all displayed a ddd splitting pattern with coupling constants of 10.1, 6.7 and 3.7. The largest coupling constant is diagnostic of this configuration, indicating an anti-configuration between the α -hydroxy proton and the adjacent methylene group C-H, which is only possible in this isomer.

For compounds **219a** and **220**, again, diagnostic interactions were observed in both NOESY NMR spectrum (500 MHz) where protons interact across the bottom of the ring, indicating they are on the same face (Figure 41, Panels B and C). Finally, the configuration of compound **221** was unambiguously determined using X-ray crystallography (Figure 41, Panel D).

The small difference in selectivity observed in the two reductions of compounds **218a** and **219a** may mean that detailed rationalisation may be inappropriate. It appears however that in the reduction of compound **218a**, L-selectride favours attack from the top face of the molecule (Figure 41, Panel A). This was unexpected due to the presence of the bridged nitrogen and aryl ring. The opposite is true for compound **219a** (Figure 41, Panel B). Indicating that attack from the bottom face of the molecule is preferred in this case.

The selectivity observed in the case of the pyrrolidine compounds **220** and **221** is far superior, with attack only proceeding from the convex face of the bowl-like structure formed between the pyrrolidine ring and the six membered rings of the core framework. Attack from the convex face is

sterically favoured and avoids unfavourable steric interactions (Figure 41, Panels C and D).

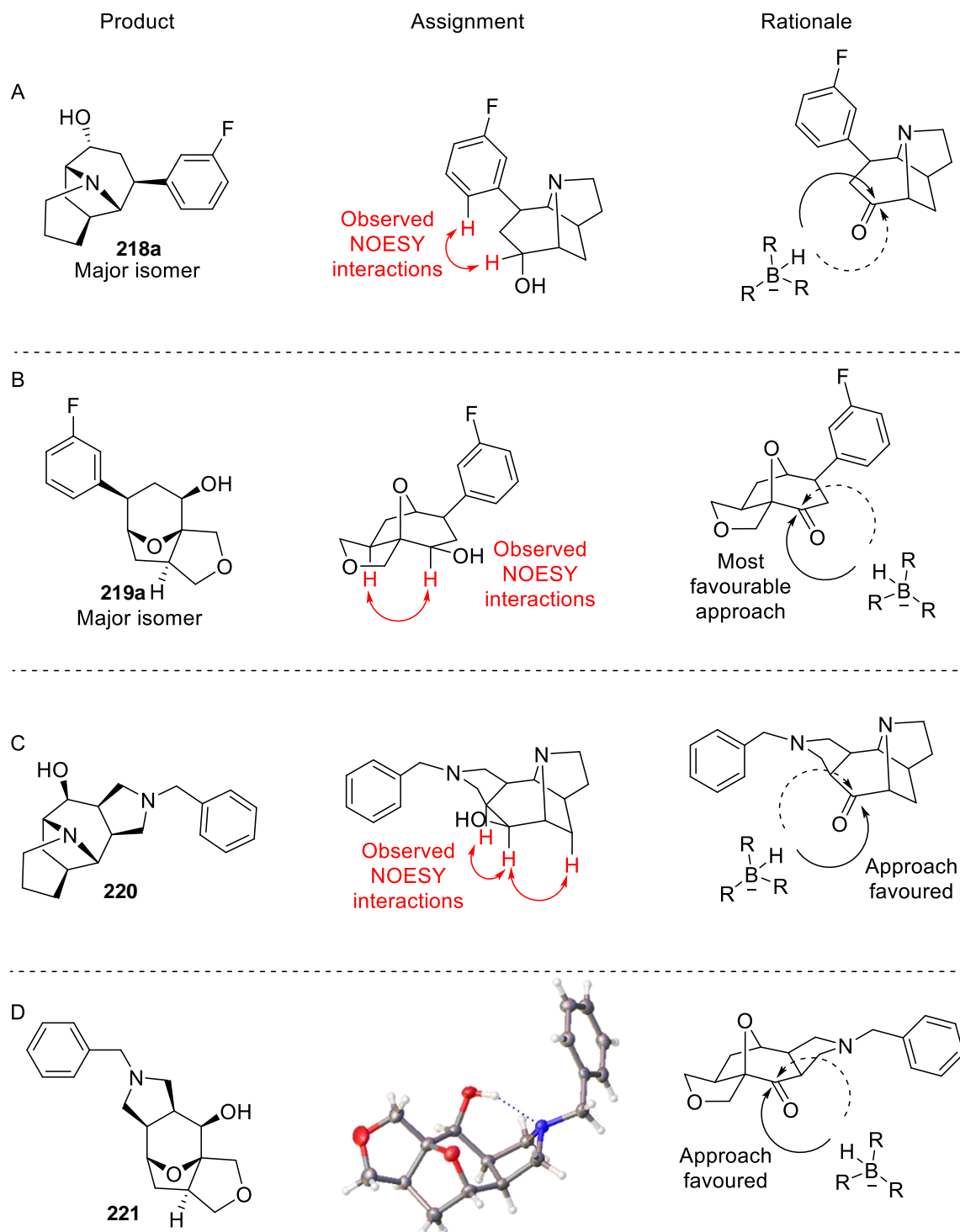


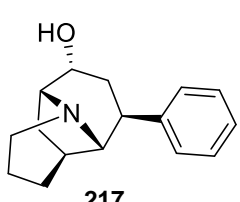
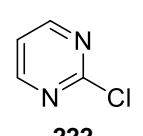
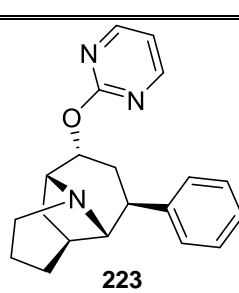
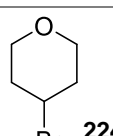
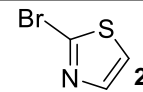
Figure 41: Assignment and rationale for the stereochemistry observed in all four reductions. Panel A, the product of the reduction of compound **218a**, the NOESY interactions (shown in red) and the rationale for the observed configuration. Panel B, the product from the reduction of **219a**, the observed NOESY interactions (shown in red) and the theorised rationale for this. Panel C, the reduced compound **220** the observed NOESY interactions (shown in red) and the rationale for the selectivity. Panel D Compound

221 and the crystal structure for this compound and the rationale for the observed stereochemistry.
R=sec-butyl

4.3.2 O-arylation via S_NAr

The successful reduction of the keto- scaffolds to the alcohols yields another functional handle suitable for decoration. Capping groups were selected from the list of exemplar capping groups outlined previously (Section 4.2.1). S_NAr and alkylation chemistry was selected to facilitate this decoration, thus alcohols were treated with sodium hydride and an appropriate aryl- or alkyl halide (Table 21).

Initially, alcohols **217** and **218a** were treated with 2-chloropyrimidine, 4-bromotetrahydropyran and 2-bromothiazole (Table 21, Entries 1 and 2). 2-chloropyrimidine was the only group to react with the alcohol, yielding the decorated compounds **223** and **226** in a 48% and 22% yield respectively. The other two capping groups showed no reactivity under these conditions with only starting material remaining as judged by 400 MHz NMR spectroscopic analysis of the crude product. As 2-chloropyrimidine was the only reactive electrophile it was applied to the remaining alcohols (Table 21, Entries 3–7) which yielded a further four final compounds in a range of yields (6-35%).

Entry	Scaffold	R-hal ^a	Product	Yield (%)
1	 217	 222	 223	48
		 224	-	<2 ^b
		 225	-	<2 ^b

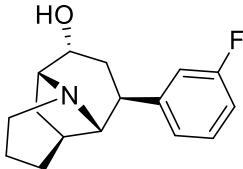
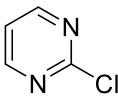
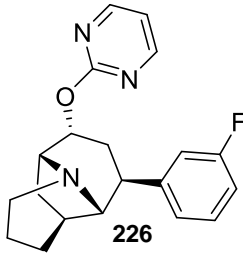
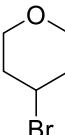
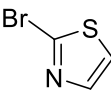
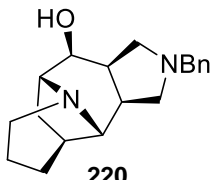
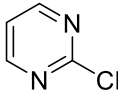
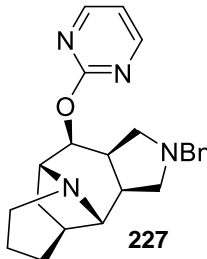
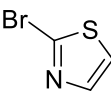
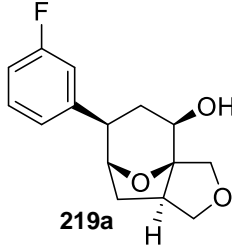
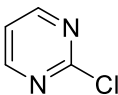
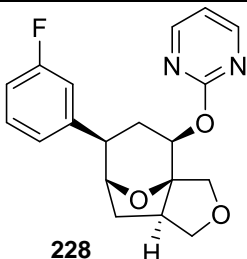
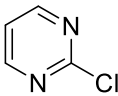
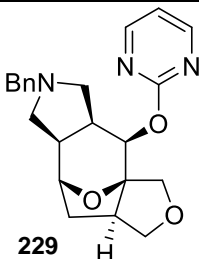
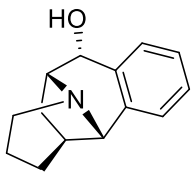
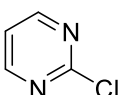
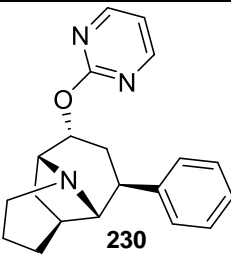
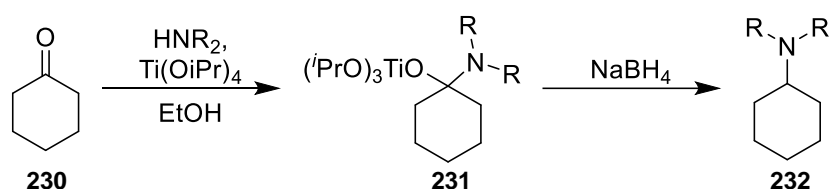
2	 218a	 222	 226	22
		 224	-	<2 ^b
		 225	-	<2 ^b
3	 220	 222	 227	24
		 225	-	<2 ^b
4	 219a	 222	 228	35
6	 221	 222	 229	6
7	 194	 222	 230	12

Table 21: decoration of the alcohol functional group. ^a Alcohol (1.0 eq.), R-hal (1.2 eq.) NaH (1.5 eq) in DMF. ^b no product isolated

4.4 Reductive aminations applied as a decoration technique

The second decoration reaction applied to the ketone containing scaffolds was reductive amination. As previously mentioned, the number of basic nitrogen atoms should be controlled to limit the polarity of the molecules. This decoration was realised on all five keto- scaffolds by treatment with titanium isopropoxide and an appropriate amine followed by the addition of sodium borohydride.¹⁷⁵ The reaction is thought to proceed *via* formation an (amino)carbinola-titanium(IV) complex **231** intermediate which can be reduced directly or *via* transient iminium species (Scheme 20).^{218,219} This method has proved tolerant of a large number of functional groups so was selected for use in this case.²¹⁹

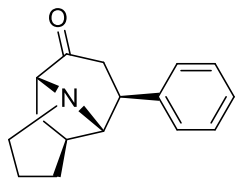
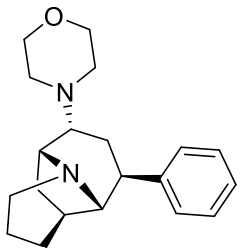
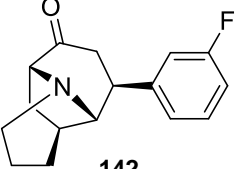
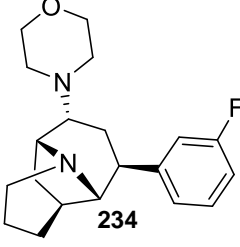


Scheme 20: The reductive amination of ketone **230** using titanium isopropoxide

The reactions progressed with varying success. Ketones **140-142** and **144** were all treated with morpholine and a saturated solution of ammonia in methanol to achieve the reductive aminations. In the case of ketones **145** and **135**, morpholine was the only amine to result in the formation of a product with yields ranging from 11–28% (Table 22, Entries 1–3). The crude diastereomeric ratios were determined by ¹H NMR analysis of the crude NMR spectrums, which highlighted a low level of selectivity observed in this reaction.

Only the major diastereomer was isolated for ketones **144** and **142** whereas for ketone **140** both diastereomers were successfully isolated, giving a product ratio of 67:33, which is a poorer *d.r* than observed in the crude product mixture. Reaction of ketone **145** with ammonia gave product **236a/b** in a 9% yield (Table 22, Entry 4). The isolated yield of this reaction was low due to challenging purification using the MDAP. Again, the selectivity of the reaction was low producing an inseparable mixture of diastereomers in a ratio of 83:17.

The ketone **135** was treated with a saturated solution of ammonia in methanol, the resulting crude material was split in two and treated with benzene sulfonyl chloride and isobutyryl chloride respectively to avoid purification of the intermediated diamine (Table 22, Entry 5). This approach also has the added benefit of decorating the newly installed amine. Amines **237** and **238** were successfully isolated, although in very low yields due to challenging purifications using the MDAP. Interestingly, the two isolated products have the opposite configuration, suggesting again the reductive amination is unselective. However, it appears the less hindered amine reacts preferentially with the larger sulfonyl chloride and the more hindered amine reacted preferentially with the smaller acid chloride as only the major product was isolated in each case.

Entry	Scaffold	Method	Product	Crude <i>d.r</i>	Yield (%)
1	 140	A	 233a Major isomer drawn	80:20	Major - 22 Minor - 11
		B/D	-	-	<2 ^b
2	 142	A	 234	80:20	20 ^c
		B/D	-	-	<2 ^b

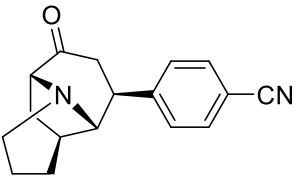
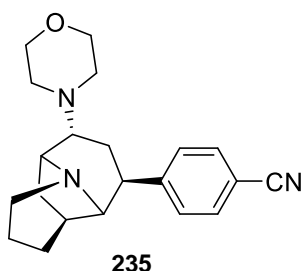
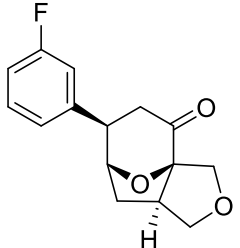
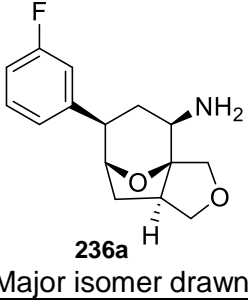
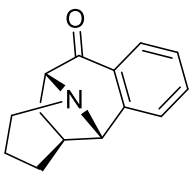
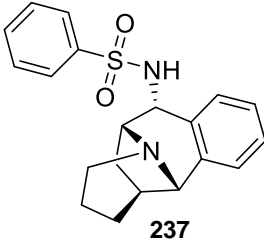
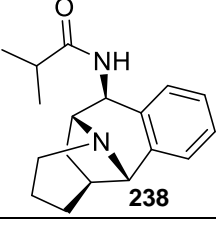
3	 144	A	 235	75:25	28 ^c
		B/D	-	-	<2 ^b
4	 145	A	-	-	<2 ^b
		B	 236a Major isomer drawn.	83:17	9 ^{d,e}
5	 135	C/E	 237	-	3 ^{c,e}
		D/F	 238	-	4 ^{c,e}
		A	-	-	<2 ^b
		C	-	-	<2 ^b

Table 22: reductive amination with titanium isopropoxide. ^a Saturated solution of ammonia in methanol
^b no product isolated ^c only the major product was isolated ^d mixture of inseparable diastereomers (83:17)
^e purified using the MDAP. Method A: Ketone (1.0 eq.), Ti(ⁱPrO)₄ (2.0 eq.) morpholine (5.0 eq.) in EtOH, 16 h then NaBH₄ (3.0 eq.). Method B: Ketone (1.0 eq.), Ti(ⁱPrO)₄ (2.0 eq.) saturated solution ammonia in methanol (as solvent), 16 h then NaBH₄ (3.0 eq.). Method C: Ketone (1.0 eq.), Ti(ⁱPrO)₄ (2.0 eq.) cyclopropyl amine (5.0 eq.) in EtOH, 16 h then NaBH₄ (3.0 eq.). Method D: Acetic anhydride (2.0 eq.) and pyridine (2.0 eq.) in CH₂Cl₂. Method E: benzene sulfonyl chloride (8.0 eq.) and pyridine (4.0 eq.) in THF. Method F: isobutyryl chloride (8.0 eq.) and pyridine (4.0 eq.) in THF.

NOESY NMR spectroscopy (500 MHz) was used to determine the configuration for all the reductive amination products (Figure 42). Compound **233a** displays a diagnostic interaction in the NOESY NMR spectrum (500 MHz), where a proton from the aromatic ring interacts with the proton highlighted in red (Figure 42, Panel A). This interaction was observed in all the 1,4-addition products from this series and therefore was assumed to be the same. Compound **236a/b** exists as an inseparable mixture of diastereomers, however the α -amino proton (shown in red) of the major isomer displays a diagnostic interaction with the α -aryl proton observed in the NOESY NMR spectrum (500 MHz), indicating they are on the same face of the molecule.

The configuration of the amines **237** and **238** was determined to be opposite. The amide demonstrated a diagnostic interaction in the NOESY NMR spectrum (500 MHz), as the two protons interact across the bottom face of the ring (Figure 42, Panel D). This interaction was not observed in the case of the sulfonamide **237**. The only observed interaction was between the bridgehead proton and the proton shown in red (Figure 42, Panel C).

Again, the selectivity of these reductive aminations is low across all substrates, therefore rationale for the selectivity may not be appropriate. The level of selectivity observed in these reductive aminations is similar to that observed in the reduction of the β -aryl ketones, suggesting there is no overwhelming steric influence to control these reactions.

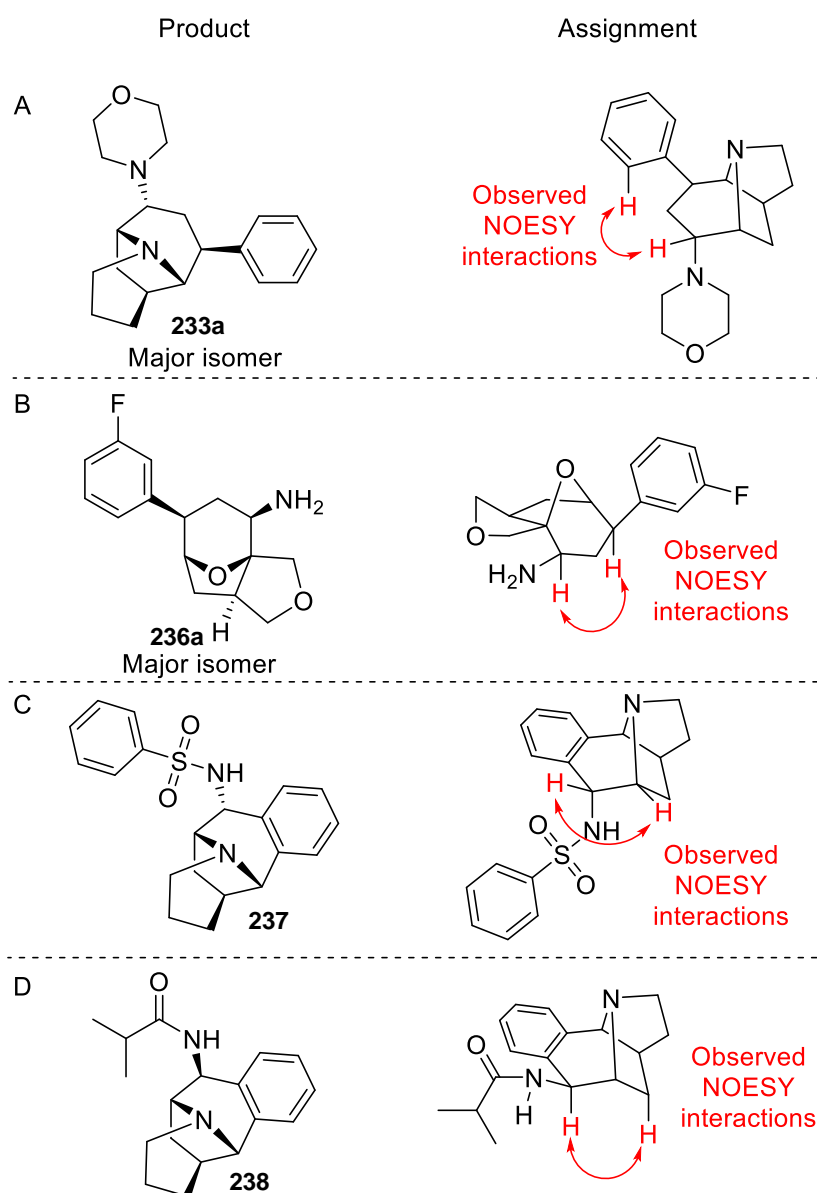


Figure 42: Assignment of the configuration in all the reductive animations. Panel A, the product of the reaction of compound **140** with morpholine with the NOESY interactions (shown in red). Panel B, the product from the reductive amination of **145** and the observed NOESY interactions (shown in red). Panel C, the sulfonamide compound **237** and the observed NOESY interactions (shown in red). Panel D amide **238** and the diagnostic NOESY interactions (shown in red).

4.5 Decorations on the nitrogen functionality

The final approach used in the synthesis of lead-like screening compounds was the decoration of the nitrogen functionality. In the previous chapter pyrrole and pyrrolidine rings were successfully fused onto the core frameworks, installing two new functional handles for decorations. There are several reactions that could be used for decoration of nitrogen including

reductive aminations, amide formations and sulfonamide formation. A mixture of these reactions should be employed with a range of capping groups creating a library of amines with varied size and electronic character.

4.5.1 Deprotection of benzylamines

Before any decorations could proceed the pyrrolidine must be deprotected, standard conditions were selected to achieve this. The benzyl amines **220** and **221** were treated with palladium hydroxide on carbon and hydrogen to yield the free amines **239** and **240** in a 70% and 97% yield respectively (Table 23, Entries 1 and 2). The final attempted deprotection was on the decorated compound **226**, however treatment with palladium hydroxide on carbon and hydrogen gave rise to a complex mixture and appeared to remove the pyrimidine group.

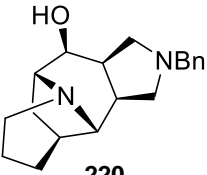
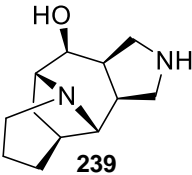
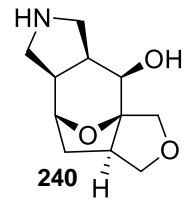
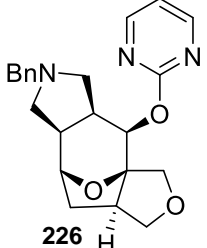
Entry	Starting material	Product	Yield %
1	 220	 239	70
2	 221	 240	97
3	 226	Complex mixture	<2 ^a

Table 23: deprotection of benzylamine with palladium hydroxide. ^a no product isolated Conditions used: Benzylamine (1.0 eq.) Pd(OH)₂/C (10 wt%), H₂, MeOH.

4.5.2 Reductive amination as a method for decoration

The first decoration method investigated on the amines **239**, **240** and **156** was reductive amination. The amines were treated with the appropriate aldehyde or ketone with molecular sieves, then sodium borohydride was

added to the reaction mixture. Amine **239** appeared to undergo a successful reaction with 2-fluoro benzaldehyde however no product was successfully isolated using the MDAP purification system (Table 24, Entry 1). Two products were successfully isolated after reaction with 2-fluorobenzaldehyde and 3-oxetanone albeit in low yields of 13% and 3% yield respectively (Table 24, Entry 3). Finally, pyrrole **156** was unreactive under these conditions and no product could be detected *via* LC-MS (Table 24, Entry 3).

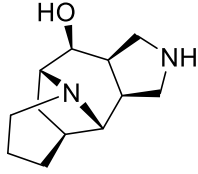
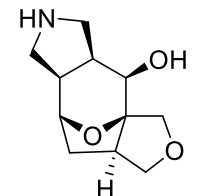
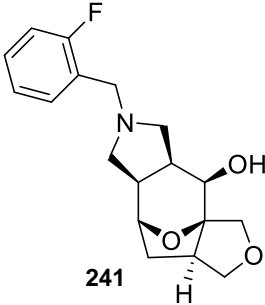
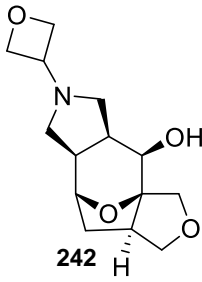
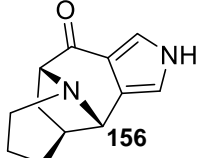
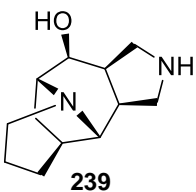
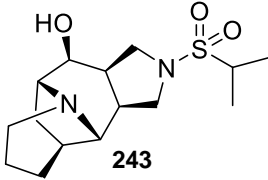
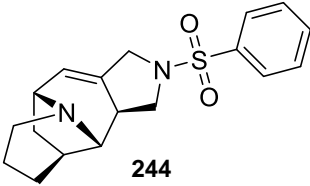
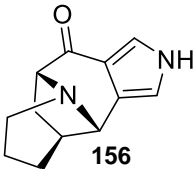
Entry	Starting material	Ketone or aldehyde	Product	Yield %
1	 239	2-fluoro benzaldehyde	-	<2 ^a
		2-pyridine carboxaldehyde	-	<2 ^a
		3-oxetanone	-	<2 ^a
2	 240	2-fluoro benzaldehyde	 241	13
		3-oxetanone	 242	3
3	 156	anisaldehyde	-	<2 ^a

Table 24: reductive aminations as a decoration reaction. ^a no product isolated. Conditions used: Amine (1.0 eq.), ketone or aldehyde (5.0 eq.) molecular sieves, DMF, 16 h, then NaBH₄ (3.0 eq.).

4.5.3 Sulfonamide formation as a decoration

The second method selected was sulfonamide formation. This capping group is electron withdrawing and thus renders the amine non-basic which is preferable for limiting polarity, especially in the case of diamine **239**. The amines were treated with pyridine followed by the addition of an appropriate sulfonyl chloride (Table 25). Only amine **239** and pyrrole **157** yielded isolatable products under these conditions. Amine **239** produced the propane sulfonamide in a 34% yield, however treatment with benzene sulfonyl chloride gave rise to an unexpected product in a 7% yield. It appears that under these conditions a dehydration occurred, which could be caused by the alcohol also reacting with the sulfonyl chloride making it a good leaving group. Pyrrole **157** reacted with benzene sulfonyl chloride to give the sulfonamide **245** in a very low yield, due to challenges in purification with the mass directed automated purification (MDAP).

Entry	Starting material	Sulfonyl chloride	Product	Yield %
1	 239	2-propane sulfonyl chloride	 243	34
		Benzenesulfonyl chloride	 244	7
		2,5-dimethoxy benzenesulfonyl chloride	-	<2 ^a
2	 156	2-propane sulfonyl chloride	-	<2 ^a
3		Benzenesulfonyl chloride	-	<2 ^a

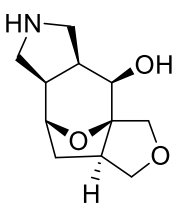
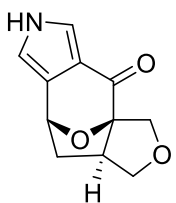
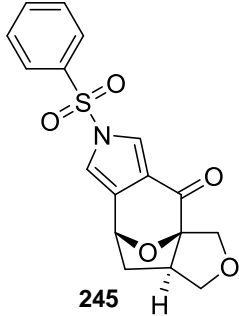
	 <p style="text-align: center;">240</p>	Pyridine 3-sulfonyl chloride	-	<2 ^a
4	 <p style="text-align: center;">157</p>	Benzenesulfonyl chloride	 <p style="text-align: center;">245</p>	2 ^b

Table 25: Sulfonamide formation as a decoration technique. ^a no product isolated ^b purified using MDAP. Conditions used: Amine (1.0 eq.), pyridine (4.0 eq.), THF, 30 mins then sulfonyl chloride (8.0 eq.), 70 °C.

4.5.4 Amide formation

The final method investigated in the functionalisation of the nitrogen containing scaffolds was amide formation. Scaffolds **239**, **240** and **157** were treated with pyridine followed by the addition of an appropriate acid chloride. Pyrrolidine scaffolds **239** and **240** also contained an alcohol functional group, therefore both an ester and amide would be formed and would require a second hydrolysis step to remove the ester. Only one of the three acid chlorides investigated with pyrrolidine **239** resulted in product formation in a low yield of 9% (Table 26, Entry 1). Compound **240** also reacted successfully with cyclohexane carbonyl chloride (Table 26, Entry 2). However, the hydrolysis was incomplete, and both the amide **247** and the ester **248** were isolated in a 4% and 5% yield respectively. Finally, pyrrole **157** gave amide **249** in an 8% yield upon treatment with cyclopropane carbonyl chloride (Table 26, Entry 3). All the products were isolated using MDAP and resulted in poor isolated yields, however the compound purity was high (as judged by ¹H NMR analysis). This method of decoration gave rise to a further four final screening compounds.

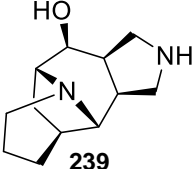
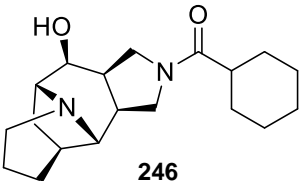
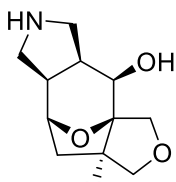
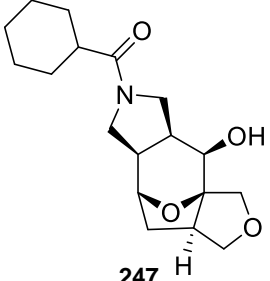
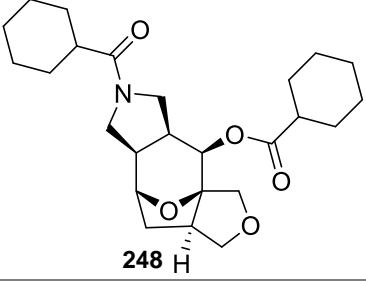
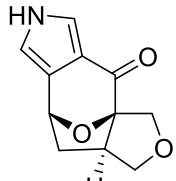
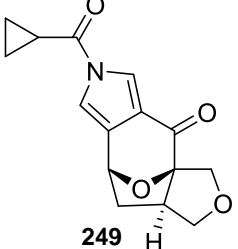
Entry	Starting material	Acid chloride	Product	Yield %
1	 239	Cyclohexane carbonyl chloride	 246	9 ^a
		Cyclopropane carbonyl chloride	-	<2 ^b
		2-furoyl chloride	-	<2 ^b
2	 240	Cyclohexane carbonyl chloride	 247	4 ^a
		Cyclohexane carbonyl chloride	 248	5 ^a
		2-furoyl chloride	-	<2 ^b
3 ^c	 157	Cyclopropane carbonyl chloride	 249	8 ^a

Table 26: The decoration of amines *via* amide formation. ^a purified using MDAP ^b no product isolated ^c step ii not required. Conditions used: Amine (1.0 eq.), pyridine (4.0 eq.), CH₂Cl₂, then acid chloride (8.0 eq.), rt, 16 h. LiOH, water, 70 °C, 16 h.

4.6 Computational assessment of the prepared screening compounds

With the synthesis of the library of screening compounds complete their molecular properties such as lipophilicity and molecular weight were analysed. LLAMA²¹¹ was used to assess these properties to see if the library compounds do indeed have the correct properties to target lead-like chemical space.

4.6.1 Analysis of the decoration reactions

When the properties of the designed library (all attempted decorations) are compared to those which were successfully synthesised, only a small drift in AlogP can be seen (Figure 43). If all decorations were successful then the average molecular weight would be 312 Da and AlogP of 1.77, compared to that of the synthesised library which has an AlogP of 1.80. The successful decorations did not result in a large drift in AlogP, as there is an equal number of failed reactions which would have resulted in compounds with a relatively low (AlogP < 1) and high (AlogP > 2.5) lipophilicity.

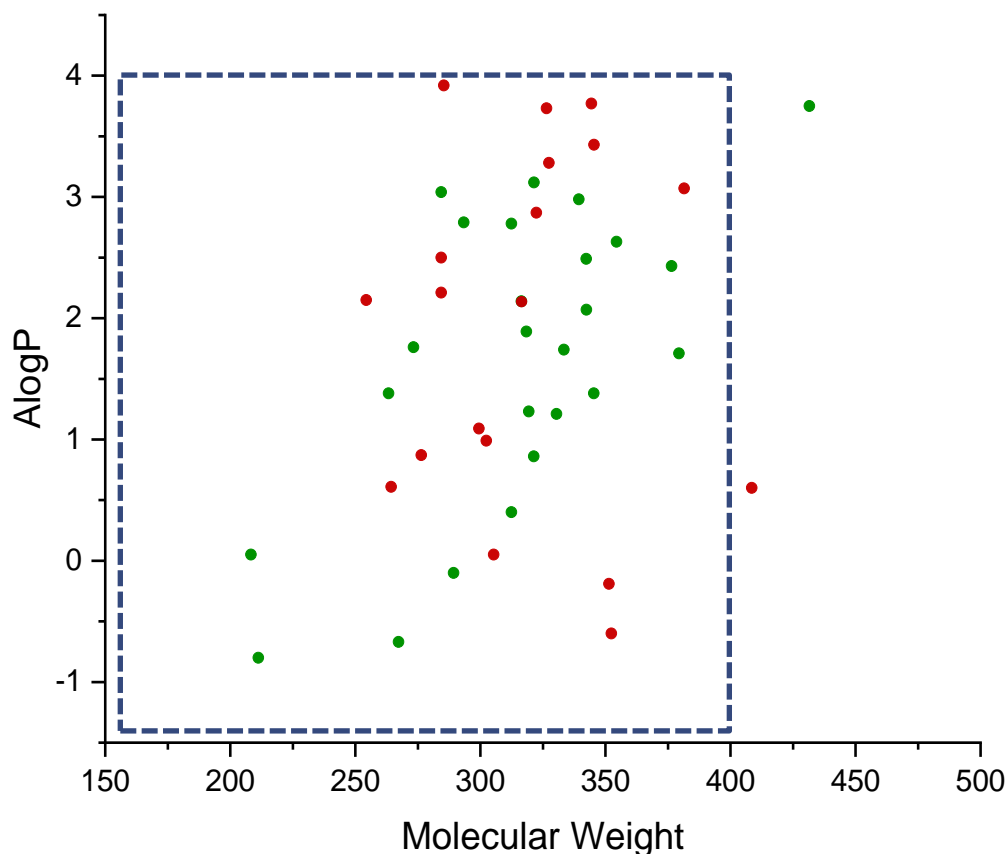


Figure 43: The lead-likeness of the products from all of the decoration compounds. The red circles indicate an unsuccessful reaction and green indicate successfully isolated products.

4.6.2 Lead-like assessment of the library of compounds

The lead-likeness of the library of compounds was assessed using LLAMA in accordance with the criteria following discussion with Dr Lindsay McMurray, whereby molecular weight is ≤ 400 Da and lipophilicity ($-1 < \text{AlogP} < 4$). Lead-likeness is assessed by plotting molecular weight against AlogP, with lead-like chemical space denoted by the dark blue box (Figure 44). All but one of the 54 compounds synthesised in this project (excluding tropone based complex intermediate and related scaffolds) have the correct properties to target lead-like chemical space. The only compound which falls outside of this space is compound **248**, where the ester could not be cleaved successfully. This compound has a molecular weight of 431 which falls outside the parameters for lead-like chemical space, even though the AlogP of 3.75 and is within the guidelines.

There are no large groups of clustering, suggesting a reasonably effective sampling of lead-like chemical space. The compounds which fall at the lower end of lead-like chemical space are some of the deprotected scaffolds used as a starting point for decoration. This highlights the rapid increase in molecular weight and lipophilicity after the addition of a capping group.

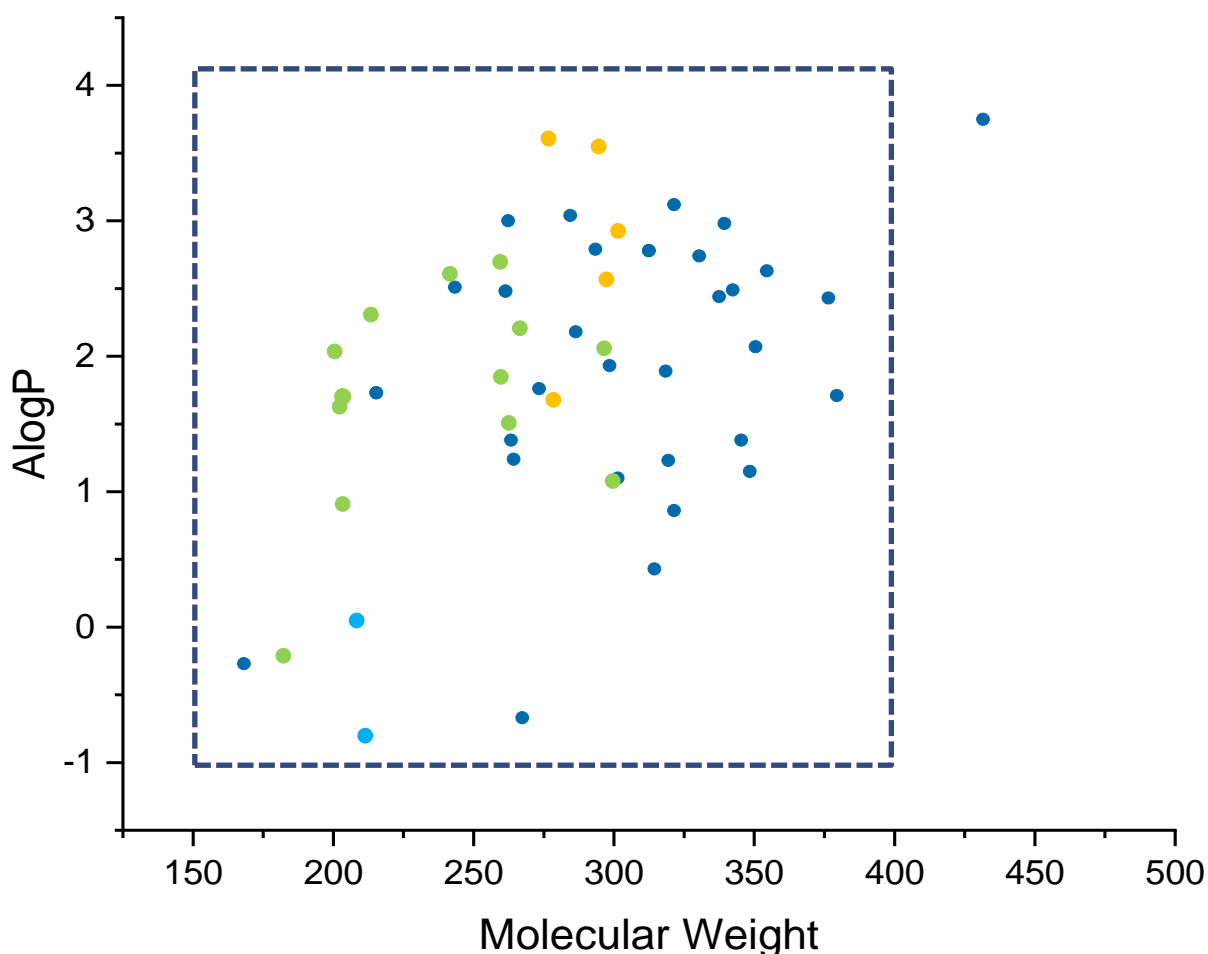


Figure 44: The lead-likeness of all 54 compounds synthesised in this project. Lead like chemical space is denoted by the dark blue box ($mw \leq 400$ and $-1 < AlogP < 4$). Dark blue dots represent a decorated compound, green dots represent scaffolds, yellow dots represent scaffolds formed from a combination of two scaffold forming reactions and pale blue dots represent reduced scaffolds with the protecting group removed.

It is clear from these results that following the principles of lead-oriented synthesis and Goldberg's requirements for capping groups,²¹⁴ has aided the design of a library of lead-like compounds, with only one outlier present. The scaffolds selected at the start of this chapter possessed an average molecular weight of 219 Da, and lipophilicity of 1.4. After decoration the average molecular weight increased by ca 30% to 283 Da and the AlogP has increased to 1.9.

4.6.3 Assessment of the shape diversity of the library of lead-like compounds

More three-dimensional compounds typically have lower attrition rates in drug discovery programmes.⁶¹⁻⁶³ The shape diversity of the scaffolds can be assessed using a principle moment of inertia (PMI) plot which is generated

using LLAMA.²¹¹ The three vertices on the PMI plot represent the extremes of shape diversity. To generate the PMI coordinates of a compound LLAMA generates the lowest energy conformer and then calculates the moments of inertia in the three axes x, y and z. I1 and I2 can then be calculated by dividing inertia(x) by inertia (y) and inertia (y) by inertia (z) respectively.

The PMI plot generated by LLAMA evidences the fact that the synthesised compounds are moving away from the overpopulated rod-disk like axis (as described previously in Section 1.3.2). The 54 library compounds synthesised in this project are represented by circles and can be seen to sample a range of three-dimensional chemical space with limited clustering observed between compound series (Figure 45).

The molecular shape of a random subset (ca 16.7 million compounds) of lead-like GDB17 compounds was assessed⁷⁸ and can be seen to be more three-dimensional than the ZINC database. The most highly populated area of three-dimensional chemical space by lead-like GDB17 compounds is represented by the pink oval (Figure 45). Many of the compounds synthesised in this project fall within or very close the most populated region of the PMI plot for the exhaustively enumerated fragments (up to 17 HA). There are also far fewer possible 'spherical' compounds which are possible to make so targeting sphere-like chemical space is very challenging, but this library of compounds has made a significant move away from the 'rod-disk' like axis and is sampling the lesser explored areas of chemical space.

Three compounds are shown on the PMI plot, highlighting how three-dimensional some of the library compounds are despite containing two aromatic rings (**198** and **226**). This could be due in part to the inherent three-dimensional nature of the parent framework and subsequent scaffolds, for example compound **239**, which is venturing far from the 'rod-disk' like axis. This is corroborated by the mean PMI coordinates (denoted by the orange cross), highlight the mean three-dimensionality of the series.

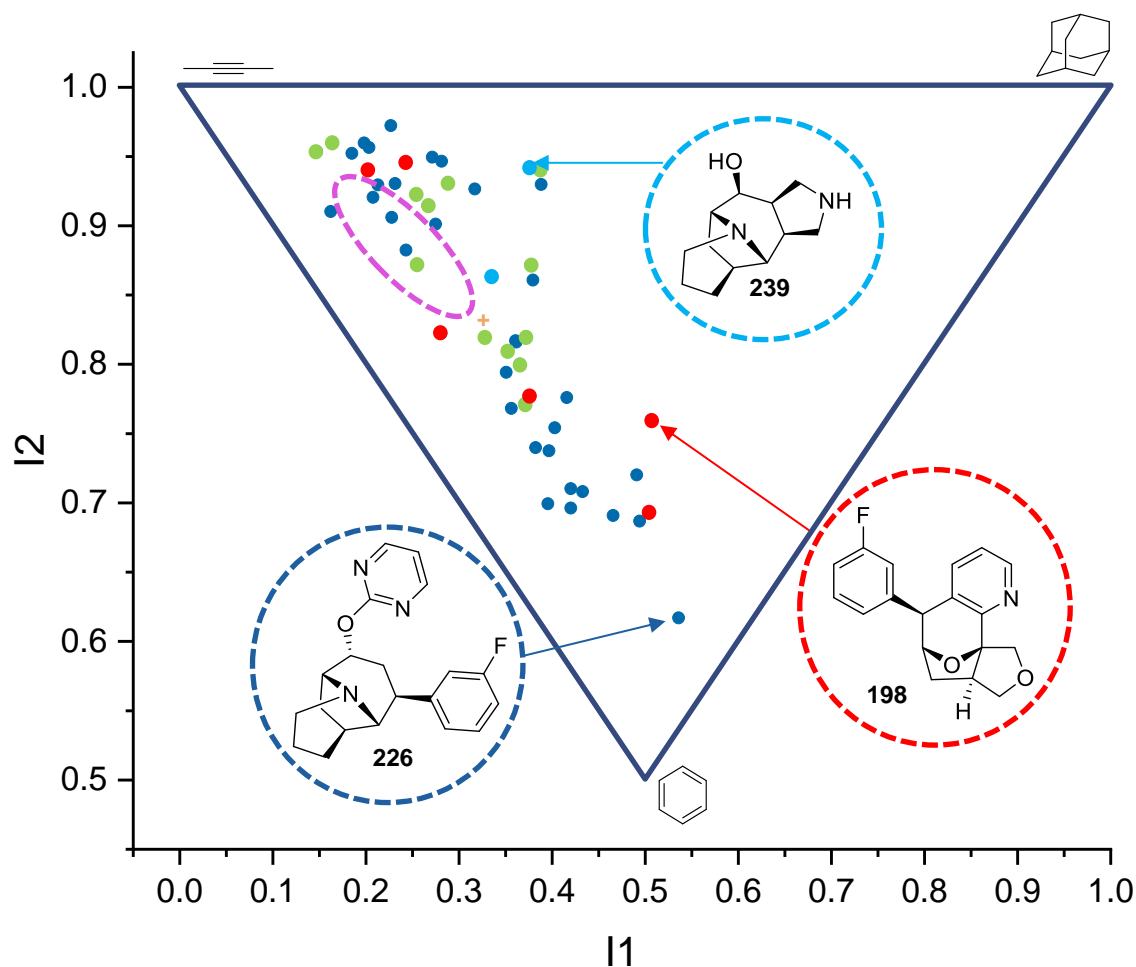


Figure 45: A PMI plot generated using LLAMA, showing the three-dimensionality of the screening compounds, with three examples highlighted. The orange cross denoted the mean PMI coordinates $I1 = 0.329$, $I2 = 0.845$. Dark blue dots represent a decorated compound, green dots represent scaffolds, red dots represent scaffolds formed from a combination of two scaffold forming reactions and pale blue dots represent scaffolds with the reduced products with protecting group removed. The pink oval represents the most populated area of three-dimensional chemical space for a random subset of lead-like compounds in GDB17.

4.6.4 Fsp³ assessment of the library compounds

The final metric analysed to assess the success of this approach was the Fsp³, as one of the aims for this project was to prepare sp³ rich lead-like compounds. Again, each of the 54 compounds were analysed by LLAMA and an Fsp³ score was calculated for each of the compounds (Figure 46). There are a range of Fsp³ scores observed for the library, the highest score achieved was 1.00. This score was achieved by four compounds in the library, one of

which can be seen below (Figure 46). Two of the lowest scores observed in this library are 0.35 and 0.40 as the compounds which these scores represent both contain two aromatic rings.

The average F_{sp^3} score for this library of lead-like screening compounds was 0.63. A random 1% of the ZINC database has an F_{sp^3} score of 0.33,¹⁷⁵ highlighting by comparison how sp^3 rich this compound collection is. Even the lowest score achieved in this library is 0.35 which is still higher than the average score achieved by the ZINC database.

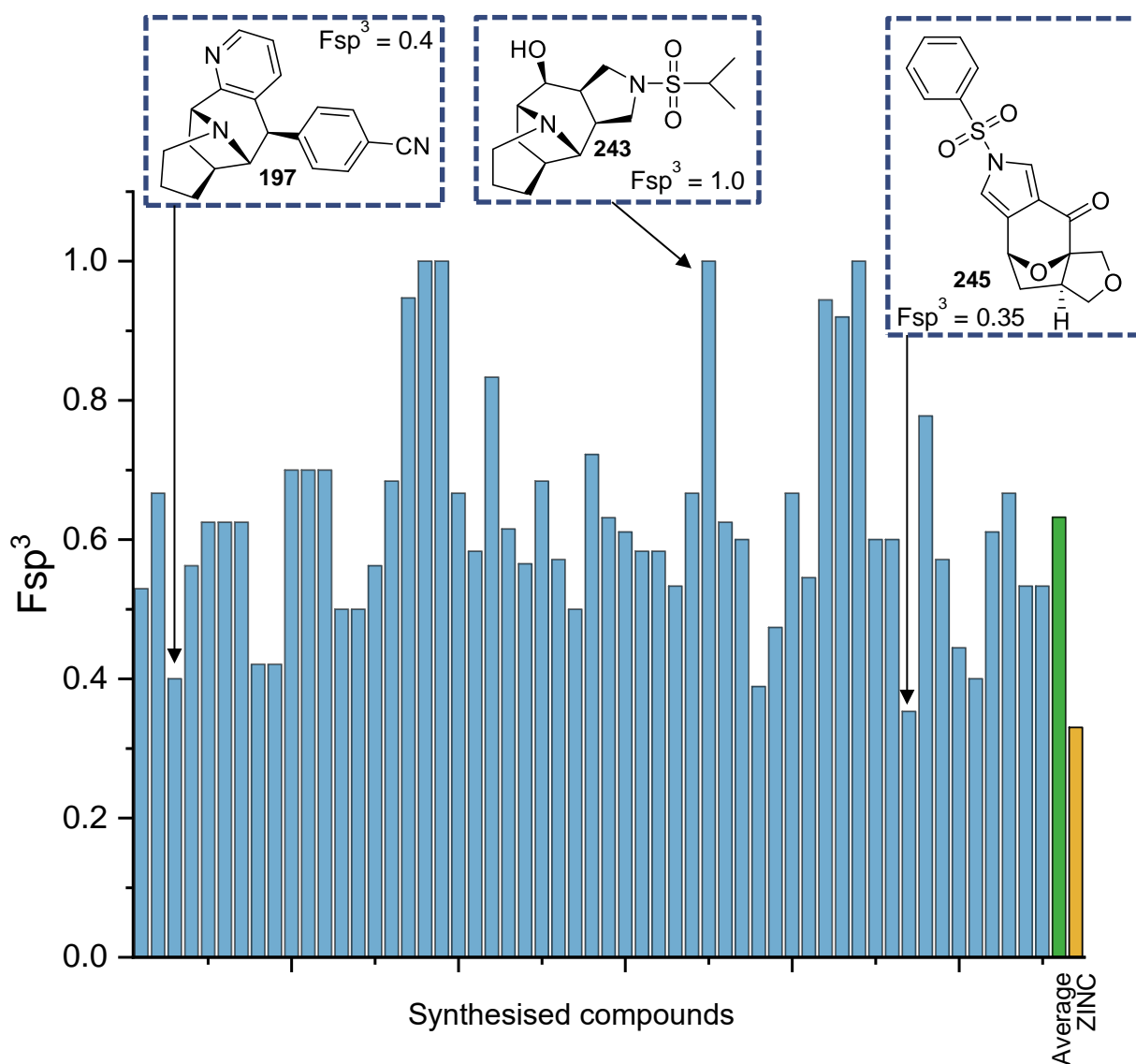


Figure 46: The F_{sp^3} scores for the synthesised compounds. Blue – synthesised compounds in this library. Green – the average F_{sp^3} for this library of compounds (0.63). Yellow – The F_{sp^3} score for a random 1% of the ZINC database (0.33).

4.6.5 Summary of the computational assessment

In summary, the careful selection of capping groups which were applied to a range of diverse scaffolds has resulted in the creation of a library of lead-like screening compounds. The application of the top-down approach has led to the synthesis of a library of screening compounds with all but one of the compounds having the correct properties to target lead-like chemical space. Analysis of the library also indicates the improved exploration of chemical space, with the compound collection moving away from the 'rod-disk' like axis. The compounds are sp^3 rich in nature, especially when compared to readily available screening compounds.

Chapter 5 Summary, conclusions and future work

Historically, the exploration of chemical space has been asymmetrical which can be attributed to a limited toolkit of reactions used by medicinal chemists,^{108–110} which has resulted in overpopulated areas of chemical space,^{98,99} with limited diversity^{105,106} and undesirable molecular properties.¹¹² This is a substantial problem as small molecules are a heavily relied upon tool in combatting disease.²²⁰ There have been several methods developed to address the challenge of the exploration of chemical space.^{39,124,126,134} Two distinct approaches known as diversity-oriented synthesis (DOS) and lead-oriented synthesis (LOS), have been developed to access new and diverse chemical matter.^{39,116}

LOS is the strategy employed to prepare compounds with lead-like molecular properties (outlined in Section 1.2.2) and was selected for use in this project.³⁹ Two approaches to LOS have been developed coined; 'bottom-up' and 'top-down'. The bottom up approach is reliant approach on a pair of building blocks which can be coupled to create a cyclisation precursor. The multiple functionalities can then be paired in several combinations to create a range of diverse frameworks.^{136,138} In contrast the 'top-down' synthetic approach to LOS utilises the formation of complex cycloadducts, which can then be converted into distinct molecular scaffolds, through the exploitation of ring expansion, ring addition and ring cleavage chemistries.²⁰⁴ The 'top-down' approach was selected to realise the synthesis of a library of Fsp³ rich lead-like compounds.

5.1 Selection of an appropriate complexity generating reaction towards the synthesis of lead-like compounds

The 'top-down' approach requires the generation of a high level of complexity, so it may be exploited in the subsequent reactions. Therefore, to ensure the correct choice was made a set of guidelines was established. It was deemed important for the reaction to construct a highly three-dimensional parent cycloadduct, ideally, a bridged or fused bi- or tricyclic ring system. Practically was also judged to be an essential characteristic (yield >40%, low

catalyst loading and <5 synthetic steps). Lastly, it was decided the reaction must contain suitable functionality to facilitate further reactions in multiple vectors.

A shortlist of five complexity generating reactions was identified from the literature and investigated. The identified Rh-catalysed C-H insertion reaction was deemed incompatible with the project due to the yield of the reaction was only 21% (Section 2.1.1). The employment of dearomatisation chemistry was successfully employed in the synthesis of a carbocyclic tricyclic framework in a 42% yield; however, this complex intermediate was deemed unsuitable as it would create a library of compounds with limited diversity and poor molecular properties (section 2.2). Despite a series of attempts neither the oxa- nor aza- analogues could be synthesised in any suitable amounts.

Tropone cycloaddition chemistry gave rise to a complex intermediate in a single step and a 57% yield (Section 2.3). Difficulties arose from this framework when the enone functionality was installed. This added four steps to the synthesis of the useful complex intermediate in a low yield of 32%. The reaction was shortlisted for further decoration due to the facile nature of the synthesis.

The penultimate complexity generating reaction was an intramolecular [5+2] oxido-pyridinium alkene cycloaddition which demonstrated its versatility by giving rise to two complex intermediates, both has yields above the desired 40% (Section 2.4). Consequently, this complexity generating reaction was a clear choice for scaffold synthesis and the fused aromatic analogue was taken forward for decoration. The final complexity generating reaction selected was complementary to the one just described as it was an intramolecular [5+2] oxido-pyrrilium alkene cycloaddition. The synthetic route was slightly longer at five steps and achieved a practical yield of 60% (Section 2.5), therefore meeting the outlined requirements. A total of three complex intermediates were prepared in synthetically useful amounts and were taken forward to investigate the synthesis of diverse molecular scaffolds.

5.2 Establishment and implementation of a toolkit of reactions for the preparation of sp^3 rich, lead-like scaffolds

To expand the chemical toolkit and following the 'top-down' approach four tactics were enlisted in the synthesis of diverse molecular scaffolds. Firstly, ring addition was investigated using a rhodium catalysed 1,4-addition reaction (Section 3.1.1). This reaction was successfully applied to all three shortlisted complex intermediates. Three different boronic acids were compatible with this reaction and gave rise to six molecular scaffolds. This reaction proved a useful tool for installing an aromatic ring into the framework without compromising the three-dimensionality of the framework.

The second tactic enlisted in this approach was ring fusion chemistry (Section 3.2) and was the most successful approach. The first reaction identified was a [3+2] dipolar cycloaddition to achieve the fusion of a pyrrolidine ring. This reaction was successfully applied to all three complex intermediates giving a further three scaffolds. The second ring fusion reaction was another [3+2] cycloaddition reaction using a tosyl isocyanate to fuse a pyrrole ring to the core framework. Again, this reaction was proved to be synthetically useful and delivered a further three scaffolds to the collection. The third and final ring fusion reaction investigated was a gold catalysed pyridine formation. This required the ketone as a starting material and was successfully applied to two of the complex intermediates, yielding a further two scaffolds. Overall this was a very successful approach using three reactions and three complex intermediates to yield eight new scaffolds.

The penultimate tactic in the 'top-down' approach was ring expansion (Section 3.3). Two methods were tested in the hope of expanding the size of the core ring. Two conditions were investigated to facilitate the Beckmann ring expansion, however all lines of enquiry proved fruitless. The Baeyer-Villiger was the only reaction to in result in a ring expanded product, producing the only scaffold from this approach.

The final approach investigated was the ring cleavage (Section 3.4), this had the potential to be the most valuable as it could result in changes to the

core framework, increasing the diversity of the scaffold collection. A range of different conditions were screened in an effort to break the carbon-carbon double bond of the enone. Unfortunately, all efforts were unsuccessful, and no bonds were cleaved. This was the only bond cleavage reaction investigated which could have been applied to both complex intermediates, suggesting this tactic is not as widely applicable to multiple frameworks as the other three approaches.

Therefore, a more tailored approach was taken, and a range of methods were identified from the literature for the activation of tertiary amines and subsequent fragmentation. Again, they were applied to the pyridinium complex intermediate which gave rise to a single product. The final attempt at ring cleavage was to break the lactone formed *via* the only successful ring cleavage reaction, but again this was unsuccessful.

Finally, a combination of the scaffold forming reactions was used as some of the scaffolds formed were unique substrates for subsequent scaffold forming reactions. A combination of ring addition and fusion reactions and ring expansion and addition yielded a further five scaffolds which could be used as screening compounds.

A total of 21 scaffolds have been synthesised, despite the limited success of the final two approaches. All but one scaffold was found to contain a novel Murcko framework and the only compound with a known Murcko framework provided a low number of hits. The scaffold set was assessed and contains eight parent frameworks. Despite the scaffold synthesis not being as evenly productive as hoped, the target of 15 scaffolds was exceeded. Therefore, the 'top-down' approach appears to be an efficient method for generating a diverse set of molecular scaffolds.

5.3 Design, preparation and evaluation of the library of decorated lead-like scaffolds

A total of ten scaffolds and one complex intermediate were selected for decorations with a range of capping groups. The capping groups were selected as not to increase molecular weight by more than 200 Da and

lipophilicity (logP) by more than two units. Capping groups of different sizes and electronics were used to sample chemical space as effectively as possible.

Using this approach 31 compounds were successfully synthesised using a range of reaction classes including reduction, S_NAr and reductive amination on both the ketone and amine functional handles. Adding the 31 decorated to the compounds synthesised previously creates a library of 54 compounds.

The lead-likeness of the library of compounds was assessed using LLAMA. All but one of the 54 compounds synthesised have the correct properties to target lead-like chemical space, highlighting the success of this approach. The three-dimensionality of the library was analysed, and the compounds were observed to be moving away from the overpopulated rod-disk like axis. Therefore, sampling some more three-dimensional chemical space. The final metric used to assess the library was the average Fsp³ score. The calculated Fsp³ score for the library of lead-like screening compounds was 0.63. When compared to a random 1% of the ZINC database which has an Fsp³ score of 0.33 it can be assessed to be much more sp³ rich.

Despite the limited success of the ring cleavage and expansion chemistries all the objectives of the project have been met. Although these approaches would have added significant value to the project by increasing the diversity of the frameworks found in the library. However, to enable this approach simpler substrates could be used which are more compatible with literature methods, however this is at odds with the top-down approach. Another option could be to select a complex intermediate which has more functionality and therefore more ring cleavage chemistries could be available.

5.4 Future perspectives

The 'top-down' approach is a broadly applicable approach to the synthesis of diverse and three-dimensional compound libraries. This approach, which utilises, and exploits complexity could be applied to a wide

number of complex intermediates. The library of scaffold forming reactions can also be adapted to suit the selected intermediates.

To effectively realise this broad application to a wide number of substrates, then practical synthetic routes for all the desired complex intermediates would have to be developed. This may involve an extensive optimisation for new complex intermediate formations or identification of further substrates from the literature. Another challenge would be the development and or identification of ring cleavage chemistry. This was the least successful approach in this project but would add significant diversity to any library. Complex intermediates could be selected which are more well suited for ring cleavage reactions, for example, containing a labile lactone or alkenes suitable for cleavage reactions.

The key challenge for the 'top-down' approach moving forward is the demonstration of biological relevance of this library of compounds. The LOS approach enables the synthesis of a library of compounds which have the correct molecular properties which target lead-like chemical space;³⁹ however, this does not guarantee biological activity. A collection of screening compounds may be tested in many distinct assays, each of which is designed to find compounds which modulate a specific biological process.²²¹ Though this is not a measure of general biological functions as it only measures one specific mode of activity and many compounds may be discounted if activity is not quickly established.²²¹

As chemists there have been many well reported methods for the generation of new diverse chemical matter.^{70,118,222223} Recently there has been a new focus on creating libraries which are not only diverse in structure but are also possess functional diversity. Aldrich has developed a library of enantiomerically enriched reduced flavone analogues with diversity observed in the appendages, stereochemistry, and chemical properties in an effort to determine which features of small molecules are most predictive of biological performance diversity (Figure 47).²²⁴ A cell painting assay was employed to assess biological function. Cell painting is a phenotypic screening which employs six dyes to stain eight cellular components and organelles method

and allows modulation of many different pathways to be assessed at the same time (within a cellular context).^{224–227} The cells are then imaged, and hundreds of features are assessed and generates a ‘barcode’ of how the compounds effects a cell and the function. This ‘barcode’ of function allows compounds to be grouped based on their similar phenotypic effects.

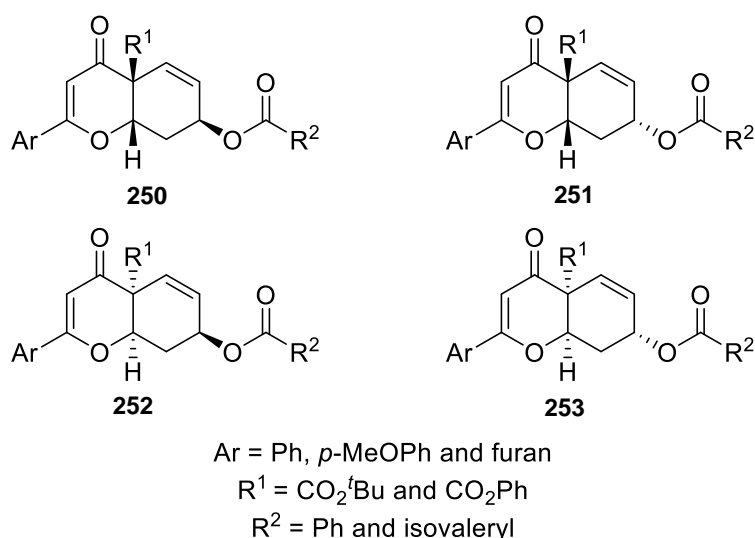


Figure 47: enantiomerically enriched reduced flavone analogues.²²⁴

Demonstration of the value of a cell painting assay and its ability to distinguish differences in biological activity arising solely from stereoisomerism.²²⁸ The different stereoisomers contained within the several selected series (Figure 48), resulted in distinct changes in cell morphology. Comparison of the concentration-dependent effects observed on cell morphology, coupled with principal component analysis (PCA) highlights the significant differences between the stereoisomers, suggesting that their biological effects are mediated by different mechanisms of action (MoA).

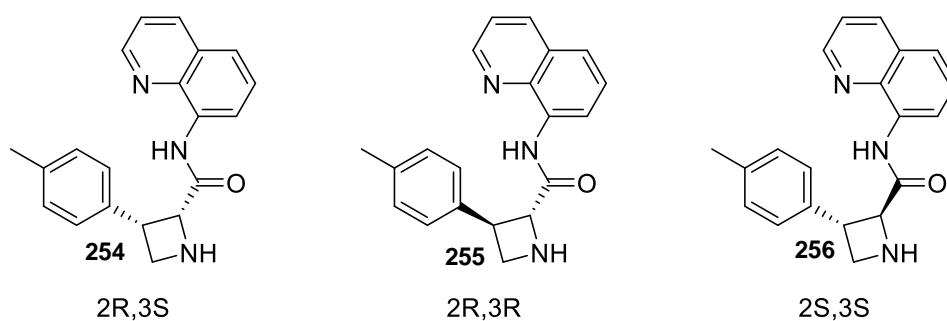


Figure 48: the stereochemical diverse library of azetidine compounds. The *cis* and *trans* isomers induce distinct changes on cell morphology.²²⁸

The cell painting assay appears to be an efficient way of annotating the activity of a diverse range of compounds that were designed with no specific biological target in mind, so would be an ideal method for screening this library. Many different functions can be screened in the same experiment, thus, giving a broad read out of biological relevance for the library of lead-like compounds.

The power of the 'top-down' approach has been demonstrated in this project via the synthesis of 21 structurally diverse scaffolds. This approach is widely adaptable and has the potential to be applied to a wide range of complex intermediates and different reaction classes. However, there is a need to establish the biological relevance of this compound library to understand the impact of the work, and as such, this will be the focus of future collaborative investigations.

Chapter 6 Experimental

6.1 General Information and Instrumentation

Commercially available starting materials were obtained from Sigma–Aldrich, Acros, Fluorochem, Alfa Aesar, Fisher Scientific, SLS (Scientific Laboratory Supplies) and Insight Biotechnology. All non-aqueous reactions were performed under a nitrogen atmosphere unless otherwise stated. Water-sensitive reactions were performed in anhydrous solvents in oven-dried glassware and cooled under nitrogen before use. Anhydrous dichloromethane (CH_2Cl_2), anhydrous tetrahydrofuran (THF), anhydrous toluene, anhydrous diethyl ether, anhydrous ethanol, anhydrous methanol and anhydrous acetonitrile were obtained from a PureSolv MD5 Purification System. Anhydrous dimethylformamide (DMF) and anhydrous 1,4- dioxane were obtained from SureSeal bottles from Sigma–Aldrich. All other solvents used were of chromatography or analytical grade. Petrol refers to petroleum spirit (b.p. 40–60 °C) and ether refers to diethyl ether. Solvents were removed under reduced pressure using a Büchi rotary evaporator and Vacuubrand PC2201 Vario diaphragm pump.

Thin layer chromatography (TLC) was performed using aluminium backed silica (Merck silica gel 60 F254) plates obtained from Merck. Ultraviolet light ($\lambda_{\text{max}} = 254 \text{ nm}$) and KMnO_4 were used for visualization. Flash column chromatography was performed using silica gel 60 (35-70 μm particles) supplied by Merck. Infrared spectra were recorded using a Bruker Alpha-P ATR FR-IR Spectrometer. Absorptions are reported in wavenumbers (cm^{-1}).

Analytical LCMS was performed using an Ultimate3000 HPLC instrument with a Bruker Amazon Speed MS Detector with electrospray ionization. The system ran with a positive and negative switching mode and UV diode array detector using a Phenomenex Kinetex C18 column (2.6 micron, 2.1x50mm) and gradient elution H_2O and MeCN each plus 0.1% formic acid. Accurate mass spectrometry was performed using electrospray ionisation on a Bruker MaXis Impact spectrometer.

Preparative LC-MS was performed using an Agilent Technologies Infinity (1260) instrument with a UV diode array detector and an Agilent 6100 series Single Quad MS detector. The system used a Phenomenex Kinetex C18 EVO 21.2 x 250 mm 5-micron column. The general preparation method used a solvent system of MeCN/H₂O (5–95%) + 0.1% Formic acid and a run time of 20 minutes.

Preparative HPLC (reverse phase) was performed using Waters XSelect (CSH C18 ODB column, 5 μ silica, 30 mm diameter, 100 mm length), using decreasingly polar mixtures of water (containing 1% by volume NH₃OH (28-30% in H₂O)) and MeCN as eluents

Proton (¹H) and carbon (¹³C) NMR data was collected on Bruker 300, 400, 500 or 500-CP(cryoprobe) MHz spectrometers using an internal deuterium lock. Data was collected at 300 K unless otherwise stated. Chemical shifts (δ) are given in parts per million (ppm) and referenced to the residual solvent peak. Coupling constants (J) are reported in Hertz (Hz) and splitting patterns are reported in an abbreviated manner: app. (apparent), s (singlet), d (doublet), t (triplet), q (quartet), sext. (sextet), hept. (heptet), m (multiplet) and br (broad). NMR data was reported in the format: ppm (number of protons, splitting pattern, coupling constant (Hz), proton ID). Assignment of signals was aided by the use of DEPT 135, COSY, HMQC, HMBC and NOESY

6.2 General experimental

A: Borohydride reduction

Sodium borohydride (1.1 eq.) was added to a solution of aldehyde/ketone (1.0 eq.) in MeOH (0.5 M), the reaction mixture was stirred at rt for 2 h and quenched with water. The aqueous phase was extracted with CH₂Cl₂ (x3) and the combined organic extracts were dried over MgSO₄ and concentrated under reduced pressure to give a crude material.

B: Pyrrolidine formation:

N-(Methoxymethyl)-*N*-(trimethylsilylmethyl)benzylamine (2.2 eq.) and lithium fluoride (2.5 eq.) were added to a solution of enone (1.0 eq.) in anhydrous

MeCN (0.2M) at rt. The reaction mixture was refluxed for 16 h cooled and then concentrated under reduced pressure to give a crude material.

C: Pyrrole formation:

The enone (1.0 eq.), tBuOK (5.0 eq.) and TosMIC (1.0 eq.) were dissolved in THF (0.2 M), cooled to 0 °C and stirred for 1 h. The reaction was then allowed to warm to rt and stirred for 16 h. The reaction was diluted with water and extracted with CH₂Cl₂ (x3) and the combined organic extracts were dried over MgSO₄ and concentrated under reduced pressure to give a crude material.

D: Rh catalysed 1,4 addition

Boronic acid (5.0 eq), chloro(1,5-cyclooctadiene)rhodium(I) dimer (2.5 mol%) and triethylamine (1.0 eq), were added to a solution of the enone (1.0 eq.) in degassed dioxane–H₂O (6:1, 0.3 M) at rt then the reaction was refluxed at 80 °C for 16 h, allowed to cool to rt and concentrated under reduced pressure to give a crude material.

E: Microwave Cyclisation

With no particular precaution to exclude air or water, 5-bromopent-1-ene (1.2 eq.) was added to a solution of an appropriate hydroxypyridine (1.0 eq.) and K₂CO₃ (1.2 eq.) in propan-2-ol (0.25 M) and the solution was refluxed overnight. The mixture was concentrated under reduced pressure to give a crude mixture which was dissolved in MeCN (0.25 M) and transferred to a microwave vial. The reaction mixture was heated at 160 °C for 6 h at 300 psi and max power. The crude reaction mixture was filtered, and the filtrate was concentrated under reduced pressure to give a crude product.

F: Gold catalysed pyridine formation:

Propargyl amine (2.0 eq.) was added to a solution of the ketone (1.0 eq.) and sodium tetrachloroaurate(III) dihydrate (2.5 mol%) in EtOH (0.1 M), the reaction mixture was refluxed at 80 °C for 16 h, allowed to cool to rt and concentrated under reduced pressure to give a crude material.

G: Titanium mediated Reductive amination:

Morpholine (5.0 eq.) and $\text{Ti}(\text{O}^i\text{Pr})_4$ (2.0 eq.) were added to a stirred solution of ketone (1.0 eq.) in EtOH (0.5 M), the reaction mixture was stirred at rt for 6 h. The reaction mixture was cooled to 0 °C and NaBH_4 (1.5 eq.) was added portion-wise, the reaction mixture was allowed to warm to rt and stirred for 3 h. The reaction was diluted with ammonium hydroxide solution (2M), filtered to remove the precipitate then extracted with EtOAc (x3) and the combined organic extracts were dried over MgSO_4 and concentrated under reduced pressure to give a crude material.

H: L-selectride reduction:

L-selectride (1M in THF, 1.5 eq.) was added to a solution of ketone (1.0 eq.) in anhydrous THF (0.3 M) cooled to -78 °C, the reaction mixture was stirred at -78 °C for 2 h and quenched with water. The aqueous phase was extracted with CH_2Cl_2 (x3) and the combined organic extracts were dried over MgSO_4 and concentrated under reduced pressure to give a crude material.

I: $\text{S}_{\text{N}}\text{Ar}$ reaction

NaH (1.5 eq.) was added to a solution of the alcohol (1.0 eq.) in THF (0.2M) cooled to 0 °C, the reaction was stirred at 0 °C for 1 h. Aryl halide (1.2 eq.) was added and the reaction was warmed to rt and stirred for 16 h, the reaction was then concentrated under reduced pressure to give a crude material.

J: Hydrogenation with Palladium hydroxide:

The benzyl protected amine (1.0 eq.), was dissolved in MeOH (0.5 M), $\text{Pd}(\text{OH})_2/\text{C}$ (10 mol%) was added and the reaction was placed under an atmosphere of hydrogen, and stirred overnight at room temp. The reaction mixture was filtered through celite and concentrated under reduced pressure to give a crude material.

K: Sulfonamide formation

Amine (1.0 eq.) was dissolved in THF (0.3 M), pyridine (4.0 eq.) was added and the mixture was stirred for 30 min. Sulfonyl chloride (8.0 eq.) was added and the reaction was heated to 70 °C overnight, the reaction was cooled to rt and quenched with water and extracted with EtOAc (3 x 10 mL), dried

(MgSO₄), filtered and concentrated under reduced pressure to give a crude material.

L: Amide formation:

Amine (1.0 eq.) was dissolved in CH₂Cl₂ (0.3 M), pyridine (4.0 eq.) was added and stirred at rt for 5 min, acid chloride (8.0 eq.) was added and the mixture was stirred at rt overnight. LiOH (5.0 eq.) and water (1.0 M) were added and the reaction was heated to 70 °C overnight, the reaction was cooled to rt and extracted with CH₂Cl₂ (3 × 10 mL), dried (MgSO₄), filtered and concentrated under reduced pressure to give a crude material.

M: Periodate cleavage

NaIO₄ (1.1 eq.) was dissolved in water-CH₂Cl₂ (1:1, 0.5 M) and the mixture was cooled to 0 °C, the diol (1.0 eq.) was added slowly, the mixture was warmed to rt and stirred for 2.5 h. The reaction was extracted with CH₂Cl₂, dried over MgSO₄ and concentrated under reduced pressure to give a crude material.

N: Lithiation

Furan (3.0 eq.) was dissolved in THF (0.6 M) and cooled to -78 °C, *n*-BuLi (2.0 eq.) was added and the mixture was stirred at -78 °C for 1.5 h, and then warmed to 0 °C for 0.5 h. The mixture was cooled to -78 °C, aldehyde (1.0 eq.) was added and the reaction was stirred at the same temperature for 1 h, and then warmed to rt for 0.5 h. The reaction was quenched with a saturated, aqueous ammonium chloride solution and extracted with EtOAc (3 × 25 mL), dried (MgSO₄), filtered and concentrated under reduced pressure to give a crude material.

O: Reductive amination:

Amine (1.0 eq.) was dissolved in DMF (0.3 M), molecular sieves were added followed by aldehyde/ketone (5.0 eq.) and the reaction was stirred overnight. NaBH₄ (3.0 eq.) was added and the reaction was stirred for 3h and quenched with water and extracted with EtOAc (3 × 10 mL), dried (MgSO₄), filtered and concentrated under reduced pressure to give a crude material.

P: Reduction of the enone with hydrogen

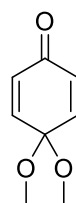
The enone (1.0 eq.), was dissolved in a solvent (0.5 M), Pd/C (10 mol%) was added and the reaction was placed under an atmosphere of hydrogen, and stirred overnight at room temp. The reaction mixture was filtered through celite and concentrated under reduced pressure to give a crude material.

Q: Luche reduction:

CeCl₃·7H₂O (1.1 eq.) was added to a solution of enone (1.0 eq.) in MeOH (0.5 M), sodium borohydride (1.1 eq.) was added and the reaction mixture was stirred at rt for 2 h and quenched with water. The aqueous phase was extracted with CH₂Cl₂ (x3) and the combined organic extracts were dried over MgSO₄ and concentrated under reduced pressure to give a crude material.

6.3 Compound Series

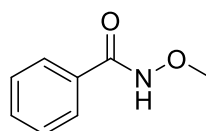
4,4-Dimethoxycyclohexa-2,5-dien-1-one 100



[Bis(trifluoroacetoxy)iodo]benzene (1.73 g, 4.20 mmol) in MeCN (24 mL), was added to a solution of 4-methoxyphenol (2.00 g, 16.1 mmol) and potassium carbonate (4.45 g, 32.2 mmol) in MeOH (40 mL) at 0 °C and stirred for 10 mins, the solution changed from colourless to dark orange. The reaction was quenched with water (30 mL), extracted with EtOAc (3 x 40 mL), dried (MgSO₄), filtered and concentrated under reduced pressure to give a crude product. The crude material was purified by flash column chromatography eluting with 20:80 EtOAc–Hexanes to give the protected quinone¹⁵² (1.31 g, 53%) as an orange oil. *R*_F 0.30 (25:75 EtOAc–Hexanes); *v*_{max}/cm⁻¹ (film) 2990, 2975, 2834, 1742, 1687, 1373, 1163 and 1034; δ_H (500 MHz, CDCl₃) 6.82 (2H, d, *J* 10.4, 2-H and 6-H), 6.28 (2H, d, *J* 10.4, 3-H and 5-H) and 3.38 (6H, s, OMe); δ_C (125 MHz,

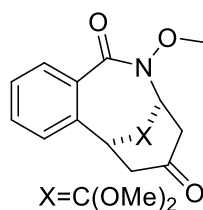
CDCl_3) 185.2, 143.3, 130.0, 114.8 and 50.4; HRMS found MH^+ , 155.0703. $\text{C}_8\text{H}_{10}\text{O}_3$ requires MH , 155.0708.

***N*-Methoxybenzamide 98**



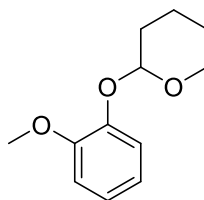
Benzoyl chloride (1.65 mL, 14.23 mmol) was added dropwise to a solution of methoxyamine hydrochloride (1.42 g, 17.1 mmol) and potassium carbonate (3.77 g, 22.7 mmol) in EtOAc–water (2:1, 325 mL) at 0 °C, and the solution was warmed to rt and stirred overnight. The reaction was extracted with EtOAc (3 x 40 mL), washed with a saturated, aqueous brine solution (3 x 50 mL) and water (3 x 50 mL), dried (MgSO_4), filtered and concentrated under reduced pressure to give a crude material. The crude material was purified by flash column chromatography eluting with 50:50 EtOAc–Hexanes, to give the amide¹⁵¹ (1.69 g, 79%) as a colourless solid. R_F 0.26 (50:50 EtOAc–Hexanes); $\nu_{\text{max}}/\text{cm}^{-1}$ (film) 3219, 3061, 3003, 2810, 1650, 1599, 1514, 1185, 1075 and 1021; δ_{H} (500 MHz, CDCl_3) 8.99 (1H, br s, NH), 7.73 (2H, d, J 8.0, 2-H and 6-H), 7.52 (1H, app t, J 7.5, 4-H), 7.42 (2H, t, J 8.0, 3-H and 5-H) and 3.87 (3H, s, methoxy); δ_{C} (125 MHz, CDCl_3) 171.2, 132.0, 131.9, 128.7, 127.1 and 64.6; HRMS found MH^+ , 152.0706. $\text{C}_8\text{H}_9\text{NO}_2$ requires MH , 152.0712.

(10*R,1*S**)-9,14,14-Trimethoxy-9-azatricyclo[8.3.1.0^{2,7}]tetradeca-2(7),3,5-triene-8,12-dione 82**



With no particular precaution to exclude air or water, $(\text{Cp}^*\text{RhCl}_2)_2$ (47 mg, 0.07 mmol, 5 mol%) was added to a solution of *N*-methoxybenzamide (0.20 g, 1.32 mmol) in trifluorotoluene (13 mL), the solution was stirred at rt for 10 min. 4-dimethoxycyclohexa-2,5-dien-1-one (0.31 g, 1.98 mmol) and CsOAc (0.25 g, 1.32 mmol) were added and the reaction was heated to 70 °C for 12 h. The reaction was diluted with a saturated, aqueous brine solution (10 mL), extracted with EtOAc (3 × 20 mL), dried (MgSO_4), filtered and concentrated under reduced pressure to give a crude material. The crude material was purified by flash column chromatography eluting with 75:25 EtOAc–Hexanes to give the ketone¹⁴⁷ (0.09 g, 21%) as an orange oil. R_F 0.21 (35:65 EtOAc–Hexanes); $\nu_{\text{max}}/\text{cm}^{-1}$ (film) 2970, 2940, 2835, 1720, 1643, 1598, 1114 and 1080; δ_{H} (500 MHz, CDCl_3) 8.24 (1H, d, J 7.5, 6-H), 7.42 (1H, t, J 7.5, 4-H), 7.32 (1H, t, J 7.5, 5-H), 7.12 (1H, d, J 7.5, 3-H), 4.45 (1H, dt, J 5.4 and 2.7, 10-H), 3.88 – 3.82 (1H, m, 1-H), 3.79 (3H, s, *N*-Omethoxy), 3.43 (3H, s, 14-methoxy_A), 3.14 (3H, s, 14-methoxy_B), 3.09 (1H, dd, J 14.9 and 7.5, 11-H_A), 2.90 (1H, dd, J 15.4 and 5.5, 13-H_A), 2.79 (1H, dt, J 15.4 and 2.2, 13-H_B) and 2.48 (1H, dt, J 14.9 and 2.2, 11-H_b); δ_{C} (126 MHz, CDCl_3) 206.1, 166.3, 136.4, 132.7, 132.1, 130.6, 130.4, 127.4, 97.0, 65.1, 62.4, 48.8, 48.6, 47.5, 46.0 and 43.1; HRMS found MNa^+ , 328.1155. $\text{C}_{19}\text{H}_{19}\text{NO}_5$ requires MNa , 328.1161.

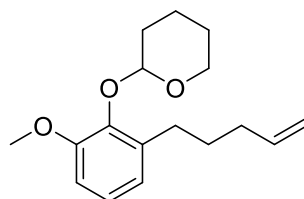
2-(2-Methoxyphenoxy)tetrahydro-2H-pyran 106



3,4-dihydro-2H-pyran (3.39 g, 40.3 mmol) was added to a solution of 2-methoxy phenol (0.50 g, 4.03 mmol) and pyridinium *p*-toluene sulfonic acid (0.10 g, 0.41 mmol) in CH_2Cl_2 (3.5 mL), which was stirred at rt for 4 h. The reaction was quenched using an aqueous NaOH solution (2 M, 5 mL), extracted with CH_2Cl_2 (3 × 30 mL), dried (MgSO_4), filtered and concentrated under reduced pressure to give a crude product. The

crude material was purified by flash column chromatography eluting with 5:95 EtOAc–Hexanes, to give the protected alcohol²²⁹ (0.71 g, 85%) as a colourless oil. R_F 0.51 (10:90 EtOAc–Hexanes); $\nu_{\max}/\text{cm}^{-1}$ (film) 3064, 2941, 2871, 2850, 2056, 1990, 1724, 1592, 1500, 1074 and 1020; δ_H (300 MHz, CDCl_3) 7.14 (1H, dd, J 7.9 and 1.4, Ar 6-H), 7.01 – 6.95 (1H, m, Ar 3-H), 6.93 – 6.88 (2H, m, Ar 4-H and Ar 5-H), 4.05 – 3.99 (1H, m, 2-H), 3.85 (3H, s, methoxy CH_3), 3.64 – 3.55 (1H, m, 6- H_A), 2.11 – 2.02 (1H, m, 6- H_B), 1.91 (2H, m, 3-H) and 1.74 – 1.54 (4H, m, 4-H and 5-H); δ_C (75 MHz, CDCl_3) 150.4, 146.4, 122.6, 121.0, 118.1, 112.5, 97.7, 62.2, 56.1, 30.9, 25.4 and 18.9; HRMS found MNa^+ , 231.0992. $\text{C}_{12}\text{H}_{16}\text{O}_3$ requires MNa , 231.0997.

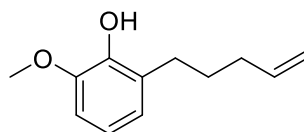
2-(2-Methoxy-6-(pent-4-en-1-yl)phenoxy)tetrahydro-2H-pyran 108



n-BuLi (65.5 mL, 91.7 mmol, 1.4 M) was added to a solution of the THP protected alcohol **106** (15.9 g, 76.4 mmol) in THF (50 mL) at 0 °C, the reaction was warmed to rt and stirred for 3 h, the reaction was then cooled to -78 °C and 5-bromopent-1-ene (9 mL, 76.4 mmol) was added, the reaction was allowed to warm to rt and stir overnight. The reaction was quenched with a saturated, aqueous ammonium chloride solution (25 mL), extracted with EtOAc (3 × 40 mL), dried (MgSO_4), filtered and concentrated under reduced pressure to give a crude product. The crude material was purified by flash column chromatography eluting with 10:90 EtOAc–Hexanes, to give the alkene²³⁰ (8.45 g, 40%) as a pale yellow oil. R_F 0.50 (10:90 EtOAc–Hexanes); $\nu_{\max}/\text{cm}^{-1}$ (film) 2938, 1584, 1474, 1438, 1199, 1033 and 1021; δ_H (300 MHz, CDCl_3) 6.97 (1H, t, J 7.9, Ar 4-H), 6.81 – 6.72 (2H, m, Ar 3-H and Ar 5-H), 5.94 – 5.78 (1H, m, pent 4-H), 5.20 (1H, t, J 3.4, 2-H), 5.03 (1H, app ddd, J 17.2, 3.6 and 1.6, pent 5- H_{trans}), 4.96 (1H, ddt, J 10.2, 2.2 and 1.2, pent 5- H_{cis}), 4.17 – 4.01 (1H, m, 6- H_A), 3.82 (3H, s, methoxy CH_3), 3.66 – 3.51 (1H, m, 6- H_B), 2.85 (1H, dt, J 13.5 and 7.8, pent 1- H_A), 2.71

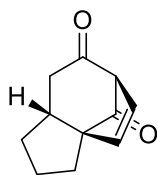
– 2.55 (1H, m, pent 1-H_B), 2.18 – 2.06 (2H, m, pent 3-H), 2.03 – 1.86 (3H, m, 3-H and 5-H_A), 1.81 – 1.69 (2H, m, pent 2-H) and 1.66 – 1.55 (3H, m, 4-H and 5-H_B); δ_C (75 MHz, CDCl₃) 152.4, 144.8, 139.8, 123.7, 122.6, 122.1, 121.0, 118.1, 114.4, 101.4, 63.3, 55.7, 33.7, 30.8, 29.7, 25.4 and 19.5; HRMS found MNa⁺, 299.1623. C₁₇H₂₄O₃ requires MNa, 299.1623.

2-Methoxy-6-(pent-4-en-1-yl)phenol **102**



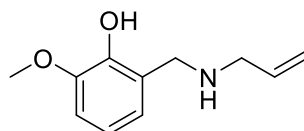
Oxalic acid (2% solution, 2.4 mL, 0.54 mmol) was added to a solution of the THP protected alcohol **108** (0.15 g, 0.54 mmol) in MeOH (3 mL), the solution was heated to 75 °C for 14 h. The reaction was quenched with a saturated, aqueous sodium bicarbonate solution (10 mL) extracted with EtOAc (3 × 25 mL), dried (MgSO₄), filtered and concentrated under reduced pressure, to give a crude material which was used without further purification to yield the phenol¹⁵⁴ (66 mg, 63%) as a yellow oil. R_F 0.54 (10:90 EtOAc–Hexanes); ν_{max}/cm^{-1} (film) 3523, 2937, 1748, 1592, 1476, 1440, 1271 and 1078; δ_H (300 MHz, CDCl₃) 6.81 – 6.71 (3H, m, 3-H, 4-H and 5-H), 5.88 (1H, m, pent 4-H), 5.07 (1H, app ddd, J 17.2, 3.5 and 1.7, pent 5-H_{trans}), 4.99 (1H, ddt, J 10.2, 2.3 and 1.2, pent 5-H_{cis}), 3.88 (3H, s, methoxy CH₃), 2.75 – 2.62 (2H, m, pent 1-H), 2.19–2.05 (2H, m, pent 3-H) and 1.83 – 1.69 (2H, m, pent 2-H); δ_C (75 MHz, CDCl₃) 146.3, 143.6, 138.9, 128.3, 122.4, 119.2, 114.5, 108.3, 56.0, 33.6, 29.3 and 29.0; HRMS found MNa⁺, 215.1043. C₁₂H₁₆O₂ requires MNa, 215.1048.

(1R*,5R*,8R*)-Tricyclo[6.2.1.0^{1,5}]undec-9-ene-7,11-dione 83



PIFA (4.93 g, 11.5 mmol) in hexafluoroisopropanol (20 mL) was added to a solution of the phenol **102** (2.00 g, 10.4 mmol) in hexafluoroisopropanol (20 mL) at 0 °C, and stirred for 20 min. The reaction was diluted with ether (20 mL) and quenched with a saturated, aqueous sodium thiosulphate solution (25 mL), extracted with Et₂O (3 × 25 mL), dried (MgSO₄), filtered and concentrated under reduced pressure to give a crude material. The crude material was purified by flash column chromatography eluting with 10:90 EtOAc–Hexanes, to give the cyclic product¹⁵⁴ (0.77 g, 42%) as a pale yellow oil. *R*_F 0.30 (10:90 EtOAc–Hexanes); *v*_{max}/cm⁻¹ (film) 2953, 2868, 2003, 1763, 1707, 1448, 1409, 1347, 1288, 1099 and 1020; δ_H (500 MHz, CDCl₃) 6.46 (1H, d, *J* 6.7, 10-H), 6.19 (1H, dd, *J* 6.7 and 3.4, 9-H), 3.52 (1H, d, *J* 3.4, 8-H), 3.03 (1H, dd, *J* 17.5 and 8.4, 8-H_A), 2.39 – 2.23 (3H, m, 8-H_B, 7-H and 6-H_A), 1.99 – 1.90 (1H, m, 6-H_B), 1.90 – 1.80 (1H, m, 5-H_A), 1.75 – 1.63 (1H, m, 4-H_A), 1.59 (1H, m, 4-H_B) and 1.22 (1H, m, 5-H_B); δ_C (75 MHz, CDCl₃) 210.0, 199.7, 141.6, 126.7, 66.2, 59.7, 45.0, 43.0, 32.4, 25.1 and 24.5.

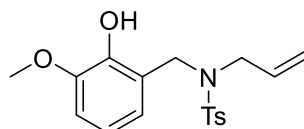
2-Methoxy-6-[(prop-2-en-1-ylamino)methyl]phenol 109



Allyl amine (0.25 mL, 3.28 mmol) was added to a solution of o-vanillin (0.50 g, 3.28 mmol) in MeOH (8 mL) and stirred at rt for 1 h, NaBH₄ (0.14 g, 3.61 mmol) was added portion wise to the solution and stirred at rt for 1 h. The reaction was quenched with water (25 mL), extracted with EtOAc (3 × 20 mL), dried (MgSO₄), filtered and concentrated under reduced pressure to give a crude material which was used without further purification to yield the the *amine* (0.59 g, 94%) as an amorphous yellow solid. *R*_F 0.06 (80:20

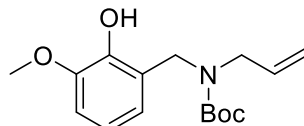
EtOAc–Hexanes); $\nu_{\max}/\text{cm}^{-1}$ (film) 3063, 3027, 2978, 2916, 2809, 1949, 1494, 1453 and 915; δ_{H} (300 MHz, CDCl_3) 6.83 (1H, dd, J 7.8 and 1.6, 5-H), 6.75 (1H, t, J 7.8, 4-H), 6.65 (1H, dd, J 7.8 and 1.6, 3-H), 5.92 (1H, ddt, J 16.3, 10.3 and 6.0, prop 2-H), 5.28 – 5.15 (2H, m, prop 3-H), 4.04 (2H, s, methyl-H), 3.89 (3H, s, methoxy H) and 3.33 (2H, dt, J 6.0 and 1.3, prop 1-H); δ_{C} (75 MHz, CDCl_3) 147.3, 135.8, 134.8, 120.7, 118.7, 117.4, 111.0, 55.9, 51.5, 50.8 and 31.6; HRMS found MH^+ , 194.1171. $\text{C}_{10}\text{H}_{15}\text{NO}_2$ requires MH , 194.1181.

***N*-[(2-Hydroxy-3-methoxyphenyl)methyl]-4-methyl-*N*-(prop-2-en-1-yl)benzenesulfonamide 110a**



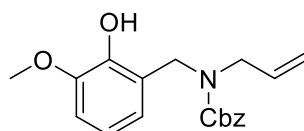
Amine **109** (0.20 g, 1.04 mmol), tosyl chloride (0.22 g, 1.14 mmol) and K_2CO_3 (0.22 g, 1.56 mmol) were dissolved in CH_2Cl_2 (8 mL) and stirred at rt for 2 h. The reaction was quenched with a saturated, aqueous sodium bicarbonate solution (10 mL) and extracted with CH_2Cl_2 (3 \times 25 mL), dried (MgSO_4), filtered and concentrated under reduced pressure to give a crude material. The crude material was purified by flash column chromatography eluting with 35:65 EtOAc–Hexanes to give the Ts protected amine¹⁵⁴ as a colourless oil (0.19 g, 53%). R_{F} 0.10 (20:80 EtOAc–Hexanes); $\nu_{\max}/\text{cm}^{-1}$ (film) 3529, 2941, 2842, 2255, 1597, 1481, 1441, 1219 and 906; δ_{H} (300 MHz, CDCl_3) 7.74 (2H, d, J 8.0, tosyl 2-H and tosyl 6-H), 7.30 (2H, d, J 8.0, tosyl 3-H and tosyl 5-H), 7.01 – 6.91 (1H, m, phenol 6-H), 6.84 – 6.74 (2H, m, phenol 4-H and phenol 5-H), 5.68 – 5.50 (1H, m, prop 2-H), 5.12 – 5.01 (2H, m, prop 3-H), 4.42 (2H, s, methyl), 3.88 (3H, s, methoxy CH_3), 3.82 (2H, d, J 6.5, prop 1-H) and 2.44 (3H, s, tosyl CH_3); δ_{C} (75 MHz, CDCl_3) 146.5, 143.9, 133.5, 131.5, 132.5, 129.6, 128.5, 127.3, 122.2, 119.6, 118.9, 110.1, 56.1, 50.2, 44.8 and 21.5; HRMS found MH^+ , 348.1264. $\text{C}_{18}\text{H}_{21}\text{NO}_4\text{S}$ requires MH , 348.1269.

Tert-butyl N-[(2-hydroxy-3-methoxyphenyl)methyl]-N-(prop-2-en-1-yl)carbamate 110b



Amine **109** (1.00 g, 5.17 mmol), boc anhydride (1.24 g, 5.69 mmol) and NEt₃ (1.45 mL, 10.4 mmol) were dissolved in CH₂Cl₂ (20 mL) and stirred at rt for 16 h. The reaction was quenched with a saturated, aqueous sodium bicarbonate solution (10 mL) and extracted with CH₂Cl₂ (3 × 25 mL), dried (MgSO₄), filtered and concentrated under reduced pressure to give a crude material. The crude material purified by flash column chromatography eluting with 30:70 EtOAc–Hexanes, to give the *boc protected amine* as a colourless oil (1.47 g, 97%). *R*_F 0.45 (30:70 EtOAc–Hexanes); *v*_{max}/cm⁻¹ (film) 3243, 2794, 2938, 1760, 1667, 1593 and 1164; δ _H (500 MHz, MeOD) 7.28 (1H, m, phenol 5-H), 7.20 – 7.17 (2H, m, phenol 4-H and phenol 6-H), 6.20 (1H, app ddt, *J* 21.8, 10.4 and 5.7, prop 2-H), 5.56-5.49 (2H, m, prop 3-H), 4.88 (2H, s, methyl), 4.28 (3H, s, OMe), 4.25 (2H, d, *J* 4.9, prop 1-H) and 1.88 (9H, s, boc ^tBu); δ _C (100 MHz, CDCl₃) 157.4, 133.4, 133.3, 125.5, 123.6, 122.8, 119.0, 116.8, 111.5, 77.2, 56.0, 49.1, 45.8 and 28.4; HRMS found MH⁺, 294.1692. C₁₆H₂₄NO₄ requires *MH*, 294.1705.

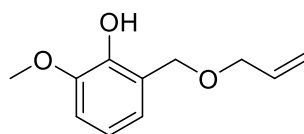
Benzyl N-[(2-hydroxy-3-methoxyphenyl)methyl]-N-(prop-2-en-1-yl)carbamate 110c



Amine **109** (1.00 g, 5.17 mmol), and K₂CO₃ (1.45 mL, 10.4 mmol) were dissolved in THF–water (2:1, 18 mL), benzyl chloroformate (0.81 mL, 5.69 mmol) was added portionwise and stirred at rt overnight. The reaction was quenched with a saturated, aqueous sodium bicarbonate solution (10 mL) and extracted with CH₂Cl₂ (3 × 25 mL), dried (MgSO₄), filtered and concentrated under reduced pressure to give a crude

material. The crude material was purified by flash column chromatography eluting with 30:70 EtOAc–Hexanes, to give the cbz *protected amine* as a colourless oil (1.57 g, 93%). R_f 0.29 (20:80 EtOAc–Hexanes); ν_{max} (neat)/ cm^{-1} 3378, 2942, 2839, 1765, 1688, 1479, 1414, 126 and 1071; δ_H (500 MHz, MeOD) 7.22 – 7.15 (5H, m, cbz phenyl), 6.77 – 6.70 (2H, m, phenol 4-H and phenol 5-H), 6.62 (1H, m, phenol 6-H), 5.66 (1H, app ddd, J 22.5, 10.8 and 5.5, prop 2-H), 5.04 (2H, s, cbz CH_2), 5.02 – 4.89 (2H, m, prop 3-H), 4.41 (2H, s, methyl), 4.35 (1H, br s, OH), 3.79 (1H, d, J 5.5, prop 1-H) and 3.73 (3H, s, OMe); δ_C (101 MHz, CDCl_3) 162.7, 148.2, 145.4, 133.0, 128.6, 128.5, 128.5, 128.3, 128.1, 127.9, 123.2, 122.7, 119.4, 117.3, 111.2, 67.9, 56.1, 48.9 and 45.8.

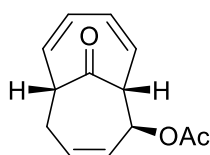
2-methoxy-6-[(prop-2-en-1-yloxy)methyl]phenol 115



NaBH_4 (1.37 g, 36.1 mmol) was added portion wise to a solution of *ortho*-Vanillin (5.00 g, 32.8 mmol) in methanol (65 mL) at 0 °C and stirred overnight at rt. The reaction was quenched with water (30 mL) extracted with EtOAc (3 x 30 mL), dried (MgSO_4) and concentrated under reduced pressure to give the crude benzyl alcohol (2.72 g, 17.7 mmol) which was dissolved in DMF (30 mL) and cooled to 0 °C. NaH (60% in mineral oil, 1.55 g, 38.9 mmol) was added and the mixture was stirred for 4 h, allyl bromide (3.36 mL, 38.9 mmol) was added and the reaction was stirred overnight at rt. The reaction was diluted with water (30 mL) and extracted with EtOAc (3 x 30 mL), dried (MgSO_4) and concentrated under reduced pressure to give a crude material. Following the literature protocol¹⁵⁷, the crude material (0.60 g, 2.56 mmol) was dissolved in KOH in methanol (10%, 60 mL), Pd/C (10% w/w, 0.10 g, 0.94 mmol) was added and the reaction was heated to 90 °C for 12 h, the reaction mixture was filtered through a short pad of celite, diluted with an aqueous saturated ammonium chloride solution (10 mL), extracted with CH_2Cl_2

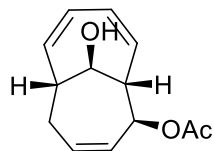
(3 x 25 mL), dried (MgSO₄) and concentrated under reduced pressure to give a crude material. The crude material was purified by flash column chromatography eluting with 10:90 EtOAc–Hexanes, to give the phenol¹⁵⁷ as a pale yellow oil (0.40 g, 81%). *R*_F 0.48 (20:80 EtOAc–Hexane); *v*_{max} (neat)/cm⁻¹ 3509, 2939, 2841, 1619, 1596, 1479, 1441, 1356, 1272, 1215 and 1058; *δ*_H (300 MHz, CDCl₃) 6.92 – 6.85 (3H, m, Ar-H), 6.33 (1H, br s, OH), 5.97 (1H, ddt, *J* 17.2, 10.4 and 5.6, prop 2-H), 5.32 (1H, app dq, *J* 17.2 and 1.4, prop 3-H_A), 5.21 (1H, ddd, *J* 10.4, 2.9 and 1.4, prop 3-H_B), 4.65 (2H, s, benzyl CH₂), 4.08 (1H, dt, *J* 5.6 and 1.4, prop 1-H) and 3.88 (3H, s, OMe); *δ*_C (75 MHz, CDCl₃) 146.9, 144.2, 134.5, 123.7, 121.2, 119.5, 117.3, 110.5, 71.3, 67.9 and 56.1; HRMS found MNa⁺, 217.0830. C₁₁H₁₄O₃ requires *MNa*, 217.0840.

(1R*,2S*,6R*)-11-oxobicyclo[4.4.1]undeca-3,7,9-trien-2-yl acetate 84



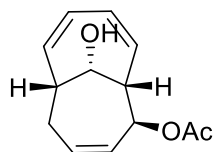
Tropone (0.46 mL, 4.72 mmol) and 1-acetoxybutadiene (1.12 mL, 9.42 mmol) were heated at 90 °C for 5 days. The crude material was purified directly by flash column chromatography eluting with 15:85 EtOAc–Hexanes, to give the bicycle¹⁶³ as a pale yellow oil (0.59 g, 51%, *d.r* >95:<5 by ¹H NMR). *R*_F 0.48 (20:80 EtOAc–Hexane); *v*_{max} (neat)/cm⁻¹ 3031, 2936, 1732, 1703, 1433, 1370, 1226, 1172 and 1019; *δ*_H (400 MHz, C₆D₆) 5.76 (1H, m, 2-H), 5.69 (2H, m, 8-H and 9-H), 5.57 – 5.51 (1H, m, 3-H), 5.40 (2H, m, 10-H and 4-H), 5.14 (1H, dd, *J* 10.8 and 5.8, 7-H), 3.78 (1H, dd, *J* 9.7 and 3.6, 1-H), 3.30 (1H, app q, *J* 6.1, 6-H), 2.17 – 2.09 (1H, m, 5-H_A), 2.04 – 1.95 (1H, m, 5-H_B) and 1.61 (3H, s, OAc); *δ*_C (100 MHz, CDCl₃) 202.9, 170.2, 131.5, 130.6, 130.0, 127.7, 126.2, 125.3, 69.6, 61.1, 55.3, 29.2 and 21.0; HRMS found MNa⁺, 241.0835. C₁₃H₁₄O₃ requires *MNa*, 241.0840.

(2R*,1S*,6R*,11R*)-11-hydroxybicyclo[4.4.1]undeca-3,7,9-trien-2-yl acetate 123



According to general procedure A, the bicyclic ketone **84** (1.00 g, 4.58 mmol) was dissolved in *i*PrOH (23 mL) to give a crude material. The crude material was purified by flash column chromatography eluting with 10:90 EtOAc–Hexanes to give the alcohol¹⁶³ as a yellow oil (0.24 g, 24%). R_F 0.46 (50:50 EtOAc–Hexane); ν_{max} (neat)/ cm^{-1} 3416, 3018, 1729, 171, 1231, 1017 and 787; δ_H (400 MHz, CDCl_3) 6.00 – 5.91 (1H, m, 4-H), 5.90 – 5.80 (1H, m, 3-H), 5.81 – 5.65 (3H, m, 7-H, 8-H and 9-H), 5.54 – 5.43 (1H, m, 10-H), 5.42 (1H, dd, J 6.5 and 5.0, 2-H), 4.52 (1H, app br s, 11-H), 3.28 (2H, dt, J 7.3 and 3.0, 1-H), 3.02 – 2.90 (2H, m, 5-H_A and 6-H), 2.21 (1H, ddd, J 13.9, 8.5 and 4.7, 6-H_B) and 2.10 (3H, s, OAc); δ_C (100 MHz, CDCl_3) 169.2, 136.0, 133.5, 130.5, 127.2, 125.7, 124.3, 74.6, 72.2, 48.2, 45.4, 25.1 and 21.3; HRMS found MNa^+ , 243.0991. $\text{C}_{13}\text{H}_{16}\text{O}_3$ requires MNa , 243.0997.

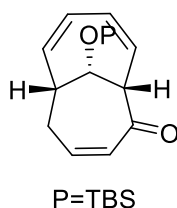
(6R*,1S*,2S*,11S*)-11-hydroxybicyclo[4.4.1]undeca-3,7,9-trien-2-yl acetate 124



According to general procedure A, the bicyclic ketone **84** (1.00 g, 4.58 mmol) was dissolved in *i*PrOH (23 mL) to give a crude material. The crude material was purified by flash column chromatography eluting with 10:90 EtOAc–Hexanes to give the alcohol¹⁶³ as a yellow oil (0.39 g, 39%). R_F 0.41 (50:50 EtOAc–Hexane); ν_{max} (neat)/ cm^{-1} 3417, 292, 1729, 1371, 1231, 1017 and 956; δ_H (400 MHz, CDCl_3) 6.01 – 5.79 (3H, m, 9-H, 8-H and 4-H), 5.77 – 5.67 (2H, m, 7-H and 3-H), 5.59 (1H, dd, J 11.3 and 6.9, 10-H), 5.36 (1H, dd, J 6.9 and 5.3, 2-H), 4.39 (1H, t, J 3.7, 11-H), 3.38 – 3.22 (1H, m, 1-H), 3.03

(1H, dq, J 6.5 and 3.7, 6-H), 2.53 – 2.40 (1H, m, 5-H_A), 2.38 – 2.27 (1H, m, 5-H_B) and 2.06 (3H, s, OAc); δ_C (100 MHz, CDCl₃) 170.1, 134.7, 134.3, 129.7, 128.5, 127.8, 125.3, 69.9, 68.4, 49.6, 46.3, 27.6 and 21.1.; HRMS found MNa^+ , 243.0991. C₁₃H₁₆O₃ requires MNa , 243.0997.

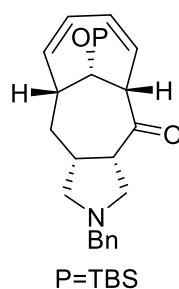
(6R*,1S*,11S*)-11-[(tert-butyldimethylsilyl)oxy]bicyclo[4.4.1]undeca-3,7,9-trien-2-one 127



The alcohol **123** (1.00 g, 4.54 mmol), TBSCl (1.03 g, 6.83 mmol) and imidazole (0.31 g, 4.54 mmol) were dissolved in the minimum amount of DMF and stirred overnight at rt. The reaction was diluted with CH₂Cl₂ (20 mL) and washed with an aqueous solution of LiCl (10% w/w, 3 x 20 mL) and a saturated aqueous brine solution (3 x 20 mL), dried (MgSO₄) and concentrated under reduced pressure. The crude product (0.68 g, 2.03 mmol) and K₂CO₃ (0.42 g, 3.04 mmol) were dissolved in MeOH (10 mL) and stirred at rt for 4 h, water (20 mL) was added and the solution was extracted with CH₂Cl₂ (3 x 25 mL), dried (MgSO₄), filtered and concentrated under reduced pressure to give a crude product (0.47 g, 1.61 mmol) which was dissolved in CH₂Cl₂ (8 mL). Dess-Martin periodinane (0.75 g, 1.77 mmol) and NaHCO₃ (0.20 g, 2.42 mmol) were added and the solution was stirred overnight at rt. The reaction was quenched with a saturated, aqueous sodium bicarbonate solution (10 mL) and extracted with CH₂Cl₂ (3 x 25 mL), dried (MgSO₄), filtered and concentrated under reduced pressure to give a crude material. The crude material was purified by flash column chromatography eluting with 15:85 EtOAc–Hexanes to give the *enone* as a yellow oil (319 mg, 32%). R_F 0.67 (30:70 EtOAc–Hexane); ν_{max} (neat)/cm⁻¹ 3026, 2888, 2855, 1670, 1450, 1211, 1104 and 940; δ_H (400 MHz, CDCl₃) 6.55 – 6.33 (1H, m, 4-H), 6.07 – 5.89 (3H, m, 3-H, 8-H and 9-H), 5.82 (1H, dd, J 11.1 and 7.1, 7-H), 5.67 (1H, dd, J 11.4 and 6.3, 10-H), 4.50 –

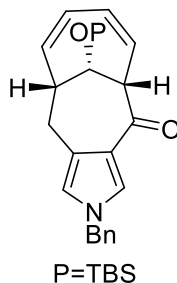
4.39 (1H, m, 11-H), 3.59 (1H, s, 1-H), 2.96 – 2.84 (1H, m, 6-H), 2.48 – 2.27 (2H, m, 5-H), 0.83 (9H, s, TBS ^tBu) and 0.03 (6H, app d, *J* 1.8, TBS Me). δ_C (100 MHz, CDCl₃) 198.7, 141.7, 135.0, 134.2, 128.0, 127.6, 125.9, 70.6, 63.6, 43.1, 29.4, 25.7, 18.0, -4.6 and -4.7; HRMS found MH⁺, 291.1775. C₁₇H₂₆O₂Si requires *MH*, 291.1780.

(7R*,1S*,3S*,9R*,14S*)-5-benzyl-14-[(tert-butyldimethylsilyl)oxy]-5-azatricyclo[7.4.1.0^{3,7}]tetradeca-10,12-dien-2-one 155



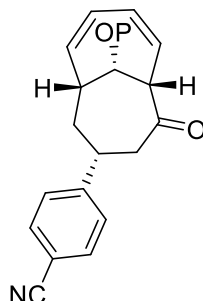
According to general procedure B, the enone **127** (0.09 g, 0.31 mmol) gave a crude material. The crude material was purified by flash column chromatography eluting with 20:80 EtOAc–Hexanes, to give the *pyrrolidine* as a yellow oil (9.00 mg, 7%). *R_F* 0.39 (30:70 EtOAc–Hexane); ν_{\max} (neat)/cm⁻¹ 3024, 2896, 1698, 1495, 1472, 1106 and 871; δ_H (400 MHz, CDCl₃) 7.27 – 7.22 (5H, m, benzyl), 6.10 – 5.95 (2H, m, 11-H and 12-H), 5.55 (2H, m, 13-H and 10-H), 4.01 (1H, t, *J* 4.5, 14-H), 3.59 – 3.54 (1H, m, 1-H), 3.49 (1H, app d, *J* 4.6, benzyl CH₂), 2.92 (1H, app t, *J* 8.2, 4-H_A), 2.86 – 2.77 (1H, m, 9-H), 2.76 – 2.65 (2H, m, 4-H_B and 6-H_A), 2.57 (1H, app t, *J* 9.4, 6-H_B), 1.74 (1H, t, *J* 8.6, 3-H), 1.62 – 1.55 (2H, m, 8-H), 1.27 – 1.15 (1H, m, 7-H), 0.78 (9H, s, TBS ^tBu), 0.01 (3H, s, TBS Me) and 0.00 (3H, s, TBS Me); δ_C (100 MHz, CDCl₃) 209.4, 132.7, 128.9, 128.3, 128.2, 127.3, 127.0, 126.7, 70.5, 66.2, 61.9, 60.4, 51.1, 46.9, 34.0, 30.5, 25.6, 17.9, -4.8 and -4.9; HRMS found MNa⁺, 446.2482. C₂₆H₃₇NO₂Si requires *MNa*, 446.2491.

(9R*,1S*,14S*)-14-[(tert-butyldimethylsilyl)oxy]-5-azatricyclo[7.4.1.0^{3,7}]tetradeca-3,6,10,12-tetraen-2-one 158



According to general procedure C, the enone **127** (0.10 g, 0.34 mmol), gave a crude material. The crude material was purified by flash column chromatography eluting with 5:95 EtOAc–Hexanes to give the *pyrrole* as a pale yellow oil (13.0 mg, 11%). R_F 0.73 (30:70 EtOAc–Hexanes); ν_{max} (neat)/ cm^{-1} 3317, 2947, 2932, 1669, 1450, 1405 and 1020; δ_H (400 MHz, $CDCl_3$) 6.04 (2H, m, 3-H and 6-H), 5.86 – 5.79 (1H, m, 11-H), 5.74 – 5.58 (3H, m, 10-H, 13-H and 12-H), 4.52 – 4.42 (1H, m, 14-H), 3.74 (1H, t, J 5.7, 1-H), 3.43 (1H, ddd, J 12.9, 5.7 and 1.9, 8-H_A), 3.28 (1H, t, J 7.3, 9-H), 2.84 (1H, dd, J 12.9 and 7.6, 8-H_B), 0.83 (9H, s, TBS ^tBu) and 0.05 (6H, s, TBS Me); δ_C (101 MHz, $CDCl_3$) 202.3, 131.3, 129.3, 128.2, 127.6, 127.4, 125.9, 124.8, 124.7, 69.2, 66.0, 49.2, 39.8, 25.6, 17.9, -4.8 and -4.8.

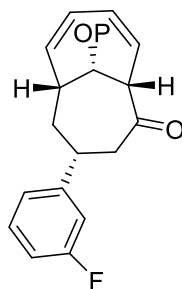
4-[(1R*,3R*,6S*,11S*)-11-[(tert-butyldimethylsilyl)oxy]-5-oxobicyclo[4.4.1]undeca-7,9-dien-3-yl]benzotrile 146



According to general procedure D, the enone **127** (0.07 g, 0.24 mmol) gave a crude material. The crude material was purified by flash column chromatography eluting with 10:90 EtOAc–Hexanes, to give the β -arylketone as a yellow oil (20.0 mg, 21%). R_F 0.35 (20:80 EtOAc–Hexane);

ν_{\max} (neat)/ cm^{-1} 2984, 1736, 1465, 1372, 1233 and 1043; δ_{H} (400 MHz, CDCl_3) 7.59 (2H, d, J 8.3, Ar 2-H and Ar 6-H), 7.39 (2H, d, J 8.3, Ar 3-H and Ar 5-H), 6.15 – 5.97 (2H, m, 7-H and 10-H), 5.69 (1H, dd, J 9.5 and 1.8, 8-H), 5.51 (1H, m, 9-H), 4.12 (1H, app d, J 6.8, 11-H), 4.04 (1H, app br s, 1-H), 2.73 (1H, dd, J 6.8 and 1.2, 4-H), 2.35 (1H, ddd, J 17.8, 5.5 and 2.4, 3- H_A), 2.17 – 2.01 (4H, m, 6-H, 3- H_B and 5-H), 0.90 (9H, s, TBS ^tBu) and 0.09 (6H, app d, J 2.8, TBS Me); δ_{C} (101 MHz, CDCl_3) 199.8, 151.0, 137.0, 132.8, 132.1, 130.5, 128.8, 128.0, 125.2, 109.5, 77.8, 56.7, 49.5, 45.7, 40.9, 35.0, 25.9, 18.1, -4.5 and -4.7; HRMS found MH^+ , 394.2188. $\text{C}_{24}\text{H}_{32}\text{NO}_2\text{Si}$ requires MH , 394.2202.

(4R*,1S*,6R*,11S*)-11-[(tert-butyldimethylsilyl)oxy]-4-(3-fluorophenyl)bicyclo[4.4.1]undeca-7,9-dien-2-one 147



According to general procedure D, the enone **127** (0.07 g, 0.24 mmol) gave a crude material. The crude material was purified by flash column chromatography eluting with 5:95 EtOAc–Hexanes, to give the β -arylketone as a yellow oil (12.5 mg, 14%). R_{F} 0.54 (20:80 EtOAc–Hexane); ν_{\max} (neat)/ cm^{-1} 2952, 2856, 1717, 1613, 1587, 1442, 1251, 1103 and 875; δ_{H} (400 MHz, CDCl_3) 7.22 – 7.14 (1H, m, Ar 5-H), 6.98 (1H, d, J 8.3, Ar 6-H), 6.90 (1H, t, J 8.3, Ar 2-H), 6.79 (1H, td, J 8.3 and 2.3, Ar 4-H), 6.02 – 5.91 (2H, m, 10-H and 9-H), 5.63 (1H, app d, J 9.6, 8-H), 5.46 – 5.37 (1H, m, 7-H), 4.03 (1H, d, J 6.8, 11-H), 3.92 (1H, app br s, 1-H), 2.65 (1H, d, J 6.8, 4-H), 2.30 – 2.19 (1H, m, 3- H_A), 2.07 – 1.77 (4H, m, 3- H_B , 6-H and 5-H), 0.81 (9H, s, TBS ^tBu) and 0.00 (6H, app d, J 3.6, TBS Me); δ_{C} (100 MHz, CDCl_3) 197.9, 163.1 (d, J 245.8), 147.7 (d, J 6.7), 137.2, 130.2, 129.9 (d, J 8.4), 128.5, 124.9, 123.1 (d, J 2.6), 114.7 (d, J 21.4), 112.8 (d, J 21.1), 77.8, 56.5, 49.4, 47.1,

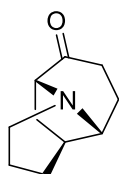
40.2, 35.1 (d, J 23.4), 26.9, 18.1, -4.5 and -4.8; HRMS found MH^+ , 387.2150. $C_{23}H_{31}FO_2Si$ requires MH , 387.2155.

(1R*, 3S*, 8S*)-7-azatricyclo[5.4.0.0.^{3,8}]undec-9-en-11-one **85**



According to general procedure E, 3-hydroxypyridine (1.00 g, 10.5 mmol) gave a crude material. The crude material was purified by flash column chromatography eluting with 100 EtOAc, to give the amine²³¹ as a dark yellow oil (1.20 g, 70%, dr >20:<1 by ¹HNMR). R_F 0.10 (50:50 EtOAc–Hexane); ν_{max} (neat)/ cm^{-1} 3367, 3045, 2936, 2861, 1686, 1567, 1451, 1382, 1136 and 1105; δ_H (400 MHz, $CDCl_3$) 7.09 (1H, dd, J 9.6 and 5.8, 9-H), 5.89 (1H, dd, J 9.6 and 1.2, 10-H), 3.68 (1H, dd, J 7.5 and 1.4, 1-H), 3.55 (1H, d, J 5.8, 8-H), 2.95 (2H, m, 6-H), 2.39 (1H, app dt, J 6.4 and 3.0, 3-H), 2.02 (1H, dd, J 13.6 and 7.7, 2- H_A), 1.78 (2H, m, 4-H), 1.63 (2H, m, 5- H_A and 2- H_B), 1.34 (1H, m, 5- H_B); δ_C (100 MHz, $CDCl_3$) 199.1, 151.8, 126.5, 70.1, 68.1, 53.9, 35.7, 30.4, 30.4 and 18.1; HRMS found MH^+ , 164.10670. $C_{10}H_{14}O$ requires MH , 164.1075.

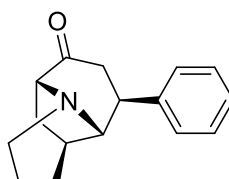
(1R*,3S*,8R*)-7-azatricyclo[5.4.0.0.^{3,8}]undecan-11-one **159**



According to general procedure P, the enone **85** (0.75 g, 4.59 mmol) in MeOH gave a yellow oil (0.66 g, 87%) which was used without further purification. R_F 0.08 (2:98 MeOH– CH_2Cl_2); ν_{max}/cm^{-1} (film) 2941, 2896, 1701, 1412, 1290 and 1205; δ_H (501 MHz, $CDCl_3$) 3.50 (1H, d, J 7.0, 6-H), 3.18 (1H, dd, J 7.8 and 0.9, 8-H), 2.99 – 2.88 (2H, m, 1- H_A and 1- H_B), 2.41 – 2.32 (1H, m, 10- H_A),

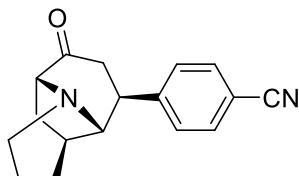
2.27 (1H, app ddd, J 17.8, 8.9, 5.5, 10-H_B), 2.22 – 2.10 (2H, m, 4-H and 9-H_A), 1.96 (1H, dd, J 13.8 and 8.2, 9-H_A), 1.75 – 1.65 (2H, m, 3-H_A and 5-H_A), 1.62 – 1.52 (2H, m, 5-H_B and 3-H_B), 1.47 – 1.39 (1H, m, 2-H_A), 1.36 – 1.28 (1H, m, 2-H_B); δ_C (101 MHz, CDCl₃) 208.6, 69.9, 65.4, 53.7, 40.2, 31.9, 31.8, 31.3, 25.8 and 18.9.

(1R*,3S*,8S*,9S*)-9-phenyl-7-azatricyclo[5.4.0.0^{3,8}]undecan-11-one 140



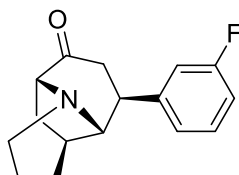
According to general procedure D, the enone **85** (1.00 g, 6.13 mmol) gave a crude material. The crude material was purified by flash column chromatography eluting with gradient elution: 0:100 → 20:80 EtOAc-hexanes to give the β -arylketone (0.36 g, 20%) as a yellow oil. R_f 0.46 (50:50 petrol–EtOAc); ν_{max}/cm^{-1} (film) 3060, 3026, 2933, 2861, 1721, 1601, 1493, 1470, 1453, 1401, 1156, 1100 and 1059; δ_H (500 MHz, CDCl₃) 7.29 – 7.35 (4H, m, Ar 2-H, Ar 3-H, Ar 5-H and Ar 6-H), 7.21 – 7.26 (1H, m, Ar 4-H), 3.60 (1H, ddd, J 8.4, 2.9 and 1.6 Hz, 1-H), 3.25 (1H, d, J 1.4 Hz, 8-H), 2.9 – 3.03 (2H, m, 6-H), 2.71 (1H, dd, J 16.8 and 9.9 Hz, 10-H_A), 2.52 – 2.57 (1H, m, 9-H), 2.44 (1H, dd, J 16.8 and 7.1 Hz, 10-H_B), 2.24 – 2.29 (1H, m, 3-H), 2.03 – 2.12 (1H, m, 2-H_A), 1.76 (1H, ddd, J 13.9, 6.7 and 3.0 Hz, 2-H_B), 1.66 – 1.72 (1H, m, 4-H_A), 1.53 – 1.65 (2H, m, 4-H_B and 5-H_A) and 1.33 (1H, dt, J 14.0, 5.2 and 5.2 Hz, 5-H_B); δ_C (126 MHz, CDCl₃) 209.1, 146.8, 128.8, 126.9, 126.6, 73.7, 68.9, 53.3, 43.1, 42.2, 40.9, 32.1, 31.1 and 19.2; HRMS found MNa^+ , 264.1359. C₁₆H₁₉NO requires MNa , 264.1364.

4-[(1R*,3S*,8S*,9S*)-11-oxo-7-azatricyclo[5.4.0.0^{3,8}]undecan-9-yl]benzonitrile 144



According to general procedure D, the enone **85** (1.00 g, 6.13 mmol) gave a crude material. The crude material was purified by flash column chromatography eluting with gradient elution: 0:100 → 20:80 EtOAc-hexanes to give the β -*arylketone* (0.39 g, 24%) as a white amorphous solid. R_f 0.25 (50:50 petrol–EtOAc); $\nu_{\max}/\text{cm}^{-1}$ (film) 2941, 2859, 2220, 1714, 1606, 1504, 1418, 1155 and 1034; δ_{H} (500 MHz, CDCl_3) 7.59 – 7.64 (2H, m, Ar 3-H and Ar 5-H), 7.41 – 7.46 (2H, m, Ar 2-H and Ar 6-H), 3.62 (1H, ddd, J 8.3, 2.9 and 1.4 Hz, 1-H), 3.13 – 3.19 (1H, m, 8-H), 2.95 – 3.03 (1H, m, 6-H_A), 2.86 – 2.96 (1H, m, 6-H_B), 2.64 – 2.7 (1H, m, 9-H), 2.46 – 2.61 (2H, m, 10-H), 2.27 – 2.33 (1H, m, 3-H), 2.10 (1H, dd, J 13.9 and 8.1 Hz, 2-H_A), 1.77 (1H, ddd, J 13.9, 6.8 and 2.9 Hz, 2-H_B), 1.67 – 1.75 (1H, m, 4-H_A), 1.53 – 1.67 (2H, m, 4-H_B and 5-H_A) and 1.34 – 1.40 (1H, m, 5-H_B); δ_{C} (126 MHz, CDCl_3) 207.3, 152.2, 132.7, 127.8, 118.8, 110.6, 73.4, 68.9, 53.5, 43.5, 41.3, 40.7, 32.1, 31.3 and 19.1; HRMS found MH^+ , 267.1494. $\text{C}_{17}\text{H}_{18}\text{N}_2\text{O}$ requires MH , 267.1497.

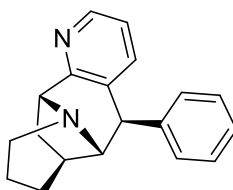
(1R*,3S*,8S*,9S*)-9-(3-fluorophenyl)-7-azatricyclo[5.4.0.0^{3,8}]undecan-11-one 142



According to general procedure D, the enone **85** (1.00 g, 6.13 mmol) gave a crude material. The crude material was purified by flash column chromatography eluting with gradient elution: 0:100 → 20:80 EtOAc-hexanes to yield to give the β -*arylketone* (0.63 g, 40%) as a yellow oil. R_f 0.31 (50:50 petrol–EtOAc); $\nu_{\max}/\text{cm}^{-1}$ (film) 2934, 1718, 1613, 1587, 1485, 1448, 1231,

1099 and 782; δ_{H} (500 MHz, CDCl_3) 7.25 – 7.30 (1H, m, Ar 5-H), 7.03 – 7.09 (2H, m, Ar 2-H and Ar 6-H), 6.9 – 6.95 (1H, m, Ar 4-H), 3.60 (1H, ddd, J 8.4, 2.9 and 1.5 Hz, 1H), 3.22 (1H, d, J 1.5 Hz, 8-H), 2.89 – 3.02 (2H, m, 6-H), 2.64 (1H, dd, J 16.4 and 9.4 Hz, 10- H_A), 2.54 – 2.6 (1H, m, 9-H), 2.46 (1H, dd, J 16.4 and 6.8 Hz, 10- H_B), 2.24 – 2.3 (1H, m, 3-H), 2.08 (1H, dd, J 13.9 and 8.4 Hz, 2- H_A), 1.73 (2H, m, 2 H_B and 4 H_A), 1.53 – 1.65 (2H, m, 4- H_B and 5- H_A) and 1.29 – 1.39 (1H, m, 5- H_B); δ_{C} (126 MHz, CDCl_3) 208.3, 163.1 (d, J 246.2 Hz), 149.3 (d, J 7.0 Hz), 130.2 (d, J 8.3 Hz), 122.5 (d, J 2.7 Hz), 113.8 (d, J 21.7 Hz), 113.4 (d, J 21.1 Hz), 73.5, 68.9, 53.4, 43.0 (d, J 1.5 Hz), 41.8, 40.8, 32.1, 31.2, 19.1; HRMS found MNa^+ , 282.1265. $\text{C}_{16}\text{H}_{18}\text{NFO}$ requires MNa , 282.1270.

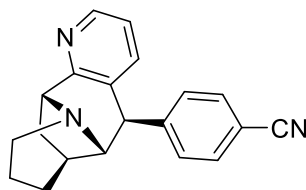
(3R*,2S*,10R*,12S*)-3-phenyl-1,8-diazatetracyclo[8.5.0.0^{2,12}.0^{4,9}]pentadeca-4(9),5,7-triene 195



According to general procedure F, ketone **140** (50.0 mg, 0.21 mmol) gave a crude material. The crude material was purified by flash column chromatography eluting with gradient elution: 0:100 \rightarrow 70:30 EtOAc-hexanes to yield the *pyridine* (23.0 mg, 40%) as a yellow oil. R_f 0.17 (50:50 petrol–EtOAc); $\nu_{\text{max}}/\text{cm}^{-1}$ (film) 3282, 3051, 3002, 2966, 2936, 2867, 2195, 1980, 1628, 1598, 1583, 1490, 1473, 1452, 1344, 1190 and 1099; δ_{H} (500 MHz, CDCl_3) 8.18 (1H, ddd, J 4.9, 1.5 and 0.9 Hz, 7-H), 7.28 – 7.34 (4H, m, Ph 2-H, Ph 3-H, Ph 5-H and Ph 6-H), 7.21 – 7.26 (1H, m, Ph 4-H), 7.07 (1H, d, J 7.7 Hz, 5-H), 6.93 (1 H, dd, J 7.7, 4.9 Hz, 6-H), 4.28 (1H, dt, J 7.3, 2.1 Hz, 10-H), 3.56 (1H, s, 3-H), 3.27 (1H, s, 2-H), 3.18 (1H, dd, J 13.3 and 5.6 Hz, 15- H_A), 2.89 – 3.01 (1H, m, 15- H_B), 2.40 (1H, t, J 5.3 Hz, 12-H), 2.27 (dd, J 13.2 and 7.4 Hz, 11- H_A), 1.79 (3H, m, 11- H_B , 14- H_A and 13- H_A), 1.61 – 1.69 (1H, m, 13- H_B) and 1.31 – 1.39 (1H, m, 14- H_B). δ_{C} (126 MHz, CDCl_3) 164.4, 146.9, 145.3, 137.9, 132.4, 128.6, 128.3, 126.6, 121.7, 74.7, 65.6, 53.8, 50.0,

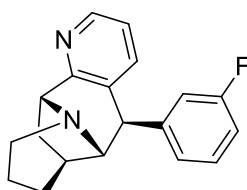
42.1, 38.3, 32.0 and 19.0; HRMS found MH^+ , 277.1714. $C_{19}H_{20}N_2$ requires MH , 277.1705.

4-[(3R*,2S*,10R*,12S*)-1,8-diazatetracyclo[8.5.0.0²,¹².0⁴,⁹]pentadeca-4(9),5,7-trien-3-yl]benzonitrile 197



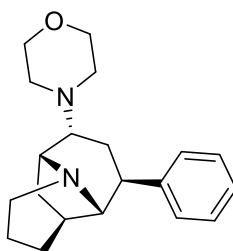
According to general procedure F, ketone **144** (50.0 mg, 0.19 mmol) gave a crude material. The crude material was purified by flash column chromatography eluting with gradient elution: 0:100 → 70:30 EtOAc-hexanes to yield the *pyridine* (41.0 mg, 73%) as a yellow oil. R_f 0.13 (50:50 petrol–EtOAc); ν_{max}/cm^{-1} (film) 3290, 3041, 2929, 2917, 2855, 2226, 2201, 1730, 1605, 1574, 1479, 1441, 1347, 1267, 1180 and 1088; δ_H (500 MHz, $CDCl_3$) 8.22 (1H, ddd, J 4.6, 1.8 and 0.8 Hz, 7-H), 7.57 – 7.61 (2H, m, Ph 3-H and Ph 5-H), 7.42 – 7.46 (2H, m, Ph 2-H and Ph 4-H), 6.94 – 7.01 (2H, m, 6-H and 5-H), 4.29 (1H, dt, J 7.3 and 1.6 Hz, 10-H), 3.64 (1H, s, 3-H), 3.12 – 3.21 (2H, m, 2-H and 15H_A), 2.83 – 3.01 (1H, m, 15-H_B), 2.39 – 2.45 (1H, m, 12-H), 2.24 – 2.32 (1H, dd, J 12.7 and 6.8, 11-H_A), 1.73 – 1.87 (3H, m, 11-H_B, 13-H_A and 14-H_A), 1.62 – 1.71 (1H, m, 13-H_B) and 1.31 – 1.39 (1H, m, 14-H_B); δ_C (126 MHz, $CDCl_3$) 164.4, 152.0, 145.9, 137.8, 132.5, 131.0, 129.1, 121.8, 118.9, 110.6, 74.4, 65.5, 53.9, 49.8, 42.0, 38.6, 32.1 and 18.9; HRMS found MH^+ , 302.1660. $C_{20}H_{19}N_3$ requires MH , 302.1657.

(3R*,2S*,10R*,12S*)-3-(3-fluorophenyl)-1,8-diazatetracyclo[8.5.0.0²,¹².0⁴,⁹]pentadeca-4(9),5,7-triene 196



According to general procedure F, ketone **142** (50.0 mg, 0.19 mmol) gave a crude material. The crude material was purified by flash column chromatography eluting with gradient elution: 0:100 → 70:30 EtOAc-hexanes to yield the *pyridine* (14.0 mg, 25%) as a yellow oil. R_f 0.16 (50:50 petrol-EtOAc); $\nu_{\max}/\text{cm}^{-1}$ (film) 3055, 2966, 2945, 2931, 2860, 1722, 1684, 1614, 1582, 1481, 1439, 1363, 1277, 1214, 1117 and 1025; δ_{H} (500 MHz, CDCl_3) 8.19 (1H, ddd, J 4.9, 1.6 and 0.9 Hz, 7-H), 7.23 – 7.29 (1H, m, Ph 5-H), 7.05 – 7.11 (3H, m, 5-H Ph 4-H and Ph 6-H), 6.87 – 6.97 (2H, m, Ph 2-H and 6-H), 4.27 (1H, dt, J 7.3, 2.0 and 1.8 Hz, 10-H), 3.56 (1H, s, 3-H), 3.24 (1H, s, 2-H), 3.21 – 3.13 (1H, m, 15- H_A), 2.89 – 3.00 (1H, m, 15- H_B), 2.37 – 2.42 (1H, m, 12-H), 2.27 (1H, dd, J 13.2 and 7.4 Hz, 11- H_A), 1.73-1.82 (3H, m, 11- H_B , 13- H_A and 14- H_A), 1.61 – 1.69 (1H, m, 13- H_B) and 1.31 – 1.39 (1H, m, 14- H_B); δ_{C} (126 MHz, CDCl_3) 164.4, 163.0 (d, J = 246.2 Hz), 149.2 (d, J = 7.2 Hz), 145.5, 137.9, 131.7, 129.9 (d, J = 8.3 Hz), 123.9 (d, J = 2.7 Hz), 121.8, 115.2 (d, J = 21.2 Hz), 113.5 (d, J = 21.1 Hz), 74.5, 65.5, 53.8, 49.6 (d, J = 1.5 Hz), 42.0, 38.4, 32.0 and 18.9; HRMS found MH^+ , 295.1624. $\text{C}_{19}\text{H}_{19}\text{FN}_2$ requires MH , 295.1611.

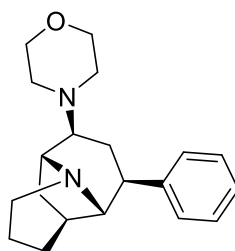
(1R*,3S*,8S*,9S*,11R*)-11-(morpholin-4-yl)-9-phenyl-7-azatricyclo[5.4.0.0^{3,9}]undecane 233a



According to general procedure G, ketone **140** (50.0 mg, 0.21 mmol) gave a crude material. The crude material was purified by flash column chromatography eluting with gradient elution: 20:80 → 100:0 EtOAc-hexanes to yield the *morpholine* (14.0 mg, 22%) as a pale yellow oil. R_f 0.24 (50:50 petrol-EtOAc); $\nu_{\max}/\text{cm}^{-1}$ (film) 2922, 2854, 1492, 1449, 1280, 1118, 1015, 947, 875 and 697; δ_{H} (500 MHz, CDCl_3) 7.41 – 7.44 (2H, m, Ar 6-H and Ar 2-H), 7.26 – 7.31 (2H, m, Ar 3-H and Ar 5-H), 7.17 (1H, m, Ar 4-H), 3.65 – 3.74

(4H, m, morpholine 3-H and 5-H), 3.52 (1H, d, J 7.3 Hz, 1-H), 2.99 (1H, s, 8-H), 2.90 (1H, dd, J 13.4 and 5.7 Hz, 6-H_A), 2.76 – 2.84 (2H, m, 6-H_B and 9-H), 2.63 (1H, ddd, J 9.5, 5.9, 3.0 Hz, 11-H), 2.44 – 2.56 (4H, m, morpholine 6-H and 2-H), 2.22 – 2.27 (1H, m, 3-H), 2.06 – 2.15 (1H, m, 2-H_A), 1.82 (1H, dd, J 13.8 and 5.9 Hz, 1H, 10-H_A), 1.61 – 1.75 (4H, m, 4-H, 5-H_A and 10-H_B), 1.54 (1H, dd, J 13.3 and 7.4 Hz, 2-H_B) and 1.22 – 1.28 (1H, m, 5-H_B); δ_C (126 MHz, CDCl₃) 147.7, 128.1, 127.9, 125.6, 72.8, 67.3, 64.2, 60.7, 54.3, 50.9, 44.0, 39.5, 32.4, 28.6, 28.3 and 19.0; HRMS found MNa^+ , 335.2094. C₂₀H₂₈N₂O requires MNa , 335.2099.

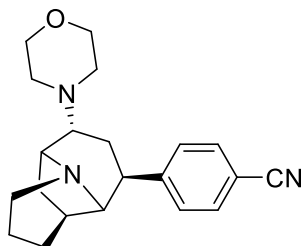
(1R*,3S*,8S*,9S*,11S*)-11-(morpholin-4-yl)-9-phenyl-7-azatricyclo[5.4.0.0^{3,8}]undecane 223b



According to general procedure G, ketone **140** (50.0 mg, 0.21 mmol) gave a crude material. The crude material was purified by flash column chromatography eluting with gradient elution: 20:80 → 100:0 EtOAc-hexanes to yield the *morpholine* (7.00 mg, 11%) as a pale yellow oil. R_f 0.07 (50:50 petrol–EtOAc); ν_{max}/cm^{-1} (film) 2921, 2845, 1492, 1450, 1306, 1118, 1070, 1015, 946, 875 and 726; δ_H (500 MHz, CDCl₃) 7.33– 7.26 (4H, m, Ar 2-H, Ar 3-H, Ar 5-H and Ar 6-H), 7.22 – 7.18 (1H, m, Ar 4-H), 3.76 – 3.67 (4H, m morph 5-H and morph 3-H), 3.29 (1H, d, J 7.8, 1-H), 3.00 (1H, s, 8-H), 2.93 – 2.88 (1H, m, 6-H_A), 2.87 – 2.78 (1H, m, 6-H_B), 2.72 – 2.64 (2H, m, morph 6-H_A and morph 2-H_A), 2.55 – 2.49 (2H, m, morph 6-H_B and morph 2-H_B), 2.29 (1H, dd, J 9.7 and 6.9, 11-H_A), 2.17 (1H, ddd, J 13.1, 5.0 and 2.6, 9-H), 2.13– 2.08 (1H, d, J 5.1, 3-H), 1.96 (1 H, dd, J 13.1 and 8.2, 2-H_A), 1.80 (1 H, td, J 12.8 and 9.9, 10-H_B), 1.59 – 1.48 (5H, m, 2-H_A, 10-H_A, 5-H_A and 4-H) and 1.28 – 1.21 (1H, m, 5-H_B); δ_C (126 MHz, CDCl₃) 148.3, 128.5, 127.1, 126.1, 72.6, 69.7,

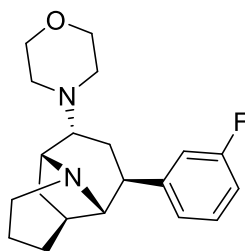
67.3, 59.3, 52.6, 50.1, 45.1, 41.2, 36.1, 30.6, 29.1 and 19.5; HRMS found MH^+ , 313.2273. $C_{20}H_{28}N_2O$ requires MH , 313.2279.

4-[(1R*,3S*,8S*,9S*,11R*)-11-(morpholin-4-yl)-7-azatricyclo[5.4.0.0^{3,8}]undecan-9-yl]benzonitrile 235



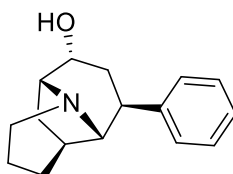
According to general procedure G, ketone **144** (50.0 mg, 0.19 mmol) gave a crude material. The crude material was purified by flash column chromatography eluting with gradient elution: 20:80 → 100:0 EtOAc-hexanes to yield the *morpholine* (18.0 mg, 28%) as a white amorphous solid. R_f 0.14 (50:50 petrol–EtOAc); ν_{max}/cm^{-1} (film) 2928, 2858, 2227, 1606, 1502, 1450, 1307, 1119, 1016, 946 and 875; δ_H (500 MHz, $CDCl_3$) 7.57 (4H, s, Ar 2-H, Ar 3-H, Ar 5-H and Ar 6-H), 3.73 – 3.64 (4H, m, morpholine 3-H and 5-H), 3.53 (1H, d, J 7.4, 1-H), 2.93 – 2.86 (2H, m, 8-H and 6- H_A), 2.83 (1H, d, J 8.1, 9-H), 2.77 (1H, ddd, J 17.1, 10.7, 5.4, 6- H_B), 2.59 – 2.54 (1H, m, 11-H), 2.54 – 2.49 (2H, m, morph 6- H_A and 2- H_A), 2.49 – 2.43 (2H, m, morph 6- H_B and 2- H_B), 2.27 – 2.23 (1H, m, 3-H), 2.10 (1H, ddd, J 13.3, 7.1 and 1.5, 2- H_A), 1.81 – 1.61 (5H, m, 10-H, 4-H and 5- H_A), 1.56 (1H, dd, J 13.3 and 7.5, 2- H_B) and 1.33 – 1.27 (1H, m, 5- H_B); δ_C (126 MHz, $CDCl_3$) 153.2, 131.9, 128.9, 119.3, 109.5, 77.3, 77.0, 76.8, 72.2, 67.2, 63.8, 54.3, 50.8, 44.1, 39.5, 32.4, 31.9, 28.6, 28.2 and 18.9; HRMS found MNa^+ , 360.2046. $C_{21}H_{27}N_3O$ requires MNa , 360.2052.

(1R*,3S*,8S*,9S*,11R*)-9-(3-fluorophenyl)-11-(morpholin-4-yl)-7-azatricyclo[5.4.0.0^{3,8}]undecane 234



According to general procedure G, ketone **142** (50.0 mg, 0.19 mmol) in EtOH (0.20 mL), gave a crude material. The crude material was purified by flash column chromatography eluting with gradient elution: 20:80 → 100:0 EtOAc-hexanes to the *morpholine* (13.0 mg, 20%) as a colourless oil. R_f 0.16 (50:50 petrol-EtOAc); $\nu_{\max}/\text{cm}^{-1}$ (film) 2925, 2856, 2808, 2226, 1613, 1585, 1449, 1281, 1121, 1016, 946 and 873; δ_{H} (500 MHz, CDCl_3) 7.26 – 7.20 (2H, m, Ar 4-H and Ar 5-H), 7.16 (1H, d, J 7.7, Ar 6-H), 6.89 – 6.83 (1H, m, Ar 2-H), 3.75 – 3.63 (4H, m, morph 3-H and morph 5-H), 3.51 (1H, d, J 7.3, 1-H), 2.97 (1H, s, 8-H), 2.90 (1H, dd, J 13.4 and 5.7, 6- H_A), 2.84 – 2.75 (2H, m, 6- H_B and 9-H), 2.59 (1H, ddd, J 9.5, 6.6 and 2.9, 11-H), 2.55 – 2.42 (4H, m, morph 2-H and morph 6-H), 2.26 – 2.20 (1H, m, 3-H), 2.09 (1H, dd, J 12.3, 7.4, 2- H_A), 1.76 – 1.59 (5H, m, 4-H, 5- H_A and 10-H), 1.54 (1 H, dd, J 12.3, 7.4, 2- H_B) and 1.31 – 1.22 (1H, m, 5- H_B); δ_{C} (126 MHz, CDCl_3) 162.7 (d, J 244.4), 150.34 (d, J 7.2), 129.3 (d, J 8.3), 123.6 (d, J 2.4), 114.9 (d, J 21.8), 112.5 (d, J 21.1), 72.4, 67.2, 63.9, 60.7, 54.3, 50.8, 43.6, 39.5, 32.4, 28.6, 28.3 and 18.9. HRMS found MH^+ , 331.2179. $\text{C}_{20}\text{H}_{27}\text{FN}_2\text{O}$ requires MH , 331.2185.

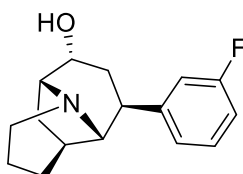
(1R*,3S*,8S*,9S*,11R*)-9-phenyl-7-azatricyclo[5.4.0.0^{3,8}]undecan-11-ol
217



According to general procedure H, ketone **140** (0.20 g, 0.83 mmol) gave a crude material. The crude material was purified by flash column chromatography eluting with gradient elution: 20:80 → 100:0 EtOAc-hexanes to yield the *alcohol* (45.0 mg, 22%) as a pale yellow oil. R_f 0.16 (50:50

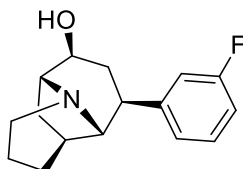
petrol-EtOAc); $\nu_{\max}/\text{cm}^{-1}$ (film); 3313 (br), 2922, 2860, 1600, 1492, 1448, 1343, 1304, 1171, 1108 and 1058. δ_{H} (500 MHz, CDCl_3) 7.42 – 7.36 (2H, m, Ar 2-H and Ar 6-H), 7.31 – 7.26 (2H, m, Ar 5-H and Ar 3-H), 7.20 – 7.14 (1H, m, Ar 4-H), 4.16 (1H, ddd, J 10.0, 6.3 and 3.7, 11-H), 3.35 – 3.27 (1H, m, 1-H), 2.96 (1H, s, 8-H), 2.93 – 2.86 (1H, m, 6-H_A), 2.85 – 2.75 (2H, m, 6-H_B and 9-H), 2.31 (1H, s, OH), 2.30 – 2.25 (1H, m, 3-H), 2.06 (1H, ddd, J 13.4, 7.1 and 1.3, 2-H_A), 1.91 (1H, dd, J 14.0 and 6.3, 10-H_A), 1.76 – 1.57 (5H, m, 5-H_B, 10-H_B, 2-H_B and 4-H) and 1.28 – 1.24 (1H, m, 5-H_B); δ_{C} (126 MHz, CDCl_3) 146.9, 128.2, 127.9, 125.7, 72.7, 69.5, 65.2, 54.0, 44.3, 39.4, 32.5, 31.8, 27.8 and 19.0; HRMS found MH^+ , 244.1703. $\text{C}_{16}\text{H}_{21}\text{NO}$ requires MH , 244.1701.

(1R*,3S*,8S*,9S*,11S*)-9-phenyl-7-azatricyclo[5.4.0.0^{3,8}]undecan-11-ol
218a



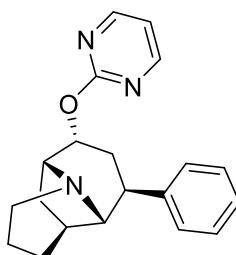
According to general procedure H, ketone **142** (0.20 g, 0.77 mmol) gave a crude material. The crude material was purified by flash column chromatography eluting with gradient elution: 20:80 → 100:0 EtOAc-hexanes to yield the *alcohol* (40.0 mg, 20%) as a pale yellow oil. R_f 0.13 (50:50 petrol-EtOAc); $\nu_{\max}/\text{cm}^{-1}$ (film) 3144, 2984, 1447, 1372, 1275, 1223, 1098, 1043, 938 and 847; δ_{H} (500 MHz, CDCl_3) 7.25 – 7.20 (2H, m, Ar 2-H and Ar 5-H), 7.15 – 7.12 (1H, m, Ar 6-H), 6.89 – 6.83 (1H, m, Ar 4-H), 4.14 (1H, ddd, J 10.1, 6.3 and 3.7, 11-H), 3.37 – 3.29 (1H, m, 1-H), 2.94 (1H, s, 8-H), 2.93 – 2.87 (1H, m, 6-H_A), 2.85 – 2.77 (2H, m, 6-H_B and 9-H), 2.30 – 2.23 (1H, m, 3-H), 2.03 (1H, ddd, J 13.5, 7.0 and 1.4, 2-H_A), 1.87 (1H, dd, J 14.0 and 6.3, 10-H_A), 1.77 – 1.68 (3H, m, 2-H_B, 10H_B and 4-H_A), 1.66 – 1.58 (2H, m, 4-H_B and 5-H_A) and 1.29 – 1.23 (1H, m, 5-H_B); δ_{C} (126 MHz, CDCl_3) 162.7 (d, J 244.3), 149.6 (d, J 7.1), 129.4 (d, J 8.3), 123.5 (d, J 2.3), 114.9 (d, J 21.8), 112.5 (d, J 21.1), 72.3, 69.4, 65.5, 54.0, 43.9 (d, J 1.5), 39.3, 32.5, 31.9, 27.7 and 19.3. HRMS found MH^+ , 262.1601. $\text{C}_{16}\text{H}_{20}\text{FNO}$ requires MH , 262.1607.

(1R*,3S*,8S*,9S*,11S*)-9-(3-fluorophenyl)-7-azatricyclo[5.4.0.0^{3,8}]undecan-11-ol 218b



According to general procedure H, ketone **142** (0.20 g, 0.77 mmol) gave a crude material. The crude material was purified by flash column chromatography eluting with gradient elution: 20:80 → 100:0 EtOAc-hexanes to yield the *alcohol* (8.00 mg, 4%) as a pale yellow oil. R_f 0.10 (50:50 petrol–EtOAc); δ_H (500 MHz, $CDCl_3$) 7.28 – 7.21 (3H, m, Ar 5-H, Ar 2-H and Ar 6-H), 6.89 – 6.82 (1H, m, Ar 4-H), 3.67 – 3.63 (1H, m, 1-H), 3.34 – 3.30 (1H, m, 11-H), 3.16 (1H, s, 8-H), 3.02 – 2.94 (1H, m, 6-H_A), 2.87 (1H, dd, J 13.9 and 6.1, 6-H_B), 2.72 (1H, d, J 9.1, 9-H), 2.34 – 2.29 (1H, m, 3-H), 2.21 – 2.12 (1H, m, 10-H_A), 1.85 – 1.60 (6H, m, 10-H_B, 2-H, 4-H and 5-H_A) and 1.38 – 1.32 (1H, m, 5-H_B); δ_C (126 MHz, $CDCl_3$) 162.9 (d, J 240.7), 150.3 (d, J 7.1), 129.5 (d, J 8.4), 123.5 (d, J 2.7), 114.6 (d, J 21.7), 112.4 (d, J 21.1), 72.1, 69.8, 65.2, 54.2, 42.0, 39.3, 32.4, 31.9, 30.9 and 18.9; HRMS found MH^+ , 262.1603. $C_{16}H_{21}FNO$ requires MH , 262.1607. Could not obtain an IR due to lack of material.

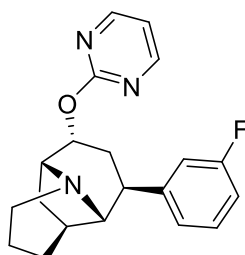
(1R*,3S*,8S*,9S*,11R*)-9-phenyl-11-(pyrimidin-2-yloxy)-7-azatricyclo[5.4.0.0^{3,8}]undecane 223



According to general procedure I, alcohol **217** (43.0 mg,) gave a crude material. The crude material was purified by flash column chromatography eluting with a 98:2 CH_2Cl_2 –MeOH to yield the *pyrimidine* (27.0 mg, 48%) as a pale yellow oil that solidified on standing. R_f 0.29 (50:50 petrol–EtOAc);

$\nu_{\max}/\text{cm}^{-1}$ (film); 3061, 3041, 2920, 2862, 1601, 1577, 1439, 1323 and 1090; δ_{H} (501 MHz, CDCl_3) 8.49 (2H, d, J 4.8, pyr 4-H and pyr 6-H), 7.48 (1H, d, J 7.5, Ph 2-H and Ph 6-H), 7.31 (2H, t, J 7.5, Ph 3-H and Ph 5-H), 7.19 (1H, t, J 7.5, Ph 4-H), 6.89 (1H, t, J 4.8, pyr 5-H), 5.48 (1H, ddd, J 10.0, 6.5 and 3.8, 11-H), 3.73 (1H, s, 1-H), 3.02 (1H, s, 8-H), 2.98 – 2.88 (2H, m, 6- H_A and 9-H), 2.87 – 2.78 (1H, m, 6- H_B), 2.37 – 2.32 (1H, m, 3-H), 2.28 (1H, dd, J 13.3 and 7.1, 2- H_A), 2.20 – 2.13 (1H, m, 10- H_A), 2.12 – 2.04 (1H, m, 10- H_B) and 1.75 – 1.60 (4H, m, 4-H, 2- H_B and 5- H_A); δ_{C} (126 MHz, CDCl_3) 164.8, 159.3, 147.0, 128.2, 127.9, 125.7, 114.8, 75.0, 73.1, 61.8, 54.1, 44.4, 39.6, 32.4, 29.0, 28.6 and 19.0; HRMS found MH^+ , 322.1918. $\text{C}_{20}\text{H}_{23}\text{N}_3\text{O}$ requires MH , 322.1919.

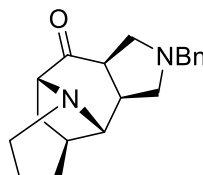
(1R*,3S*,8S*,9S*,11R*)-9-(3-fluorophenyl)-11-(pyrimidin-2-yloxy)-7-azatricyclo[5.4.0.0^{3,8}]undecane **226**



According to general procedure I, alcohol **218a** (25.0 mg,) gave a crude material. The crude material was purified by flash column chromatography eluting with 98:2 CH_2Cl_2 -MeOH to yield the *pyrimidine* (7.00 mg, 22%) as a colourless oil. R_f 0.37 (50:50 petrol-EtOAc); $\nu_{\max}/\text{cm}^{-1}$ (film); 2928, 1577, 1561, 1485, 1416, 1333, 1108, 1029, 902 and 808; δ_{H} (501 MHz, CDCl_3) 8.49 (2H, d, J 4.7, pyr 4-H and pyr 6-H), 7.34 – 7.29 (1H, m, pyr 5-H), 7.25 – 7.17 (2H, m, Ph 5-H and Ph 6-H), 6.91 – 6.85 (2H, m, Ph 4-H and Ph 2-H), 5.43 (1H, ddd, J 10.1, 6.7 and 3.7, 11-H), 3.74 – 3.69 (1H, m, 1-H), 3.01 (1H, s, 8-H), 2.95 (1H, dd, J 13.7 and 6.2, 6- H_A), 2.90 (1H, d, J 7.8, 9-H), 2.88 – 2.79 (1H, m, 6- H_B), 2.37 – 2.32 (1H, m, 3-H), 2.30 – 2.23 (1H, m, 2- H_A), 2.14 – 2.03 (2H, m, 10-H), 1.77 – 1.61 (2H, m, 2- H_B , 4-H and 5- H_B) and 1.33 – 1.19 (1H, m, 5- H_B); δ_{C} (126 MHz, CDCl_3) 164.8, 162.8 (d, J 244.3), 159.3, 149.6 (d, J 7.1), 129.4 (d, J 8.3), 123.6 (d, J 2.6), 115.0 (d, J 21.2), 114.9, 112.6 (d, J

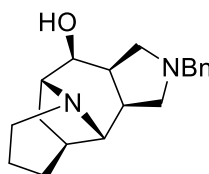
21.1), 74.7, 72.8, 61.8, 54.0, 44.0 (d, J 1.6), 39.5, 32.4, 28.7 and 18.9; HRMS found MNa^+ , 362.1639. $C_{20}H_{22}FN_3O$ requires MNa , 362.1644.

(7R*,2S*,3S*,9R*,11S*)-5-benzyl-1,5-diazatetracyclo[7.5.0.0²,¹¹.0³,⁷]tetradecan-8-one 153



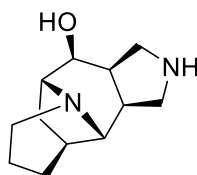
According to general procedure B, enone **85** (1.00 g, 6.13 mmol) gave a crude material. The crude material was purified by flash column chromatography eluting with 98:2 CH_2Cl_2 -MeOH to yield the *pyrrolidine* (723 mg, 40%) as a yellow oil. R_f 0.14 (50:50 petrol-EtOAc); ν_{max}/cm^{-1} (film) 3028, 2928, 2862, 2794, 1715, 1679, 1453, 1327, 1148, 1100, 731 and 698; δ_H (500 MHz, $CDCl_3$) 7.31 – 7.27 (5H, m, Ar 2-H, Ar 3-H, Ar 5-H and Ar 6-H), 7.26 – 7.21 (1H, m, Ar 4-H), 3.60 (1H, d, J 12.6, benzyl CH_2), 3.54 (1H, d, J 12.6, benzyl CH_2), 3.46 (1H, dd, J 8.0 and 2.5, 9-H), 3.27 (1H, app t, J 9.3, 6- H_A), 3.08 – 3.04 (1H, m, 4- H_A), 2.97 – 2.83 (4H, m, 14-H, 2-H and 7-H), 2.34 – 2.22 (4H, m, 6- H_B , 4- H_B , 11-H and 3-H), 1.92 (1H, dd, J 13.7 and 8.0, 10- H_A), 1.75 – 1.66 (2H, m, 10- H_B and 12- H_A), 1.62 – 1.54 (2H, m, 13- H_A and 12- H_B) and 1.39 – 1.31 (1H, m, 13- H_B); δ_C (126 MHz, $CDCl_3$) 207.1, 138.8, 128.9, 128.3, 127.0, 69.0, 68.9, 60.1, 59.5, 57.4, 54.3, 44.7, 42.2, 39.8, 31.5, 31.3 and 19.2; HRMS found MH^+ , 297.1965. $C_{19}H_{24}N_2O$ requires MH , 297.1966.

(7R*,2S*,3S*,8S*,9R*,11S*)-5-benzyl-1,5-diazatetracyclo[7.5.0.0²,¹¹.0³,⁷]tetradecan-8-ol 220



According to general procedure H, ketone **152** (415 mg, 1.40 mmol) gave a crude material. The crude material was purified by flash column chromatography eluting with 98:2 CH₂Cl₂-sat. NH₃ in MeOH to yield the γ -alcohol pyrrolidine (**322** mg, 77%) as a yellow oil. *R*_f 0.02 (99:01 CH₂Cl₂-sat. NH₃ in MeOH); $\nu_{\text{max}}/\text{cm}^{-1}$ (film) 3394, 2924, 2858, 2795, 1600, 1494, 1453, 1407, 1343, 1322, 1201, 1145, 1027, 973, 912, and 808; δ_{H} (500 MHz, CDCl₃) 7.33 – 7.27 (4H, m, Ar 2-H, Ar 3-H, Ar 5-H and Ar 6-H), 7.25 – 7.20 (1H, m, Ar 4-H), 3.74 (1H, d, *J* 12.9, benzyl CH₂), 3.54 (1H, d, *J* 12.9, benzyl CH₂), 3.51 (1H, dd, *J* 6.2 and 3.9, 8-H), 3.28 – 3.23 (1H, m, 9-H), 2.95 – 2.87 (2H, m, 6-H_A and 14-H_A), 2.87 – 2.77 (2H, m, 4-H_A and 14-H_B), 2.71 (1H, s, 2-H), 2.48 (1H, t, *J* 9.3, 4-H_B), 2.37 (1H, dd, *J* 8.4 and 6.4, 6-H_B), 2.27 – 2.19 (1H, m, 7-H), 2.19 – 2.13 (1H, m, 11-H), 2.13 – 2.06 (1H, m, 3-H), 1.69 – 1.50 (5H, m, 12-H, 10-H and 13-H_A) and 1.28 – 1.22 (1H, m, 13-H_B); δ_{C} (126 MHz, CDCl₃) 138.7, 128.8, 128.3, 127.0, 70.3, 68.4, 65.8, 60.0, 57.4, 55.9, 54.8, 42.3, 38.7, 34.3, 31.9, 30.5 and 19.2; HRMS found MH⁺, 299.2118. C₁₉H₂₆N₂O requires *MH*, 299.2124.

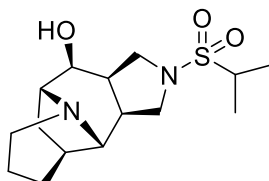
(7R*,2S*,3S*,8S*,9R*,11S*)-1,5-diazatetracyclo[7.5.0.0^{2,11}.0^{3,7}]tetradecan-8-ol **239**



According to general procedure J amine **220** (322 mg, 1.08 mmol) gave a crude material which was used without further purification to yield the γ -alcohol deprotected pyrrolidine (**157** mg, 70%) as a pale yellow oil which solidified on standing. *R*_f 0.00 (100 EtOAc); $\nu_{\text{max}}/\text{cm}^{-1}$ (film) 3322, 2942, 2831, 1449, 1402, 1022 and 786; δ_{H} (500 MHz, MeOD) 3.66 – 3.62 (1H, m, 8-H), 3.46 (1H, app d, *J* 11.6, 6-H_A), 3.43 – 3.38 (1H, m, 10-H), 3.32 – 3.30 (2H, m 14-H), 3.12 (1H, dd, *J* 11.6 and 7.1, 6-H_B), 2.98 (1H, s, 2-H), 2.96 – 2.92 (2H, m, 4-H), 2.57 (1H, dd, *J* 13.4 and 7.0, 7-H), 2.43 – 2.33 (2H, m, 3-H and 11-H), 1.87 – 1.71 (5H, m, 13-H_A, 10-H and 12-H) and 1.68 – 1.62 (1H, m, 13-

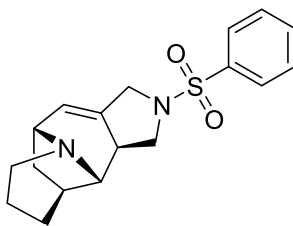
H_B); δ_C (126 MHz, MeOD) δ 70.6, 67.5, 66.7, 55.5, 50.0, 49.8, 43.3, 39.7, 36.7, 32.7 and 31.2.

(7R*,2S*,3S*,8S*,9R*,11S*)-5-(propane-2-sulfonyl)-1,5-diazatetracyclo[7.5.0.0²,¹¹.0³,⁷]tetradecan-8-ol 243



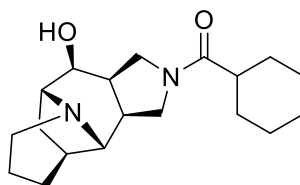
According to general procedure K the amine **239** (50.0 mg, 0.24 mmol) gave a crude material. The crude material was purified by flash column chromatography eluting with 98:2 CH₂Cl₂– sat. NH₃ in MeOH to yield the *sulfonamide* (25.1 mg, 34%) as a yellow oil. *R_f* 0.07 (05:95 MeOH–EtOAc); $\nu_{\max}/\text{cm}^{-1}$ (film) 3256, 2931, 1640, 1400, 1319, 1201, 1143, 1073, 1013 and 817; δ_H (500 MHz, CDCl₃) 3.68 (1H, t, *J* 8.9, 6-H_A), 3.61 – 3.56 (1H, m, 4-H_A), 3.54 (1H, dd, *J* 9.3 and 1.8, 4-H_B), 3.49 (1H, app t, *J* 4.6, 8-H), 3.38 – 3.34 (1H, m, 9-H), 3.26 (2H, m, *i*Pr CH and 6-H_B), 2.89 – 2.83 (2H, m, 14-H), 2.75 (1H, s, 2-H), 2.42 – 2.36 (1H, m, 3-H), 2.30 – 2.20 (2H, m, 7-H and 11-H), 1.76 – 1.64 (5H, m, 13-H_A, 12-H and 10-H), 1.41 – 1.32 (7H, m, *i*Pr CH₃_A and *i*PrCH₃_B and 13-H_B); δ_C (126 MHz, CDCl₃) 69.8, 66.6, 66.3, 54.4, 53.8, 51.4, 51.3, 49.9, 43.1, 38.8, 35.9, 31.3, 30.1, 17.2 and 17.0; HRMS found MH⁺, 315.1737. C₁₅H₂₆N₂O₃S requires *MH*, 315.1742.

(9R*,2S*,3S*,11S*)-5-(benzenesulfonyl)-1,5-diazatetracyclo[7.5.0.0²,¹¹.0³,⁷]tetradec-7-ene 244



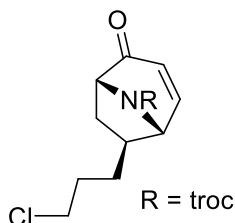
According to general procedure K, the amine **239** (63.0 mg, 0.30 mmol) gave a crude material. The crude material was purified by flash column chromatography eluting with 98:2 CH₂Cl₂–sat. NH₃ in MeOH to yield the *aryl sulfonamide* (7.2 mg, 7%) as a yellow oil. *R*_f 0.11 (05:95 MeOH–EtOAc); *v*_{max}/cm⁻¹ (film); 3107, 2933, 2863, 1735, 1713, 1608, 1402, 1222 and 1108; δ_H (500 MHz, CDCl₃) 7.82 – 7.78 (1H, m, Ar 2-H and Ar 6-H), 7.57 (1H, t, *J* 7.5, Ar 4-H), 7.50 (1H, app t, *J* 7.5, Ar 5-H and Ar 3-H), 6.32 – 6.23 (1H, m, OH), 3.95 (1H, d, *J* 12.9), 3.79 – 3.71 (1 H, m), 3.59 (1 H, d, *J* 13.0), 3.45 (1 H, t, *J* 6.8), 3.04 – 2.95 (1 H, m), 2.92 – 2.74 (1 H, m), 2.33 – 2.22 (1 H, m), 1.92 (1 H, dd, *J* 12.6, 7.3), 1.79 (1 H, dd, *J* 11.4, 7.0), 1.71 – 1.52 (2 H, m), 1.36 – 1.30 (1 H, m); δ_C (126 MHz, CDCl₃) 137.5, 135.2, 132.8, 131.1, 129.3, 127.5, 64.7, 57.7, 52.9, 50.7, 49.5, 46.4, 42.5, 38.5, 31.1 and 18.5.

(7R*2S*,3S*,8S*,9R*,11S*)-5-cyclohexanecarbonyl-1,5-diazatetracyclo[7.5.0.0²,¹¹.0³,⁷]tetradecan-8-ol **246**



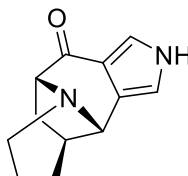
According to general procedure L, the amine **239** (50.0 mg, 0.24 mmol) gave a crude material. The crude material was purified by flash column chromatography eluting with 98:2 CH₂Cl₂–MeOH to yield the *amide* (6.6 mg, 9%) as a yellow oil. *R*_f 0.10 (100 EtOAc); δ_H (500 MHz, CDCl₃) 3.73 – 3.66 (H, m, 6-H_A), 3.63 – 3.32 (5H, m, 4-H, 8-H, 9-H and 6-H_B), 3.05 – 2.78 (3H, br m, 2-H and 14-H), 2.35 – 2.21 (3H, m, 7-H, 11-H and 3-H), 2.20 – 2.17 (1H, m, 3-H), 1.81 (1H, br d, *J* 13.0, 2-H_A), 1.76 – 1.52 (10H, m, 10-H, 12-H, 13-H, hex 3-H_A, hex 2-H_B and hex 6-H), 1.50 – 1.31 (3H, m, hex 3-H and hex 5-H_A), 1.22 – 1.14 (3H, m, hex 5-H_A and 4-H); δ_C (126 MHz, CDCl₃, mix of rotamers) 174.7, 174.3, 77.3, 77.0, 76.8, 70.1, 66.6, 66.5, 65.6, 54.3, 54.2, 49.3, 48.8, 42.9, 42.8, 42.6, 40.7, 38.5, 35.9, 31.5, 30.2, 28.9, 28.8, 28.8, 25.9, 25.9, 25.9, 18.7; HRMS found MNa⁺, 341.2197. C₁₉H₃₀N₂O₂Na requires *MNa*, 341.2204. Could not obtain an IR due to lack of material.

2,2,2-trichloroethyl(1R*,5S*,7R*)-7-(3-chloropropyl)-4-oxo-8-azabicyclo[3.2.1]oct-2-ene-8-carboxylate **183**



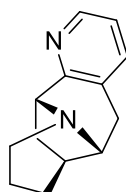
2,2,2-trichloroethylchloroformate (0.63 mL, 4.69 mmol) was added to a solution of the enone **85** (0.70 g, 4.27 mmol) and K_2CO_3 (0.59 g, 4.27 mmol) in toluene (8 mL), the reaction was heated at reflux overnight. Water (5 mL) was added to the mixture and extracted with EtOAc (3 × 25 mL), dried ($MgSO_4$), filtered and concentrated under reduced pressure to give a crude material. The crude material was purified by flash column chromatography eluting with 20:80 EtOAc–Hexanes to yield the *alkyl chloride* (125 mg, 8%). R_f 0.18 (80:20 petrol–EtOAc); ν_{max}/cm^{-1} (film) 2954, 1773, 1718, 1431, 1314, 1285, 1229, 1146, 1059, 996 and 824; δ_H (400 MHz, $CDCl_3$, Mix of rotamers 1.3:1) 7.35 (1H, dd, J 9.8 and 5.3, rot_A 2-H), 7.30 (1H, dd, J 9.7 and 5.3, rot_B 2-H), 5.99 (1H, d, J 1.2, rot_A 3-H), 5.97 (1H, d, J 1.2, rot_B 3-H), 4.85 – 4.65 (6H, m, rot_A 5-H, rot_B 5-H, rot_A troc CH_2 and rot_B troc CH_2), 4.60 (1H, d, J 5.2, rot_A 1-H), 4.55 (1H, d, J 5.2, rot_B 1-H), 3.60 – 3.49 (4H, m, rot_A prop 3-H and rot_B prop 3-H), 2.25 – 2.11 (2H, m, rot_A 7-H and rot_B 7-H), 2.10 – 1.92 (4H, m, rot_A 6-H and rot_B 6-H), 1.90 – 1.77 (4H, m, rot_A prop 2-H and rot_B prop 2-H) and 1.74 – 1.57 (3H, m, rot_A prop 1-H and rot_B prop 1-H). δ_C (100 MHz, $CDCl_3$) 195.5, 194.8, 152.8, 152.5, 152.2, 151.3, 126.9, 74.8, 64.4, 64.1, 59.2, 59.1, 44.5, 42.4, 41.6, 33.1, 31.9, 31.1 and 30.8; HRMS found MNa^+ , 395.9698. $C_{13}H_{15}NO_2Cl_4Na$ requires MNa , 395.9704.

(9R*, 2S*, 11S*)-1,5-diazatetracyclo[7.5.0.0²,¹¹.0³,⁷]tetradeca-3,6-dien-8-one 156



According to general procedure C, enone **85** (1.00 g, 6.13 mmol) gave a crude material. The crude material was purified by preparative HPLC (Waters XSelect CSH C18 ODB column, 5 μ silica, 30 mm diameter, 100 mm length), eluting with gradient elution: 5:95 \rightarrow 95:5 MeCN–water (containing 1% by volume NH₃OH (28-30% in H₂O)) to yield the *pyrrole* (29.0 mg, 24%). *R*_f 0.13 (50:50 petrol–EtOAc); $\nu_{\max}/\text{cm}^{-1}$ (film) 3054, 2937, 2863, 2671, 1453, 1264, 1140 and 733; δ_{H} (500 MHz, DMSO) 11.26 (1H, s, NH), 7.20 (1H, dd, *J* 2.9 and 1.9, 6-H), 6.65 (1H, t, *J* 1.9, 4-H), 3.96 (1H, s, 2-H), 3.48 (1H, d, *J* 6.2, 9-H), 2.89 – 2.81 (2H, m, 14-H), 2.13 (1H, d, *J* 5.0, 11-H), 2.02 – 1.93 (1H, m, 10-H_A), 1.82 (1H, dd, *J* 17.1 and 12.0, 12-H_A), 1.63 (2H, m, 12-H_B and 13-H_A), 1.51 (1H, ddd, *J* 13.1, 6.7 and 2.3, 10-H_B) and 1.27 – 1.19 (1H, m, 13-H_B); δ_{C} (126 MHz, DMSO) 194.9, 129.9, 119.1, 118.8, 112.7, 70.2, 65.9, 53.9, 32.3, 30.6 and 18.7; HRMS found MH⁺, 203.1179. C₁₂H₁₄N₂O requires *MH*, 203.1184.

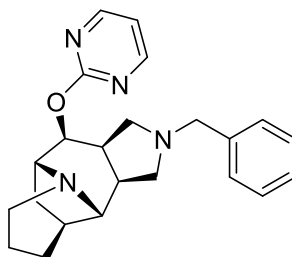
(2R*,10R*,12S*)-1,8-diazatetracyclo[8.5.0.0²,¹².0⁴,⁹]pentadeca-4(9),5,7-triene 163



According to general procedure F, ketone **159** (55.0 mg, 0.33 mmol) gave a crude material. The crude material was purified by flash column chromatography eluting with 95:5 CH₂Cl₂ – sat. NH₃ in MeOH to yield the *pyridine* (27.7 mg, 42 %) as a yellow oil. *R*_f 0.11 (10:90 MeOH – EtOAc); δ_{H} (500 MHz, CDCl₃) 8.16 (1H, d, *J* 45.0, 7-H), 7.34 (1H, d, *J* 7.6, 5-H), 7.01 (1H,

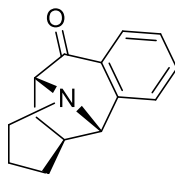
dd, J 7.6 and 5.0, 6-H), 4.17 (1H, d, J 7.4, 10-H), 3.36 – 3.27 (2H, m, 3-H_A and 2-H), 3.17 (1H, dd, J 14.0, 5.7, 15-H_A), 3.09 – 3.02 (1H, m, 15-H_B), 2.55 – 2.46 (2H, m, 2-H and 3-H_B), 2.34 – 2.30 (1H, m, 12-H), 2.22 (2H, dd, J 13.2 and 7.5, 11-H_A), 1.81 – 1.73 (4H, m, 11-H_B, 13-H and 14-H_A) and 1.64 – 1.60 (1H, m, 14-H_B); δ_C (126 MHz, CDCl₃) 144.9, 136.6, 121.6, 77.3, 77.0, 76.8, 65.73, 65.3, 53.7, 42.5, 38.3, 33.7, 31.7 and 18.8; HRMS found MH⁺, 201.1386. C₁₃H₁₆N₂ requires MH , 201.1391.

(7R*,2S*,3S*,8S*,9R*,11S*)-5-benzyl-8-(pyrimidin-2-yloxy)-1,5-diazatetracyclo[7.5.0.0^{2,11}.0^{3,7}]tetradecane 227



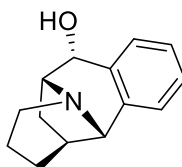
According to general procedure I, the alcohol **220** (43.0 mg, 0.14 mmol) gave a crude material. The crude material was purified by flash column chromatography eluting with 99:1 CH₂Cl₂–sat. NH₃ in MeOH to yield the *pyrimidine* (12.5 mg, 24%) as a yellow oil. R_f 0.15 (100 EtOAc); δ_H (500 MHz, CDCl₃) 8.51 (2H, d, J 4.8, pyrim 3-H and pyrim 5-H), 7.39 (1H, m, benzyl 4-H), 7.33 – 7.21 (4H, m, benzyl 2-H, benzyl 3-H, benzyl 5-H and benzyl 6-H), 6.91 (1H, t, J 4.8, pyrim 4-H), 4.99 (1H, dd, J 7.7, 2.7, 8-H), 3.94 – 3.71 (3H, m, Benzyl CH₂ and), 3.62 – 3.48 (1 H, m), 3.28 – 3.21 (1 H, m), 3.10 (1 H, s,), 2.93 – 2.86 (1H, m, 14-H_A), 2.80 – 2.69 (2H, m, 14-H_B), 2.69 – 2.60 (1 H, m), 2.27 – 2.08 (3H, m, 3-H, 7-H and 11-H), 1.81 (1H, dd, J 13.4 and 8.1, 10-H_A), 1.73 – 1.50 (4H, m, 13-H_A, 12-H, 10-H_B) and 1.31 – 1.20 (1H, m, 13-H_B); δ_C (126 MHz, CDCl₃) 163.9, 158.2, 128.3, 127.8, 127.3, 126.1, 113.9, 73.9, 64.7, 61.3, 58.9, 53.8, 53.3, 41.3, 32.9 and 30.4; HRMS found MH⁺, 377.2329. C₂₃H₂₈N₄O requires MH , 377.2341. Unable to obtain an IR due to lack of material.

(10R*, 2S*, 12S*)-1-azatetracyclo[8.5.0.0^{2,12}.0^{3,8}]pentadeca-3(8),4,6-trien-9-one **135**



According to general procedure E, isoquinolin-4-ol (250 mg, 1.72 mmol) gave a crude material. The crude material was purified by flash column chromatography eluting with 30:70 EtOAc–Hexanes to give the *fused aryl amine* as a gold amorphous solid (163 mg, 45%). R_f 0.14 (70:30 Hexanes–EtOAc); ν_{max}/cm^{-1} (film); 3067, 3032, 2957, 2931, 2860, 1691, 1603, 1480, 1324, 1304, 1116, 1017, 988 and 877; δ_H (500 MHz, $CDCl_3$) 7.97 – 7.93 (1H, m, 7-H), 7.44 (1H, td, J 7.5 and 1.4, 5-H), 7.31 (1H, td, J 7.5 and 1.4, 6-H), 7.27 – 7.24 (1H, m, 4-H), 4.03 (1H, s, 2-H), 3.89 – 3.83 (1H, m, 10-H), 3.03 (2H, dd, J 10.2 and 3.3, 15-H), 2.37 (1H, t, J 4.7, 12-H), 2.06 (1H, dd, J 13.7 and 7.8, 11-H_A), 1.92 (1H, tdd, J 12.8, 5.2 and 1.5, 13-H_A), 1.81 – 1.74 (1H, m, 13-H_B), 1.73 – 1.64 (1H, m, 14-H_A), 1.61 (1H, ddd, J 13.7, 6.8 and 2.5, 11-H_B) and 1.42 – 1.36 (1H, m, 14-H_B); δ_C (126 MHz, $CDCl_3$) 196.0, 146.7, 132.9, 129.5, 127.5, 127.3, 125.6, 72.1, 69.4, 54.3, 38.6, 30.8, 30.4 and 18.6; HRMS found MNa^+ , 236.1044. $C_{14}H_{15}NO$ requires MNa , 236.1051.

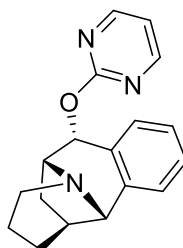
(9R*, 2S*,10R*,12S*)-1-azatetracyclo[8.5.0.0^{2,12}.0^{3,8}]pentadeca-3(8),4,6-trien-9-ol **191**



According to general procedure J, the ketone **135** (60.0 mg, 0.28 mmol) gave a crude material. The crude material was used without further purification to give the *benzylic alcohol* as a yellow oil (56.0 mg, 93%). R_f 0.13 (100 EtOAc); ν_{max}/cm^{-1} (film); 3286, 2936, 2863, 2831, 2716, 2559, 1635, 1455, 1353, 1312, 1150, 1077 and 1023; δ_H (500 MHz, MeOD) 7.95 (1H, d, J 7.5, 7-H), 7.71 (1H,

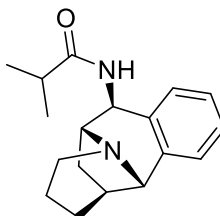
td, J 7.5 and 1.2, 6-H), 7.63 (1H, t, J 7.5, 5-H), 7.50 (1H, d, J 7.5, 4-H), 5.54 (1H, d, J 4.7, 9-H), 4.23 (1H, s, 2-H), 4.04 (1H, td, J 4.7 and 1.9, 10-H), 3.53 – 3.39 (2H, m, 15-H), 2.90 – 2.81 (1H, m, 12-H), 2.48 (1H, ddd, J 13.5, 6.8 and 2.3, 11-H_A), 2.36 – 2.07 (4H, m, 11-H_B, 13-H_A and 14-H) and 1.91 (1H, dt, J 7.9 and 4.2, 13-H_B); δ_c (126 MHz, MeOD) 139.2, 136.4, 127.5, 126.9, 124.9, 71.2, 70.4, 64.1, 53.5, 42.6, 30.3, 26.9 and 18.1; HRMS found MH^+ , 216.1383. $C_{14}H_{17}NO$ requires MH , 216.1388.

(9R*,2S*,10R*,12S*)-9-(pyrimidin-2-yloxy)-1-azatetracyclo[8.5.0.0^{2,12}.0^{3,8}]pentadeca-3(8),4,6-triene 230



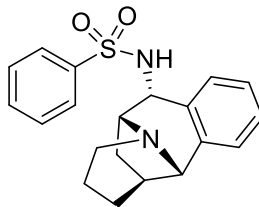
According to general procedure I, the alcohol **191** (56.0 mg, 0.26 mmol) gave a crude material. The crude material was purified using HPLC eluting with gradient elution: 5:95 → 95:5 MeCN–water to give the *pyrimidine* as a yellow oil (10.2 mg, 12%). R_f 0.08 (50:50 hexanes–EtOAc); ν_{max}/cm^{-1} (film); 3036, 2928, 2860, 1577, 1562, 1414, 1325, 1299 and 998; δ_H (500 MHz, $CDCl_3$) 8.58 (2H, d, J 4.8, pyrim 3-H and pyrim 5-H), 7.42 (1H, d, J 7.0, 7-H), 7.29 – 7.20 (2H, m, 5-H and 6-H), 7.11 – 7.06 (1H, m, 4-H), 7.02 (1H, t, J 4.8, pyrim 4-H), 6.65 (1H, d, J 4.4, 9-H), 4.26 – 4.16 (1H, m, 10-H), 4.05 (1H, s, 2-H), 3.32 – 3.21 (2H, m, 15-H), 2.55 – 2.50 (1H, m, 12-H), 2.31 (1H, ddd, J 13.6, 6.8 and 2.0, 11-H_A), 1.92 – 1.66 (4H, m, 14-H_A, 11-H_B and 13-H) and 1.62 – 1.52 (1H, m, 14-H_B); δ_c (126 MHz, $CDCl_3$) 166.9, 165.0, 159.6, 137.8, 132.2, 128.2, 128.1, 127.9, 125.4, 115.7, 75.7, 69.9, 60.4, 52.9, 42.4, 29.9, 27.4 and 17.7; HRMS found MH^+ , 294.1611. $C_{18}H_{19}N_3O$ requires MH , 294.1606.

N-[(9R*,2S*,10R*,12S*)-1-azatetracyclo[8.5.0.0²,¹².0³,⁸]pentadeca-3(8),4,6-trien-9-yl]-2-methylpropanamide 238



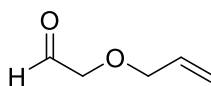
According to general procedure G, the ketone **135** (79 mg, 0.37 mmol) gave a crude material, which was dissolved in CH_2Cl_2 (0.8 mL), pyridine (0.12 mL, 1.48 mmol) was added and stirred at rt for 5 min, acid chloride (0.31 mL, 2.96 mmol) was added and the mixture was stirred at rt overnight and concentrated under reduced pressure. The crude material was purified by flash column chromatography eluting with 95:05 EtOAc–MeOH to give the *alkyl amide* (4.41 mg, 4%) as a colourless oil. R_f 0.14 (05:95 MeOH–EtOAc); δ_{H} (500 MHz, CDCl_3) 7.32 – 7.28 (1H, m, 5-H), 7.20 – 7.16 (2H, m, 4-H and 6-H), 7.04 (1H, m, 7-H), 6.30 (1H, br d, J 8.3, *N*-H), 4.88 (1H, dd, J 9.1 and 2.3, 2-H), 3.75 (1H, s, 9-H), 3.46 (1H, d, J 7.7, 12-H), 3.08 – 2.97 (1H, m, 14- H_A), 2.97 – 2.90 (1H, m, 14- H_B), 2.34 – 2.26 (2H, m, 10-H and prop 2-H), 1.86 – 1.76 (2H, m, 15- H_A and 11- H_A), 1.72 – 1.65 (2H, m, 16- H_A and 11- H_B), 1.45 (1H, ddd, J 13.3, 6.7 and 2.7, 15- H_B), 1.39 – 1.27 (1H, m, 16- H_B), 1.15 (3H, d, J 6.9, methyl) and 1.13 (3H, d, J 6.9, prop 3-H); δ_{C} (126 MHz, CDCl_3) 175.8, 130.3, 127.5, 127.1, 125.5, 70.1, 63.9, 53.9, 52.8, 42.1, 35.7, 31.3, 30.6, 19.6, 19.5 and 18.6; HRMS found MH^+ , 285.1978. $\text{C}_{18}\text{H}_{24}\text{N}_2\text{O}$ requires *MH*, 285.1967. An IR could not be obtained due to a lack of material.

N-[(9R*,2S*,10R*,12S*)-1-azatetracyclo[8.5.0.0²,¹².0³,⁸]pentadeca-3(8),4,6-trien-9-yl]benzenesulfonamide **237**



According to general procedure G, the ketone **135** (79 mg, 0.37 mmol) gave a crude material, which was dissolved in CH_2Cl_2 (0.8 mL), pyridine (0.12 mL, 1.48 mmol) was added and stirred at rt for 5 min, sulfonyl chloride (0.38 mL, 2.96 mmol) was added and the mixture was stirred at rt overnight and concentrated under reduced pressure. The crude material was purified by flash column chromatography eluting with 95:05 EtOAc–MeOH to give the *aryl sulfonamide* (3.51 mg, 3%) as a yellow oil. R_f 0.25 (05:95 MeOH–EtOAc); δ_H (500 MHz, MeOD) 8.03 – 7.99 (2H, m, sulf Ar 2-H and sulf Ar 6-H), 7.72 – 7.68 (1H, m, sulf Ar 4-H), 7.67 – 7.62 (2H, m, sulf Ar 3-H and sulf Ar 5-H), 7.18 – 7.13 (1H, m, 7-H), 7.12 – 7.05 (2H, m, 6-H and 5-H), 6.93 (1H, d, J 7.7, 4-H), 4.85 (1H, m, 2-H), 3.84 (1H, s, 9-H), 3.51 (1H, ddd, J 7.1, 4.0 and 2.5, 12-H), 3.00 – 2.90 (2H, m, 14-H), 2.40 – 2.34 (1H, m, 10-H), 1.91 – 1.79 (2H, m, 11- H_A and 16- H_A), 1.74 – 1.52 (3H, m, 15- H_A , 11- H_B and 16- H_B) and 1.45 – 1.33 (1H, m, 15- H_B); δ_C (126 MHz, MeOD) 141.9, 139.7, 132.9, 132.4, 129.8, 129.0, 127.3, 127.1, 126.6, 125.5, 69.8, 63.2, 57.2, 53.0, 43.1, 29.6, 27.3 and 17.6; HRMS found MNa^+ , 377.1290. $\text{C}_{20}\text{H}_{22}\text{N}_2\text{O}_2\text{S}$ requires MNa , 377.1299. IR could not be obtained due to a lack of material.

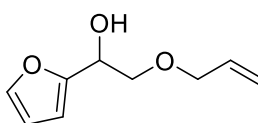
2-(prop-2-en-1-yloxy)acetaldehyde **137**



According to general procedure M, 3-allyloxy-1,2-diol (0.47 mL, 3.78 mmol) gave a crude material which was used without further purification to give the aldehyde²³² as a colourless oil (0.19 g, 50%). R_f 0.61 (50:50 petrol–EtOAc); $\nu_{\text{max}}/\text{cm}^{-1}$ (film) 3092, 2981, 2888, 1735, 1651, 1431, 1092,

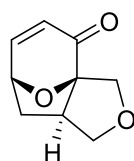
1000 and 942; δ_{H} (400 MHz, CDCl_3) 9.73 (1H, s, aldehyde-H), 5.91 (1H, app ddd, J 17.2, 11.0 and 5.8, prop 2-H), 5.32 (1H, app dd, J 17.2 and 1.4, prop 3- H_{trans}), 5.25 (1H, app dd, J 11.0 and 1.4, prop 3- H_{cis}), 4.09 (2H, d, J 5.8, prop 1-H) and 4.08 (H, s, CH_2 acetyl CH_2); δ_{C} (101 MHz, CDCl_3) 200.6, 133.5, 118.5, 75.3 and 72.7; HRMS could not be obtained due to the low molecular weight of the molecule.

1-(furan-2-yl)-2-(prop-2-en-1-yloxy)ethanol **138**



According to general procedure N, aldehyde **137** (1.00 g, 9.99 mmol) gave a crude material. The crude material was purified by flash column chromatography eluting with 20:80 EtOAc–Hexanes to yield the alcohol¹⁷¹ as an orange oil (0.50 g, 60%). R_f 0.21 (50:50 petrol–EtOAc); $\nu_{\text{max}}/\text{cm}^{-1}$ (film) 3413, 3061, 2863, 1692, 1646, 1572, 1505, 1466, 1147, 1105, 1063 and 1005; δ_{H} (400 MHz, CDCl_3) 7.41 – 7.34 (1H, m, furan 5-H), 6.35 – 6.28 (2H, m, furan 3-H and furan 4-H), 5.92 (1H, app ddd, J 17.1, 10.4 and 5.7, prop 2-H), 5.29 (1H, app dd, J 17.1 and 1.5, prop 3- H_{trans}), 5.21 (1H, dd, J 10.4 and 1.5, prop 3- H_{cis}), 4.90 (1H, dd, J 9. and, 5.7, ethanol 1-H), 4.06 (2H, d, J 5.7, ethanol 2-H), 3.74 – 3.68 (2H, m, prop 1-H) and 2.74 (1H, app d, J 3.8, OH); δ_{C} (100 MHz, CDCl_3) 153.5, 142.2, 134.3, 117.6, 110.3, 107.0, 72.4, 72.4 and 66.9; HRMS found MNa^+ , 191.0678. $\text{C}_9\text{H}_{12}\text{O}_3$ requires MNa , 191.0684.

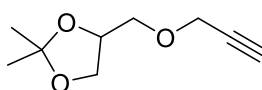
(7R*, 1S*, 5S*)-11-oxatricyclo[5.3.1.0^{1,5}]undec-8-en-10-one **86**



The alcohol **138** (2.60 g, 15.5 mmol) was dissolved in THF–water (38 mL, 4:1), NBS (2.70 g, 15.5 mmol) was added portionwise over 30 mins. The reaction was then quenched with water (25 mL) and extracted

with EtOAc (3 × 25 mL), dried and concentrated under reduced pressure to give a crude material which was dissolved in CH₂Cl₂ (30 mL) and cooled to 0 °C. Pyridine (3.13 mL, 38.7 mmol) and acetyl chloride (1.42 mL, 20.1 mmol) was added and stirred at 0 °C for 2 hours. The reaction was then quenched with water (25 mL) and extracted with CH₂Cl₂ (3 × 25 mL), dried and concentrated under reduced pressure to give a crude material which was dissolved in MeCN (155 mL), NMP (6.60 mL, 61.9 mmol) was added and the solution was heated at 60 °C for 6 h, the mixture was then concentrated under reduced pressure to give a crude product. The crude material was purified by flash column chromatography eluting with 30:70 EtOAc–Hexanes to yield the enone¹⁷¹ as an orange oil (1.00 g, 64%). *R*_f 0.26 (50:50 hexanes–EtOAc); *v*_{max}/cm⁻¹ (film) 2964, 2875, 1736, 1699, 1447, 1372, 1233 and 1098; *δ*_H (400 MHz, CDCl₃) 7.21 (1H, dd, *J* 9.8 and 4.5, 9-H), 6.01 (1H, d, *J* 9.8, 10-H), 5.04 (1H, dd, *J* 6.3 and 4.5, 8-H), 4.43 (1H, d, *J* 10.6, 3-H_A), 4.13 (1H, t, *J* 8.9, 5-H_A), 3.87 (1H, d, *J* 10.6, 3-H_B), 3.72 (1H, dd, *J* 8.9 and 6.1, 5-H_B), 2.72 (1H, ddd, *J* 13.9, 8.1 and 6.1, 6-H), 2.15 (1H, dd, *J* 12.1 and 8.5, 7-H_A) and 2.09 – 1.98 (1H, m, 7-H_B); *δ*_C (101 MHz, CDCl₃) 194.4, 152.3, 126.3, 98.1, 77.6, 74.0, 70.3, 46.8 and 34.5.

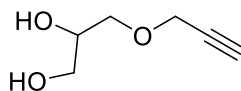
2,2-dimethyl-4-[(prop-2-yn-1-yloxy)methyl]-1,3-dioxolane



NaH (1.83 g, 46.2 mmol) was added to a solution of Solketal (5.74 mL, 46.2 mmol) dissolved in THF (84 mL) and stirred at rt for 20 min. Propargyl bromide (80% in toluene, 4.68 mL, 42.0 mmol) was added and the reaction was heated to 70 °C overnight, the reaction was then quenched with water (50 mL), extracted with EtOAc (3 x 40 mL), dried and concentrated under reduced pressure to give a crude product. The crude material was purified by flash column chromatography eluting with 10:90 EtOAc–Hexanes to yield the acetal²³³ (3.82 g, 53%) as a colourless oil. *R*_f 0.76 (50:50 hexanes–EtOAc); *v*_{max}/cm⁻¹ (film) 3272, 2987, 2936, 2873, 2116, 1456, 1371, 1253, 1213, 1157, 1095, 1045 and 842; *δ*_H (500 MHz, CDCl₃) 4.33 – 4.27 (1H,

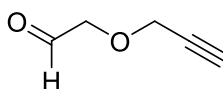
m, 4-H), 4.21 (2H, m, prop 1-H), 4.07 (1H, dd, J 8.3 and 6.5, methyl-H_A), 3.74 (1H, dd, J 8.3 and 6.3, methyl-H_B), 3.59 (2H, t, J 5.8, 5-H), 2.44 (1H, t, J 2.4, prop 3-H), 1.43 (3H, s, acetal-CH₃) and 1.36 (3H, s, acetal-CH₃); δ_{C} (126 MHz, CDCl₃) 109.6, 79.4, 74.8, 74.5, 70.8, 66.7, 58.7, 26.8 and 25.4; HRMS found $M\text{Na}^+$, 193.0835. C₉H₁₄O₃ requires $M\text{Na}$, 193.0841.

3-(prop-2-yn-1-yloxy)propane-1,2-diol



Propargyl acetal (11.8 g, 69.5 mmol) was dissolved in EtOAc (100 mL), HCl (1M, 100 mL) was added and the reaction was stirred at rt for 2 hours. The reaction was neutralised with sodium hydroxide (1M), extracted with EtOAc (3 x 100 mL), dried and concentrated under reduced pressure to give the alcohol²³³ (9.00g, 99%) which was used without further purification. R_{f} 0.16 (50:50 hexanes–EtOAc); $\nu_{\text{max}}/\text{cm}^{-1}$ (film) 3406, 3289, 2928, 2877, 1443, 1359, 1097 and 1038; δ_{H} (500 MHz, CDCl₃) 4.20 (2H, d, J 2.4, prop 1-H), 3.94 – 3.87 (1H, m, 2-H), 3.73 (1H, dd, J 11.4 and 3.9, 3-H_A), 3.67 – 3.58 (3H, m, 3-H_B and 1-H), 2.47 (1H, t, J 2.4, prop 3-H), 2.01 (3H, br s, OH); δ_{C} (126 MHz, CDCl₃) 79.2, 77.3, 77.0, 76.8, 75.0, 71.5, 70.5, 63.9 and 58.7; HRMS found $M\text{Na}^+$, 153.0519. C₆H₁₀O requires $M\text{Na}$, 153.0527.

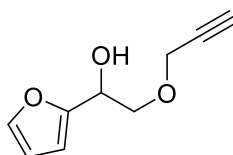
2-(prop-2-yn-1-yloxy)acetaldehyde



According to general procedure M, propargyl diol (1.48 g, 10.9 mmol) gave a crude product which was used without further purification to give the aldehyde²³⁴ (0.30 g, 29%) as a yellow oil. R_{f} 0.11 (20:80 EtOAc–Hexanes); $\nu_{\text{max}}/\text{cm}^{-1}$ (film) 3285, 2923, 1725, 1361, 1078, 948 and 712; δ_{H} (500 MHz, CDCl₃) 9.75 (1H, t J 0.8, aldehyde), 4.30 (2H, d J 2.4, prop-1H), 4.20 (2H, d J 0.8, acetal CH₂) and 2.50 (1H, t, J 2.4, prop 3-H); δ_{C} (126 MHz, CDCl₃) 199.7,

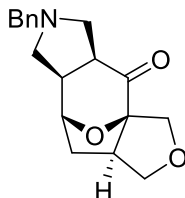
78.4, 75.9, 74.6 and 58.7; HRMS could not be obtained due to the low molecular weight of the molecule.

1-(furan-2-yl)-2-(prop-2-yn-1-yloxy)ethanol



According to general procedure N, the propargyl aldehyde (0.30 g, 3.06 mmol) gave a crude material. The crude product which was purified via column chromatography eluting with 20:80 EtOAc–Hexanes, to give the *furyl alcohol* as an orange oil (0.18 g, 36%). R_f 0.18 (80:20 Hexanes–EtOAc); $\nu_{\max}/\text{cm}^{-1}$ (film) 3405, 2911, 2865, 1645, 1504, 1422, 1222, 1147, 1064, 1007, 927, 883 and 738; δ_{H} (500 MHz, CDCl_3) 7.39 (1H, dd, J 1.7 and 0.9, furan 5-H), 6.36 – 6.32 (2H, m, furan 3-H and furan 4-H), 4.94 (1H, dd, J 7.5 and 3.8, ethanol 1-H), 4.25 (2H, dd, J 5.7 and 2.4, prop 1-H), 3.86 – 3.81 (2H, m, ethanol 2-H) and 2.47 (1H, t, J 2.4, prop 1-H); δ_{C} (126 MHz, CDCl_3) 153.1, 142.3, 110.3, 107.2, 79.2, 77.3, 77.0, 76.8, 75.1, 72.2, 66.8 and 58.7; HRMS could not be obtained due to the low molecular weight of the molecule.

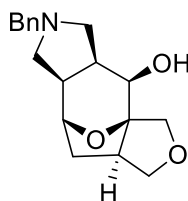
(1R*,3S*,7R*,8R*,10R*)-5-benzyl-12,14-dioxo-5-diazatetracyclo[6.5.1.0^{1,10}.0^{3,7}]tetradecane-2-one 154



According to general procedure B, the enone **86** (1.00 g, 6.02 mmol) gave a crude material. The crude material was purified by flash column chromatography eluting with gradient elution: 0:100 → 5:95 Sat. NH_3 in MeOH–EtOAc to give the *pyrrolidine* as a yellow oil (1.33 g, 74%). R_f 0.11 (100% EtOAc); $\nu_{\max}/\text{cm}^{-1}$ (film) 2969, 2953, 2927, 2911, 2898, 2860,

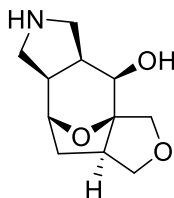
2821, 2788, 2769, 2742, 1717, 1475, 1379, 1331, 1249, 1202, 1152, 1094, 1051, 924 and 754; δ_{H} (500 MHz, CDCl_3) 7.33 – 7.28 (4H, m, benzyl), 7.28 – 7.25 (1H, m, benzyl 4-H), 4.58 (1H, d, J 6.8, 8-H), 4.32 (1H, d, J 10.6, 13- H_A), 4.06 – 4.01 (1H, m, 11- H_A), 3.88 (1H, d, J 10.6, 13- H_B), 3.68 – 3.58 (3H, m, 11- H_B and benzyl CH_2), 3.20 (1H, t, J 9.2, 4- H_A), 3.06 (1H, t, J 7.9, 6- H_A), 3.00 (1H, app dd, J 16.5 and 8.9, 3-H), 2.82 (1H, ddd, J 14.0, 8.3 and 5.7, 10-H), 2.57 – 2.41 (3H, m, 4- H_B , 6- H_B and 7-H), 2.14 (1H, dd, J 12.6 and 9.0, 9- H_A), 2.08 – 2.00 (1H, m, 9- H_B); δ_{C} (126 MHz, CDCl_3) 204.9, 138.2, 128.9, 128.4, 127.3, 96.6, 80.2, 74.8, 70.4, 59.9, 58.6, 56.5, 48.3, 45.9, 44.8 and 36.6; HRMS found MNa^+ , 322.1414. $\text{C}_{18}\text{H}_{21}\text{NO}_3$ requires MNa , 322. 1419.

(1R*,2R*,3S*,7R*,8R*,10R*)-5-benzyl-12,14-dioxa-5-azatetracyclo[6.5.1.0¹,¹⁰.0³,⁷]tetradecan-2-ol 221



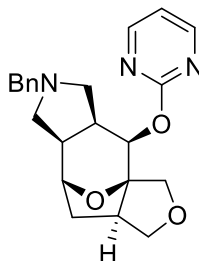
According to the general procedure H, the ketone **154** (1.00 g, 3.34 mmol.) gave a crude material. The crude material was purified by flash column chromatography eluting with gradient elution: 2:98 → 10:90 Sat. NH_3 in MeOH–EtOAc to give the *alcohol* as a yellow oil (0.86 g, 86%); R_f 0.04 (50:50 hexanes–EtOAc); $\nu_{\text{max}}/\text{cm}^{-1}$ (film) 3142, 3083, 3026, 2946, 2904, 2864, 2826, 2804, 1670, 1494, 1450, 1343, 1333, 1210, 1190, 1010, 916, and 831; δ_{H} (500 MHz, CDCl_3) 7.34 – 7.24 (5H, m, benzyl), 4.45 (1H, d, J 6.6, 8-H), 4.06 – 3.98 (2H, m, 13- H_A and 11- H_A), 3.84 (1H, d, J 10.4, 13- H_B), 3.75 (1H, d, J 12.6, benzyl CH_2), 3.67 (1H, d, J 5.8, 2- H_A), 3.63 – 3.55 (2H, m, benzyl CH_2 and 11- H_B), 3.09 (1H, dd, J 9.5 and 6.2, 6- H_A), 3.02 (1H, d, J 8.7, 4- H_A), 2.53 – 2.45 (2H, m, 6- H_B and 10-H), 2.41 – 2.31 (2H, m, 3-H and 4- H_B), 2.14 – 2.07 (1H, m, 7-H) and 1.99 – 1.86 (2H, m, 9-H); δ_{C} (126 MHz, CDCl_3) δ 137.6, 128.7, 128.6, 127.5, 95.3, 79.1, 77.3, 77.1, 76.8, 75.6, 75.4, 69.8, 59.6, 56.2, 55.2, 44.2, 41.4, 36.1 and 35.8; HRMS found MNa^+ , 324.1566. $\text{C}_{18}\text{H}_{23}\text{NO}_3$ requires MNa , 324.1575; melting point 159.6 – 162.4 °C.

(1R*,2R*,3S*,7R*,8R*,10R*)-12,14-dioxa-5-azatetracyclo[6.5.1.0¹,¹⁰.0³,⁷]tetradecan-2-ol 240



According to general procedure J, the benzyl amine **221** (0.60 g, 1.99 mmol) gave a crude material. The crude material was used without further purification to give the *amine* as a yellow oil (0.41 g, 97 %). R_f 0.24 (100 EtOAc); $\nu_{\max}/\text{cm}^{-1}$ (film) 3490, 3054, 2871, 2736, 1521, 1423, 1285, 1200, 1127, 1076, 983, 921 and 832; δ_H (500 MHz, CDCl_3) 6.73 (2H, br s, OH and NH), 4.53 (1H, d, J 6.7, 8-H), 4.01 (1H, t, J 8.6, 11- H_A), 3.95 (1H, d, J 10.4, 13- H_A), 3.80 – 3.75 (2H, m, 2-H and 13- H_B), 3.63 (1H, d, J 11.4, 4- H_A), 3.55 (1H, dd, J 8.6 and 6.4, 11- H_B), 3.40 – 3.35 (2H, m, 6-H), 3.22 (1H, dd, J 11.4 and 6.5, 4- H_B), 2.57 – 2.49 (1H, m, 10-H and 3-H), 2.26 – 2.17 (1H, m, 7-H), 2.04 (1H, dd, J 12.7 and 8.8, 9- H_A) and 1.99 – 1.90 (1H, m, 9- H_B); δ_C (126 MHz, CDCl_3) 95.4, 77.3, 77.1, 76.8, 76.5, 75.5, 75.1, 68.5, 48.1, 47.0, 44.6, 41.9, 37.6 and 35.8; HRMS found MH^+ , 212.1281. $\text{C}_{11}\text{H}_{17}\text{NO}_3$ requires MH , 212.1287.

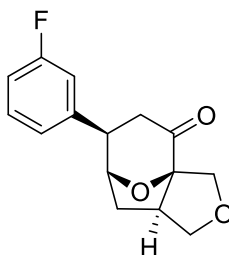
(1R*,2R*,3S*,7R*,8R*,10R*)-5-benzyl-2-(pyrimidin-2-yloxy)-12,14-dioxa-5-azatetracyclo[6.5.1.0¹,¹⁰.0³,⁷]tetradecane 229



According to general procedure I, the alcohol **240** (100 mg, 0.33 mmol) gave a crude material. The crude material was purified using HPLC eluting with gradient elution: 5:95 → 95:5 MeCN–water to give the *pyrimidine* as a yellow oil. R_f 0.10 (100 EtOAc); δ_H (500 MHz, CDCl_3) 8.59 (2H, d, J 4.8, pyrim 3-H and pyrim 5-H), 7.51 – 7.46 (2H, m, benzyl 2-H and benzyl 6-H), 7.35 – 7.30

(3H, m, benzyl 3-H, benzyl 4-H and benzyl 5-H), 7.08 (1H, t, J 4.8, pyrim 4-H), 5.48 (1H, d, J 5.6, 2-H), 4.61 (1H, d, J 6.8, 8-H), 4.39 (1H, d, J 12.5, benzyl CH₂), 4.32 (1H, d, J 12.5, benzyl CH₂), 4.07 – 4.01 (1H, m, 11-H_A), 3.85 (2H, app q, J 10.4, 13-H), 3.76 (1H, dd, J 12.1 and 8.4, 4-H_A), 3.65 (1H, dd, J 9.1 and 5.5, 11-H_B), 3.51 – 3.43 (2H, m, 6-H), 2.90 – 2.82 (1H, m, 3-H), 2.78 – 2.68 (2H, m, 4-H_B and 10-H), 2.59 – 2.50 (1H, m, 7-H), 2.17 (1H, dd, J 12.9 and 8.9, 9-H_A) and 2.10 – 2.02 (1H, m, 9-H_B); δ_C (126 MHz, CDCl₃) 168.8, 164.8, 159.7, 130.1, 129.0, 128.9, 116.2, 94.3, 77.3, 77.0, 76.8, 76.3, 75.4, 74.4, 72.7, 58.1, 54.9, 53.1, 45.4 and 41.78; HRMS found MH⁺, 380.1968. C₂₂H₂₅N₃O₃ requires MH , 380.1974.

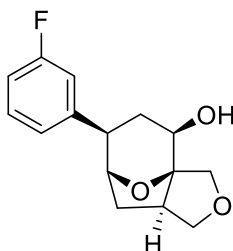
(1R*,5R*,7R*,8R*)-8-(3-fluorophenyl)-3,11-dioxatricyclo[5.3.1.0^{1,5}]undecan-10-one 145



According to general procedure D, enone **86** (1.00 g, 6.02 mmol) gave a crude material. The crude material was purified by flash column chromatography eluting with 20:80 EtOAc–Hexanes, to give the β -aryl ketone as a pale yellow oil that solidified on standing (0.78 g, 49%). R_f 0.53 (50:50 hexanes–EtOAc); ν_{max}/cm^{-1} (film) 3059, 2999, 2972, 2937, 2867, 1712, 1613, 1586, 1479, 1450, 1299, 1279, 1118, 1096, 1067, 989, 925, 820 and 750; δ_H (500 MHz, CDCl₃) 7.32–7.27 (1H, m, phenyl 5-H), 7.02 (1H, d, J 7.7, phenyl 6-H), 7.00 – 6.93 (2H, m, phenyl 2-H and phenyl 4-H), 4.75 (1H, d, J 6.6, 7-H), 4.37 (1H, d, J 10.6, 2-H_A), 4.11 (1H, t, J 8.3, 4-H_A), 3.93 (1H, d, J 10.6, 2-H_B), 3.66 (1H, dd, J 8.8 and 6.4, 4-H_B), 3.15 – 3.08 (1H, m, 8-H), 2.98 – 2.89 (1H, m, 5-H), 2.84 – 2.70 (2H, m, 9-H), 2.25 (1H, ddd, J 12.8, 8.7 and 0.5, 6-H_A) and 2.14 – 2.06 (1H, m, 6-H_B); δ_C (126 MHz, CDCl₃) 205.2, 163.0 (d, J 246.5), 146.4 (d, J 7.0), 130.4 (d, J 8.3), 122.9 (d, J 2.9), 114.3 (d, J 21.7), 113.9 (d, J 21.0), 97.7, 84.2, 74.7, 70.5, 49.5, 47.1 (d, J 1.6), 41.0, 36.6; HRMS

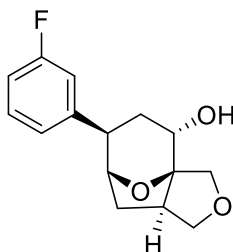
found MNa^+ , 285.0897. $C_{15}H_{15}FO_3$ requires MNa , 285.0902; Melting point 111.6 – 113.7 °C.

(1R*,5R*,7R*,8R*,10R*)-8-(3-fluorophenyl)-3,11-dioxatricyclo[5.3.1.0^{1,5}]undecan-10-ol 129a



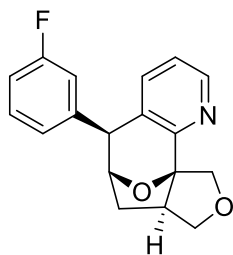
According to general procedure H, the ketone **145** (250 mg, 0.95 mmol) gave a crude material. The crude material was purified by flash column chromatography eluting with 100 CH_2Cl_2 , to give the *alcohol* as a colourless amorphous solid (94.0 mg, 38%). R_f 0.26 (50:50 hexanes–EtOAc); ν_{max}/cm^{-1} (film) 3481, 2939, 2921, 2876, 1614, 1584, 1486, 1441, 1234, 1185, 1107, 1016, 919, and 777; δ_H (500 MHz, $CDCl_3$) 7.36 – 7.27 (3H, m, phenyl 2-H, phenyl 4-H and phenyl 5-H), 6.94 – 6.88 (1H, m, phenyl 6-H), 5.07 (1H, d, J 6.5, 5-H), 4.11 (1H, t, J 8.6, 8- H_A), 3.99 (1H, d, J 10.5, 10- H_A), 3.84 (1H, d, J 10.5, 10- H_B), 3.71 (1H, br s, 2-H), 3.61 (1H, dd, J 8.6, 7.3, 8- H_B), 2.71 – 2.62 (2H, m, 4-H and 7-H), 2.36 (1H, ddd, J 15.2, 7.6, 4.2, 3- H_A) and 2.16 – 2.04 (3H, m, 3- H_B and 6-H); δ_C (126 MHz, $CDCl_3$) 163.1 (d, J 245.8), 147.5 (d, J 6.9), 130.3 (d, J 8.4), 123.2 (d, J 2.8), 114.7 (d, J 21.9), 113.3 (d, J 21.0), 95.3, 81.7, 75.5, 75.0, 69.9, 46.2, 40.9 (d, J 1.6), 35.2, 33.1; HRMS found MNa^+ , 287.1054. $C_{15}H_{17}FO_3$ requires MNa , 287.1059.

(1R*,5R*,7R*,8R*,10S*)-8-(3-fluorophenyl)-3,11-dioxatricyclo[5.3.1.0^{1,5}]undecan-10-ol 219b



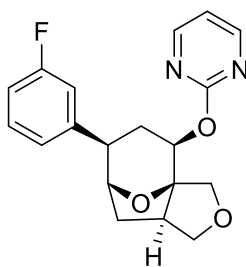
According to general procedure H, the ketone **145** (250 mg, 0.95 mmol) gave a crude material. The crude material was purified by flash column chromatography eluting with 100 CH₂Cl₂, to give the *alcohol* as a colourless oil (38.0 mg, 15%). *R*_f 0.16 (50:50 hexanes–EtOAc); *v*_{max}/cm⁻¹ (film) 3480, 2941, 2921, 2876, 1615, 1584, 1487, 1440, 1185, 1106, 1011 and 919; δ _H (500 MHz, CDCl₃) 7.28 – 7.22 (1H, m, phenyl 5-H), 7.19 – 7.11 (2H, m, phenyl 6-H and phenyl 2-H), 6.90 (1H, tdd, *J* 8.4, 2.5 and 0.8, phenyl 4-H), 4.73 (1H, app t, *J* 3.8, 7-H), 4.13 – 4.01 (3H, m, 2-H_A, 4-H_A and 10-H), 3.85 (1H, d, *J* 10.0, 2-H_B), 3.54 (1H, dd, *J* 8.6 and 7.6, 4-H_B), 2.99 – 2.90 (1H, m, 7-H), 2.85 (1H, d, *J* 7.1, 8-H), 2.22 – 2.13 (1H, m, 9-H_A), 2.09 – 2.04 (2H, m, 6-H) and 1.91 (1H, ddd, *J* 13.8, 10.7 and 7.2, 9-H_B); δ _C (126 MHz, CDCl₃) 162.8 (d, *J* 245.1), 146.9 (d, *J* 7.0), 129.8 (d, *J* 8.3), 123.5 (t, *J* 34.4), 115.0 (d, *J* 21.7), 113.1 (d, *J* 21.0), 95.8, 82.4, 75.5, 72.1, 64.7, 46.0 (d, *J* 1.6), 41.7, 36.1 and 34.2; HRMS found MNa⁺, 287.1054. C₁₅H₁₇FO₃ requires *MNa*, 287.1059.

(9R*,1S*,8S*,11R*)-8-(3-fluorophenyl)-13,15-dioxazetetracyclo[7.5.1.0^{1,11}.0^{2,7}]pentadeca-2(7),3,5-triene 198



According to general procedure F, ketone **145** (75.0 mg, 0.28 mmol) gave a crude material. The crude material was purified using HPLC eluting with gradient elution: 5:95 → 95:5 MeCN–water to give the *pyridine* as a yellow oil (17.0 mg, 21%). R_f 0.29 (50:50 hexanes–EtOAc); $\nu_{\max}/\text{cm}^{-1}$ (film) 3053, 2951, 2873, 1613, 1586, 1484, 1441, 1420, 1253, 1218, 1136, 1066, 988, 917, 840 and 702; δ_{H} (500 MHz, CDCl_3) 8.38 (1H, dd, J 4.8 and 1.2, 4-H), 7.31 – 7.22 (2H, m, 6-H and phenyl 5-H), 7.11 (1 H, dd, J 7.8 and 4.8, 5-H), 7.03 (1H, br d, J 7.7, phenyl 6-H), 6.98 – 6.87 (2H, m, phenyl 2-H and phenyl 4-H), 5.09 (1H, d, J 10.2, 14- H_A), 4.81 (1H, d, J 7.3, 9-H), 4.27 (1H, d, J 10.2, 14- H_B), 4.20 (1H, t, J 8.3, 12- H_A), 3.73 (1H, s, 8-H), 3.64 (1H, t, J 8.4, 12- H_B), 2.96 (1H, qd, J 8.3 and 3.1, 11-H), 2.21 (1H, ddd, J 13.2, 7.3 and 3.1, 10- H_A) and 2.06 (1H, ddd, J 13.2, 8.4 and 1.3, 10- H_B); δ_{C} (126 MHz, CDCl_3) 162.9 (d, J 246.3), 156.7, 147.3 (d, J 7.0), 147.1, 138.7, 130.8, 130.0 (d, J 8.2), 124.1 (d, J 2.8), 122.9, 115.6 (d, J 21.7), 113.9 (d, J 21.1), 94.3, 83.3, 74.9, 71.4, 54.5, 51.2 and 35.4; HRMS found MNa^+ , 320.1057. $\text{C}_{18}\text{H}_{16}\text{FNO}_2$ requires MNa , 320.1062.

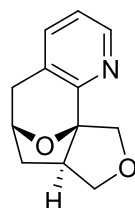
2-[[[(1R*,5R*,7R*,8R*,10R*)-8-(3-fluorophenyl)-3,11-dioxatricyclo[5.3.1.0^{1,5}]undecan-10-yl]oxy}pyrimidine



According to general procedure I, alcohol **129a** (48.0 mg, 0.18 mmol) gave a crude material. The crude material was purified using HPLC eluting with gradient elution: 5:95 → 95:5 MeCN–water to give the *I pyrimidine* as a yellow oil (21.3 mg, 35%). R_f 0.52 (100 EtOAc); $\nu_{\max}/\text{cm}^{-1}$ (film) 3051, 2950, 2860, 1614, 1576, 1562, 1485, 1416, 1318, 1267, 1185, 1123, 1050, 1014, 807 and 731; δ_{H} (500 MHz, CDCl_3) 8.43 (2H, d, J 4.8, pyrim 3-H and pyrim 5-H), 7.37 (1H, d, J 7.8, phenyl 6-H), 7.35 – 7.30 (1H, m, phenyl 2-H), 7.21 (1H, app td, J 8.1 and 6.3, phenyl 5-H), 6.87 (1H, t, J 4.8, pyrim 4-H), 6.83 (1H, td,

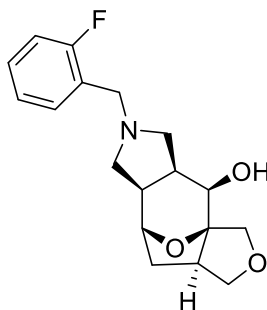
J 8.1 and 1.9, phenyl 4-H), 5.16 (1H, dd, J 5.0 and 1.3, 10-H), 4.83 (1H, d, J 6.6, 7-H), 4.20 (1H, d, J 10.5, 2-H_A), 4.12 (1H, t, J 8.5, 4-H_A), 3.86 (1H, d, J 10.5, 2-H_B), 3.64 (1H, dd, J 8.5 and 7.0, 4-H_B), 2.80 (1H, app qd, J 8.0 and 5.0, 5-H), 2.67 (1H, d, J 7.9, 8-H), 2.48 (1H, ddd, J 15.9, 7.9 and 5.1, 9-H_A), 2.23 (1 H, dd, J 15.0, 1.3, 9-H_B) and 2.16 – 2.05 (2H, m, 6-H); δ_c (126 MHz, CDCl₃) 164.4, 162.9 (d, J 244.5), 159.4, 147.5 (d, J 7.2), 129.7 (d, J 8.2), 124.1 (d, J 2.6), 115.6 (d, J 21.8), 115.2, 113.1 (d, J 21.0), 93.8, 82.8, 75.4, 75.1, 73.3, 46.9, 43.0, 35.9 and 28.6; HRMS found MH⁺, 343.1452. C₁₉H₁₉N₂O₃ requires *MH*, 343.1458.

(9R*, 1S*, 11R*)-13, 15-dioxa-3-azatetracyclo[7.5.1.0^{1,11}.0^{2,7}]pentadeca-2(7), 3, 5-triene 198



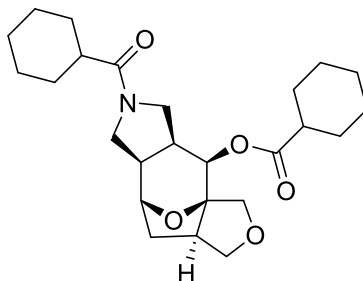
According to general procedure F, ketone **161** (100 mg, 0.60 mmol) gave a crude material. The crude material was purified by flash column chromatography eluting with 05:95 Sat. NH₃ in MeOH–EtOAc to give the *pyridine* as a dark yellow oil (4.0 mg, 3%). R_f 0.24 (50:50 hexanes–EtOAc); δ_H (500 MHz, CDCl₃) 8.34 (1H, d, J 4.9, 4-H), 7.45 (1H, d, J 7.6, 6-H), 7.16 (1H, dd, J 7.6 and 4.9, 5-H), 5.02 (1H, d, J 10.3, 14-H_A), 4.98 (1H, t, J 6.5, 9-H), 4.19 (1H, d, J 10.3, 14-H_B), 4.16 (1H, t, J 8.4, 12-H_A), 3.67 – 3.62 (1H, m, 12-H_B), 3.44 (1H, ddd, J 17.0, 6.5 and 0.9, 8-H_A), 2.95 (1H, qd, J 8.1 and 3.5, 11-H), 2.59 (1H, d, J 17.0, 8-H_B), 2.17 – 2.09 (1H, m, 10-H_A) and 2.03 (1H, ddd, J 13.0, 8.5, 1.1, 10-H_B); δ_c (126 MHz, CDCl₃) 157.5, 146.2, 138.1, 129.2, 123.3, 94.3, 77.8, 77.6, 77.3, 75.7, 71.9, 55.5, 37.0 and 35.8; HRMS found MH⁺, 204.1019. C₁₂H₁₃NO₂ requires *MH*, 204.1024. Unable to obtain an IR due to lack of material.

(1R*,2R*,3S*,7R*,8R*,10R*)-5-[(2-fluorophenyl)methyl]-12,14-dioxo-5-azatetracyclo[6.5.1.0^{1,10}.0^{3,7}]tetradecan-2-ol 241



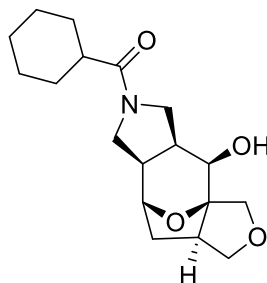
According to general procedure O, ketone **240** (75.0 mg, 0.35 mmol) gave a crude material. The crude material was purified using HPLC eluting with gradient elution: 5:95 → 95:5 MeCN–water to give the *alkyl amine* as a yellow oil (15.0 mg, 13%). R_f 0.31 (100 EtOAc); ν_{max}/cm^{-1} (film); 3154, 2861, 2726, 1601, 1496, 1459, 1349, 1237, 1144, 1107, 987, 916, 831 and 737; δ_H (500 MHz, MeOD) 7.60 (1H, td, J 7.5 and 1.5, phenyl 4-H), 7.56 – 7.49 (1H, m, phenyl 3-H), 7.32 (1H, td, J 7.5 and 0.9, phenyl 5-H), 7.29 – 7.24 (1H, m, phenyl 6-H), 4.53 (1H, d, J 6.9, 8-H), 4.45 (1H, d, J 13.1, benzyl CH₂), 4.40 (1H, d, J 13.1, benzyl CH₂), 4.08 – 3.95 (2H, m, 13-H_A and 11-H_A), 3.77 (2H, m, 2-H and 13-H_B), 3.61 (1H, dd, J 8.9 and 5.8, 11-H_B), 3.50 (2H, m, 4-H_A and 6-H_A), 3.38 – 3.30 (2H, m, 4-H_B and 6-H_B), 2.80 – 2.73 (1H, m, 3-H), 2.72 – 2.64 (1H, m, 10-H), 2.39 – 2.29 (1H, m, 7-H), 2.18 (1H, dd, J 13.0, 9.0, 9-H_A) and 2.06 – 1.93 (1H, m, 9-H_B); δ_C (126 MHz, MeOD) 161.4 (d, J 247.3), 132.1 (d, J 3.0), 131.6 (d, J 8.5), 124.8 (d, J 3.7), 119.4 (d, J 15.6), 115.6 (d, J 21.7), 76.6, 75.3, 74.6, 67.7, 55.6, 55.5, 51.5 (d, J 2.8), 44.1, 41.3, 36.9 and 35.7; HRMS found MH^+ , 320.1656. C₁₈H₂₂FNO₃ requires MH , 320. 1661.

**(1R*, 2R*, 3S*, 7R*, 8R*, 10R*)-5-cyclohexanecarbonyl-12,14-dioxa-5-azatetracyclo[6.5.1.0^{1,10}. 0^{3,7}]tetradecane-2-yl cyclohexane carboxylate
248**



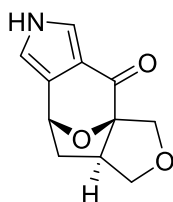
According to general procedure L, the amine **240** (75.0 mg, 0.36 mmol) gave a crude material. The crude material was dissolved in MeOH (1.5 mL), a precipitate was formed and collected via filtration, giving the *amide* as a colourless amorphous solid (7.8 mg, 5.2%). R_f 0.11 (50:50 hexanes–EtOAc); $\nu_{\max}/\text{cm}^{-1}$ (film); 2918, 2850, 1718, 1628, 1429, 1347, 1321, 1246, 1207, 1160, 1075, 963, 911 and 838; δ_{H} (400 MHz, CDCl_3) 5.15 (1H, d, J 5.6, 2-H), 4.60 (1H, app dd, J 17.8 and 6.3, 8-H), 4.06 – 3.97 (1H, m, 13- H_A), 3.86 – 3.69 (2H, m, 11- H_A and 4- H_A), 3.67 – 3.49 (3H, m, 13- H_B , 11- H_B and 6- H_A), 3.41 – 3.30 (2H, m, 6- H_B and 4- H_B), 2.74 – 2.56 (2H, m, 3-H and 10-H), 2.39 – 2.29 (1H, m, 7-H), 2.27 – 1.96 (4H, m, 9-H, cyclohexane 1-H and cyclohexane carboxylate 1-H) and 1.90 – 1.13 (20H, br m, cyclohexane-H and cyclohexane carboxylate-H); δ_{C} (100 MHz, CDCl_3 , mixture of rotamers, rotamer A is major) 176.3 (rotamer B), 175.7 (rotamer A), 174.3 (rotamer A), 174.3 (rotamer B), 94.2 (rotamer A), 93.9 (rotamer B), 76.9 (rotamer A), 75.5 (rotamer A), 75.4 (rotamer B), 74.4 (rotamer B), 74.3 (rotamer A), 70.3 (rotamer B), 69.7 (rotamer A), 48.0 (rotamer B), 47.9 (rotamer A), 47.7 (rotamer A), 47.4 (rotamer B), 45.3 (rotamer B), 45.2 (rotamer A), 43.3 (rotamer B), 43.3 (rotamer A), 42.9 (rotamer A), 42.7 (rotamer B), 42.5 (rotamer A), 40.7 (rotamer B), 36.8 (rotamer B), 36.5 (rotamer A), 36.2 (rotamer B), 34.8 (rotamer A), 29.2 (rotamer B), 29.0 (rotamer A), 28.9 (rotamer A), 28.9 (rotamer A) 28.8 (rotamer B), 28.8 (rotamer B), 28.8 (rotamer A), 25.9 (rotamer A), 25.9 (rotamer A), 25.8 (rotamer A), 25.8 (rotamer A), 25.6 (rotamer A), 25.4 (rotamer A), 25.4 (rotamer A) and 25.2 (rotamer B); HRMS found MNa^+ , 454.2564. $\text{C}_{25}\text{H}_{37}\text{NO}_5$ requires MNa , 454. 2569.

(1R*,2R*,3S*,7R*,8R*,10R*)-5-cyclohexanecarbonyl-12,14-dioxa-5-azatetracyclo[6.5.1.0^{1,10}.0^{3,7}]tetradecan-2-ol 247



According to general procedure L, amine **240** (75.0 mg, 0.36 mmol) gave a crude material. The crude material was purified using HPLC eluting with gradient elution: 5:95 → 95:5 MeCN–water to give the *amide* as a yellow oil (4.3 mg, 4%). R_f 0.10 (100 EtOAc); $\nu_{\max}/\text{cm}^{-1}$ (film); 3051, 2928, 2853, 1607, 1449, 1278, 1196, 1136, 1075, 970 and 919; δ_{H} (500 MHz, CDCl_3) 4.53 – 4.45 (1H, m, 8-H), 4.02 – 3.88 (2H, m, 13- H_A and 11- H_A), 3.81 – 3.70 (3H, m, 4- H_A , 6- H_A and 13- H_B), 3.63 – 3.53 (2H, m, 11- H_B and 2-H), 3.53 – 3.42 (1H, m, 4- H_B), 3.40 – 3.27 (1H, m, 6- H_B), 2.54 (1H, app ddd, J 14.0, 8.2 and 5.9, 10-H), 2.39 (1H, m, 3-H), 2.31 – 2.21 (1H, m, 7-H), 2.20 – 1.91 (3H, m, cyclohexane 1-H and 9-H), 1.86 – 1.57 (6H, m, cyclohexane 2-H, cyclohexane 6-H and cyclohexane 5- H_A and cyclohexane 3- H_A), 1.45 – 1.36 (2H, m, cyclohexane 5- H_B and cyclohexane 3- H_B) and 1.19 (2H, m, cyclohexane 4-H); δ_{C} (126 MHz, CDCl_3) 175.1, 95.6, 78.1, 75.7, 75.3, 75.2, 71.1, 48.7, 48.6, 44.8, 43.1, 42.9, 40.8, 38.2, 36.3, 28.9, 28.8, 26.1, 25.9 and 25.9; HRMS found MNa^+ , 344.1833. $\text{C}_{18}\text{H}_{27}\text{NO}_4$ requires MNa , 344.1837.

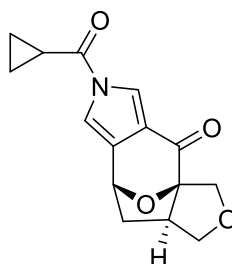
(1R*, 8R*, 10R*)-12,14-dioxa-5-azatetracyclo[6.5.1.0^{1,10}.0^{3,7}] tetradeca-3,6-dien-2-one 157



According to general procedure C, enone **86** (1.00 g, 6.02 mmol) gave a crude material. The crude material was purified by flash column chromatography

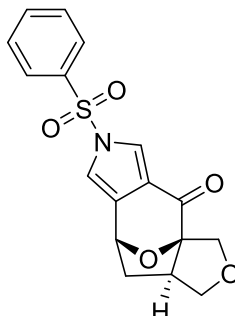
eluting with 60:40 EtOAc–Hexanes to give the *pyrrole* as a dark orange amorphous solid (413 mg, 34%). R_f 0.55 (100 EtOAc); $\nu_{\max}/\text{cm}^{-1}$ (film); 3310, 3163, 3126, 2988, 2965, 2914, 2848, 1668, 1567, 1517, 1449, 1433, 1354, 1318, 1103, 1080, 1054 and 985; δ_{H} (500 MHz, CDCl_3) 8.89 (1H, br s, NH), 7.36 (1H, dd, J 2.9 and 1.7, 4-H), 6.62 (1H, t, J 1.9, 6-H), 5.58 (1H, t, J 3.3, 8-H), 4.51 (1H, d, J 10.5, 13- H_A), 4.12 – 4.03 (1H, m, 11- H_A), 3.97 (1H, d, J 10.5, 13- H_B), 3.77 (1H, dd, J 9.0 and 4.9, 11- H_B), 2.88 – 2.80 (1H, m, 10-H) and 2.20 – 2.13 (2H, m, 9-H); δ_{C} (126 MHz, CDCl_3) 191.7, 129.9, 119.9, 118.5, 111.6, 97.5, 74.3, 70.3, 48.3 and 39.1; HRMS found MNa^+ , 228.0631. $\text{C}_{11}\text{H}_{11}\text{NO}_3$ requires MNa , 228.0636.

(1R*,8R*,10R*)-5-cyclopropanecarbonyl-12,14-dioxa-5-azatetracyclo[6.5.1.0^{1,10}.0^{3,7}]tetradeca-3,6-dien-2-one 249



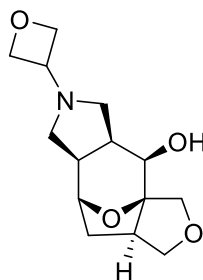
According to general procedure L, the pyrrole **157** (100 mg, 0.49 mmol) gave a crude material. The crude material was purified using HPLC eluting with gradient elution: 5:95 → 95:5 MeCN–water to give the *pyrrole amide* as a yellow oil (8.1 mg, 6%). R_f 0.26 (50:50 hexanes–EtOAc); δ_{H} (500 MHz, MeOD) 8.12 (1H, d, J 1.9, 4-H), 7.46 (1H, d, J 1.9, 6-H), 5.59 (1H, d, J 5.9, 8-H), 4.41 (1H, d, J 10.4, 13- H_A), 4.09 – 3.99 (1H, m, 11- H_A), 3.88 (1H, d, J 10.4, 13- H_B), 3.75 (1H, dd, J 9.0 and 5.0, 11- H_B), 2.98 – 2.84 (1H, m, 10-H), 2.54 (1H, ddd, J 12.5, 7.7 and 4.7, cycloprop 1-H), 2.32 – 2.14 (2H, m, 9-H) and 1.26 – 1.14 (4H, m, cycloprop 2-H and cycloprop 3-H); δ_{C} (126 MHz, MeOD) 191.9, 172.5, 131.7, 121.3, 120.1, 112.8, 97.4, 77.1, 73.9, 69.6, 48.5, 38.3, 12.2, 10.2 and 10.2; HRMS found MNa^+ , 296.0894. $\text{C}_{15}\text{H}_{15}\text{NO}_4$ requires MNa , 296.0898. Unable to obtain an IR due to lack of material.

(1R*,8R*,10R*)-5-(benzenesulfonyl)-12,14-dioxa-5-azatetracyclo[6.5.1.0^{1,10}.0^{3,7}]tetradeca-3,6-dien-2-one 245



According to general procedure K, the pyrrole **157** (100 mg, 0.49 mmol) gave a crude material. The crude material was purified using HPLC eluting with gradient elution: 5:95 → 95:5 MeCN–water to give the *sulfonamide* as a yellow oil (2.9 mg, 2%). R_f 0.31 (50:50 hexanes–EtOAc); δ_H (500 MHz, $CDCl_3$) 7.92 (1H, d, J 7.7, Ar 2-H and Ar 6-H), 7.72 (1H, d, J 2.0, 4-H), 7.68 (1H, t, J 7.7, Ar 4-H), 7.57 (1H, t, J 7.7, Ar 3-H and Ar 5-H), 7.00 (1H, d, J 2.0, 6-H), 5.48 (1H, d, J 4.5, 8-H), 4.40 (1H, d, J 10.6, 13-H_A), 4.05 – 3.99 (1H, m, 11-H_A), 3.93 (1H, d, J 10.6, 13-H_B), 3.76 (1H, dd, J 9.1 and 4.6, 11-H_B), 2.81 (1H, qd, J 7.4 and 4.6, 10-H) and 2.20 – 2.16 (2H, m, 9-H); δ_C (126 MHz, $CDCl_3$) 190.6, 134.8, 132.2, 129.8, 127.3, 122.1, 121.6, 113.7, 97.6, 77.3, 77.0, 76.8, 76.6, 74.2, 70.1, 48.1, 38.7 and 29.7; HRMS found MH^+ , 346.0736. $C_{17}H_{15}NO_5S$ requires MH , 346.0748. Unable to obtain an IR due to lack of material.

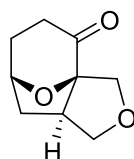
(1R*,2R*,3S*,7R*,8R*,10R*)-5-(oxetan-3-yl)-12,14-dioxa-5-azatetracyclo[6.5.1.0^{1,10}.0^{3,7}]tetradecan-2-ol 242



According to general procedure O, the pyrrole **240** (100 mg, 0.49 mmol) gave a crude material. The crude material was purified by flash column chromatography eluting with 05:95 Sat. NH_3 in MeOH–EtOAc to give the

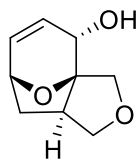
oxetane (3.0 mg, 3%) as a colourless amorphous solid. R_f 0.03 (100 EtOAc); δ_H (500 MHz, MeOD) 4.74 (2H, m, oxetane 2-H_A and oxetane 4-H_A), 4.64 (1H, t, J 6.0, oxetane 2-H_B), 4.60 (1H, t, J 6.0, oxetane 4-H_B), 4.47 (1H, d, J 6.8, 8-H), 4.03 – 3.95 (2H, m, 11-H_A and 13-H_A), 3.84 – 3.77 (1H, m, oxetane 3-H), 3.75 – 3.68 (2H, m, 13-H_B and 2-H), 3.60 (1H, dd, J 8.9 and 5.5, 11-H_B), 3.00 – 2.90 (2H, m, 4-H), 2.66 (1H, ddd, J 13.8, 8.6 and 5.5, 10-H), 2.58 – 2.50 (3H, m, 7-H and 3-H), 2.20 – 2.09 (2H, m, 7-H and 9-H_A) and 1.94 – 1.88 (1H, m, 9-H_B); δ_C (126 MHz, MeOD) 96.5, 80.0, 77.1, 76.9, 76.8, 76.2, 70.6, 58.6, 53.6, 53.2, 45.2, 42.8, 37.7 and 37.1; HRMS found MNa^+ , 290.1359. $C_{14}H_{21}NO_4$ requires MNa , 290.1367. Unable to obtain an IR due to lack of material.

(1R*, 5R*, 7S*)-3,11-dioxaricyclo[5.3.1.0^{1,5}]undecane-10-one 161



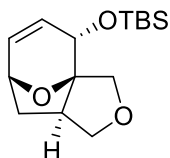
According to general procedure P, the enone **86** (70.0 mg, 0.42 mmol) in EtOAc (0.5 mL) gave a crude material. The crude material was used without further purification to give the *ketone* as a pale yellow oil (58.0 mg, 83%). R_f 0.76 (50:50 hexanes–EtOAc); ν_{max}/cm^{-1} (film); 2924, 2872, 1718, 1458, 1371, 1235, 1177, 1077, 1053 and 923; δ_H (500 MHz, $CDCl_3$) 4.82 (1H, t, J 6.1, 7-H), 4.36 (1H, d, J 10.6, 2-H_A), 4.09 (1H, t, J 8.4, 4-H_A), 3.83 (1H, d, J 10.6, 2-H_B), 3.60 (1H, dd, J 8.7 and 6.9, 4-H_B), 2.83 (1H, app ddd, J 15.2, 8.1 and 5.0, 5-H), 2.54 (1H, ddd, J 16.8, 8.3 and 3.4, 9-H_A), 2.50 – 2.41 (1H, m, 9-H_B), 2.40 – 2.30 (1H, m, 8-H_A), 2.11 (1H, dd, J 12.7 and 8.8, 6-H_A), 2.07 – 1.99 (1H, m, 6-H_B) and 1.86 – 1.78 (1H, m, 8-H_B); δ_C (126 MHz, $CDCl_3$) 204.6, 97.5, 78.4, 74.8, 70.2, 49.4, 35.1, 33.4 and 30.9; HRMS found MH^+ , 169.0859. $C_9H_{11}O_3$ requires MH , 169.0864.

(1R*, 5R*, 7R*, 10S*)-3,11-dioxatricyclo[5.3.1.0^{1,5}]undec-8-en-10-ol 178



According to general procedure Q, the enone **86** (0.10 g, 0.60 mmol) gave a crude material. The crude material was used without further purification to give the *allylic alcohol* as a yellow oil (54.0 mg, 53%). R_f 0.15 (100 EtOAc); $\nu_{\max}/\text{cm}^{-1}$ (film); 3345, 2954, 2882, 1641, 1454, 1370, 1229, 1072, 1049 and 920; δ_H (500 MHz, CDCl_3) 6.01 – 5.95 (1H, m, 8-H), 5.53 (1H, dd, J 9.7 and 1.6, 9-H), 4.65 (1H, br s, 10-H), 4.63 – 4.60 (1H, m, 7-H), 3.91 (2H, m, 2- H_A and 4- H_A), 3.78 – 3.72 (2H, m, 4- H_B and 2- H_B), 3.09 (1H, ddd, J 11.2, 8.0 and 3.7, 5-H), 2.24 (1H, dd, J 11.7, 8.8, 6- H_A) and 1.83 (1H, app dt, J 12.2, 6.3, 6- H_B); δ_C (126 MHz, CDCl_3) 133.6, 128.1, 76.9, 74.8, 71.9, 67.3, 41.7 and 40.0; HRMS found MNa^+ , 191.0679. $\text{C}_9\text{H}_{12}\text{O}_3$ requires MNa , 191.0684.

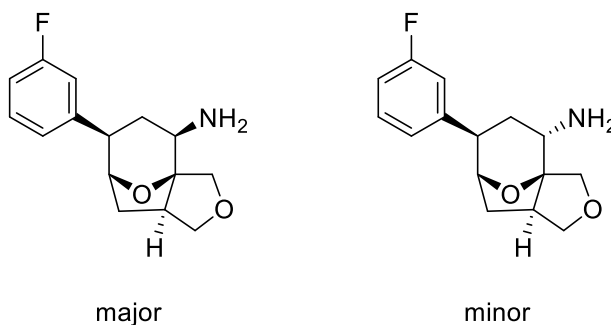
tert-butyl[(1R*,5R*,7R*,10S*)-3,11-dioxatricyclo[5.3.1.0^{1,5}]undec-8-en-10-yloxy]dimethylsilane 179



The alcohol **178** (54.0 mg, 0.32 mmol), TBSCl (53.0 mg, 0.35 mmol) and imidazole (23.9 mg, 0.35 mmol) were dissolved in the minimum amount of DMF and stirred overnight at rt. The reaction was diluted with CH_2Cl_2 (20 mL) and washed with an aqueous solution of LiCl (10% w/w, 3 x 20 mL) and a saturated aqueous brine solution (3 x 20 mL), dried (MgSO_4) and concentrated under reduced pressure. The crude material was purified by flash column chromatography eluting with 50:50 EtOAc–Hexanes to give the *protected alcohol* as a colourless oil (35.0 mg, 39%). R_f 0.51(50:50 hexanes–EtOAc); $\nu_{\max}/\text{cm}^{-1}$ (film); 2943, 2831, 1449, 1421, 1114, 1022 and 629; δ_H (501 MHz, CDCl_3) 5.90 (1H, ddd, J 9.7, 3.9 and 1.4, 9-H), 5.44 (1H, dd, J 9.7 and 1.8, 8-H), 4.62 (1H, s, 10-H), 4.60 – 4.57 (1H, m, 7-H), 3.87 (1H,

d, J 9.9, 2-H_A), 3.83 – 3.75 (2H, m, 4-H), 3.63 (1H, d, J 9.9, 2-H_B), 3.20 – 3.15 (1H, m, 5-H), 2.25 (1H, dd, J 11.6, 8.8, 6-H_A), 1.85 – 1.77 (1H, m, 6-H_B), 0.90 (9H, s, ^tBu), 0.09 (3H, s, CH₃ TBS) and 0.07 (3H, s, CH₃ TBS); δ_c (126 MHz, CDCl₃) 132.4, 128.7, 94.8, 74.6, 71.5, 67.2, 41.8, 40.4, 25.6, 17.8, -4.2 and -5.1; HRMS found MNa⁺, 305.1547. C₁₅H₂₆O₃Si requires MNa, 305.1549.

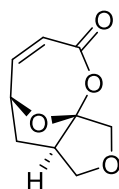
(5R*,1S*,7R*,8R*,10R*)-8-(3-fluorophenyl)-3,11-dioxatricyclo[5.3.1.0^{1,5}]undecan-10-amine and (5R*,1S*,7R*,8R*,10S*)-8-(3-fluorophenyl)-3,11-dioxatricyclo[5.3.1.0^{1,5}]undecan-10-amine
236a/b



According to general procedure G, the ketone **145** (100 mg, 0.44 mmol) gave a crude material. The crude material was purified using HPLC eluting with gradient elution: 5:95 → 95:5 MeCN–water to give the *amines* as a yellow oil (10.0 mg, 9%). R_f 0.13 (100 EtOAc); ν_{max}/cm^{-1} (film); 3266, 2944, 2867, 1614, 1595, 1487, 1444, 1345, 1268, 1186, 1147, 1072, 922 and 785; δ_H (500 MHz, MeOD and CDCl₃, mixture of diastereomers 5:1) 8.29 (5H, br s, NH), 7.38 – 7.13 (18H, m, Ar 2-H_{maj}, Ar 4-H_{maj}, Ar 5-H_{maj}, Ar 2-H_{min}, Ar 4-H_{min}, Ar 5-H_{min}), 6.97 – 6.88 (6H, m, Ar 6-H_{maj} and Ar 6-H_{min}), 5.14 (5H, d, J 6.5, 7-H_{maj}), 4.78 (1H, d, J 6.5, 7-H_{min}), 4.10 (6H, m, 4-H_Amaj and 4-H_Amin), 3.98 (6H, m, 9-H_Amaj and 9-H_Amin), 3.83 (1H, d, J 10.4, 9-H_Bmin), 3.72 (5H, d, J 10.4, 9-H_Bmaj), 3.66 (5H, dd, J 9.0 and 6.5, 4-H_Bmaj), 3.54 (1H, dd, J 9.0 and 6.5, 4-H_Bmin), 3.42 – 3.36 (1H, m, 10-H_{min}), 3.19 (5H, br s, 10-H_{maj}), 3.00 – 2.93 (1H, m, 5-H_{min}), 2.88 – 2.79 (6H, m, 5-H_{maj} and 8-H_{min}), 2.75 (5H, d, J 7.4, 8-H_{maj}), 2.61 – 2.52 (5H, m, 9-H_Amaj), 2.53 – 2.45 (1H, m, 9-H_Amin), 2.26 – 2.04 (16H, m, 9-H_Bmaj, 6-H_{maj} and 6-H_{min}) and 2.00 – 1.90 (1H, m, 9-H_Bmin); δ_c (126 MHz, MeOD and CDCl₃) 163.1 (d, J 246.0, major), 161.26 (d, J 246.0, minor), 146.6 (d, J 7.2,

major), 130.3 (d, *J* 8.4, major), 129.8 (d, *J* 8.4, minor), 123.6 (d, *J* 2.8, minor), 123.2 (d, *J* 2.8, major), 114.8 (d, *J* 21.8, minor), 114.5 (d, *J* 22.0, major), 113.33 (d, *J* 22.0, major), 113.11 (d, *J* 21.8, minor), 82.4 (minor), 81.3 (major), 75.6 (major), 75.3 (minor), 74.4 (minor), 73.9 (major), 71.9 (minor), 50.3 (major), 46.8 (major), 44.5 (minor), 41.8 (minor), 39.9 (major), 36.3 (major), 36.2 (minor) and 32.1 (minor); HRMS found MH^+ , 264.1394. $C_{15}H_{18}FNO_2$ requires *MH*, 264.1399.

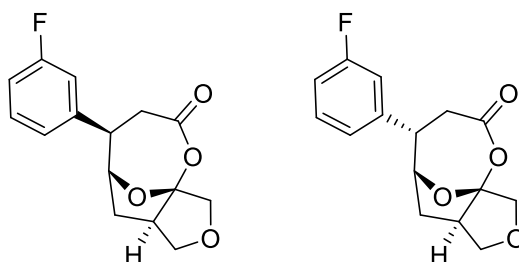
(5*R,1*S**,7*S**)-3,11,12-trioxatricyclo[5.4.1.0^{1,5}]dodec-8-en-10-one 173**



Enone **86** (70 mg, 0.42 mmol) was diluted in CH_2Cl_2 (2.0 mL), *m*-CPBA (145 mg, 0.84 mmol) was added and stirred at room temperature for 16 h, the reaction mixture was quenched with Na_2SO_3 (10 mL) then extracted with CH_2Cl_2 (3 × 25 mL). The reaction was then concentrated under reduced pressure to give a crude material. The crude material was purified by flash column chromatography eluting with 20:80 EtOAc–Hexanes to give the *lactone* as a pale yellow oil (22.0 mg, 28%). R_f 0.16 (50:50 EtOAc–Hexanes); δ_H (500 MHz, $CDCl_3$) 6.57 (1H, dd, *J* 12.0 and 4.2, 8-H), 6.03 (1H, d, *J* 12.0, 9-H), 4.99 (1H, dd, *J* 7.3 and 4.1, 7-H), 4.12 (1H, d, *J* 10.0, 2- H_A), 3.96 (1H, dd, *J* 9.6 and 5.9, 4- H_A), 3.84 (1H, d, *J* 9.6, 4- H_B), 3.70 (1H, d, *J* 10.0, 2- H_B), 3.15 – 3.07 (1H, m, 5-H), 2.44 (1H, dd, *J* 12.4 and 8.2, 6- H_A) and 2.11 (1H, ddd, *J* 12.4, 9.1 and 7.3, 6- H_B); δ_C (126 MHz, $CDCl_3$) 165.1, 147.1, 122.7, 118.4, 81.6, 74.7, 73.2, 48.9 and 40.7; HRMS found MNa^+ , 205.0467. $C_9H_{10}O_4$ requires *MNa*, 205.0476. Unable to obtain an IR due to lack of material.

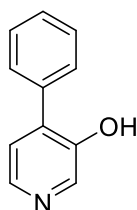
(5R*,1S*,7S*,8R*)-8-(3-fluorophenyl)-3,11,12-trioxatricyclo[5.4.1.0^{1,5}]dodecan-10-one 199a and

(5R*,1S*,7S*,8S*)-8-(3-fluorophenyl)-3,11,12-trioxatricyclo[5.4.1.0^{1,5}]dodecan-10-one 199b



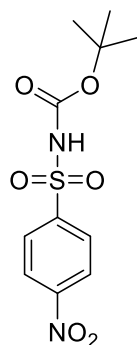
According to general procedure D, enone **173** (10 mg, 0.06 mmol) gave a crude material. The crude material was purified by flash column chromatography eluting with 20:80 EtOAc–Hexanes, to give the β -aryl lactone as a pale yellow oil that solidified on standing (5.01 mg, 33%). R_f 0.38 (50:50 Hexanes–EtOAc); δ_H (500 MHz, $CDCl_3$, mixture of diastereomers 7:5) 7.40 – 7.32 (12H, m, Ar 5- H_{maj} and Ar 5- H_{min}), 7.08 – 6.99 (24H, m, Ar 2- H_{maj} , Ar 2- H_{min} , Ar 4- H_{maj} and Ar 4- H_{min}), 6.99 – 6.92 (12H, m, Ar 6- H_{maj} and Ar 6- H_{min}), 4.62 – 4.54 (14H, m, 4- H_A maj and 7- H_{maj}), 4.50 (5H, t, J 8.9, 4- H_A min), 4.40 (5H, td, J 8.8 and 3.3, 5- H_{min}), 4.09 (5H, d, J 6.7, 2- H_A min), 4.05 (7H, d, J 6.7, 2- H_A maj), 3.83 – 3.70 (24H, m, 2- H_B maj, 2- H_B min, 4- H_B maj and 4- H_B min), 3.38 – 3.31 (5H, m, 8- H_{min}), 3.31 – 3.24 (7H, m, 8- H_{maj}), 2.98 (12H, m, 9- H_A maj, 9- H_A min), 2.82 – 2.70 (17H, m, 9- H_B maj, 9- H_B min and 5- H_{min}), 2.61 (7H, qd, J 9.2 and 5.8, 5- H_{maj}), 2.24 – 2.13 (7H, m, 6- H_A maj), 1.77 (5H, ddd, J 14.7, 10.0 and 3.3, 6- H_{Amin}) and 1.68 – 1.60 (2 H, m, 6- H_B maj, 6- H_B min); δ_C (126 MHz, $CDCl_3$) 174.3 (major), 174.2 (minor), 140.35 (d, J 7.1 major), 140.3 (d, J 6.8, minor), 131.0 (d, J 8.7, major), 129.8 (d, J 5.1, minor), 122.9 (d, J 3.0, major), 122.9 (d, J 3.2, minor), 115.2 (d, J 21.0, major), 114.3 (d, J 21.9, major), 114.3 (d, J 22.0, minor), 87.8 (major), 86.2 (minor), 84.9 (major), 83.5 (minor), 72.6 (major), 71.8 (minor), 70.8 (minor), 70.7 (major), 48.0 (d, J 1.6, major), 47.4 (d, J 1.5, minor), 45.4 (major), 43.8 (minor), 37.3 (major), 37.1 (minor), 32.1 (major), and 31.2 (minor); HRMS found MNa^+ , 301.0858. $C_{18}H_{19}N_3O$ requires MNa , 301.0852.

4-Phenylpyridin-3-ol



According to the literature procedure²³⁵, 4-bromo-3-hydroxypyridine (0.30 g, 1.72 mmol) and Pd(PPh)₄ (57.0 mg, 0.05 mmol, 3 mol%) were dissolved in toluene (3.5 mL, 0.5 M), then Na₂CO₃ (1.72 mL, 3.44 mmol, 2M) was added. Phenyl boronic acid (230 mg, 1.89 mmol) was dissolved in the minimum amount of EtOH and added into the toluene solution, the reaction was then heated at 100 °C and stirred vigorously for 6 h. The reaction was then concentrated under reduced pressure to give a crude material. The crude material was purified by flash column chromatography eluting with 20:80 EtOAc–Hexanes to give the hydroxy pyridine²³⁶ as a pale yellow amorphous solid (156 mg, 52%). *R*_f 0.40 (100 EtOAc); $\nu_{\max}/\text{cm}^{-1}$ (film); 3316, 2943, 2831, 1449, 1418, 1115, 1021 and 630; δ_{H} (500 MHz, CDCl₃) 8.47 (1H, s, pyridine 2-H), 8.19 (1H, d, *J* 5.0, pyridine 6-H), 7.67 – 7.63 (2H, m, Phenyl 2-H and phenyl 6-H), 7.53 – 7.48 (2H, m, phenyl 3-H and phenyl 5-H), 7.46 – 7.41 (1H, m, phenyl 4-H) and 7.30 (1H, d, *J* 5.0, pyridine 5-H); δ_{C} (126 MHz, CDCl₃) 151.2, 140.7, 137.8, 136.6, 135.2, 128.9, 128.7 and 124.8; HRMS found MH⁺, 172.0759. C₁₁H₉NO requires *MH*, 172.0762.

tert-butyl N-(4-nitrobenzenesulfonyl)carbamate 169



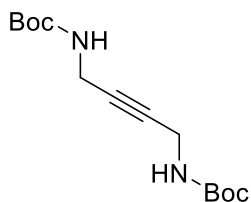
According to the literature procedure²³⁷, 4-nitrobenzenesulfonamide (2.00 g, 9.90 mmol), DMAP (119 mg, 0.98 mmol, 10 mol%), Boc anhydride (2.60 g, 11.9 mmol) and NEt₃ (2.08 mL, 14.8 mmol) were all dissolved in CH₂Cl₂ (40 mL) and stirred at rt for 1 h. The reaction mixture was poured into HCl (1M, 40 mL) and the mixture was extracted with Et₂O (3 × 25 mL), dried (MgSO₄), filtered and concentrated under reduced pressure to give a crude material. The crude material was used without further purification to give the amine²³⁷ as a yellow oil (2.94 g, 98%). *R*_f 0.47 (50:50 hexanes–EtOAc); *v*_{max}/cm⁻¹ (film); 3107, 2866, 1746, 1533, 1350, 1146, 1089 and 906; δ _H (500 MHz, CDCl₃) 8.41 – 8.37 (2H, m, Ar 3-H and Ar 5-H), 8.25 – 8.21 (2H, m, Ar 2-H and Ar 6-H) and 1.41 (9H, s, Boc ^tBu); δ _C (126 MHz, CDCl₃) 189.9, 148.6, 144.4, 129.9, 124.3, 85.3 and 28.0; HRMS found MNa⁺, 325.0472. C₁₁H₁₄N₂O₆S requires *MNa*, 325.0470.

***tert*-butyl-N-(4-{N-[(*tert*-butoxy)carbonyl]4-nitrobenzenesulfonamido}but-2-yn-1-yl)-N-(4-nitrobenzenesulfonyl)carbamate 170**



According to the literature procedure,¹⁹⁶ the protected amine **169** (2.94 g, 9.73 mmol), butyne-1,4-diol (0.42 g, 4.86 mmol), PPh₃ (2.55 g, 9.73 mmol) and DIAD (1.90 mL, 9.73 mmol) were dissolved in THF (20 mL) and stirred overnight at rt. The reaction mixture was then concentrated under reduced pressure to give a crude material. The crude material was purified by flash column chromatography eluting with 30:70 EtOAc–Hexanes to give the *amine* as a cream amorphous solid (163 mg, 45%). *R*_f 0.64 (100 EtOAc); *v*_{max}/cm⁻¹ (film) 3109, 2983, 2937, 1731, 1608, 1531, 1477, 1349, 1307, 1277, 1174 and 1027 δ _H (501 MHz, CDCl₃) 8.40 – 8.35 (4H, m, nosyl 3-H and nosyl 5-H), 8.26 – 8.20 (4H, m, nosyl 2-H and nosyl 6-H), 4.74 (4H, br s, butyn 1-H and butyn 4-H) and 1.33 – 1.26 (18H, m, boc ^tBu); δ _C (126 MHz, CDCl₃) 150.4, 149.5, 144.9, 129.4, 124.1, 86.2, 79.4, 35.7 and 27.7; HRMS found MNH₄⁺, 672.1643. C₂₆H₃₀N₄O₁₂S requires *MNH*₄, 672.1645.

***tert*-butyl N-(4-[[*tert*-butoxy]carbonyl]amino}but-2-yn-1-yl)carbamate
171**



The protected diamine **170** (2.54 g, 4.14 mmol) was dissolved in DMF (41 mL), K_2CO_3 (1.71 g, 12.4 mmol) was added followed by chlorothiophenol (1.43 g, 12.4 mmol) and the mixture was stirred overnight at rt. The reaction mixture was quenched with a saturated solution of sodium bicarbonate (40 mL) and extracted with EtOAc (3 × 40 mL), dried ($MgSO_4$), filtered and concentrated under reduced pressure to give a crude material. The crude material was purified by flash column chromatography eluting with 20:80 EtOAc–Hexanes to give the *N*-Boc amine as a colourless oil (0.52 g, 44%). R_f 0.19 (80:20 Hexanes–EtOAc); ν_{max}/cm^{-1} (film) 3337, 3308, 2979, 2933, 2253, 1697, 1510, 1367, 1249, 1249, 1164 and 905; δ_H (500 MHz, $CDCl_3$) 4.65 (2H, br s, NH), 3.91 (4H, d, J 3.3, CH_2) and 1.45 (18H, s, Boc t Bu); δ_C (126 MHz, $CDCl_3$) 155.3, 80.0, 79.3, 30.6 and 28.4; HRMS found MH^+ , 285.1804. $C_{14}H_{24}N_2O_4$ requires MNH , 285.1814.

List of References

- 1 Food and Drug Administration (FDA), *Advancing Health through innovation 2019 New Drug therapy approvals*, 2020.
- 2 D. Cook, D. Brown, R. Alexander, R. March, P. Morgan, G. Satterthwaite and M. N. Pangalos, *Nat. Rev. Drug Discov.*, 2014, **13**, 419–31.
- 3 B. S. Slusher, P. J. Conn, S. Frye, M. Glicksman and M. Arkin, *Nat. Rev. Drug Discov.*, 2013, **12**, 811–812.
- 4 B. Munos, *Nat. Rev. Drug Discov.*, , DOI:10.1038/nrd2961.
- 5 J. A. DiMasi, H. G. Grabowski and R. W. Hansen, *J. Health Econ.*, 2016, **47**, 20–33.
- 6 P. Gleeson, G. Bravi, S. Modi and D. Lowe, *Bioorganic Med. Chem.*, 2009, **17**, 5906–5919.
- 7 S. M. Paul, D. S. Mytelka, C. T. Dunwiddie, C. C. Persinger, B. H. Munos, S. R. Lindborg and A. L. Schacht, *Nat. Rev. Drug Discov.*, 2010, **9**, 203–14.
- 8 J. P. Hughes, S. S. Rees, S. B. Kalindjian and K. L. Philpott, *Br. J. Pharmacol.*, 2011, **162**, 1239–1249.
- 9 R. E. Hubbard, in *Structure Based Drug Discovery*, 2005, vol. 1, pp. 391–406.
- 10 Y. Tang, W. Zhu, K. Chen and H. Jiang, *Drug Discov. Today*, 2006, **3**, 307–313.
- 11 D. G. Brown and J. Boström, *J. Med. Chem.*, 2018, **61**, 9442–9468.
- 12 L. M. Mayr and D. Bojanic, *Curr. Opin. Pharmacol.*, 2009, **9**, 580–588.
- 13 K. E. Hevener, R. Pesavento, J. H. Ren, H. Lee, K. Ratia and M. E. Johnson, in *Methods in Enzymology*, Academic Press Inc., 2018, vol. 610, pp. 265–309.
- 14 G. Wu and S. K. Doberstein, *Drug Discov. Today*, 2006, **11**, 718–724.
- 15 P. Szymański, M. Markowicz and E. Mikiciuk-Olasik, *Int. J. Mol. Sci.*, 2012, **13**, 427–452.
- 16 G. M. Keseru and G. M. Makara, *Drug Discov. Today*, 2006, **11**, 741–748.
- 17 K. H. Bleicher, H.-J. Böhm, K. Müller and A. I. Alanine, *Nat. Rev. Drug Discov.*, 2003, **2**, 369–378.
- 18 J. U. Adams, Drug Discovery and Development: A Complex Team Sport, http://sciencecareers.sciencemag.org/career_magazine/previous_issues/articles/2008_03_07/science.opms.r0800049, (accessed 9 November 2016).
- 19 B. E. Maryanoff, *Future Med. Chem.*, 2009, **1**, 11–15.

- 20 S. L. Kidd, T. J. Osberger, N. Mateu, H. F. Sore and D. R. Spring, *Front. Chem.*, 2018, 6, 460.
- 21 W. R. J. D. Galloway and D. R. Spring, *Divers. Oriented Synth.*, 2013, 1, 21–28.
- 22 A. Guarnieri-Ibez, F. Medina, C. Besnard, S. L. Kidd, D. R. Spring and J. Lacour, *Chem. Sci.*, 2017, 8, 5713–5720.
- 23 D. Chen, Y. Chen, F. Lian, L. Chen, Y. Li, D. Cao, X. Wang, L. Chen, J. Li, T. Meng, M. Huang, M. Geng, J. Shen, N. Zhang and B. Xiong, *Eur. J. Med. Chem.*, 2019, 163, 597–609.
- 24 D. A. Erlanson, S. W. Fesik, R. E. Hubbard, W. Jahnke and H. Jhoti, *Nat. Rev. Drug Discov.*, 2016, 15, 605–619.
- 25 R. G. Doveston, P. Tosatti, M. Dow, D. J. Foley, H. Y. Li, A. J. Campbell, D. House, I. Churcher, S. P. Marsden and A. Nelson, *Org. Biomol. Chem.*, 2015, 13, 859–65.
- 26 S. J. Chawner, M. J. Cases-Thomas and J. A. Bull, *European J. Org. Chem.*, 2017, 2017, 5015–5024.
- 27 T. Cernak, K. D. Dykstra, S. Tyagarajan, P. Vachal and S. W. Krska, *Chem. Soc. Rev.*, 2016, 45, 546–576.
- 28 P. S. Engl, A. P. Ha, F. Berger, G. Berger, A. Pe and T. Ritter, , DOI:10.1021/jacs.9b07323.
- 29 C. N. Neumann and T. Ritter, *Angew. Chemie Int. Ed.*, 2015, 54, 3216–3221.
- 30 T. W. J. Cooper, I. B. Campbell and S. J. F. Macdonald, *Angew. Chemie Int. Ed.*, 2010, 49, 8082–8091.
- 31 ABPI, Worldwide pharmaceutical company R&D expenditure | ABPI, <https://www.abpi.org.uk/facts-and-figures/science-and-innovation/worldwide-pharmaceutical-company-rd-expenditure/>, (accessed 8 January 2020).
- 32 M. Riley, 2018.
- 33 Deloitte, *DTTL LSHC Ind. Gr.*, 2018, 9 ff.
- 34 A. Mullard, *Nat. Rev. Drug Discov.*, 2019, 18, 85–89.
- 35 R. K. Harrison, *Nat. Rev. Drug Discov.*, 2016, 15, 817–818.
- 36 I. Khanna, *Drug Discov. Today*, 2012, 17, 1088–1102.
- 37 I. Kola and J. Landis, *Nat. Rev. Drug Discov.*, 2004, 3, 1–5.
- 38 M. E. Bunnage, *Nat. Chem. Biol.*, 2011, 7, 335–339.
- 39 A. Nadin, C. Hattotuwigama and I. Churcher, *Angew. Chemie - Int. Ed.*, 2012, 51, 1114–1122.
- 40 C. Harrison, *Nat. Rev. Drug Discov.*, 2011, 10, 12–13.
- 41 C. H. Song and J. W. Han, *Springerplus*, 2016, 5, 692.
- 42 P. Morgan, D. G. Brown, S. Lennard, M. J. Anderton, J. C. Barrett, U.

- Eriksson, M. Fidock, B. Hamrén, A. Johnson, R. E. March, J. Matcham, J. Mettetal, D. J. Nicholls, S. Platz, S. Rees, M. A. Snowden and M. N. Pangalos, *Nat. Rev. Drug Discov.*, 2018, **17**, 167–181.
- 43 W. P. Walters and M. A. Murcko, 2002, **54**, 255–271.
- 44 P. J. Lipinski, C.A.; Lombardo, F.; Dominy, B.W.; Feeney, *Adv. Drug Deliv. Rev.*, 2012, **64**, 4–17.
- 45 C. A. Lipinski, *Drug Discov. Today Technol.*, 2004, **1**, 337–341.
- 46 C. A. Lipinski, F. Lombardo, B. W. Dominy and P. J. Feeney, *Adv. Drug Deliv. Rev.*, 1997, **23**, 3–25.
- 47 J. Hodgson, *Nat. Biotechnol.*, 2001, **19**, 722–726.
- 48 P. D. Leeson and B. Springthorpe, *Nat. Rev. Drug Discov.*, 2007, **6**, 881–90.
- 49 J. D. Hughes, J. Blagg, D. A. Price, S. Bailey, G. A. DeCrescenzo, R. V. Devraj, E. Ellsworth, Y. M. Fobian, M. E. Gibbs, R. W. Gilles, N. Greene, E. Huang, T. Krieger-Burke, J. Loesel, T. Wager, L. Whiteley and Y. Zhang, *Bioorganic Med. Chem. Lett.*, 2008, **18**, 4872–4875.
- 50 C. W. Murray and D. C. Rees, *Angew. Chemie - Int. Ed.*, 2016, **55**, 488–492.
- 51 M. M. Hann and T. I. Oprea, *Curr. Opin. Chem. Biol.*, 2004, **8**, 255–263.
- 52 T. I. Oprea, A. M. Davis, S. J. Teague and P. D. Leeson, *J. Chem. Inf. Model.*, 2001, **41**, 1308–1315.
- 53 G. M. Keserü and G. M. Makara, *Nat. Rev. Drug Discov.*, 2009, **8**, 203–212.
- 54 E. Perola, *J. Med. Chem.*, 2010, **53**, 2986–2997.
- 55 M. M. Hann, *Med. Chem. Commun.*, 2011, **2**, 349–355.
- 56 J. L. Reymond, R. Van Deursen, L. C. Blum and L. Ruddigkeit, *Medchemcomm*, 2010, **1**, 30–38.
- 57 P. G. Polishchuk, T. I. Madzhidov and A. Varnek, *J. Comput. Aided. Mol. Des.*, 2013, **27**, 675–679.
- 58 A. R. Leach and M. M. Hann, *Curr. Opin. Chem. Biol.*, 2011, **15**, 489–496.
- 59 F. Lovering, J. Bikker and C. Humblet, *J. Med. Chem.*, 2009, **52**, 6752–6756.
- 60 F. Lovering, *Medchemcomm*, 2013, **4**, 515–519.
- 61 F. Lovering, J. Bikker and C. Humblet, *J. Med. Chem.*, 2009, **52**, 6752–6756.
- 62 F. Lovering, *Medchemcomm*, 2013, **4**, 515–519.
- 63 N. C. Firth, N. Brown and J. Blagg, *J. Chem. Inf. Mod.*, 2012, Accepted.

- 64 M. J. Waring, J. Arrowsmith, A. R. Leach, P. D. Leeson, S. Mandrell, R. M. Owen, G. Pairaudeau, W. D. Pennie, S. D. Pickett, J. Wang, O. Wallace and A. Weir, *Nat. Rev. Drug Discov.*, 2015, **14**, 475–486.
- 65 T. J. Ritchie and S. J. F. Macdonald, *Drug Discov. Today*, 2009, **14**, 1011–1020.
- 66 J. Meyers, M. Carter, N. Y. Mok and N. Brown, *Future Med. Chem.*, 2016, **8**, 1753–1767.
- 67 W. P. Janzen, *Chem. Biol.*, 2014, **21**, 1162–1170.
- 68 T. Kogej, N. Blomberg, P. J. Greasley, S. Mundt, M. J. Vainio, J. Schamberger, G. Schmidt and J. Hüser, *Drug Discov. Today*, 2013, **18**, 1014–1024.
- 69 A. Karawajczyk, F. Giordanetto, J. Benningshof, D. Hamza, T. Kalliokoski, K. Pouwer, R. Morgentin, A. Nelson, G. Müller, A. Piechot and D. Tzalis, *Drug Discov. Today*, 2015, **20**, 1310–1316.
- 70 R. Morgentin, M. Dow, A. Aimon, G. Karageorgis, T. Kalliokoski, D. Roche, S. Marsden and A. Nelson, *Drug Discov. Today*, 2018, **23**, 1578–1583.
- 71 R. MacArron, M. N. Banks, D. Bojanic, D. J. Burns, D. A. Cirovic, T. Garyantes, D. V. S. Green, R. P. Hertzberg, W. P. Janzen, J. W. Paslay, U. Schopfer and G. S. Sittampalam, *Nat. Rev. Drug Discov.*, 2011, **10**, 188–195.
- 72 S. Fox, S. Farr-Jones, L. Sopchak, A. Boggs, H. Wang, R. Khoury and M. Biro, , DOI:10.1177/1087057106292473.
- 73 P. Dorr, M. Westby, S. Dobbs, P. Griffin, B. Irvine, M. Macartney, J. Mori, G. Rickett, C. Smith-Burchnell, C. Napier, R. Webster, D. Armour, D. Price, B. Stammen, A. Wood and M. Perros, *Antimicrob. Agents Chemother.*, 2005, **49**, 4721–4732.
- 74 D. Price, D. Armour, M. de Groot, D. Leishman, C. Napier, M. Perros, B. Stammen and A. Wood, *Curr. Top. Med. Chem.*, 2008, **8**, 1140–1151.
- 75 D. Armour, M. J. De Groot, M. Edwards, M. Perros, D. A. Price, B. L. Stammen and A. Wood, *ChemMedChem*, 2006, **1**, 706–709.
- 76 D. R. Armour, M. J. De Groot, D. A. Price, B. L. C. Stammen, A. Wood, M. Perros and C. Burt, *Chem. Biol. Drug Des.*, 2006, **67**, 305–308.
- 77 C. Abell and C. Dagostin, *RSC Drug Discov. Ser.*, 2015, **47**, 1–18.
- 78 L. Ruddigkeit, R. Van Deursen, L. C. Blum and J.-L. Reymond, *J. Chem. Inf. Model.*, 2012, **52**, 2864–2875.
- 79 R. S. Bohacek, C. McMartin and W. C. Guida, *Med. Res. Rev.*, 1996, **16**, 3–50.
- 80 S. Howard and C. Abell, Eds., *Fragment-Based Drug Discovery*, Royal Society of Chemistry, Cambridge, 2015.
- 81 D. A. Erlanson, S. W. Fesik, R. E. Hubbard, W. Jahnke and H. Jhoti,

Nat. Rev. Drug Discov., 2016, **15**, 605–619.

- 82 A. Schuffenhauer, S. Ruedisser, A. L. Marzinzik, W. Jahnke, M. Blommers, P. Selzer and E. Jacoby, *Curr. Top. Med. Chem.*, 2005, **5**, 751–762.
- 83 C. W. Murray and D. C. Rees, *Nat. Chem.*, 2009, **1**, 187–192.
- 84 A. L. Hopkins, C. R. Groom and A. Alex, *Drug Discov. Today*, 2004, **9**, 430–431.
- 85 A. L. Hopkins, G. M. Keserü, P. D. Leeson, D. C. Rees and C. H. Reynolds, *Nat. Rev. Drug Discov.*, 2014, **13**, 105–21.
- 86 K. Retra, H. Irth and J. E. Van Muijlwijk-Koezen, *Drug Discov. Today Technol.*, 2010, **7**, e181–e187.
- 87 E. H. Mashalidis, P. Śledź, S. Lang and C. Abell, *Nat. Protoc.*, 2013, **8**, 2309–2324.
- 88 C. A. Shepherd, A. L. Hopkins and I. Navratilova, *Prog. Biophys. Mol. Biol.*, 2014, **116**, 113–123.
- 89 J. Schoepfer, W. Jahnke, G. Berellini, S. Buonamici, S. Cotesta, S. W. Cowan-Jacob, S. Dodd, P. Drueckes, D. Fabbro, T. Gabriel, J.-M. Groell, R. M. Grotzfeld, A. Q. Hassan, Il Chrystè Le Henry, V. Iyer, D. Jones, F. Lombardo, A. Loo, P. W. Manley, X. Pellé, Pellé, G. Rummel, B. Salem, M. Warmuth, A. A. Wylie, T. Zoller, A. L. Marzinzik and P. Furet, *J. Med. Chem.*, 2018, **61**, 8120–8135.
- 90 M. Zender, F. Witzgall, A. Kiefer, B. Kirsch, C. K. Maurer, A. M. Kany, N. Xu, S. Schmelz, C. Börger, W. Blankenfeldt and M. Empting, *ChemMedChem*, 2020, **15**, 188–194.
- 91 A. J. Whitehouse, S. E. Thomas, K. P. Brown, A. Fanourakis, D. S. H. Chan, M. D. J. Libardo, V. Mendes, H. I. M. Boshoff, R. A. Floto, C. Abell, T. L. Blundell and A. G. Coyne, *J. Med. Chem.*, 2019, **62**, 7210–7232.
- 92 D. A. Carcache, A. Vulpetti, J. Kallen, H. Mattes, D. Orain, R. Stringer, E. Vangrevelinghe, R. M. Wolf, K. Kaupmann, J. Ottl, J. Dawson, N. G. Cooke, K. Hoegenauer, A. Billich, J. Wagner, C. Guntermann and S. Hintermann, *J. Med. Chem.*, 2018, **61**, 6724–6735.
- 93 U. Grädler, D. Schwarz, M. Blaesse, B. Leuthner, T. L. Johnson, F. Bernard, X. Jiang, A. Marx, M. Gilardone, H. Lemoine, D. Roche and C. Jorand-Lebrun, *Bioorganic Med. Chem. Lett.*, , DOI:10.1016/j.bmcl.2019.126717.
- 94 C. W. Murray, M. G. Carr, O. Callaghan, G. Chessari, M. Congreve, S. Cowan, J. E. Coyle, R. Downham, E. Figueroa, M. Frederickson, B. Graham, R. McMenemy, M. A. O'Brien, S. Patel, T. R. Phillips, G. Williams, A. J. Woodhead and A. J. A. Woolford, *J. Med. Chem.*, 2010, **53**, 5942–5955.
- 95 F. H. Schopf, M. M. Biebl and J. Buchner, *Nat. Rev. Mol. Cell Biol.*, 2017, **18**, 345–360.

- 96 U. S. F. and D. Administration and C. of D. E. and Research, .
- 97 M. Paul Gleeson, P. D. Leeson and H. van de Waterbeemd, *CHAPTER 1. Physicochemical Properties and Compound Quality*, 2015.
- 98 M. Dow, M. Fisher, T. James, F. Marchetti and A. Nelson, *Org. Biomol. Chem.*, 2012, **10**, 17–28.
- 99 Z. Deng, C. Du, X. Li, B. Hu, Z. Kuang, R. Wang, S. Feng, H. Zhang and D. Kong, *J. Chem. Inf. Model*, 2013, **53**, 2820–2828.
- 100 J. L. Reymond, *Acc. Chem. Res.*, 2015, **48**, 722–730.
- 101 A. M. Virshup, J. Contreras-García, P. Wipf, W. Yang and D. N. Beratan, *J. Am. Chem. Soc.*, 2013, **135**, 7296–7303.
- 102 P. G. Polishchuk, • T I Madzhidov and • A Varnek, , DOI:10.1007/s10822-013-9672-4.
- 103 D. R. Spring, *Org. Biomol. Chem.*, 2003, **1**, 3867–3870.
- 104 J. L. Reymond, *Acc. Chem. Res.*, 2015, **48**, 722–730.
- 105 A. H. Lipkus, Q. Yuan, K. a Lucas, S. a Funk, W. F. B. Iii, R. J. Schenck and A. J. Trippe, *J. Org. Chem.*, 2008, **5**, 4443–4451.
- 106 A. H. Lipkus, S. P. Watkins, K. Gengras, M. J. McBride and T. J. Wills, *J. Org. Chem.*, 2019, **84**, 13948–13956.
- 107 S. R. Langdon, N. Brown and J. Blagg, *J. Chem. Inf. Model.*, 2011, **51**, 2174–2185.
- 108 D. G. Brown and J. Boström, *J. Med. Chem.*, 2016, **59**, 4443–4458.
- 109 J. Boström, D. G. Brown, R. J. Young and G. M. Keserü, *Nat. Rev. Drug Discov.*, 2018, **17**, 709–727.
- 110 D. C. Blakemore, L. Castro, I. Churcher, D. C. Rees, A. W. Thomas, D. M. Wilson and A. Wood, *Nat. Chem.*, 2018, **10**, 383–394.
- 111 S. D. Roughley and A. M. Jordan, *J. Med. Chem.*, 2011, **54**, 3451.
- 112 W. P. Walters, J. Green, J. R. Weiss and M. A. Murcko, *J. Med. Chem.*, 2011, **54**, 6405–6416.
- 113 J. Boström, D. G. Brown, R. J. Young and G. M. Keserü, *Nat. Rev. Drug Discov.*, 2018, **17**, 709–727.
- 114 D. G. Brown and J. Boström, *J. Med. Chem.*, 2016, **59**, 4443–4458.
- 115 U. of L. Foley, Daniel Jason. PhD thesis, .
- 116 W. J. D. Galloway and D. Spring, *Nature*, 2011, 470, 43.
- 117 C. J. Gerry and S. L. Schreiber, *Curr. Opin. Chem. Biol.*, 2020, 56, 1–9.
- 118 T. E. Nielsen and S. L. Schreiber, *Angew. Chemie - Int. Ed.*, 2008, **47**, 48–56.
- 119 N. Kato, E. Comer, T. Sakata-Kato, A. Sharma, M. Sharma, M.

- Maetani, J. Bastien, N. M. Brancucci, J. A. Bittker, V. Corey, D. Clarke, E. R. Derbyshire, G. L. Dornan, S. Duffy, S. Eckley, M. A. Itoe, K. M. J. Koolen, T. A. Lewis, P. S. Lui, A. K. Lukens, E. Lund, S. March, E. Meibalan, B. C. Meier, J. A. McPhail, B. Mitasev, E. L. Moss, M. Sayes, Y. Van Gessel, M. J. Wawer, T. Yoshinaga, A. M. Zeeman, V. M. Avery, S. N. Bhatia, J. E. Burke, F. Catteruccia, J. C. Clardy, P. A. Clemons, K. J. Dechering, J. R. Duvall, M. A. Foley, F. Gusovsky, C. H. M. Kocken, M. Marti, M. L. Morningstar, B. Munoz, D. E. Neafsey, A. Sharma, E. A. Winzeler, D. F. Wirth, C. A. Scherer and S. L. Schreiber, *Nature*, 2016, **538**, 344–349.
- 120 A. W. Hung, A. Ramek, Y. Wang, T. Kaya, J. A. Wilson, P. A. Clemons and D. W. Young, *Proc. Natl. Acad. Sci.*, 2011, **108**, 6799–6804.
- 121 J. Zhang, M. Mulumba, H. Ong and W. D. Lubell, *Angew. Chemie Int. Ed.*, 2017, **56**, 6284–6288.
- 122 N. Mateu, S. L. Kidd, T. J. Osberger, H. L. Stewart, S. Bartlett, W. R. J. D. Galloway, A. J. P. North, H. F. Sore and D. R. Spring, *The Application of Diversity-oriented Synthesis in Chemical Biology*, .
- 123 O. C. CJ, H. S. Beckmann and D. R. Spring, *Chem Soc Rev*, 2012, **41**, 4444–4456.
- 124 M. D. Burke and S. L. Schreiber, *Angew. Chemie - Int. Ed.*, 2004, **43**, 46–58.
- 125 W. R. J. D. Galloway, A. Bender, M. Welch and D. R. Spring, *Chem. Commun.*, 2009, 2446–2462.
- 126 R. J. Spandl, A. Bender and D. R. Spring, *Org. Biomol. Chem.*, 2008, **6**, 1149–1158.
- 127 M. E. Fitzgerald, C. A. Mulrooney, J. R. Duvall, J. Wei, B. C. Suh, L. B. Akella, A. Vrcic and L. A. Marcaurelle, *ACS Comb. Sci.*, 2012, **14**, 89–96.
- 128 D. Brossard, P. Retailleau, V. Dumontet, P. Breton, S. Desrat and F. Roussi, *Org. Biomol. Chem.*, 2017, **15**, 5585–5592.
- 129 K. T. Mortensen, T. J. Osberger, T. A. King, H. F. Sore and D. R. Spring, , DOI:10.1021/acs.chemrev.9b00084.
- 130 H. Oguri and S. L. Schreiber, *Org. Lett.*, 2005, **7**, 47–50.
- 131 O. Kwon, S. B. Park and S. L. Schreiber, *J. Am. Chem. Soc.*, 2002, **124**, 13402–13404.
- 132 A. H. Bansode, P. Chimala and N. T. Patil, *ChemCatChem*, 2017, **9**, 30–40.
- 133 J. E. Ha, S. J. Yang and Y. D. Gong, *ACS Comb. Sci.*, 2018, **20**, 82–97.
- 134 N. Mateu, S. L. Kidd, L. Kalash, H. F. Sore, A. Madin, A. Bender and D. R. Spring, *Chem. - A Eur. J.*, 2018, **24**, 13681–13687.
- 135 D. Foley, R. Doveston, I. Churcher, A. Nelson and S. P. Marsden,

- Chem. Commun.*, 2015, **51**, 11174–11177.
- 136 J. Mayol-Llinàs, W. Farnaby and A. Nelson, *Chem. Commun.*, 2017, **53**, 12345–12348.
- 137 T. T. Wager, X. Hou, P. R. Verhoest and A. Villalobos, *ACS Chem. Neurosci.*, 2010, **1**, 435–449.
- 138 L. G. Baud, M. A. Manning, H. L. Arkless, T. C. Stephens and W. P. Unsworth, *Chem. - A Eur. J.*, 2017, **23**, 2225–2230.
- 139 A. K. Clarke and W. P. Unsworth, *Chem. Sci.*, 2020, **11**, 2876–2881.
- 140 C. Kitsiou, J. J. Hindes, P. I'Anson, P. Jackson, T. C. Wilson, E. K. Daly, H. R. Felstead, P. Hearnshaw and W. P. Unsworth, *Angew. Chemie - Int. Ed.*, 2015, **54**, 15794–15798.
- 141 I. Colomer, C. J. Empson, P. Craven, Z. Owen, R. G. Doveston, I. Churcher, S. P. Marsden and A. Nelson, *Chem. Commun.*, 2016, **52**, 7209–7212.
- 142 D. J. Foley, P. G. E. Craven, P. M. Collins, R. G. Doveston, A. Aimon, R. Talon, I. Churcher, F. von Delft, S. P. Marsden and A. Nelson, *Chem. - A Eur. J.*, 2017, **23**, 15227–15232.
- 143 S. Z. Tasker, A. E. Cowfer and P. J. Hergenrother, *Org. Lett.*, 2018, **20**, 5894–5898.
- 144 K. C. Morrison and P. J. Hergenrother, *Nat. Prod. Rep.*, 2014, **31**, 6–14.
- 145 M. Weber, K. Owens, A. Masarwa and R. Sarpong, *Org. Lett.*, 2015, **17**, 5432–5435.
- 146 M. J. Harner, B. A. Chauder, J. Phan and S. W. Fesik, *J. Med. Chem.*, 2014, **57**, 9687–9692.
- 147 W. Yang, J. Dong, J. Wang and X. Xu, *Org. Lett.*, 2017, **19**, 616–619.
- 148 R. Wang, X. Xie, H. Liu and Y. Zhou, *Catalysts*, 2019, **9**, 823.
- 149 Z. Shi, C. Grohmann and F. Glorius, *Angew. Chemie - Int. Ed.*, 2013, **52**, 5393–5397.
- 150 S. Cui, Y. Zhang, D. Wang and Q. Wu, *Chem. Sci.*, 2013, **4**, 3912–3916.
- 151 N. J. Webb, Leeds, 2014.
- 152 Y. Tamura, T. Yakura, J. Haruta and Y. Kita, *J. Org. Chem.*, 1987, **52**, 3927–3930.
- 153 N. Guimond, S. I. Gorelsky and K. Fagnou, *J. Am. Chem. Soc.*, 2011, **133**, 6449–6457.
- 154 C. He, J. Hu, Y. Wu and H. Ding, *J. Am. Chem. Soc.*, 2017, **139**, 6098–6101.
- 155 K. C. Nicolaou, Q. Y. Toh and D. Y. K. Chen, *J. Am. Chem. Soc.*, 2008, **130**, 11292–11293.

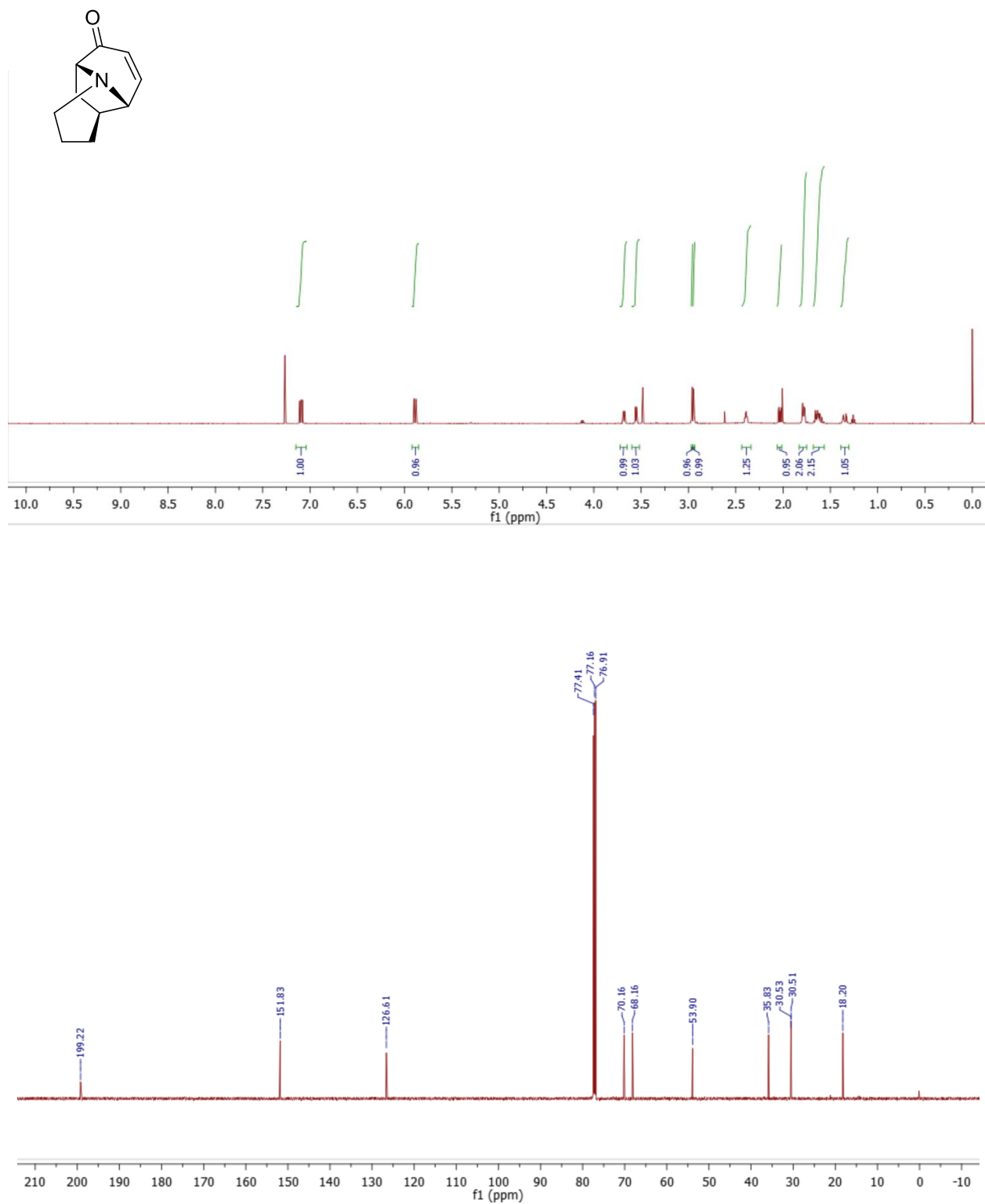
- 156 T. Javorskis and E. Orentas, *J. Org. Chem.*, 2017, **82**, 13423–13439.
- 157 M. Ishizaki, M. Yamada, S. I. Watanabe, O. Hoshino, K. Nishitani, M. Hayashida, A. Tanaka and H. Hara, *Tetrahedron*, 2004, **60**, 7973–7981.
- 158 Y. Fujise, T. Shiokawa, Y. Mazaki, Y. Fukazawa, M. Fujii and S. Ito, *Tetrahedron Lett.*, 1982, **23**, 1601–1604.
- 159 J. H. Rigby and S. V. Cuisiat, *J. Org. Chem.*, 1993, **58**, 6286–6291.
- 160 H. Liu, Y. Wu, Y. Zhao, Z. Li, L. Zhang, W. Yang, H. Jiang, C. Jing, H. Yu, B. Wang, Y. Xiao and H. Guo, *J. Am. Chem. Soc.*, 2014, **136**, 2625–2629.
- 161 S. Zheng and X. Lu, *Org. Lett.*, 2008, **10**, 4481–4484.
- 162 J. H. Rigby, in *Organic Reactions*, John Wiley & Sons, Inc., Hoboken, NJ, USA, 1996, pp. 331–425.
- 163 J. H. Rigby and S. V Cuisiat, *J. Org. Chem.*, 1993, **58**, 6286–6291.
- 164 I. Fleming, *Molecular orbitals and Organic Chemical Reactions*, John Wiley & Sons, Ltd, Refernece., 2010.
- 165 Z. Wang, in *Comprehensive Organic Name Reactions and Reagents*, John Wiley & Sons, Inc., Hoboken, NJ, USA, 2010.
- 166 H. C. Brown, S. Krishnamurthy and N. M. Yoon, *J. Org. Chem.*, 1976, **41**, 1778–1791.
- 167 K. E. O. Ylijoki and J. M. Stryker, *Chem. Rev.*, 2013, **113**, 2244–66.
- 168 M. A. Battiste, P. M. Pelphrey and D. L. Wright, *Chem. - A Eur. J.*, 2006, **12**, 3438–3447.
- 169 S. M. Bromidge, D. A. Archer and P. G. Sammes, *J. Chem. Soc. Perkin Trans. 1*, 1990, 353–359.
- 170 L. P. Bejcek and R. P. Murelli, *Tetrahedron*, 2018, **74**, 2501–2521.
- 171 R. H. Kaufman, C. M. Law, J. A. Simanis, E. L. Woodall, C. R. Zwick, H. B. Wedler, P. Wendelboe, C. G. Hamaker, J. R. Goodell, D. J. Tantillo and T. A. Mitchell, *J. Org. Chem.*, 2018, **83**, 31.
- 172 P. Tian, H. Q. Dong and G. Q. Lin, *ACS Catal.*, 2012, **2**, 95–119.
- 173 R. Itooka, Y. Iguchi and N. Miyaura, *J. Org. Chem.*, 2003, **68**, 6000–6004.
- 174 F. Albrecht, O. Sowada, M. Fistikci and M. M. K. Boysen, *Org. Lett.*, 2014, **16**, 5212–5215.
- 175 R. A. Lowe, D. Taylor, K. Chibale, A. Nelson and S. P. Marsden, *Bioorganic Med. Chem.*, 2020, **28**, 115442.
- 176 F. Le Boucher D'Herouville, A. Millet, M. Scalone and V. Michelet, *J. Org. Chem.*, 2011, **76**, 6925–6930.
- 177 T. Konno, T. Tanaka, T. Miyabe, A. Morigaki and T. Ishihara, *Tetrahedron Lett.*, 2008, **49**, 2106–2110.

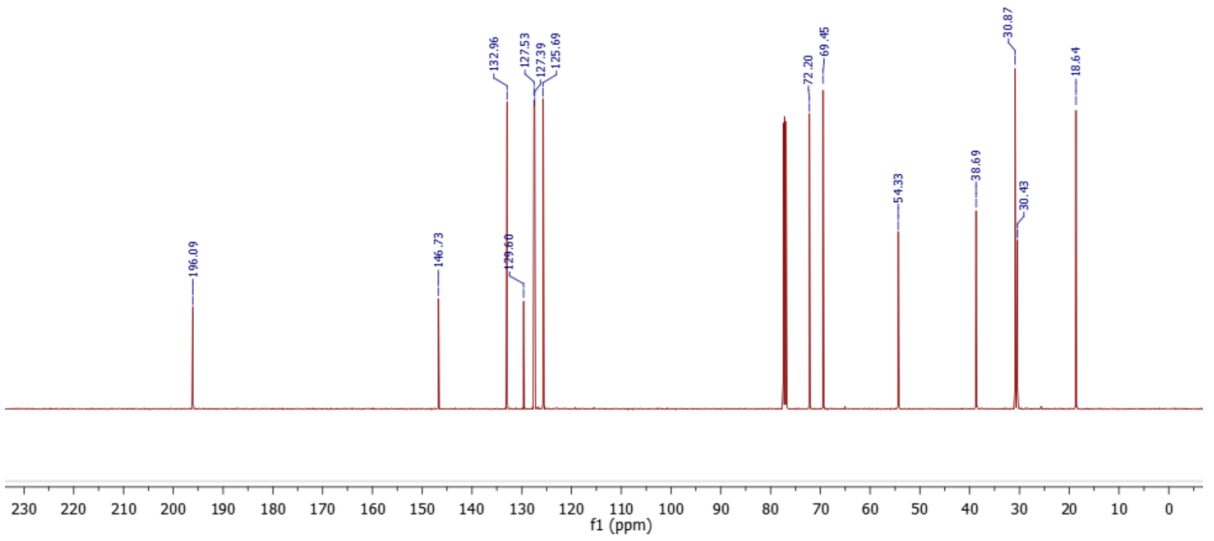
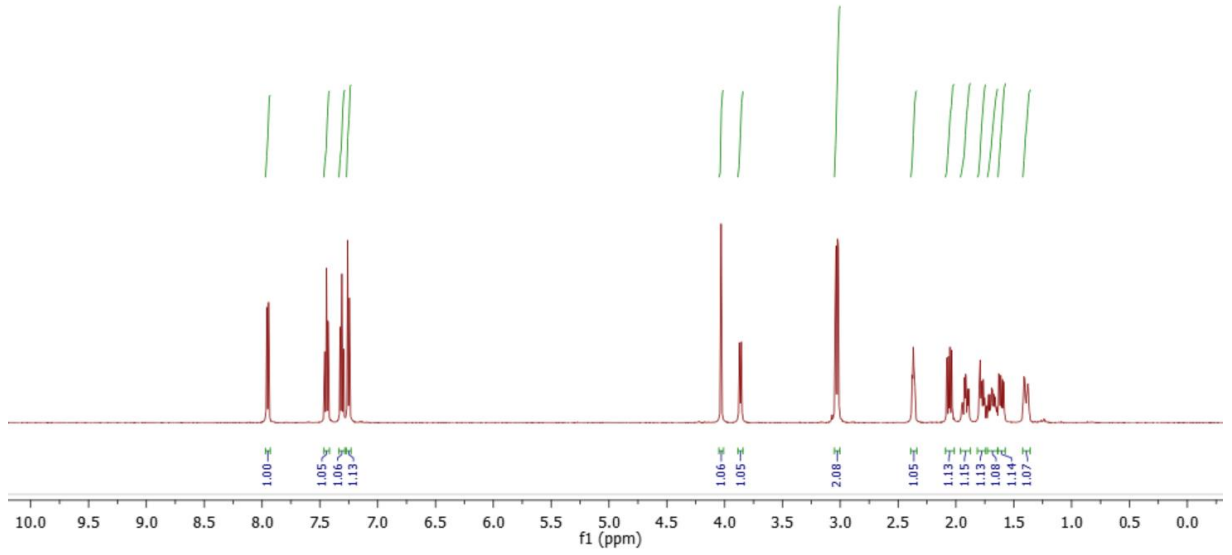
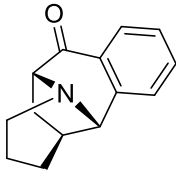
- 178 G. Kumaraswamy, G. Ramakrishna, P. Naresh, B. Jagadeesh and B. Sridhar, *J. Org. Chem.*, 2009, **74**, 8468–8471.
- 179 Y. Miura, N. Hayashi, S. Yokoshima and T. Fukuyama, *J. Am. Chem. Soc.*, 2012, **134**, 11995–11997.
- 180 C. Navarro, A. Moreno and A. G. Csáký, *J. Org. Chem.*, 2009, **74**, 466–469.
- 181 M. Jean, B. Casanova, S. Gnoatto and P. Van De Weghe, *Org. Biomol. Chem.*, 2015, **13**, 9168–9175.
- 182 F. Albrecht, O. Sowada, M. Fistikci and M. M. K. Boysen, *Org. Lett.*, 2014, **16**, 5212–5215.
- 183 T. Hayashi, *Synlett*, 2001, 879–887.
- 184 E. Vitaku, D. T. Smith and J. T. Njardarson, *J. Med. Chem.*, 2014, **57**, 10257–10274.
- 185 J. Li, Y. Ye and Y. Zhang, *Org. Chem. Front.*, 2018, **5**, 864–892.
- 186 G. Pandey, P. Banerjee and S. R. Gadre, *Chem. Rev.*, 2006, **106**, 4484–4517.
- 187 M. Grafton, A. C. Mansfield and M. J. Fray, *Tetrahedron Lett.*, 2010, **51**, 1026–1029.
- 188 A. G. H. Wee, *J. Chem. Soc. Perkin Trans. 1*, 1989, 1363–1364.
- 189 K. Miyajima, *Chem. Pharm. Bull.*, 1991, **39**, 3175–3179.
- 190 J. T. Gupton, in *Heterocyclic Antitumor Antibiotics*, Springer Berlin Heidelberg, Berlin, Heidelberg, 2nd edn., 2006, vol. 2, pp. 53–92.
- 191 V. Bhardwaj, D. Gumber, V. Abbot, S. Dhiman and P. Sharma, *RSC Adv.*, 2015, **5**, 15233–15266.
- 192 A. M. van Leusen, H. Siderius, B. E. Hoogenboom and D. van Leusen, *Tetrahedron Lett.*, 1972, **13**, 5337–5340.
- 193 Y. Hamada, in *Pyridine*, ed. P. P. Pandey, InTech, 2018.
- 194 E. Vessally, A. Hosseinian, L. Edjlali, A. Bekhradnia and M. D. Esrafil, *RSC Adv.*, 2016, **6**, 71662–71675.
- 195 G. Abbiati, A. Arcadi, G. Bianchi, S. Di Giuseppe, F. Marinelli and E. Rossi, *J. Org. Chem.*, 2003, **68**, 6959–6966.
- 196 T. James, I. Simpson, J. A. Grant, V. Sridharan and A. Nelson, *Org. Lett.*, 2013, **15**, 6094–6097.
- 197 H. Fujiwara, T. Kurogi, S. Okaya, K. Okano and H. Tokuyama, *Angew. Chemie - Int. Ed.*, 2012, **51**, 13062–13065.
- 198 J. Clayden, K. Tchabanenko, S. A. Yasin and M. D. Turnbull, *Synlett*, 2001, **2**, 302–304.
- 199 C. J. Young, H. Y. Cheol, E. Tuross, S. Y. Kyung and W. J. Kyung, *J. Org. Chem.*, 2007, **72**, 10114–10122.
- 200 J. Moursounidis and D. Wege, *Aust. J. Chem.*, 1983, **36**, 2473–2482.

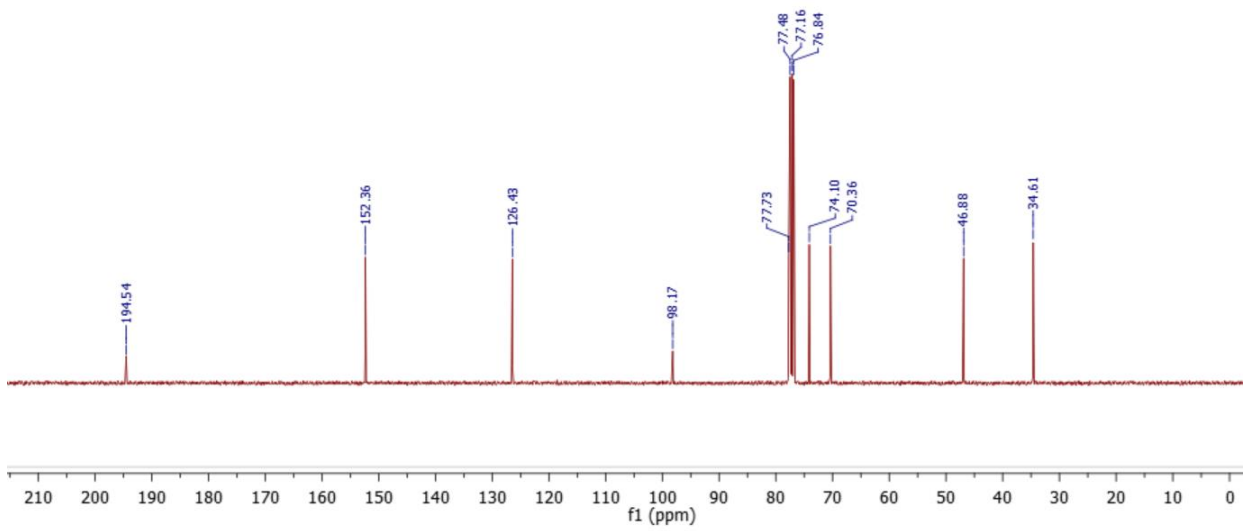
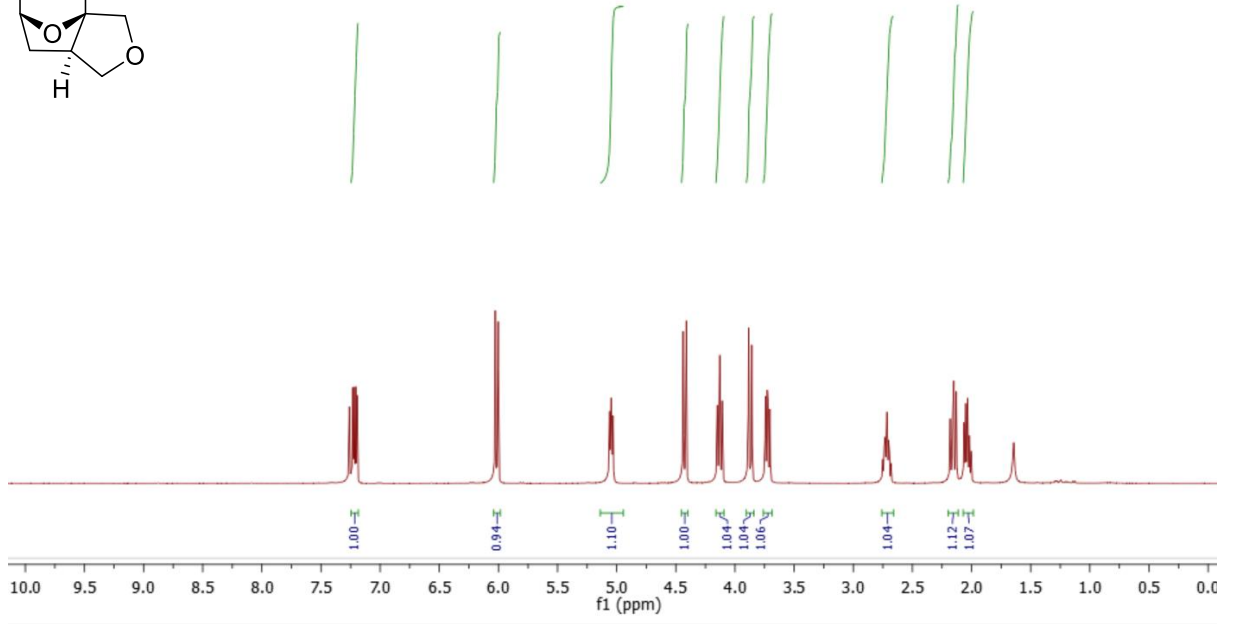
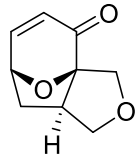
- 201 A. S. Goldman, *Nature*, 2010, **463**, 435–436.
- 202 S. Rice, D. J. Cox, S. P. Marsden and A. Nelson, *Tetrahedron*, 2019, **75**, 130513.
- 203 A. Vijay Kumar, V. Prakash Reddy, R. Sridhar, B. Srinivas and K. Rama Rao, *Synlett*, 2009, 0739–0742.
- 204 A. Foley, Daniel. J. Craven, Phillip. G. E. Collins, Patrick. M. Doveston, Richard. G. Aimon, Anthony. Talon, Romain. Churcher, Ian. von Delft, Frank. Marsden, Stephen. P. Nelson, *Unified synthesis and Demonstration of the Biological Relevance of Natural Product Paralogues*, 2017.
- 205 Y. Li, F. Jia and Z. Li, *Chem. - A Eur. J.*, 2013, **19**, 82–86.
- 206 R. A. Olofson, R. C. Schnur, L. Bunes and J. P. Pepe, *Tetrahedron Lett.*, 1977, **18**, 1567–1570.
- 207 A. Aimon, G. Karageorgis, J. Masters, M. Dow, P. G. E. Craven, M. Ohsten, A. Willaume, R. Morgentin, N. Ruiz-Llamas, H. Lemoine, T. Kalliokoski, A. J. Eatherton, D. J. Foley, S. P. Marsden and A. Nelson, *Org. Biomol. Chem.*, 2018, **16**, 3160–3167.
- 208 G. Stork and M. Kahn, *J. Am. Chem. Soc.*, 1985, **107**, 500–501.
- 209 S. Bracegirdle and E. A. Anderson, *Chem. Soc. Rev.*, 2010, 39, 4114–4129.
- 210 G. Stork, T. Y. Chan and G. A. Breault, *J. Am. Chem. Soc.*, 1992, **114**, 7578–7579.
- 211 I. Colomer, C. J. Empson, P. Craven, Z. Owen, R. G. Doveston, I. Churcher, S. P. Marsden and A. Nelson, *Chem. Commun.*, 2016, **52**, 7209–7212.
- 212 G. W. Bemis and M. A. Murcko, *J. Med. Chem.*, 1996, **39**, 2887–2893.
- 213 A. Schuffenhauer, P. Ertl, S. Roggo, S. Wetzel, M. A. Koch and H. Waldmann, *J. Chem. Inf. Model.*, 2007, **47**, 47–58.
- 214 F. W. Goldberg, J. G. Kettle, T. Kogej, M. W. D. Perry and N. P. Tomkinson, *Drug Discov. Today*, 2015, **20**, 11–17.
- 215 B. C. Doak, B. Over, F. Giordanetto and J. Kihlberg, *Chem. Biol.*, 2014, **21**, 1115–1142.
- 216 A. Gautier and M. J. Hinner, *Methods Mol Biol.*, 2015, **1266**, 29–53.
- 217 P. Matsson and J. Kihlberg, *J. Med. Chem.*, 2017, **60**, 1662–1664.
- 218 Sukanta Bhattacharyya, *Tetrahedron Lett.*, 1994, **35**, 2401–2404.
- 219 S. Bhattacharyya, *J. Org. Chem.*, 1995, 60, 4928–4929.
- 220 H. X. Ngo and S. Garneau-Tsodikova, *Medchemcomm*, 2018, **9**, 757–758.
- 221 M. J. Wawer, K. Li, S. M. Gustafsdottir, V. Ljosa, N. E. Bodycombe, M. A. Marton, K. L. Sokolnicki, M.-A. Bray, M. M. Kemp, E. Winchester, B. Taylor, G. B. Grant, S.-Y. Hon, J. R. Duvall, J. A. Wilson, J. A. Bittker,

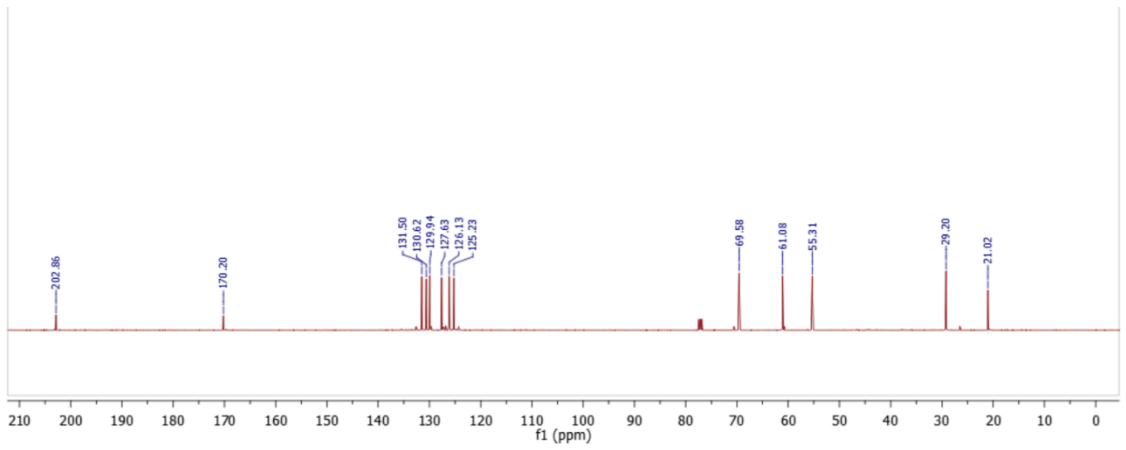
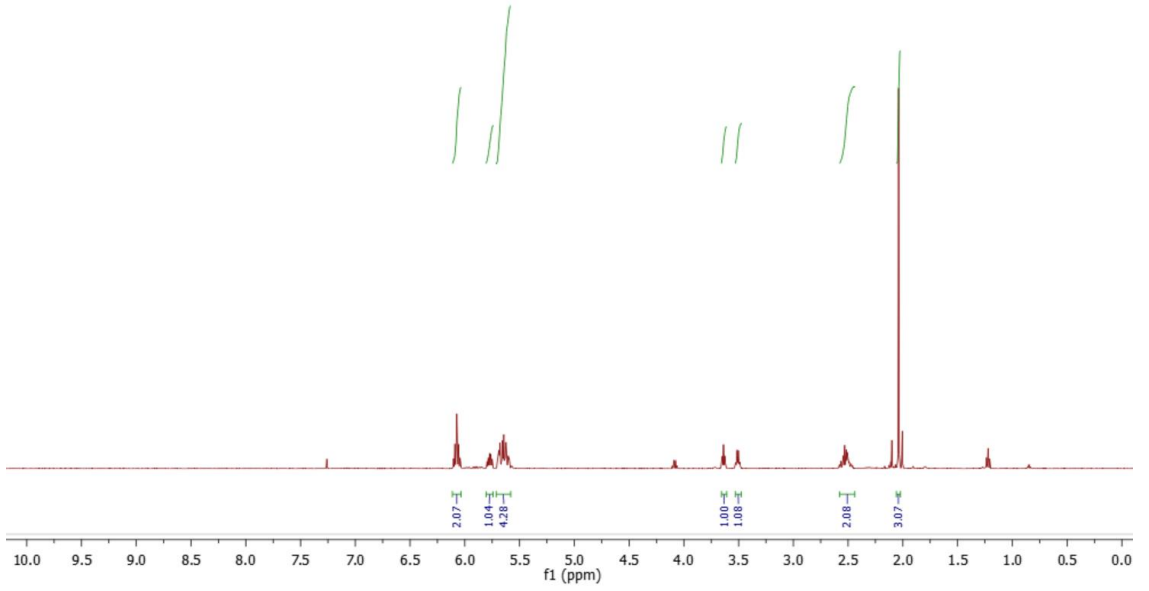
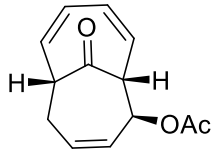
- V. Dančák, R. Narayan, A. Subramanian, W. Winckler, T. R. Golub, A. E. Carpenter, A. F. Shamji, S. L. Schreiber and P. A. Clemons, , DOI:10.1073/pnas.1410933111.
- 222 B. M. Ibbeson, L. Laraia, E. Alza, C. J. O' Connor, Y. S. Tan, H. M. L. Davies, G. McKenzie, A. R. Venkitaraman and D. R. Spring, *Nat. Commun.*, 2014, **5**, 3155–3163.
- 223 I. Pavlinov, E. M. Gerlach and L. N. Aldrich, *Org. Biomol. Chem.*, 2019, **17**, 1608–1623.
- 224 E. M. Gerlach, M. A. Korkmaz, I. Pavlinov, Q. Gao and L. N. Aldrich, *ACS Chem. Biol.*, 2019, **14**, 1536–1545.
- 225 S. S. H. H. C. T. D. B. B. C. H. Mark-Anthony Bray¹ and S. M. G. C. C. G. & A. E. C. Maria Kost-Alimova³, *Nat. Protoc.*, 2016, **11**, 1757–1774.
- 226 L. Laraia, L. Robke and H. Waldmann, *CHEMPR*, 2018, **4**, 705–730.
- 227 N. Aulner, A. Danckaert, J. Ihm, D. Shum and S. L. Shorte, *Trends Parasitol.*, 2019, **35**, 559–570.
- 228 B. Melillo, J. Zoller, B. K. Hua, O. Verho, J. C. Borghs, S. D. Nelson, M. Maetani, M. J. Wawer, P. A. Clemons and S. L. Schreiber, *J. Am. Chem. Soc.*, 2018, **140**, 11784–11790.
- 229 J. S. Byck and C. R. Dawson, *JACS*, 1966, **32**, 1084–1088.
- 230 H. Cheng, L. Xu, D. L. Chen, Q. H. Chen and F. P. Wang, *Tetrahedron*, 2012, **68**, 1171–1176.
- 231 P. G. Sammes and R. A. Watt, *J. Chem. Soc. Chem. Commun.*, 1976, 367–368.
- 232 D. Farquhar, A. Cherif, E. Bakina and J. Arly Nelson, *J. Med. Chem.*, 1998, **41**, 965–972.
- 233 F. Reise, J. E. Warias, K. Chatterjee, N. R. Krekiahn, O. Magnussen, B. M. Murphy and T. K. Lindhorst, *Chem. - A Eur. J.*, 2018, **24**, 17497–17505.
- 234 2010.
- 235 J. Stavenuiter, M. Hamzink, R. van der Hulst, G. Zomer, G. Westra and E. Kriek, *Heterocycles*, 1987, **26**, 2711–2716.
- 236 W. X. Huang, B. Wu, X. Gao, M. W. Chen, B. Wang and Y. G. Zhou, *Org. Lett.*, 2015, **17**, 1640–1643.
- 237 M. Barbazanges, M. Augé, J. Moussa, H. Amouri, C. Aubert, C. Desmarests, L. Fensterbank, V. Gandon, M. Malacria and C. Ollivier, *Chem. - A Eur. J.*, 2011, **17**, 13789–13794.

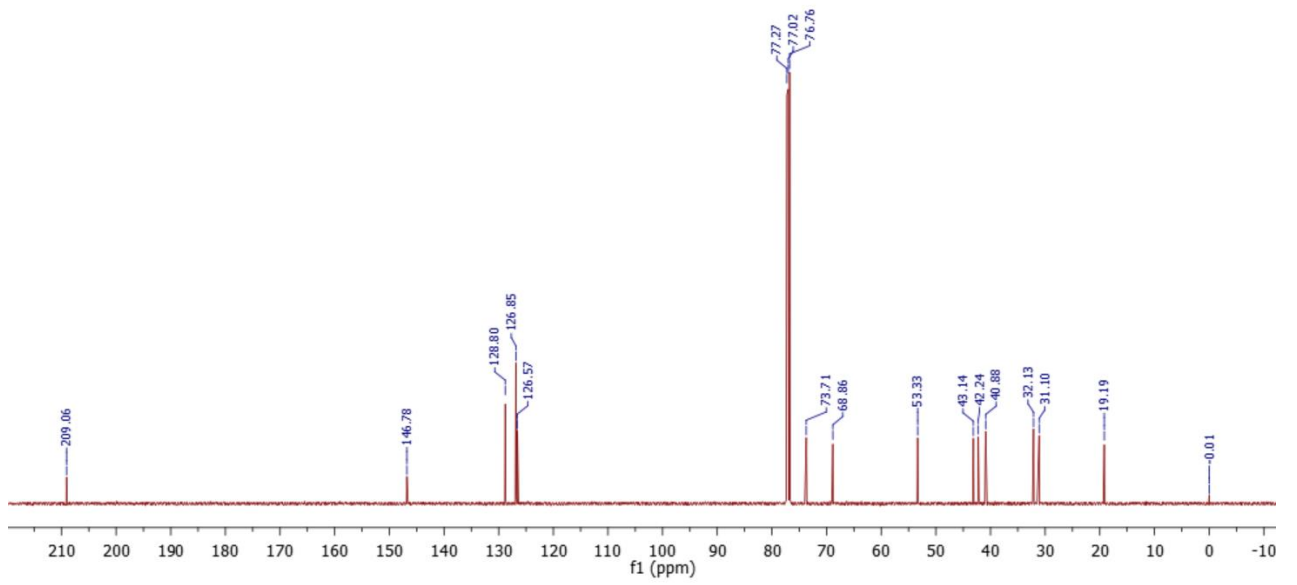
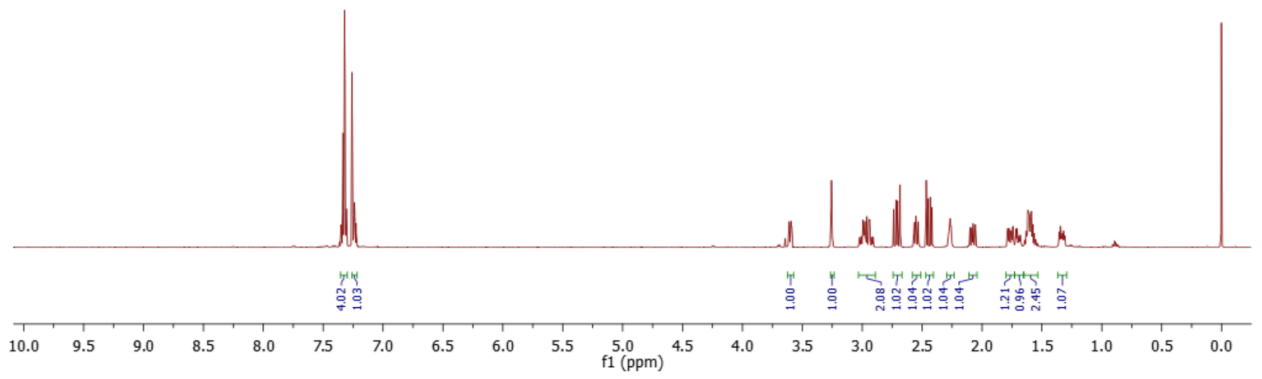
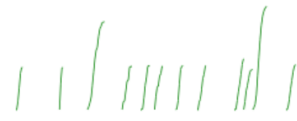
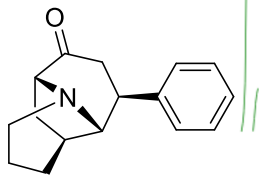
Appendix A: NMR data for complex intermediates and scaffolds included in the final library.

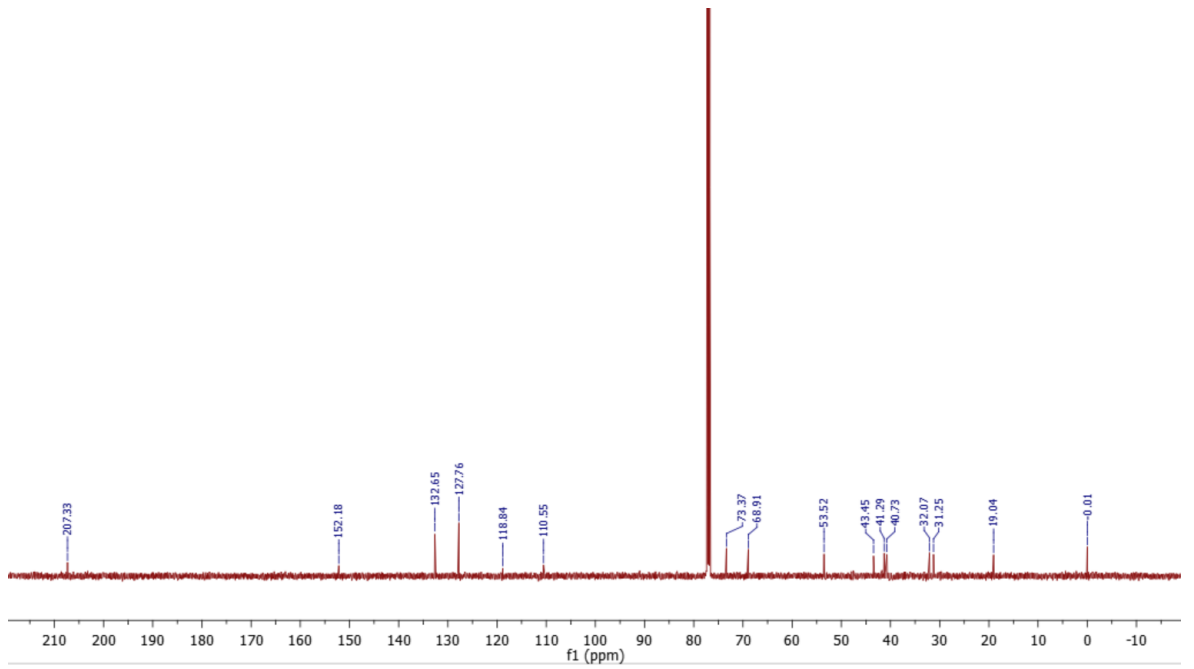
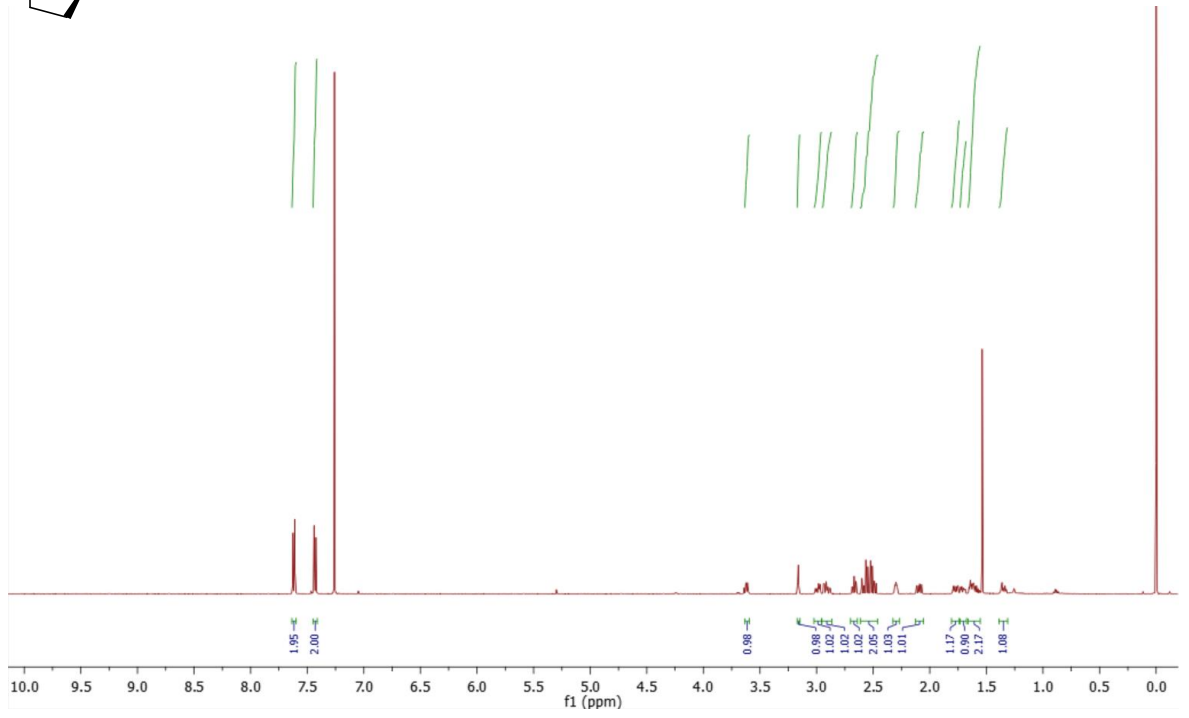
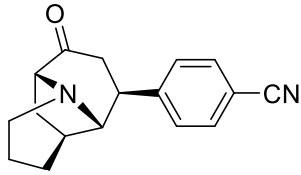


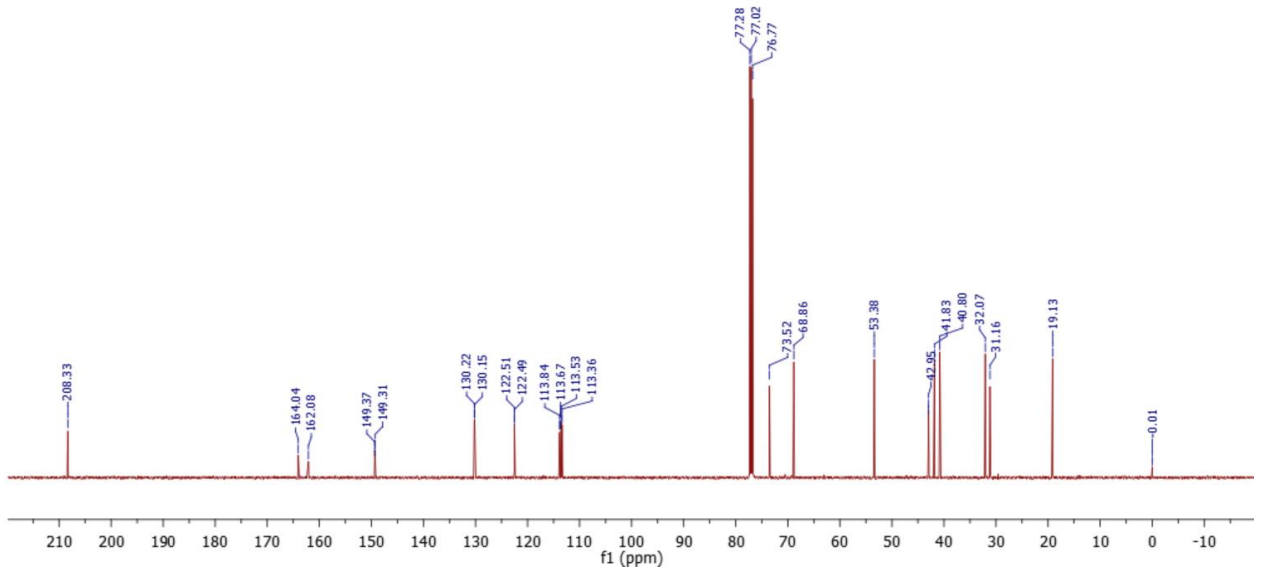
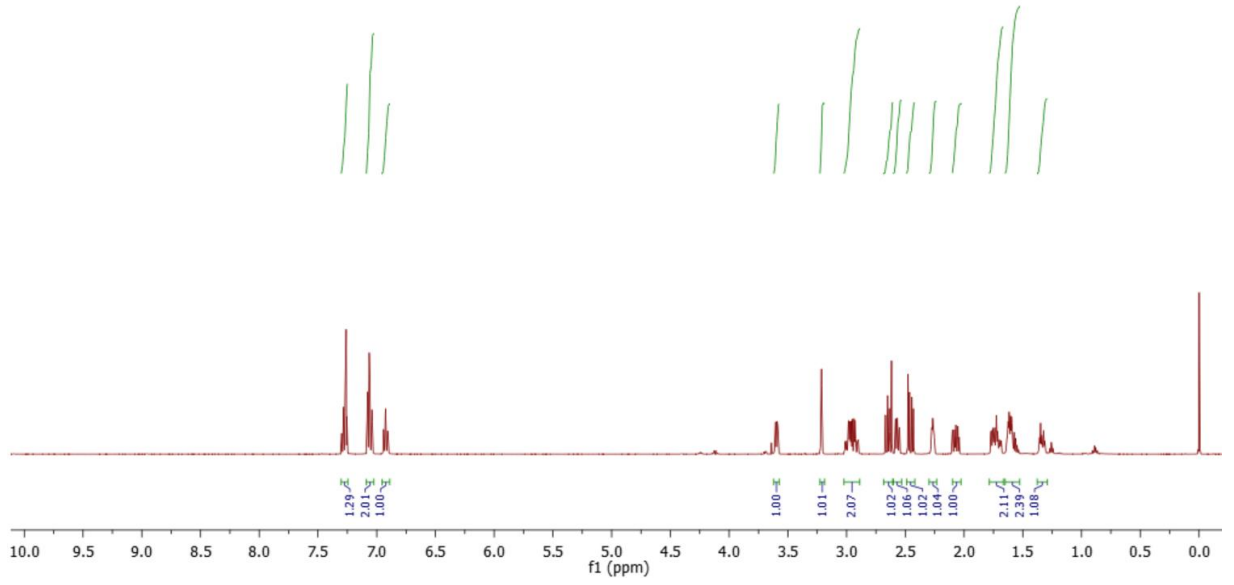
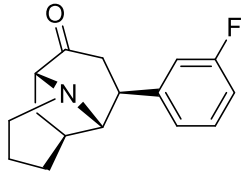


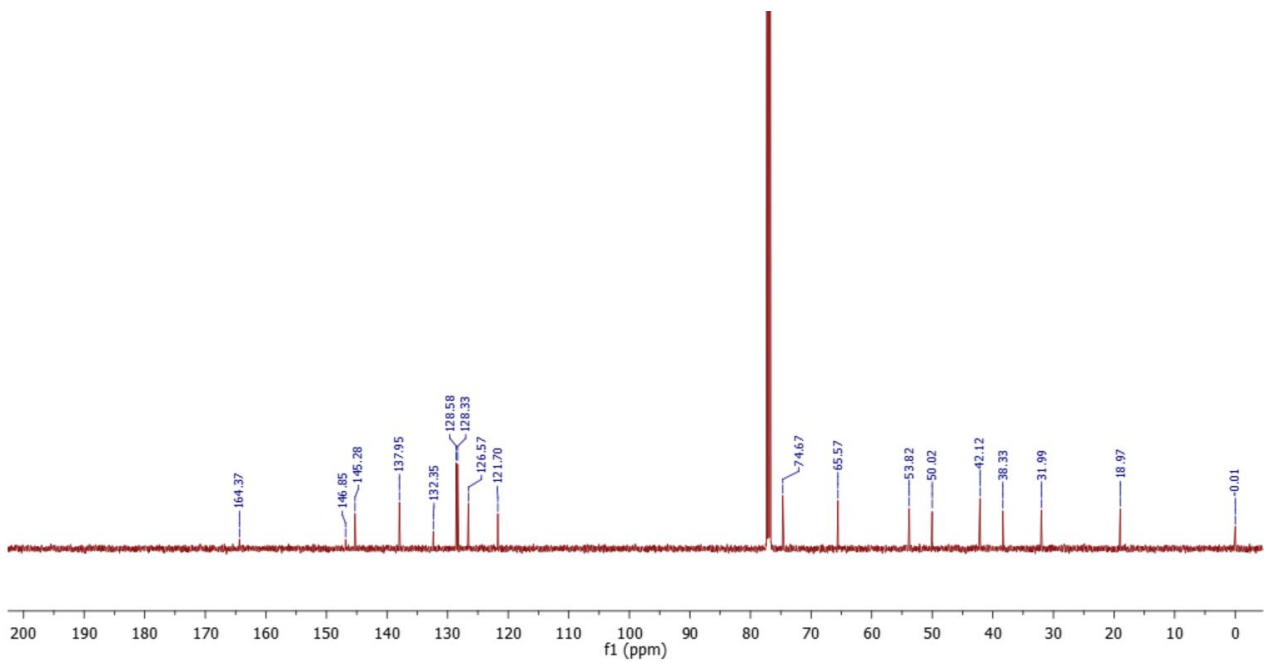
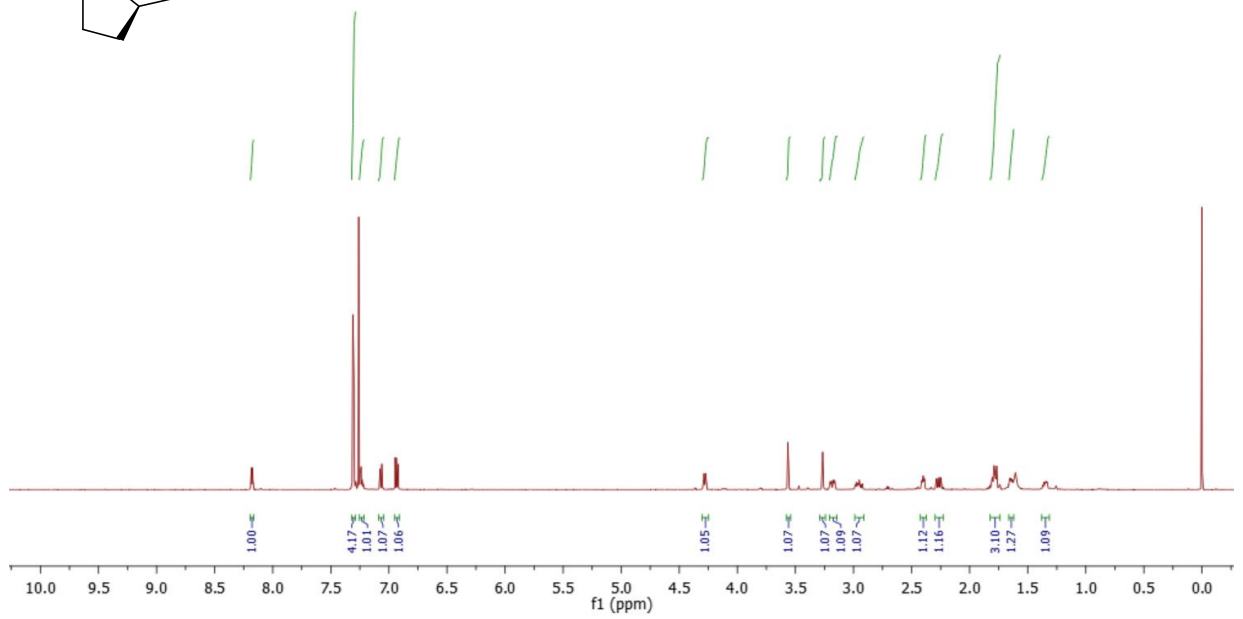
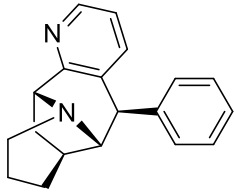


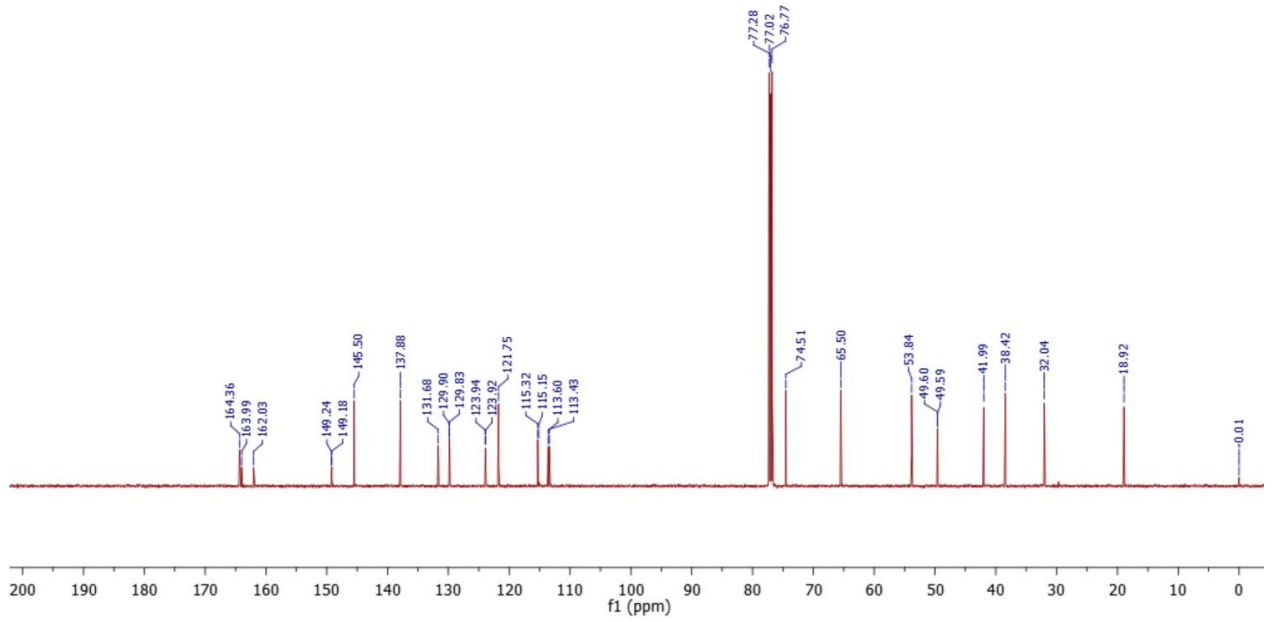
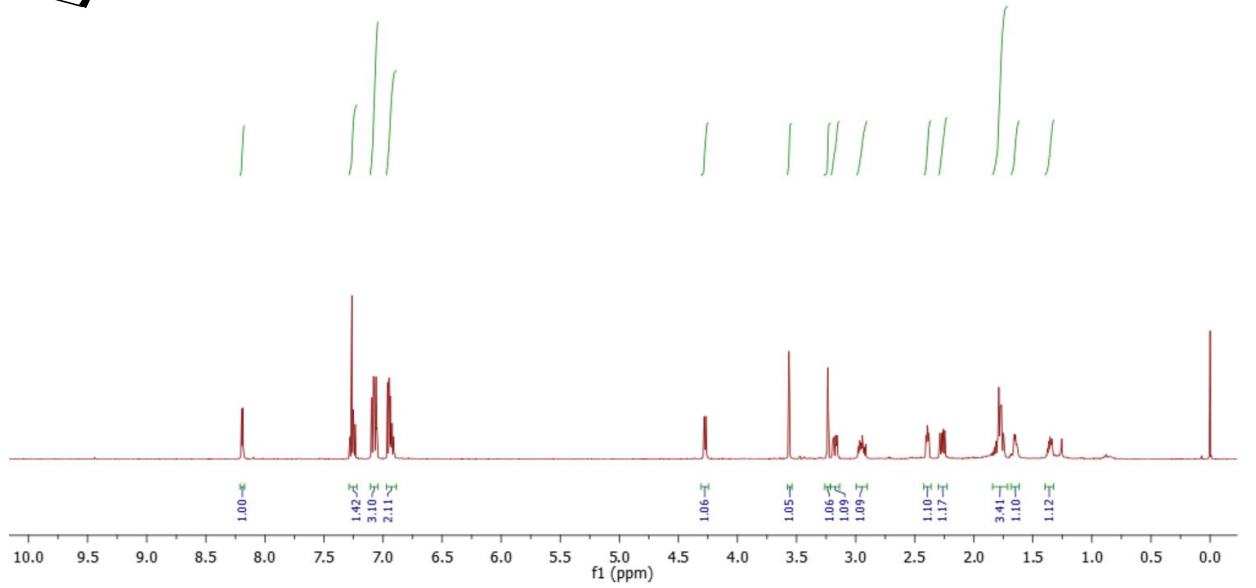
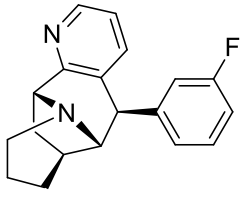


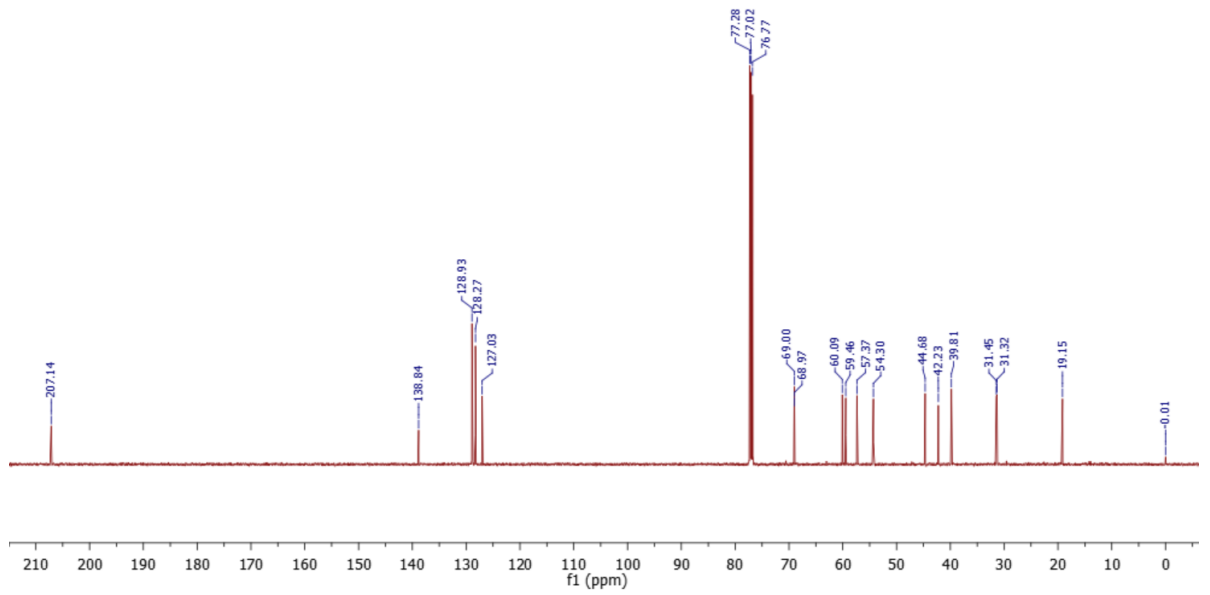
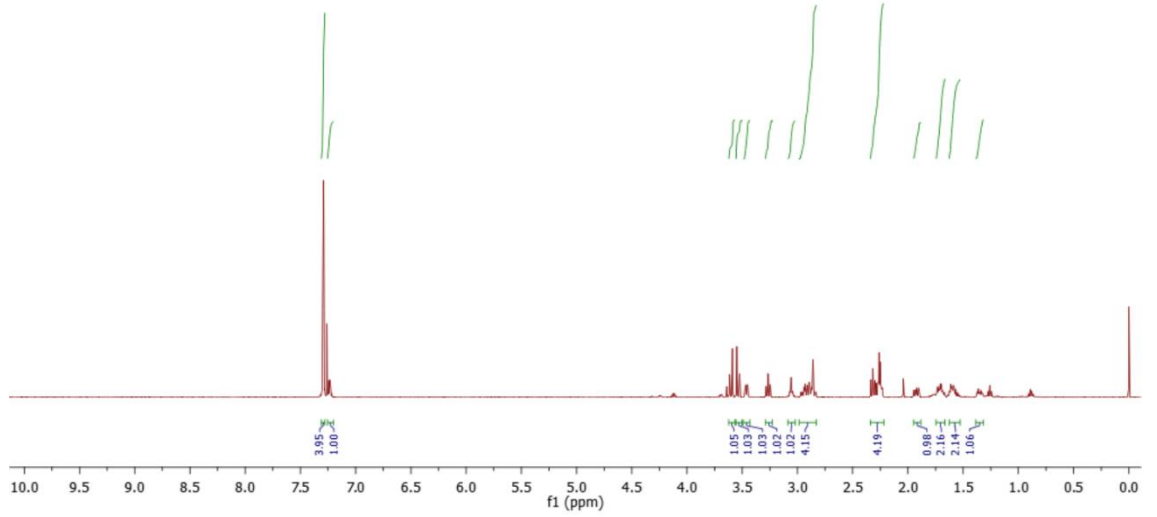
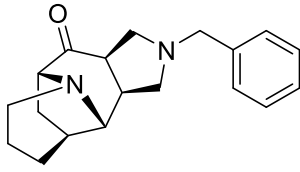


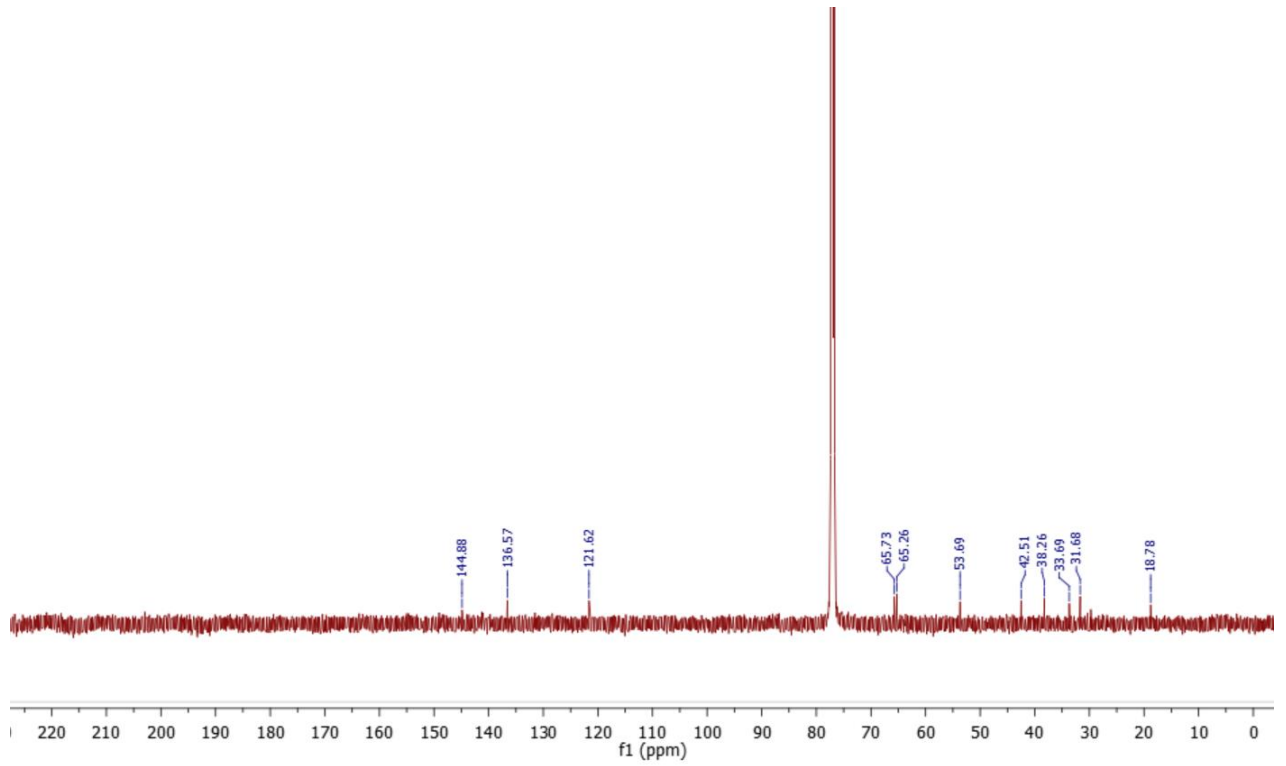
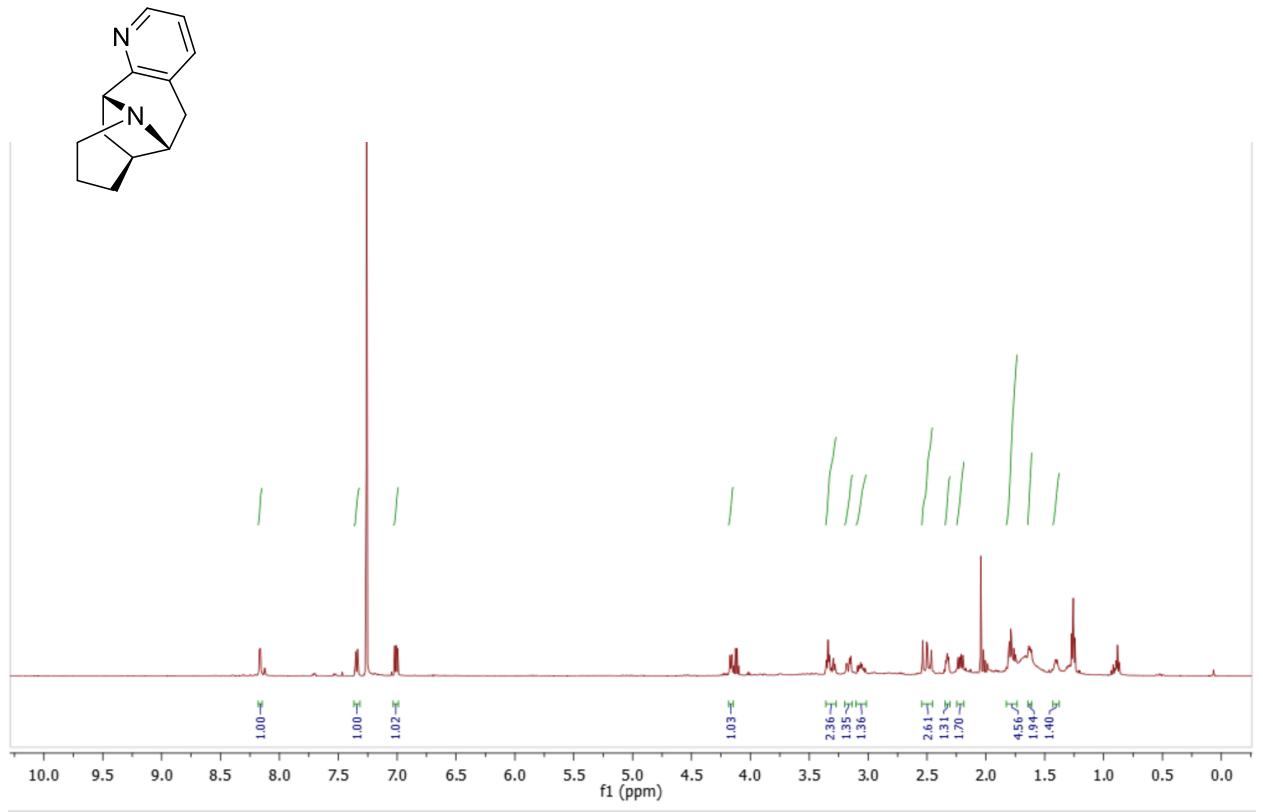


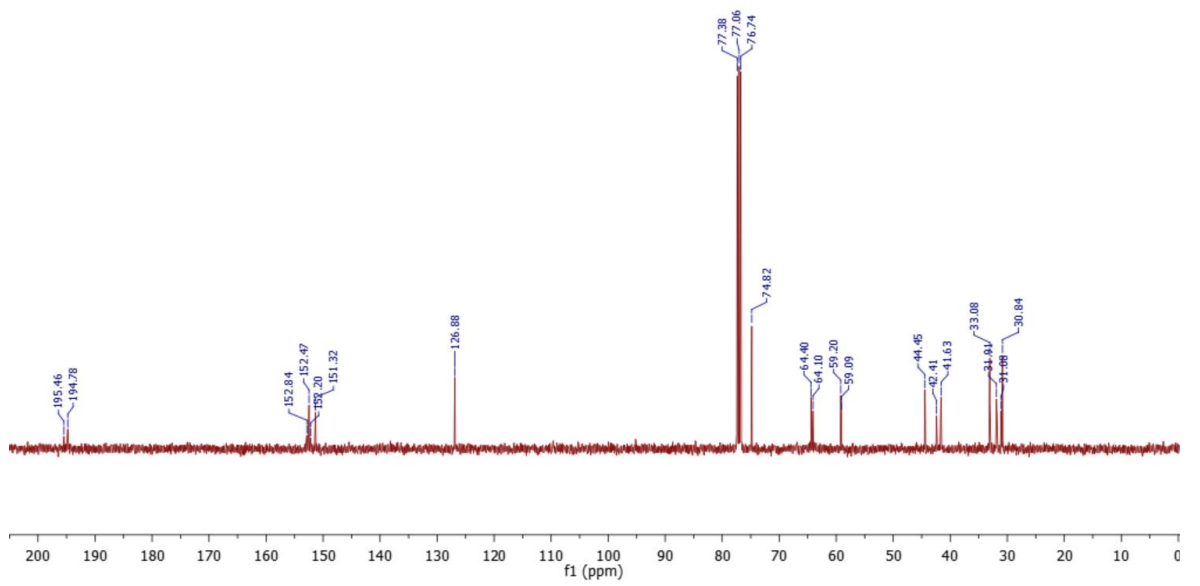
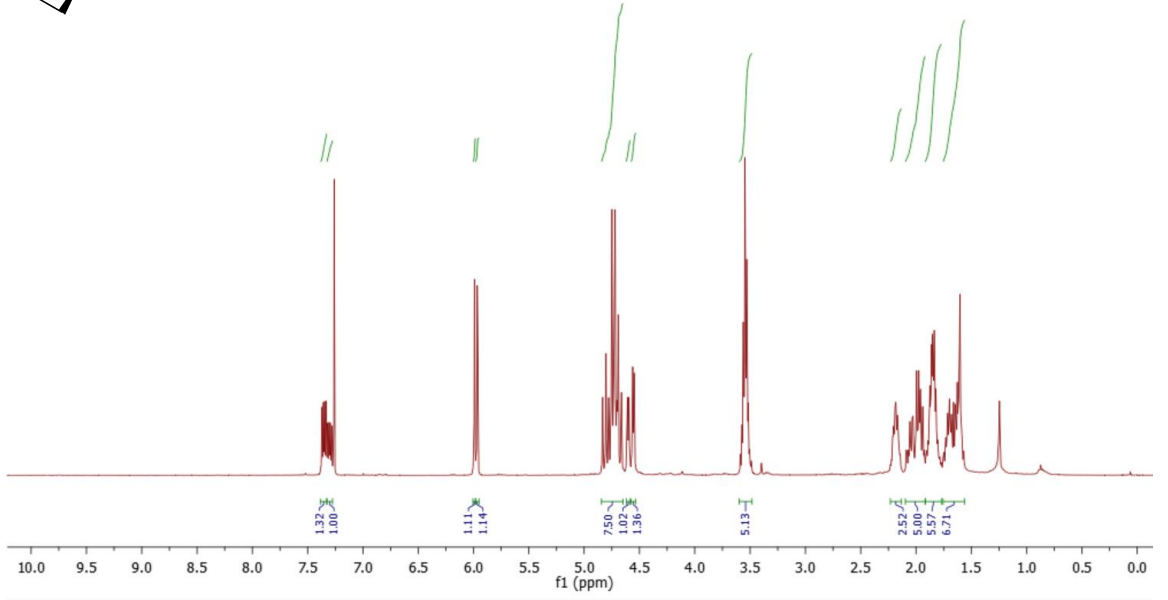
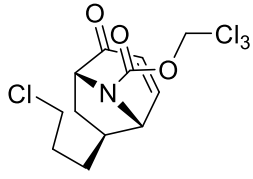


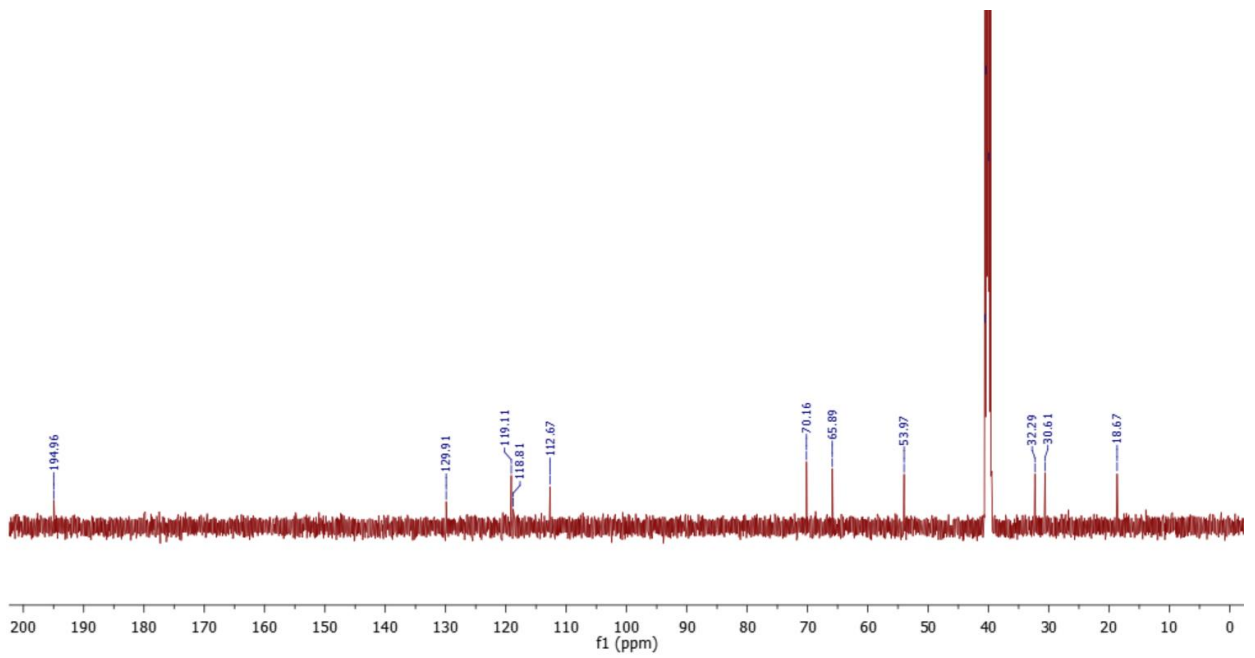
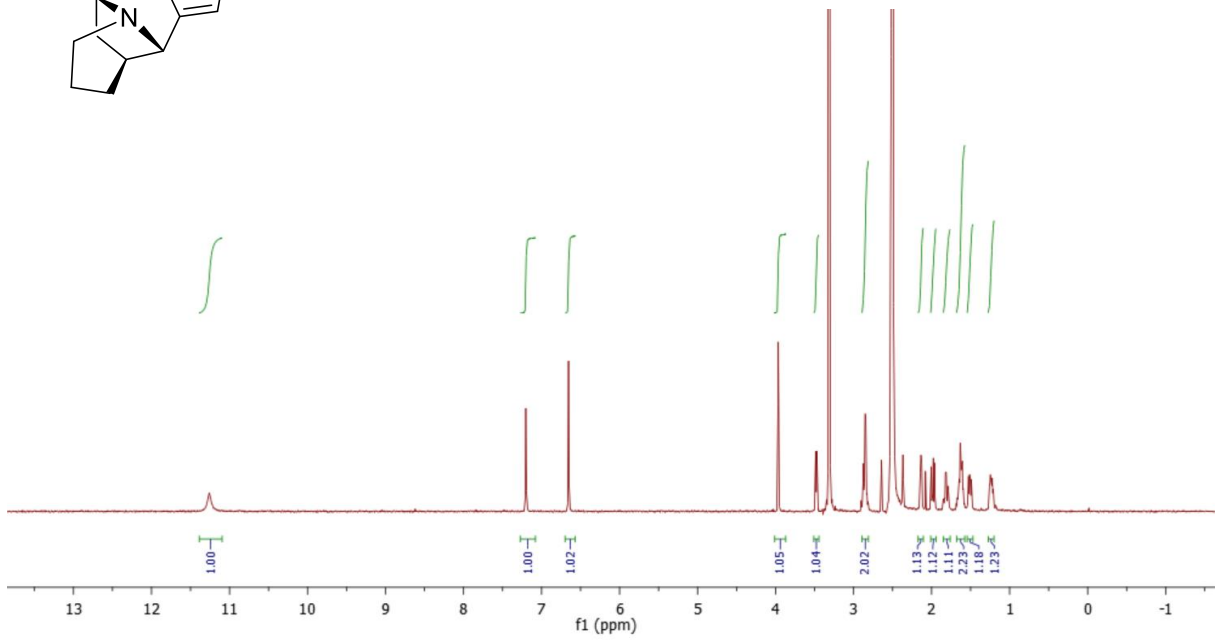
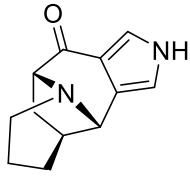


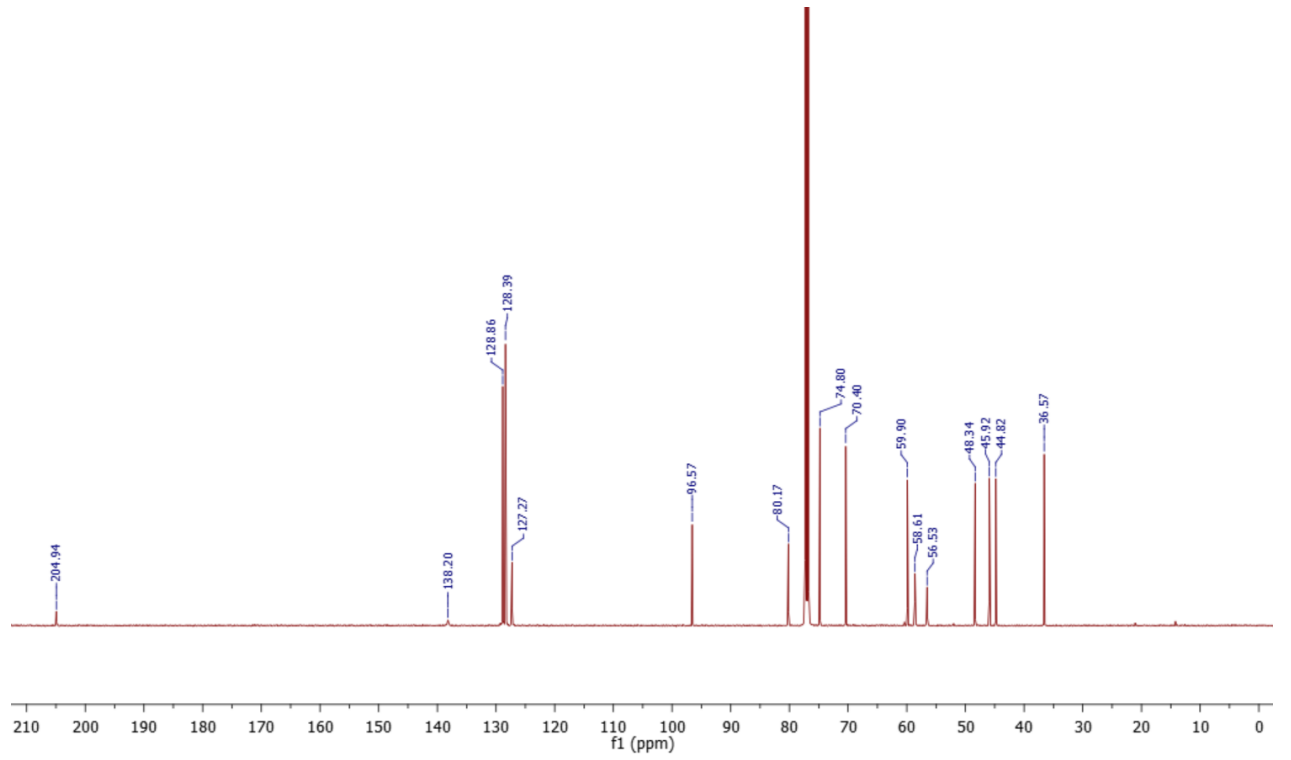
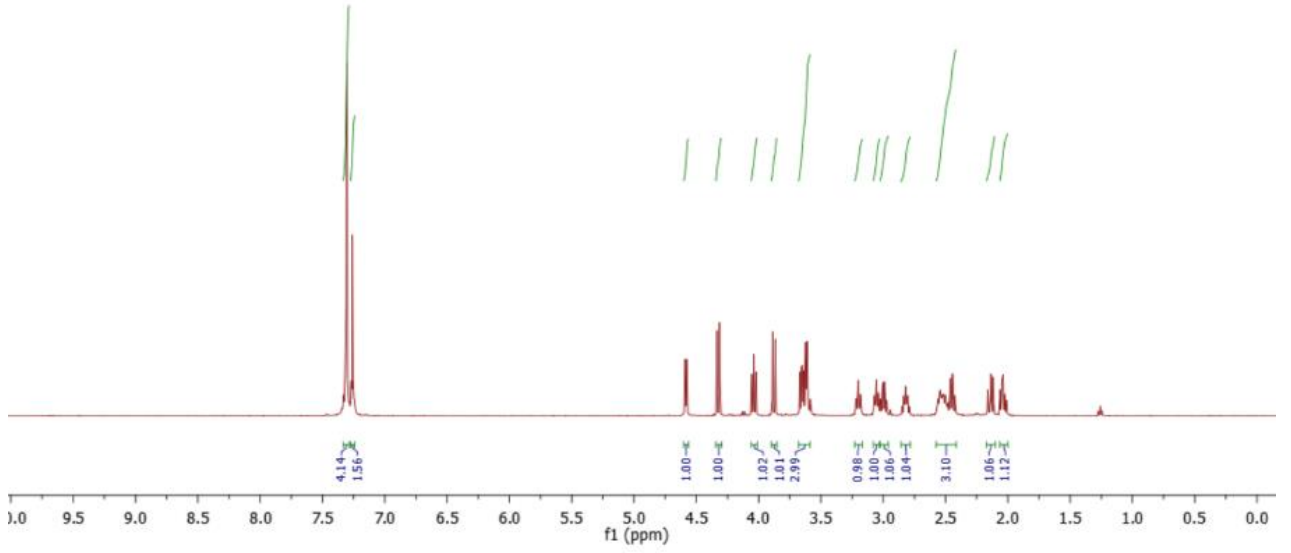
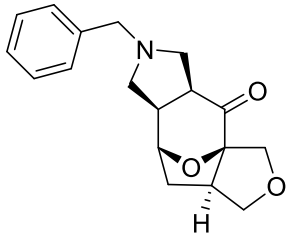


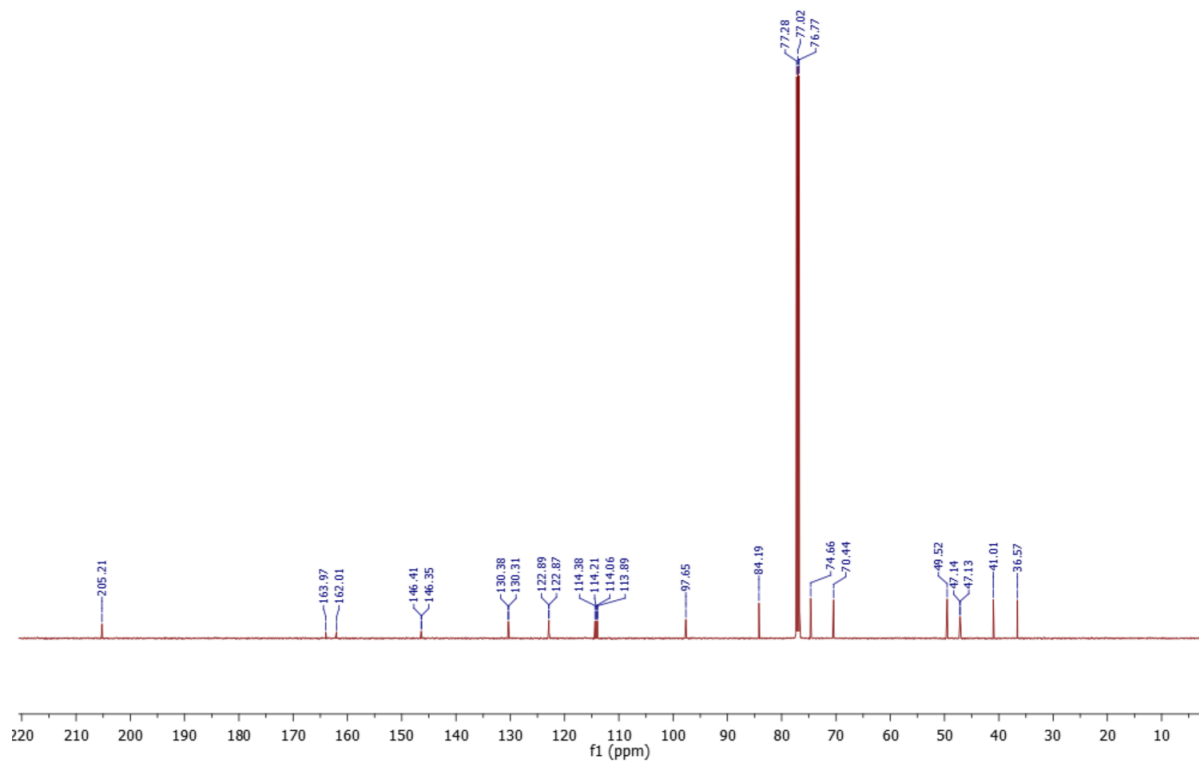
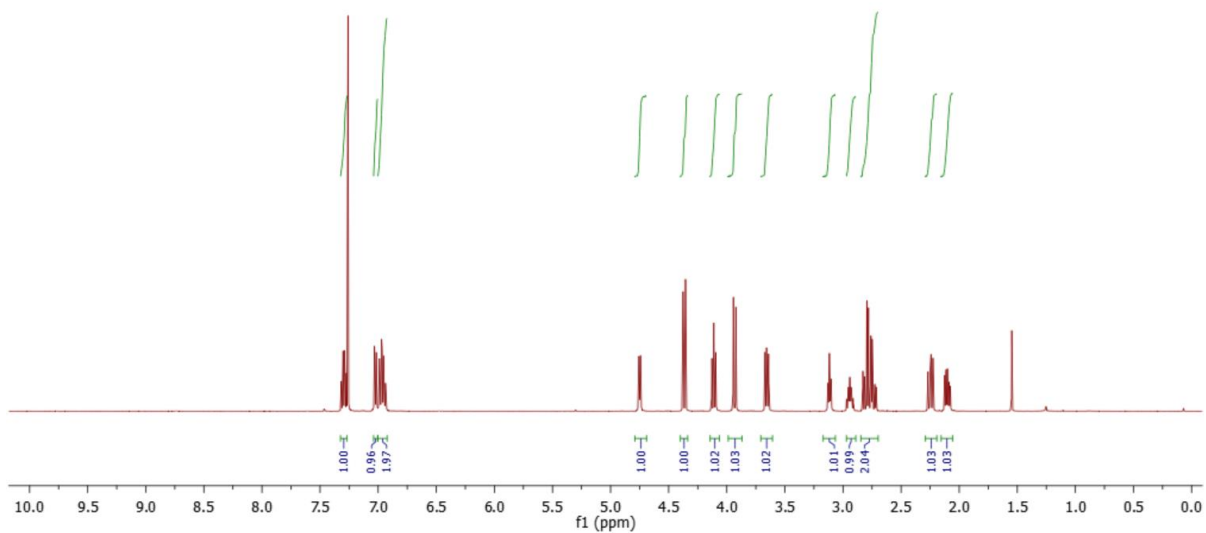
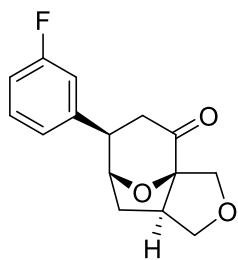


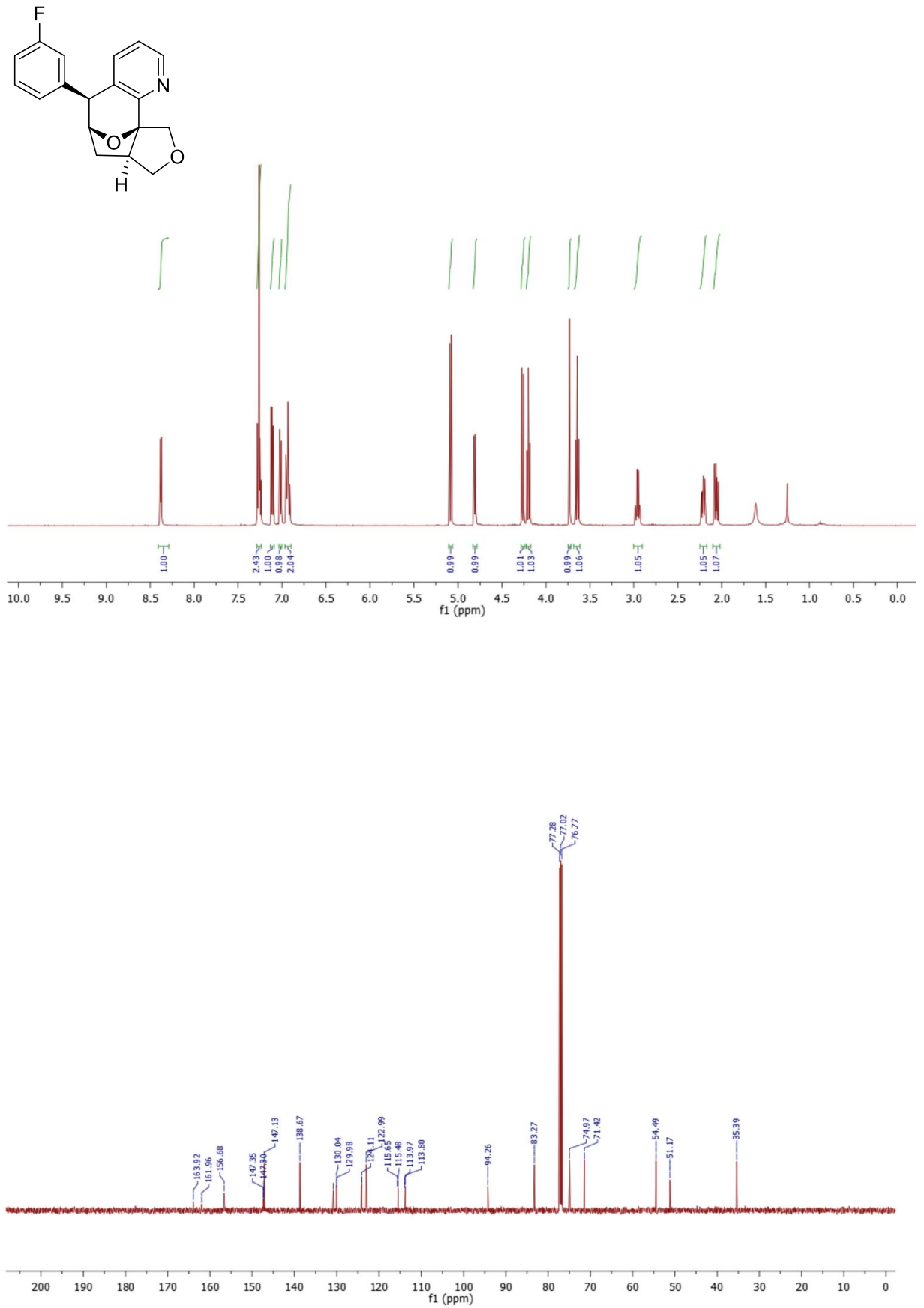


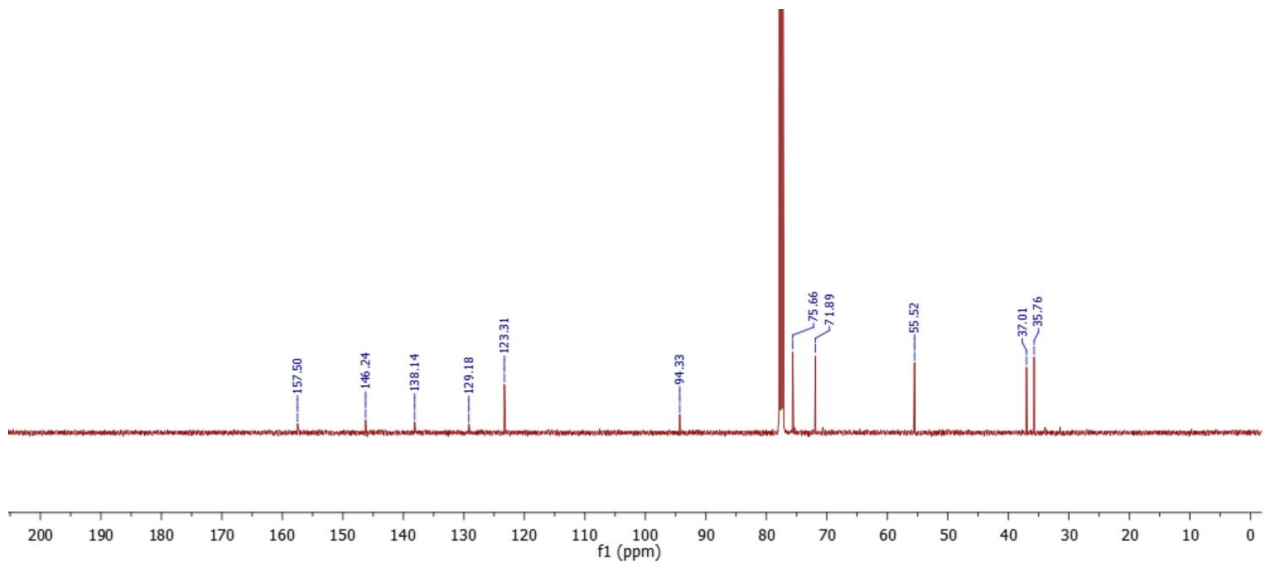
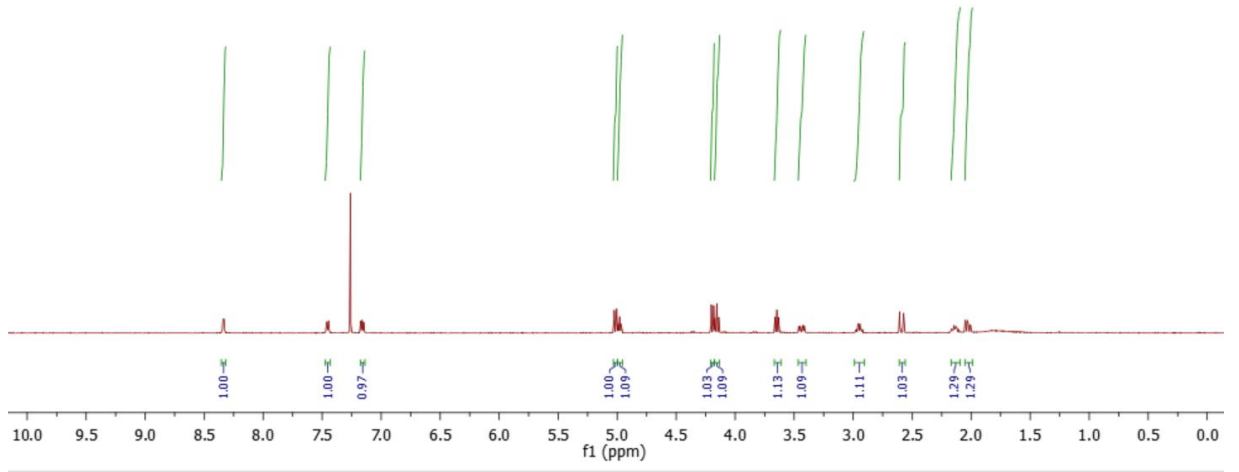
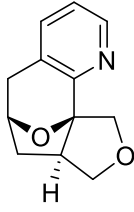


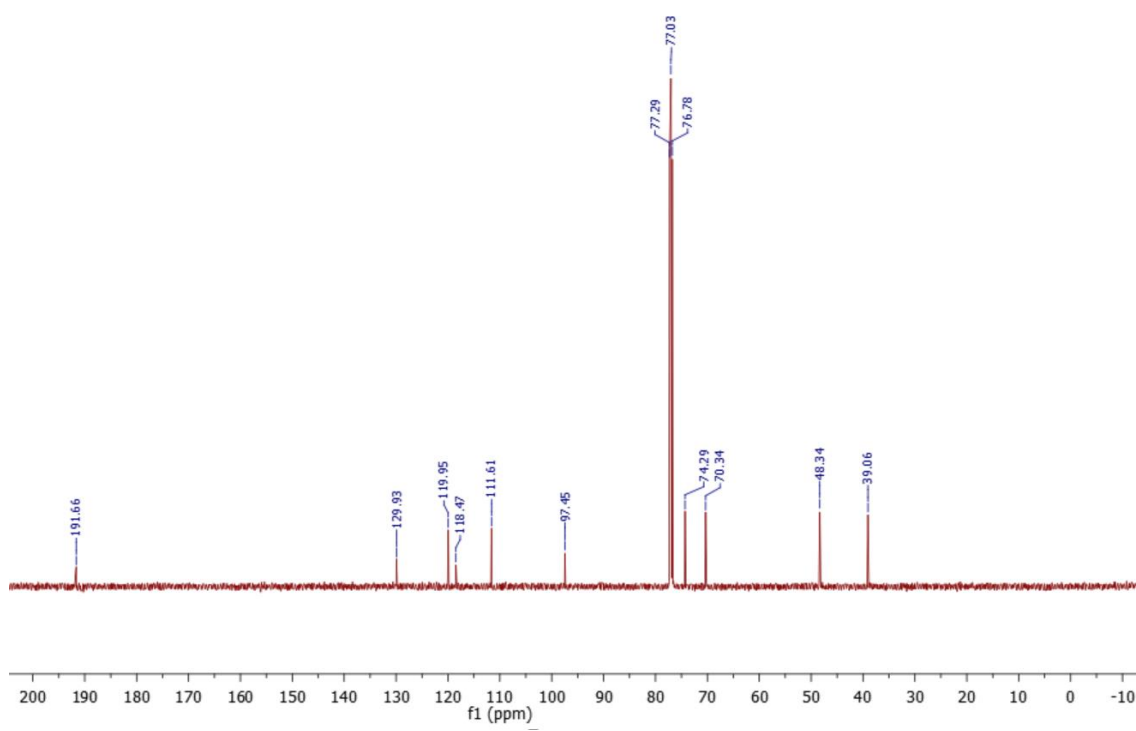
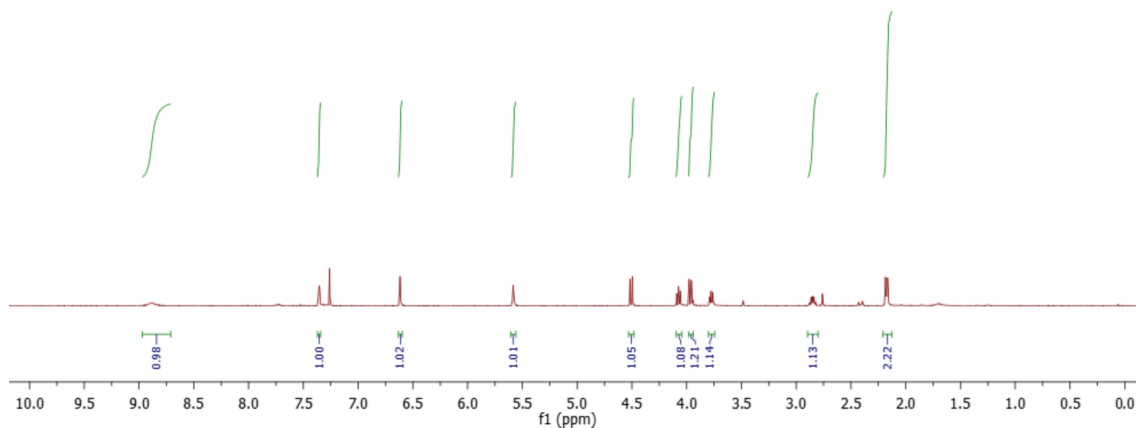
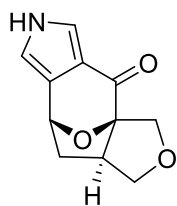


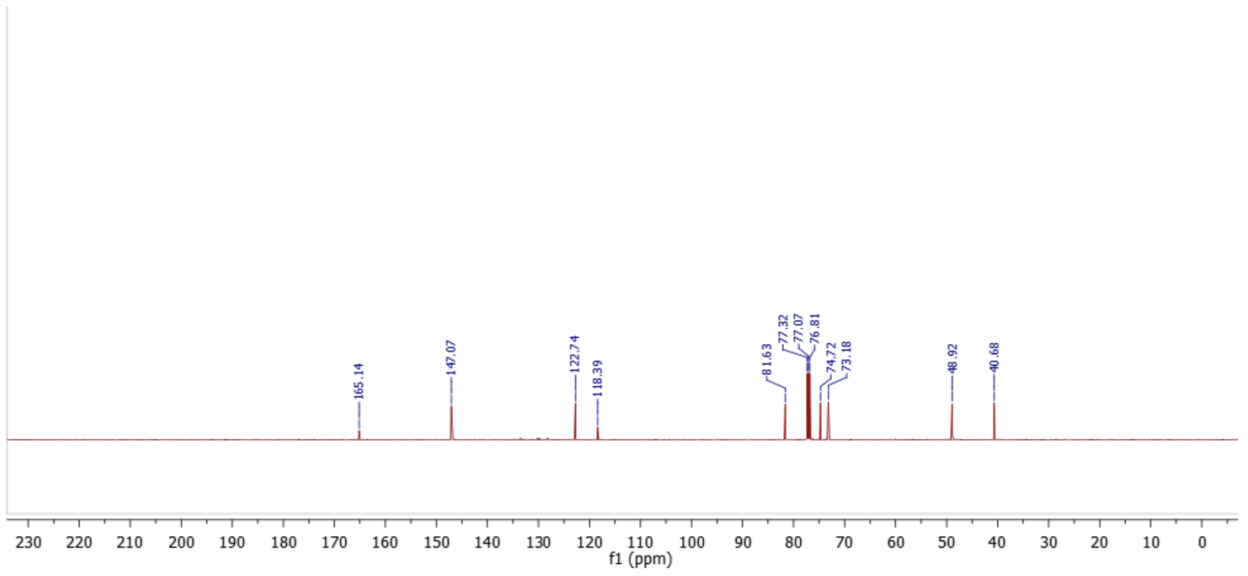
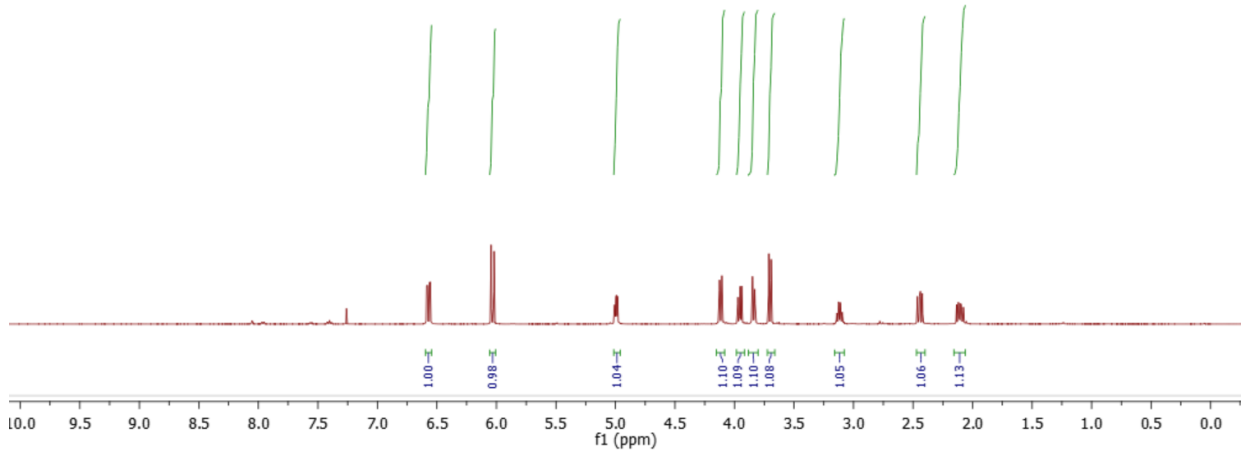
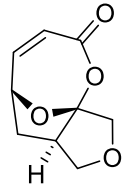


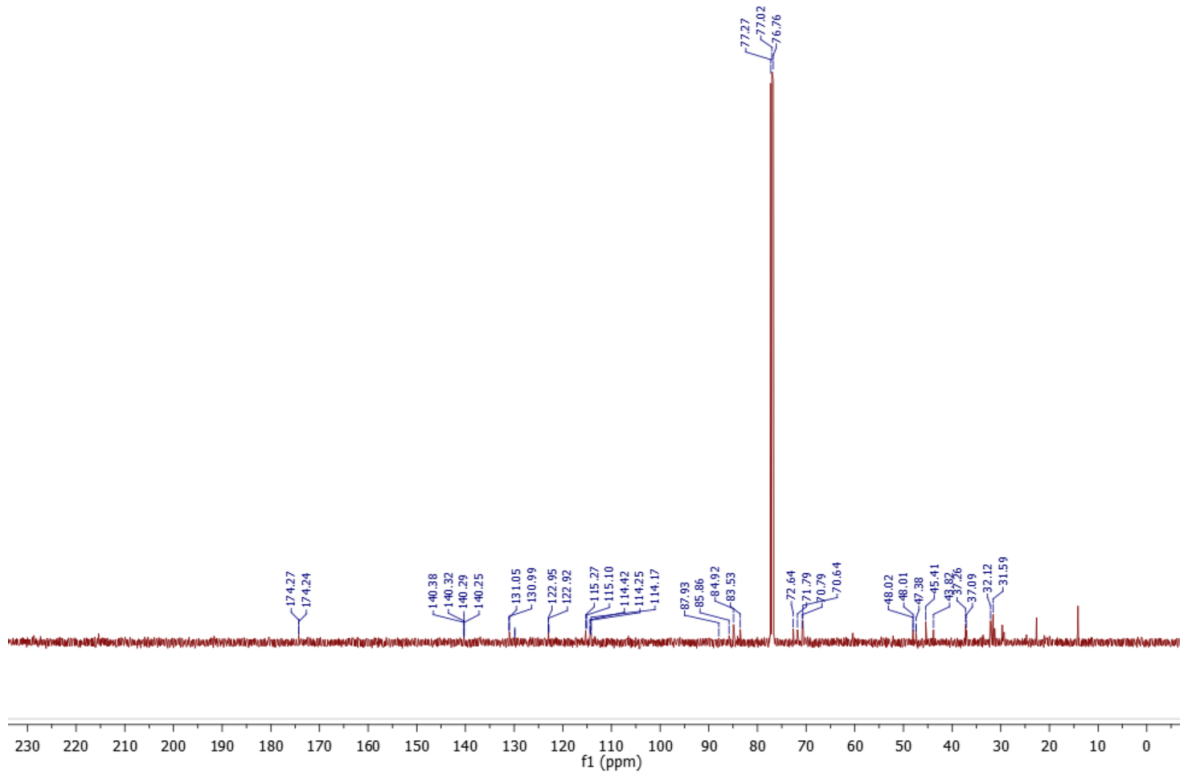
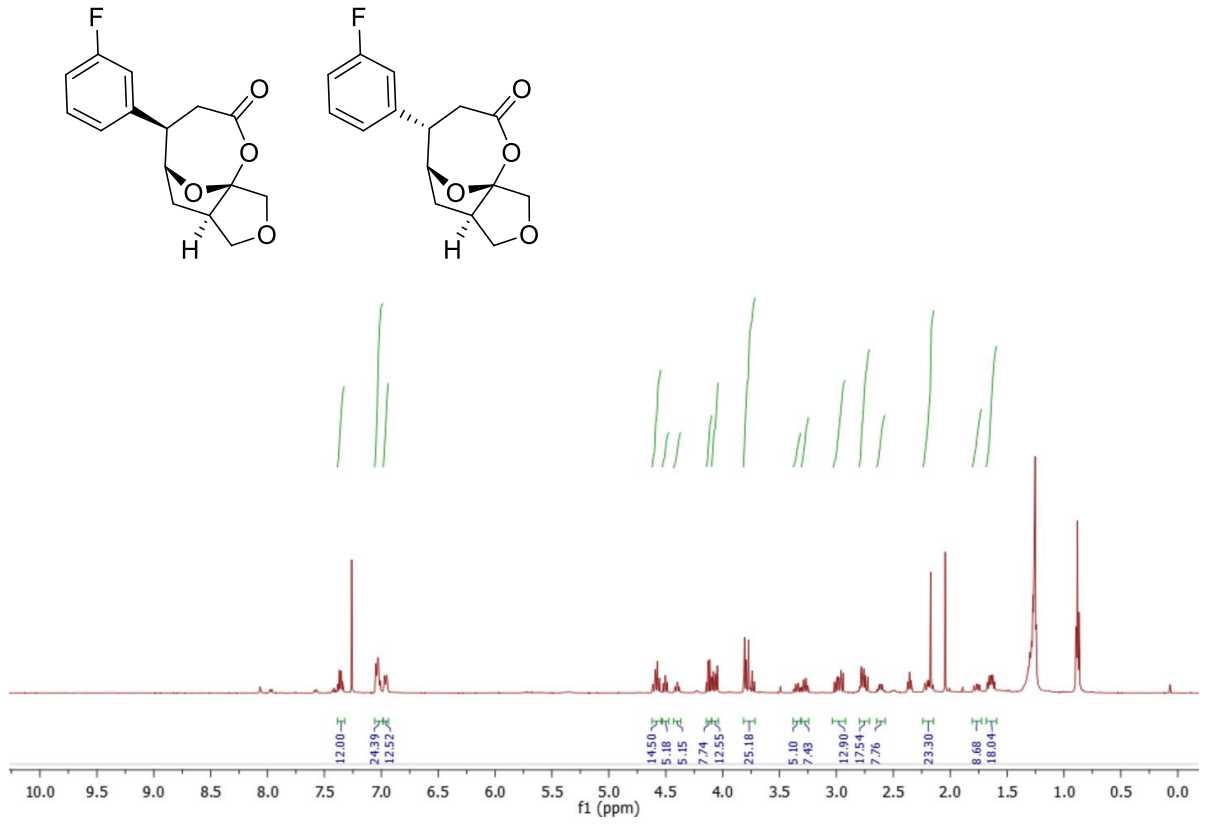












Appendix B

NOESY NMR Spectrum's used in the assignment of stereochemistry.

